ISSN 0021-9673

ISHED
LY

VOL. 238 NO. 1 APRIL 2, 1982

NAL OF

HROMATOGRAPHY

RNATIONAL JOURNAL ON CHROMATOGRAPHY, ELECTROPHORESIS AND RELATED METHODS

ELSEVIER SCIENTIFIC PUBLISHING COMPANY
AMSTERDAM

JOURNAL OF CHROMATOGRAPHY

Scope. The *Journal of Chromatography* publishes papers on all aspects of chromatography, electrophoresis and related methods. Contributions consist mainly of research papers dealing with chromatographic theory, instrumental development and their applications. The section *Biomedical Applications,* which is under separate editorship, deals with the following aspects: developments in and applications of chromatographic and electrophoretic techniques related to clinical diagnosis (including the publication of normal values); screening and profiling procedures with special reference to metabolic disorders; results from basic medical research with direct consequences in clinical practice; combinations of chromatographic and electrophoretic methods with other physicochemical techniques such as mass spectrometry. In *Chromatographic Reviews,* reviews on all aspects of chromatography, electrophoresis and related methods are published.

Submission of Papers. Papers in English, French and German may be submitted, in three copies. Manuscripts should be submitted to: The Editor of *Journal of Chromatography,* P.O. Box 681, 1000 AR Amsterdam, The Netherlands, or to: The Editor of *Journal of Chromatography, Biomedical Applications,* P.O. Box 681, 1000 AR Amsterdam, The Netherlands. Review articles are invited or proposed by letter to the Editors and will appear in *Chromatographic Reviews* or *Biomedical Applications.* An outline of the proposed review should first be forwarded to the Editors for preliminary discussion prior to preparation. Submission of an article is understood to imply that the article is original and unpublished and is not being considered for publication elsewhere. For copyright regulations, see below.

Subscription Orders. Subscription orders should be sent to: Elsevier Scientific Publishing Company, P.O. Box 211, 1000 AE Amsterdam, The Netherlands. The *Journal of Chromatography* and the *Biomedical Applications* section can be subscribed to separately.

Publication. The *Journal of Chromatography* (incl. *Biomedical Applications, Chromatographic Reviews* and *Cumulative Author and Subject Indexes, Vols. 221–230, 231–240* and *241–250*) has 25 volumes in 1982. The subscription prices for 1982 are:

J. Chromatogr. (incl. *Chromatogr. Rev.* and *Cum. Indexes Vols. 221–230, 231–240 and 241–250*) + *Biomed. Appl.* (Vols. 227–251):
Dfl. 3625.00 plus Dfl. 500.00 (postage) (total *ca.* US$ 1650.00)

J. Chromatogr. (incl. *Chromatogr. Rev.* and *Cum. Indexes Vols. 231–240* and *241–250*) only (Vols. 234–251):
Dfl. 2826.00 plus Dfl. 360.00 (postage) (total *ca.* US$ 1274.50)

Biomed. Appl. (incl. *Cum. Indexes Vols. 221–230*) only (Vols 227–233):
Dfl. 1050.00 plus Dfl. 140.00 (postage) (total *ca.* US$ 476.00).

Journals are automatically sent by airmail to the U.S.A. and Canada at no extra costs, and to Japan, Australia and New Zealand, with a small additional postal charge. Back volumes of the *Journal of Chromatography* (Vols. 1 through 226) are available at Dfl. 173.00 (plus postage). Claims for issues not received should be made within three months of publication of the issue. If not, they cannot be honoured free of charge. For customers in the U.S.A. and Canada, wishing additional bibliographic information on this and other Elsevier journals, please contact Elsevier Science Publishing Company Inc., Journal Information Center, 52 Vanderbilt Avenue, New York, NY 10017. Tel: (212) 867-9040.

Abstracts/Contents Lists published in Analytical Abstracts, Biochemical Abstracts, Biological Abstracts, Chemical Abstracts, Chemical Titles, Current Contents/Physical, Chemical & Earth Sciences, Current Contents/Life Sciences, Index Medicus, Mass Spectrometry Bulletin, and Science Citation Index.

See page 3 of cover for Publication Schedule, Information for Authors, and information on the News Section and Advertisements.

Printed in The Netherlands

VOL. 238, NO. 1 JOURNAL OF CHROMATOGRAPHY APRIL 2, 1982

CONTENTS

(Abstracts/Contents Lists published in Analytical Abstracts, Biochemical Abstracts, Biological Abstracts, Chemical Abstracts, Chemical Titles, Current Contents/Physical, Chemical & Earth Sciences, Current Contents/Life Sciences, Index Medicus, Mass Spectrometry Bulletin, and Science Citation Index)

(Continued overleaf)

Contents (continued)

Notes

INSTRUMENTATION FOR HIGH-PERFORMANCE LIQUID CHROMATOGRAPHY

J. F. K. HUBER, *Institute of Analytical Chemistry, University of Vienna, Austria (Editor).*

Journal of Chromatography Library: Volume 13.

A practical guide for all those involved in the application of column liquid chromatography, this book provides a valuable, up-to-date review of the large selection of instrumentation currently available. Special emphasis is given to discussion of the general principles of design which will remain relevant even if new technical solutions are found in the future.

CONTENTS: Chapters. 1. The chromatographic apparatus from the viewpoint of system theory *(J. F. K. Huber).* 2. Pump systems *(M. Martin and G. Guiochon).* 3. Solvent gradient systems *(M. Martin and G. Guiochon).* 4. Sample introduction systems *(J. C. Kraak).* 5. Column design selection *(J. C. Kraak).* 6. Components and accessories for preparative high-performance liquid chromatography *(A. Wehrli).* 7. Detectors based on the measurement of optical and electrical properties of the mobile phase *(H. Poppe).* 8. Electrochemical Detectors *(H. Poppe).* 9. Radiometric detectors *(P. Markl).* 10. Combination of liquid chromatography and mass spectrometry *(E. Kenndler and E. R. Schmid).* 11. Specifications of commercial liquid chromatographs *(R. R. Becker).* Subject index. Manufacturer index.

"...this book provides useful practical information for the neophyte. It is well produced and in line with the high standard set by the publishers."

– Faraday Transactions

1978 xii + 204 pages US $ 39.00/Dfl. 80.00
ISBN 0-444-41648-X

POROUS SILICA

Its Properties and Use as Support in Column Liquid Chromatography

K. K. UNGER, *Professor of Chemistry at the University of Mainz, West Germany.*

Journal of Chromatography Library: Volume 16.

This book provides the chromatographer with full information on the properties of silica and its chemically bonded derivatives in context with its chromatographic behaviour. The book will be useful to all those who use silica in HPLC and who seek to choose the optimum silica packing for a given separation problem.

CONTENTS: Chapters. 1. General Chemistry of Silica. 2. Pore Structure of Silica. 3. Surface Chemistry of Porous Silica. 4. Particle Characteristics. 5. Silica Columns – Packing Procedures and Performance Characteristics. 6. Silica and Its Chemically Bonded Derivatives as Adsorbents in Liquid-Solid Chromatography. 7. Silica as a Support in Liquid-Liquid Chromatography. 8. Chemically Modified Silica as Packings in Ion Exchange Chromatography. 9. Silica as a Packing in Size-Exclusion Chromatography. Subject Index.

"...no book previously published has so thoroughly investigated the surface properties of a material in relation to its uses in chromatography."

– Chromatographia

1979 xii + 336 pages US $ 58.50/Dfl. 120.00
ISBN 0-444-41683-8

P.O. Box 211,
1000 AE Amsterdam,
The Netherlands,

52 Vanderbilt Ave,
New York, N.Y. 10017.

The Dutch guilder price is definitive US $ prices are subject to exchange rate fluctuations

ELSEVIER

JOURNAL OF CHROMATOGRAPHY

VOL. 238 (1982)

JOURNAL *of* CHROMATOGRAPHY

INTERNATIONAL JOURNAL ON CHROMATOGRAPHY, ELECTROPHORESIS AND RELATED METHODS

ELSEVIER SCIENTIFIC PUBLISHING COMPANY
AMSTERDAM

J. Chromatogr., Vol. 238 (1982)

Printed in The Netherlands

Journal of Chromatography, 238 (1982) 1–12
Elsevier Scientific Publishing Company, Amsterdam – Printed in The Netherlands

CHROM. 14,567

OPTIMIZATION OF EXPERIMENTAL CONDITIONS FOR THE ANALYSIS OF COMPLEX MIXTURES BY GAS CHROMATOGRAPHY

J. KRUPČÍK, J. MOCÁK, A. ŠIMOVÁ and J. GARAJ
Slovak Technical University, Chemical Faculty, Department of Analytical Chemistry, 880 37 Bratislava (Czechoslovakia)
and
G. GUIOCHON*
École Polytechnique, Laboratoire de Chimie Analytique Physique, 91128 Palaiseau Cedex (France)
(First received June 15th, 1981; revised manuscript received October 30th, 1981)

SUMMARY

An optimization procedure for the gas chromatography of complex mixtures is described and has been applied to the analysis of a mixture of 40 polychlorobiphenyls on a column made by connecting an Apiezon L-coated column with a Carbowax 20M-coated column.

INTRODUCTION

Open-tubular gas chromatographic columns are used mainly for the analysis of complex mixtures of organic compounds. Their development in the last 12 years has been speeded up by pressing needs for trace analysis, the identification of components of complex mixtures and faster analyses. It was made possible by the ease with which such columns can be prepared from glass tubes.

Analytical results are strongly dependent upon working conditions and up to now the adjustment of experimental parameters has been empirical. The analysis of complex mixtures is long, however, and empirical optimization is tedious and time consuming and the results depend heavily on the experience and skill of the analyst.

The optimization of analytical conditions for the separation of a binary mixture is easy to achieve or even to formulate, as we have to maximize only the resolution, R_{ij}, between the two peaks:

$$R_{ij} = \frac{\sqrt{n_i}}{4} \cdot \frac{k_j}{1 + k_j} \cdot \frac{\alpha_{ij} - 1}{\alpha_{ij}} \qquad (1)$$

(see list of symbols) and to adjust the analysis time to achieve the necessary resolution.

The problem becomes more complicated when we have to separate a multicomponent mixture, where there are always several pairs of compounds the resolution

0021-9673/82/0000–0000/$02.75

of which is more critical than others. Morgan and Deming[1], for example, have shown how to optimize the temperature and the carrier gas flow-rate in the analysis of two- to five-component mixtures using a sequential simplex method and carrying out calculations with a computer. In the cases they discussed, however, the elution order remained unchanged. This is not what happens in actual situations of current interest when we attempt to optimize the temperature, the phase ratio and the selectivity of the stationary phase to separate a complex mixture with a large number of components whose retention order will change markedly in the range of experimental conditions that can be achieved. For each such change there is a corresponding narrow range of conditions in which total resolution of the mixture is impossible in practice. A systematic approach to the problem is extremely difficult and time consuming, and has not been achieved up to now, although Laub *et al.*[2] have suggested an interesting scheme with mixed stationary phases. We have previously explained why we prefer to use series of columns prepared with different stationary phases and how it is possible to predict retention data on such series of columns[3].

We describe here a systematic approach using some simple approximations and demonstrate its application to the analysis of mixtures of 40 polychlorinated biphenyls (PCBs) by optimizing the column temperature and the length of the second column of a series of two columns.

EXPERIMENTAL

Samples were prepared by dissolving 100 mg of Aroclor 1242 (Monsanto, St. Louis, MO, U.S.A.), which is a mixture of PCBs containing 42% (w/w) of chlorine, in 1 ml of *n*-hexane.

Open-tubular columns manufactured from soda-lime glass were used. The inner surface of the glass tube was treated with gaseous hydrogen chloride using the procedure described previously[4]. The columns were coated with stationary phase using a dynamic procedure[5].

Column A

Apiezon L was purified by column liquid chromatography on alumina[6], and a 114-m glass capillary column of 0.25 mm I.D. was coated with 0.3 ml of a 10% solution of Apiezon L in *n*-hexane using the dynamic procedure with a mercury plug[5]. The column was divided into six 19-m long sections. The thickness of the stationary phase film was checked by measuring the capacity ratio for 2,5,2′-trichlorobiphenyl. The capacity ratios in the four middle parts were 1.70 ± 0.085. These four parts were connected by shrinkable Teflon tubing and a 75.6-m long column (A) was obtained.

Column B

A 90-m glass capillary column of 0.25 mm I.D. was coated with 0.3 ml of a 5% solution of polyethylene glycol 20,000 (Carbowax 20M) in dichloromethane, using the dynamic procedure with a mercury plug. The column was divided into six parts. The four middle parts formed columns B_1 (15.5-m long), B_2 (14.3 m), B_3 (14.7 m) and B_4 (12.1 m). These individual parts were successively connected with column A by shrinkable Teflon tubing to make series of two columns with a variable length of the second column[3].

TABLE I

CHARACTERISTICS OF THE COLUMNS USED, MEASURED WITH 2,5,2′-TRICHLOROBIPHENYL AT 180°C

Column designation	*Characteristics**			
	$\bar{u}$ *(cm/sec)*	k'	n	N
A	13.90	1.70	287,500	114,000
$A+B_1$	12.60	1.76	349,500	142,000
$A+B_1+B_2$	12.86	1.86	387,000	164,000
$A+B_1+B_2+B_3$	13.60	1.92	419,500	181,000
$A+B_1+B_2+B_3+B_4$	14.00	2.04	452,500	204,000

* n = number of theoretical plates found for 2,5,2′-trichlorobiphenyl; $\bar{u}$ = average carrier gas (nitrogen) velocity; k' = capacity ratio for 2,5,2′-trichlorobiphenyl; N = number of effective plates $\left[N = n\left(\frac{k'}{1+k'}\right)^2\right]$.

The characteristics of the columns are summarized in Table I.

Equipment

A Fractovap Model 2300 gas chromatograph (Carlo Erba, Milan, Italy) equipped with a flame-ionization detector and a sampling splitter was used, which allowed the easy use of glass capillary columns. The end of the column was carefully inserted into the detector jet to minimize the equipment contribution to band broadening. Nitrogen was used as the carrier gas.

Retention times for the calculation of Kováts retention indices were measured with a stopwatch.

The calculation of the optimal values of the temperature and column selectivity was performed using a Siemens 4004-150 computer and a FORTRAN program called OPTIM[7].

THEORETICAL

The optimal carrier gas velocities of the columns used were in the range 7–10 cm/sec for nitrogen and 25–30 cm/sec for hydrogen, in agreement with the findings of Schomburg *et al.*[8]. Further, a change in the velocity of nitrogen between 7 and 14 cm/sec caused a relative decrease in resolution of less than 10%, which is approximatively equal to the error of the resolution measurement and to the difference between the resolutions obtained with hydrogen and nitrogen. There is little need to optimize further that velocity except in an attempt to minimize the analysis time, which is not the topic of this work. Therefore, all the experiments were made using a stream of nitrogen at an average velocity around 13–14 cm/sec (*cf.*, Table I).

The last two factors on the right-hand side of eqn. 1 depend greatly on the column temperature. The influence of temperature on the effective plate number:

$$N_j = n_j\left(\frac{k'_j}{1+k'_j}\right)^2 \tag{2}$$

has been discussed previously[9].

The selectivity of the stationary phase is also a function of temperature. It can also be changed by using another liquid phase. Unfortunately, only a small number of liquid phases can be used to prepare good, efficient capillary columns. They do not mix easily and the preparation of mixed-phase open-tubular columns is impaired by wettability problems; glass has to be treated in different ways in order to be wetted properly by different stationary phases. The approach used by Laub *et al.* with packed columns[2] cannot, therefore, be used with capillary columns, whether well founded or not[3].

On the other hand, the ease with which open-tubular columns can be connected without any loss in efficiency, using shrinkable Teflon tubing[4], allows the systematic use of series of columns prepared with different stationary phases. This permits a virtually continuous change in the selectivity of column series, by changing the length of the second column[3]. The only problem will be that the longer the second column, the higher the efficiency of the column series, and this will have to be taken into account in the calculations.

Finally, our previous work has shown that, in practice, retention indices of many compounds increase linearly with the length of the second column, provided that this column is shorter than the first one[3]. This fact will make the calculations fairly simple. The retention index of a compound i, I_i, is defined as

$$I_i = 100z + 100 \cdot \frac{\log (t'_{R,i}/t'_{R,z})}{\log (t'_{R,z+1}/t'_{R,z})} \tag{3}$$

If compounds i and j are both eluted between the n-alkanes with z and $z + 1$ carbon atoms, the difference between their retention indices is

$$\Delta I = I_j - I_i = 100 \cdot \frac{\log \alpha_{ij}}{\log (t'_{R,z+1}/t'_{R,z})} \tag{4}$$

Combination of eqns. 1, 2 and 4 gives

$$R_{ij} = \frac{\sqrt{N_j}}{4} \left[1 - \left(\frac{t'_{R,z}}{t'_{R,z+1}} \right)^{\Delta I/100} \right] \tag{5}$$

When ΔI becomes small, R_{ij} tends towards zero. For most stationary phases $t'_{R,Z+1}/t'_{R,Z}$ is around 1.5. Hence we can approximate eqn. 5, for small differences between retention indices, by

$$R_{ij} \approx \frac{\sqrt{N_j}}{4} \cdot \frac{\Delta I}{100} \cdot \ln \left(\frac{t'_{R,Z+1}}{t'_{R,z}} \right) \approx 10^{-3} \, \Delta I \sqrt{N_j} \tag{6}$$

This shows that a resolution of unity can be obtained between two compounds whose retention indices differ only by 1 if the effective plate number is 10^6, which is very high[8].

As we have shown above, the retention index can be written as a linear function of temperature and of the length of the second column of the series:

$$I_i = A_i + B_i T + C_i L + D_i LT \tag{7}$$

As the two partial differentials of I depend only on the other parameter, it is possible to calculate the four coefficients of eqn. 7 for a given compound from experimental data using the linear least-squares method.

If the components of the mixture are arranged in order of increasing retention indices, the difference

$$\Delta I_i = I_{i+1} - I_i \tag{8}$$

between the retention indices of two adjacent compounds gives an estimate of their resolution for a given system. As a first approximation it can be predicted that the two compounds will be resolved if ΔI_i exceeds a threshold δ, determined as a function of the desired resolution and of the range of the effective plate number of the column used for the separation of the components of the mixture. We know that for capillary columns the effective plate number increases very rapidly for column capacity factors between 0 and 1 and then much more slowly, so that the approximation will be valid for compounds that are significantly retained, but not for those which are eluted early and are difficult to separate anyway[10].

The basic tasks of the program will thus be as follows: (i) to calculate the retention indices of all compounds in a given set of conditions; (ii) to arrange compounds in order of increasing retention indices; (iii) to calculate all retention indices increments, ΔI_i; (iv) to determine how many increments are below the threshold and what is the lowest increment above the threshold.

Optimal conditions are those in which there is the smallest number of unresolved pairs of compounds. If there are several sets of conditions in which the numbers of such pairs are equal, the optimal conditions are those in which the smallest increment above the threshold is the largest (the compounds with an increment below the threshold are unresolved so that it is pointless to use their increments, unless the column can be made longer and therefore the threshold decreased).

Using experimental data covering a given range of temperature and column length (*cf.*, eqn. 7), it is possible to calculate retention indices for any combination of T and L in this range. Thus, the calculation of optimal conditions is possible using a variety of techniques. It must be emphasized, however, that altough eqn. 7 is linear in L and in T, ΔI_i is not regular but exhibits discontinuities each time the order of elution of the components of the mixture is changed. The use of conventional optimization methods such as the simplex method becomes difficult and has not been contemplated at this stage.

Main characteristics of the calculation program

The main operations carried out by the program are the following:

(i) Reading retention indices measured for all components of the mixture at different temperatures and second column lengths. Calculation of the coefficients of eqn. 7 for each component.

(ii) For each selected value of temperature and the second column length chosen for this investigation, calculation of retention indices of all components. The compounds are then ordered according to increasing retention index and differences ΔI_i are calculated. Usually the network chosen for these calculations is regular, dense and contained in the range of temperatures and column lengths investigated in the measurements of experimental data.

(iii) The smallest ΔI_i is divided by the threshold δ, selected for the particular analysis. If the result is larger than 1, this result minus one $(\Delta I_i/\delta) - 1$ is the value of the optimization criterion for this particular set of conditions. If the result is smaller than 1, a value equal to -10 is taken for the optimization criterion and then the same operation is repeated for the second smallest ΔI_i. Again, if the result is larger than 1, $(\Delta I_i/\delta) - 1$ is added to the criterion and the program passes on to the next set of conditions; if the result is smaller than 1, -10 is added to the criterion and the next larger ΔI_i is considered.

The final value of the optimization criterion for a given set of experimental conditions is equal to -10 multiplied by the number of unresolved pairs $(\Delta I_i \leqslant \delta)$ plus the term $(\Delta I_i/\delta) - 1$ corresponding to the smallest I_i larger than the threshold.

(iv) The procedure described under operations (ii) and (iii) is repeated for all the sets of experimental conditions corresponding to the network defined by the instructions given to the computer.

(v) When the calculation is finished, the computer prints out the optimal experimental conditions (T and L), the corresponding value of the optimization criterion and the list of retention indices of all components of the mixture in increasing order under these optimal conditions.

The values of the optimization criterion under other conditions (for example, optimal column length at any given temperature), retention indices under any given conditions, regression coefficients or standard deviations can also be printed on request.

RESULTS AND DISCUSSION

This optimization procedure was applied to the analysis of the mixture of polychlorinated biphenyls (Aroclor 1242) on the glass capillary columns described above. Measurements were made on Apiezon L column A alone and then on series of columns made by connecting to column A the four sections of the Carbowax column B as indicated in Table I. All measurements were carried out at 170, 175 and 180°C.

As an example, a chromatogram showing the separation of the mixture of

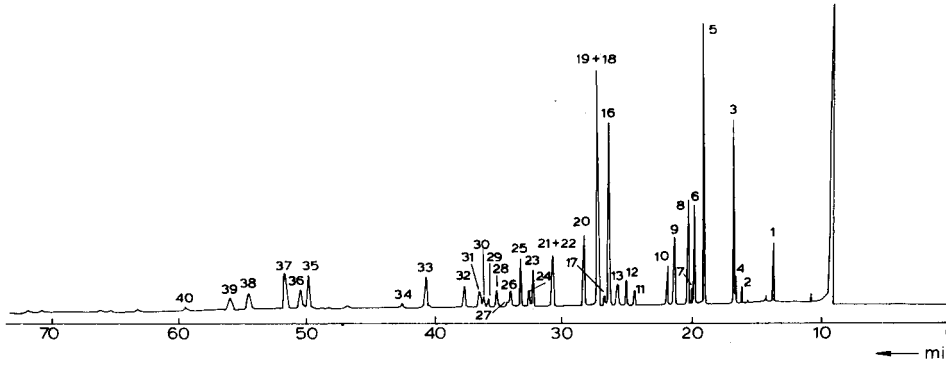

Fig. 1. Separation of Aroclor 1242 on a glass capillary column coated with Apiezon L at 180°C. Peak numbers refer to the same compounds as those in all other figures and in Table II, except for Fig. 3. Peak identification is given in ref. 11.

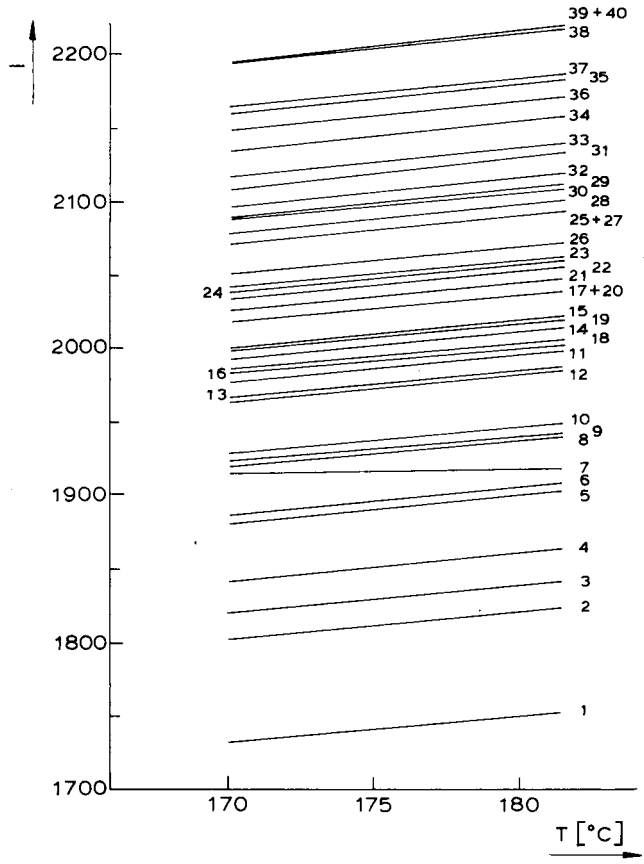

Fig. 2. Plots of retention indices (I) *versus* temperature (T) for PCBs, using column system A + B_1 + B_2 + B_3 + B_4 (*cf.*, Table I).

chlorinated biphenyls on column A at 180°C is shown in Fig. 1. Forty components of the mixture have been identified, but a few trace components have not. The numbers used are the same as those given elsewhere[3]. Several peaks on this chromatogram overlap and the resolution of a few other pairs is inadequate.

The influence of temperature on the separation of the 40 components identified in Aroclor 1242 is illustrated in Fig. 2, where plots of retention indices on columns A + B *versus* temperature are given for these compounds. We observe that although the resolution of several pairs of components could be improved by a decrease in temperature, a significant improvement can be obtained only by a marked decrease in temperature resulting in an excessively long analysis time; most of the straight lines in Fig. 2 are almost parallel.

When Aroclor 1242 is analysed on column B (B_1 + B_2 + B_3 + B_4), the separation of some pairs of PCBs improves in comparison with that obtained by analysis on the apolar column A but, as shown in Fig. 3, other components overlap. Note that the numbers in Fig. 3 do not correspond to those in Figs. 1 and 2 or those used below, because the peaks have not been all identified in this chromatogram.

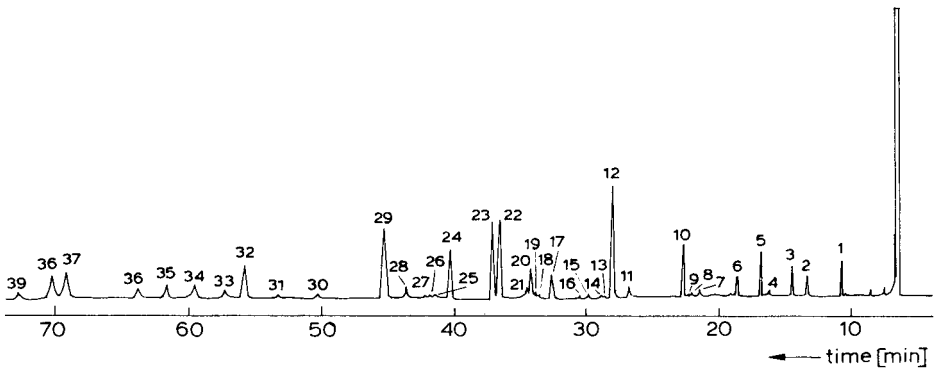

Fig. 3. Separation of PCBs on a glass capillary column coated with Carbowax 20M at 180 C. Peaks are still unidentified.

Similar problems were observed in the analysis of Aroclor 1242 on glass capillary columns coated with OV-101 silicone oil or with the hydrocarbon C_{87} phase[2,11]. Further, a considerable disadvantage in changing the stationary phase is the necessity to repeat the qualitative analysis of the mixture whenever a new phase is used. Moreover, the change in the stationary phase selectivity is discontinuous and cannot be controlled.

When the selectivity of the stationary phase is changed by connecting different column sections of increasing length but coated with the same polar stationary phase to a fixed, non-polar column, the selectivity changes with the length and film thickness of the added column. When sufficiently short parts of the polar column are used, the selectivity of the resulting column varies almost continuously. If the properties of the added columns (k') remain unchanged when their length is increased, the selectivity of the resulting column increases linearly with increasing length of the added column, as can be seen in Fig. 4, which shows graphs of retention indices of a column series *versus* the length of the Carbowax 20M column added to the fixed Apiezon L column.

The plots in Figs. 2 and 4 exhibit perfect linearity, in agreement with the correlation coefficients of both dependences, which are greater than 0.998 for all components. The difference in the slopes of the lines can be explained, *inter alia*, by the different number of chlorine atoms and by their various positions in the PCB molecules.

For the optimization of column temperature and the selectivity of the stationary phase system, we measured retention indices corresponding to fifteen different experimental conditions: three temperatures (170, 175 and 180°C) and five different lengths of the added column (*cf.*, Table I). The network $T \times L$ was defined by the temperature range (170–180°C), the increment $\Delta T = 1$°C (altogether eleven chosen T-values), the range of length of the added column (0.0–60.0 m) and the increment $\Delta L = 0.5$ m (121 chosen L-values in all). Thus the investigated network consisted of 1331 points for each of the 40 components, and 53,240 values of retention indices were calculated by linear regression from 600 experimental measurements.

The threshold δ was derived from chromatograms recorded as follows. The

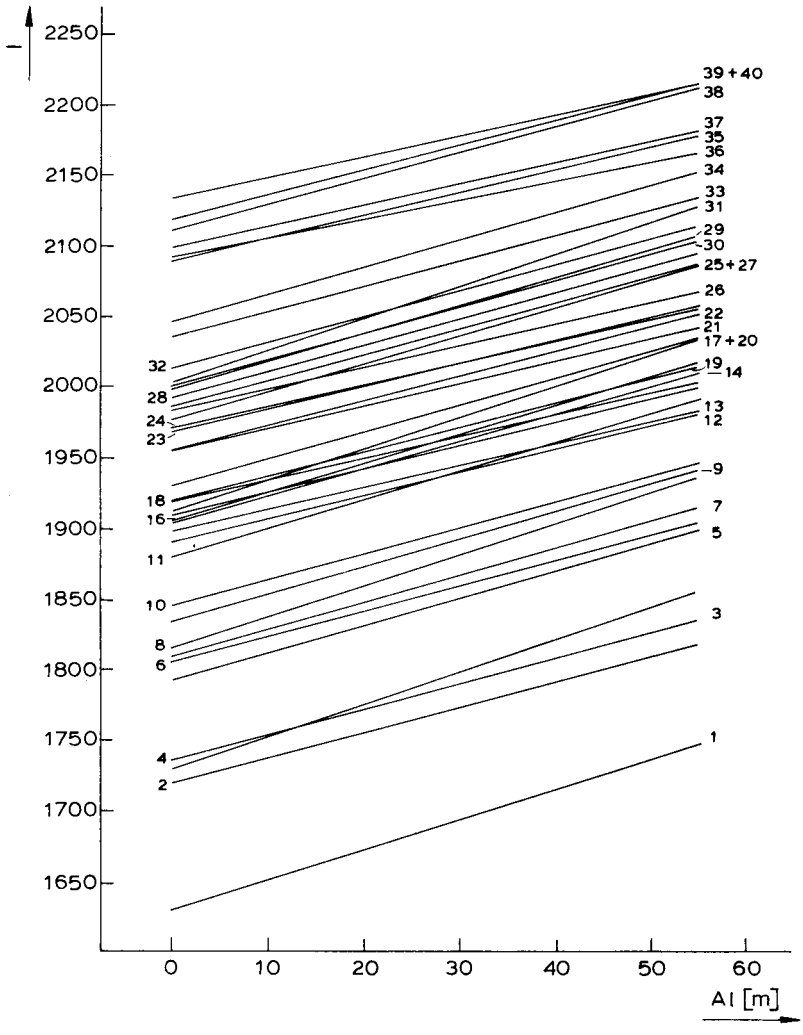

Fig. 4. Plots of retention indices (I) *versus* length of the Carbowax 20M column (A) coupled to a fixed Apiezon L glass capillary column at 180°C.

minimum degree of resolution between two peaks of equal size at which there appears a valley is 0.50. When we add sections of a polar column to increase selectivity we also increase efficiency. On column A the first serious interference problem occurs for $k' = 1.7$, and then $N = 114{,}000$ (*cf.*, Table I). Thus, if we increase the column length and the apparent k' (ref. 3), the effective plate number will increase and we shall be able to resolve compounds with closer retention indices. With column A (Apiezon L), we found that at 170°C, $\log (t'_{R,z+1}/t'_{R,z}) = 0.192$, and hence $\ln (t'_{R,z+1}/t'_{R,z}) = 0.442$. Then for $k_j = 1.7$ and $N_j = 114{,}000$, to the R_{ij} value of 0.50 there corresponds a value $\Delta I_i = I_{i+1} - I_i = 1.34$, which was used as the threshold δ. The consequence of this approach is that the optimization procedure used tends to produce a greater polar column length than would be necessary simply on the basis of selectivity.

TABLE II

KOVÁTS RETENTION INDICES (I_i) OF PCBs FOUND UNDER OPTIMAL CONDITIONS (T_{opt} = 170°C, L_{opt} = 40.0 m): OUTPUT FROM COMPUTER

i	*Peak reference number*	I_i	ΔI*
1	1	1701.80	
2	2	1777.50	6.70
3	3	1794.10	16.60
4	4	1809.03	14.93
5	5	1854.32	45.29
6	6	1862.12	7.80
7	7	1876.79	14.67
8	8	1888.46	11.67
9	9	1896.19	7.73
10	10	1902.21	6.02
11	12	1940.46	38.25
12	13	1943.93	3.47
13	11	1947.83	3.90
14	16	1959.11	11.28
15	18	1964.09	4.98
16	14	1965.57	1.48
17	15	1970.25	4.68
18	19	1972.95	2.70
19	17	1985.10	12.15
20	20	1990.67	5.57
21	21	2003.32	12.65
22	22	2009.44	6.12
23	24	2016.30	6.86
24	23	2018.07	1.77
25	26	2028.55	10.48
26	25	2041.77	13.22
27	27	2043.21	1.44
28	28	2051.18	7.97
29	29	2060.25	9.07
30	30	2061.19	0.94
31	32	2069.99	8.80
32	31	2075.83	5.84
33	33	2090.86	15.03
34	34	2107.41	16.55
35	36	2129.97	12.56
36	35	2137.79	7.82
37	37	2142.85	5.06
38	38	2168.45	25.60
39	39	2170.71	2.26
40	40	2174.82	4.11

* $\Delta I = I_{i+1} - I_i$.

The optimal conditions found in the analysis of Aroclor 1242 by the computer program are T_{opt} = 170°C and optimal length of added Carbowax column L_{opt} = 40.0 m. The value of the optimization criterion OPTTOT = −9.93 corresponds to one unresolved pair of peaks.

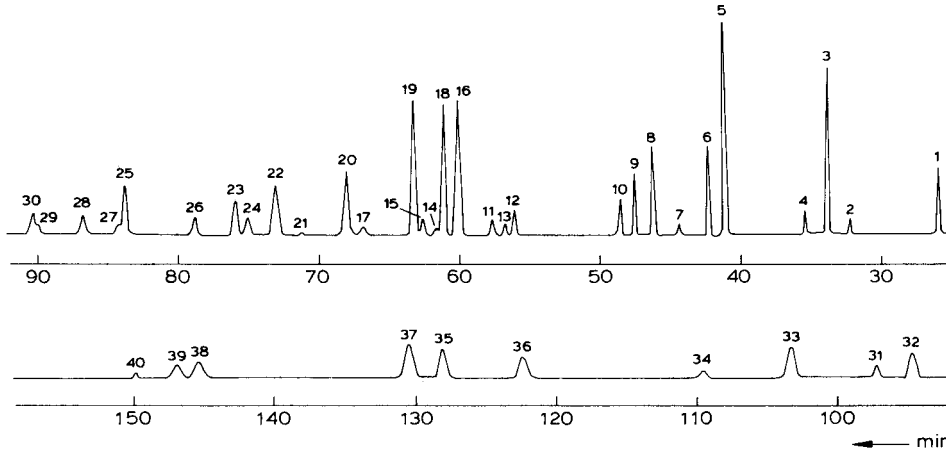

Fig. 5. Separation of Aroclor 1242 at the optimal temperature (170°C) and optimal column polarity (40.0 m Carbowax 20M capillary column connected to a 75.6 m Apiezon L glass capillary column).

Table II lists the retention indices calculated and ordered by the program, corresponding to the components of the PCB mixture under the optimal conditions. The difference between the retention indices corresponding to peaks 29 and 30 is 0.94 (Table II), which is less than the threshold (1.34), so that this pair of peaks is considered to be unresolved, which is in agreement with the poor resolution of these peaks on the chromatogram shown in Fig. 5: calculated $R_{ij} = 0.35$; from the chromatogram it seems that R_{ij}, which is closer to 0.5, may be slightly larger, as can be expected from the use of an almost twice as long column and a value of N_j probably close to 200,000 (Table II). We also observe in Fig. 5 the poor separations of peaks 25 and 27 ($\delta_i = 1.44$, $R_{ij} = 0.54$) and of peaks 18 and 14 ($\delta_i = 1.48$, $R_{ij} = 0.55$). The separation of these last two pairs is further complicated by the different concentration of the two compounds.

The optimization criterion introduced in this paper unambiguously prefers conditions at which the maximal number of peaks is resolved. This is ensured by a sufficiently large contribution to the value of the optimization criterion for each unresolved pair (-10) which, in the separation of PCBs, was considerably greater than the secondary part of the criterion: in the example discussed, OPTTOT* = $1 \cdot (-10) + (1.44 - 1.34)/1.34 = -10 + 0.07 = -9.93$. Some difficulty can arise when the contribution of the secondary part is too big [*i.e.*, if $(\delta_i - \delta)/\delta > 10$]; in such a case, however, the optimization problem would simply become optimization of a binary separation.

Finally, if the data are extrapolated to a lower temperature, we find that at 163°C the difference in retention indices for peaks 29 and 30 increases from 0.94 to 1.19, but this marginal improvement in separation is obtained at the cost of an increase in analysis time from 2.5 to almost 4 h.

LIST OF SYMBOLS

A, B, C, D	Coefficients in eqn. 7
I_i	Retention index of compound i (eqn. 3)
k'_j	Column capacity factor for compound j (eqn. 1)
L	Column length (eqn. 7)
N_i	Number of effective theoretical plates for compound i (eqn. 2)
n_j	Number of theoretical plates for compounds j (eqn. 1)
R_{ij}	Resolution between the peaks of compounds i and j (eqn. 1)
$t'_{R,i}$	Adjusted retention time of compound i (eqn. 3)
T	Temperature (eqn. 7)
z	Number of carbon atoms in a normal alkane (eqn. 3)
α_{ij}	Relative retention of compounds i and j (eqn. 1)
ΔI_{ij}	Difference between retention indices of compounds i and j (eqn. 4)
δ	Retention index difference threshold

ACKNOWLEDGEMENT

One of us (J.K.) thanks the Foundation SEA for a research fellowship.

REFERENCES

1 S. L. Morgan and S. N. Deming, *J. Chromatogr.*, 112 (1975) 267.
2 R. J. Laub, J. H. Purnell and P. S. Williams, *J. Chromatogr.*, 134 (1977) 249.
3 J. Krupčík, G. Guiochon and J. M. Schmitter, *J. Chromatogr.*, 213 (1981) 189.
4 J. Krupčík, M. Kristín, M. Valachovičová and Š. Janiga, *J. Chromatogr.*, 126 (1976) 147.
5 G. Schomburg, H. Husmann and F. Weeke, *J. Chromatogr.*, 99 (1974) 63.
6 E. W. Cieplinski, L. S. Ettre, B. Kolb and G. Kemmer, *Z. Anal. Chem.*, 205 (1964) 357.
7 J. Mocák, *Computer program OPTIM2*; a listing is available on request.
8 G. Schomburg, R. Dielmann, H. Borwitzky and H. Husmann, *J. Chromatogr.*, 167 (1978) 337.
9 L. Soják, J. Krupčík and L. Janák, *J. Chromatogr.*, in press.
10 J. H. Purnell, *J. Chem. Soc.*, (1960) 1268.
11 E. sz. Kováts, *Advan. Chromatogr.*, 1 (1965) 229.

Journal of Chromatography, 238 (1982) 13–28
Elsevier Scientific Publishing Company, Amsterdam — Printed in The Netherlands

CHROM. 14,609

DETERMINATION OF MACROPORE DIFFUSION IN MOLECULAR SIEVE PARTICLES BY PULSE GAS CHROMATOGRAPHY

A. BAIKER* and M. NEW
Swiss Federal Institute of Technology (ETH), Department of Industrial and Engineering Chemistry, CH-8092 Zurich (Switzerland)
(Received October 20th, 1981)

SUMMARY

The experimental conditions necessary for reliable determination of the intraparticle diffusivity of gases in porous solids by pulse gas chromatography (PGC) are investigated. Diffusivity measurements carried out with non-adsorbable tracer gases in packings of molecular sieve particles of different sizes indicate that the experimentally observed contributions of external mass transfer and intraparticle diffusion resistance may not depend on the particle size as theory predicts. With decreasing particle diameter the external mass transfer resistance becomes increasingly dominant as compared to intraparticle diffusion resistances. This finding follows from comparative experiments with packings of non-porous glass beads and porous molecular sieve particles of equal size. The sensitivity of the mass transfer rate parameter determination is markedly improved by using an experimental arrangement with a column to particle diameter ratio which corresponds to a "single pellet string reactor" (S.P.S.R.). The reliability of the determination of the intraparticle diffusivity with an S.P.S.R. has been checked by independent diffusivity measurements carried out on pressed single pellets of the molecular sieve. Steady-state counter-diffusion and dynamic pulse response measurements yielded an effective diffusivity comparable to that determined with the PGC method using an S.P.S.R. arrangement.

INTRODUCTION

In the last decade, pulse gas chromatography (PGC) has gained acceptance as a rapid and versatile technique for the determination of the effective intraparticle diffusivity of gases in porous solids, *e.g.*, adsorbents and catalysts[1–6]. The reliability of the PGC technique for the determination of intraparticle diffusivity is strongly dependent on the experimental conditions under which the measurements are carried out[7,8]. The main objective of the present work is therefore to study the suitability of different experimental conditions for the determination of intraparticle diffusivity with the PGC technique and to check the diffusivity results obtained with independent measurements on single pellets in a diffusion cell.

0021-9673/82/0000–0000/$02.75

THEORY

The theory most often applied in recent years to the estimation of intraparticle diffusivity is generally referred to as the Kubin–Kucera model after the authors of the original papers[9–11] published in 1965. Initially, the model was applied to describe the dispersion of an adsorbable tracer gas pulse in a packed bed of porous adsorbent through which an inert gas is flowing. Later it was shown that the theory can also be applied if a non-adsorbable tracer is used. In this theory the moments of the chromatographic peak leaving the bed are related to the parameters describing the mass transfer process. An analytical solution of the Kubin–Kucera model is not possible in the time domain; however, solutions can be given in the Laplace or Fourier domains[12]. Moment expressions can be derived from these solutions in terms of various model parameters.

For a Dirac delta-input signal of a non-adsorbable tracer one obtains the following results for the first absolute, μ_1, and second central moments, μ_2' (ref. 1)

$$\mu_1 = (z/u)\,(1 + \delta_0) \tag{1}$$

$$\mu_2' = 2\,(z/u)\left[\delta_1 + (E_A/\alpha)\,(1 + \delta_0)^2 \cdot \frac{1}{u^2}\right] \tag{2}$$

where:

$$\delta_0 = \frac{1 - \alpha}{\alpha} \cdot \varepsilon \tag{3}$$

$$\delta_1 = \delta_e + \delta_i \tag{4}$$

The contribution of δ_1 to the second moment function (eqn. 2) is the sum of the external mass transfer, δ_e, and the intraparticle diffusion contribution, δ_i, which have different dependences on the average particle radius, R, of the packing:

$$\delta_e = \left(\frac{1 - \alpha}{\alpha} \cdot \varepsilon\right)\left(\frac{R^2\varepsilon}{15}\right) \cdot \frac{5}{k_f R} \tag{5}$$

$$\delta_i = \left(\frac{1 - \alpha}{\alpha} \cdot \varepsilon\right)\left(\frac{R^2\varepsilon}{15}\right) \cdot \frac{1}{D_e} \tag{6}$$

The first absolute and second central moments of the tracer concentration curve $c(z,t)$ are defined as

$$\mu_1 = m_1/m_0 \tag{7}$$

$$\mu_2' = \frac{1}{m_0} \int_0^\infty (t - \mu_1)^2\, c(z,t)\mathrm{d}t \tag{8}$$

where the integrals m_0 and m_1 are given by:

$$m_n = \int_0^{\infty} t^n c(z,t)\mathrm{d}t \qquad \text{for } n = 0, 1 \tag{9}$$

Eqn. 1 contains the bed length, z, the interstitial gas velocity, u, the particle porosity, ε, and the column void fraction, α, all of which can be measured independently of the chromatographic technique. This is not the case with the parameters determining the second moment given in eqn. 2. The axial dispersion, E_A, may be obtained from the slope of a plot of μ_2' against $1/u^2$; however, the extraction of the effective intraparticle diffusivity, D_e, and of the fluid-particle mass transfer coefficient, k_f, from the intercept of this plot is difficult. Theoretically, it is possible to derive expressions for the third and higher moments in terms of these parameters. However, in practice, only zero, first and second moments are useful since higher moments can rarely be determined with appropriate accuracy from experimental response curves. An approach to avoid the application of higher moments is to calculate k_f from other approximate relations. Different expressions have been suggested[13–16] for the estimation of the fluid-particle mass transfer coefficient.

EXPERIMENTAL

Apparatus and procedure

The experimental arrangement employed is shown schematically in Fig. 1. It basically consists of three parts, the gas supply and control part, the test section (gas chromatographic column) and the data collection system.

The purity of the gases used in the experiments (He,Ar,N_2) was better than

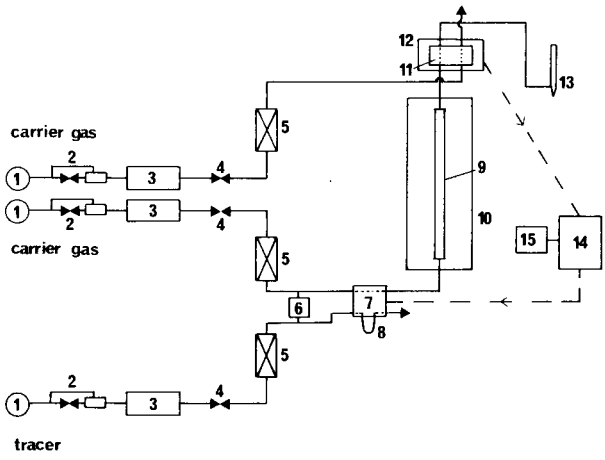

Fig. 1. Experimental arrangement used for pulse gas chromatography measurements. 1 = Gas cylinder; 2 = pressure controller; 3 = molecular sieve packing; 4 = low flow valve; 5 = flow meter; 6 = precision pressure gauge; 7 = tracer injection valve; 8 = sample loop; 9 = gas chromatographic column or single pellet string arrangement; 10 = temperature-controlled oven; 11 = hot-wire detector; 12 = detector heating block; 13 = soap bubble flow meter; 14 = PDP 11/10 process computer; 15 = x,y recorder.

99.99%, as quoted by the manufacturers. All gases were taken from commercial steel cylinders and dried before use by passing them through a packed bed of activated molecular sieve (Linde, 5A). The carrier gas flow-rates were controlled by a Dual GC Mass Flow Controller (Brooks Inst. Div., Model 5840). The tracer gas pulses were introduced by a COV Series eight-ports gas changeover valve (Mechanism Ltd.) equipped with two 0.15-cm^3 sampling loops. Pulses of pure gases were fed to the column inlet after it had been confirmed by varying the pulse inlet concentration that non-linearities due to concentration effects did not effect the experimental moment results.

The column (test section) was mounted in a gas chromatograph oven where the temperature could be held constant to within ± 1°K. Column lengths were determined before the tube was coiled and, from residence time measurements in the void column, the inner diameter of the tubing was determined to be 5.8 mm. The pressure drop in the column was measured by means of a high precision pressure difference gauge (Revue Thommen, Type 19 A2) and was at most 8% of the inlet pressure at the highest gas velocities reported.

The connection between the sample valve and the column as well as between the column end and the detector was of stainless-steel tubing (2 mm O.D.). To keep extra-column dispersion to a minimum, the length of all pulse-carrying tubing was kept as small as possible. By short-circuiting the column the system dead volume (including the sampling loop volume) was determined (1.07 cm^3) and all first moment results reported below were corrected for holding times in the connecting lines. Contributions of the system dead volume and the constriction at the column outlet to the experimental second moments were ignored since they never exceeded 2%.

The detector was a Gow Mac Model 69-552. A bridge current of 140 mA was set and the detector bridge element was run at 420°K. The bridge element was controlled by means of a control unit (Carlo Erba, Model 230). The linearity of the detector response was periodically checked by means of an exponential dilution flask (Carlo Erba). Experimental tracer gas concentration functions were recorded with a PDP 11/10 process computer. The analogue detector control unit signal ranging between 0 and 10 V was divided down into equisized digitized levels between 0 and 4096. The response time, typically between 10 and 500 sec, was recorded at 2000 equally spaced but variable units of time.

Material

Commercially available molecular sieve particles were employed for the measurements (Chemische Fabrik Uetikon, Type IG2-4Å). The physical properties of the porous particles were: surface area (BET), 12 m^2/g; void fraction, $\varepsilon = 0.305$; void volume, $V_t = 0.252$ cm^3/g; apparent density, $\sigma_a = 1.30$ g/cm^3; solid density, $\sigma_s = 1.87$ g/cm^3. The solid density was measured in a helium pycnometer, and the apparent density by mercury displacement. The differential macropore size distribution measured with the mercury intrusion method is presented in Fig. 2. Before being packed into the column, the molecular sieve particles were kept in a vacuum-drying oven at 420°K and *ca.* 7 kPa for about 12 h. Prior to experimental runs the packed column was left overnight in the gas chromatograph oven at 420°K with inert carrier gas flowing. The packing porosity, α, of the column was calculated from the apparent density of the particles and the bed bulk density.

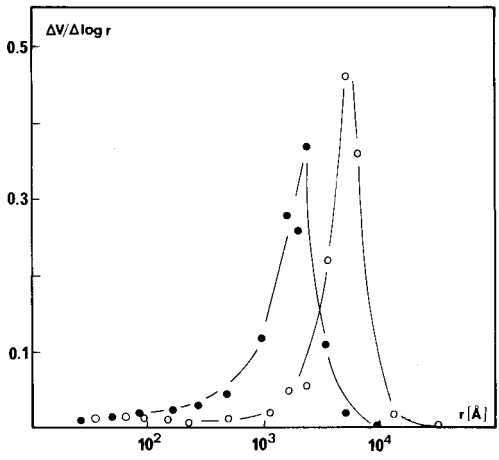

Fig. 2. Differential macropore size distribution of commercial (●) and pressed (○) molecular sieve pellets.

RESULTS

Measurements with different ratios of column to particle diameter

First the influence of the ratio of column to particle diameter on the determination of the mass transfer parameters was investigated. Experiments were carried out with four packings of different ratios of column to particle diameter (d_c/d_p). The properties of the column packings of length 40 cm are given in Table I. Packings I and II consisted of well defined spherical particles as supplied by the manufacturer, whereas packings III and IV comprised crushed material of a less well defined shape. Pulse response experiments were carried out at $T_1 = 313°K$ and $T_2 = 375°K$ under a pressure of 100 kPa. Nitrogen was the carrier and argon the tracer gas. The interstitial carrier gas velocity range investigated with the four packings was 0.3–2 cm/sec. Fig. 3 shows a linearized plot of the experimentally observed dependence of first moments on the carrier gas flow-rate, F, for experiments carried out with packing IV. The plotted carrier gas flow-rates were measured at room temperature at the detector outlet. To calculate the interstitial gas velocity, u, under the experimental conditions this value was corrected for the effective column temperature assuming ideal gas behaviour. After this correction, identical slopes were obtained within the experimental error for the relation μ_1 *vs.* $1/u$ for both temperatures and for the four different column packings. This result indicates that no marked adsorption was occurring in the system.

TABLE I

PROPERTIES OF MOLECULAR SIEVE PACKINGS EMPLOYED

Packing	*Mesh size (μm)*	α	d_c/d_p
I	1870–2000	0.472	2.99
II	1000–1070	0.332	5.60
III	400– 430	0.404	13.97
IV	150– 200	0.412	33.14

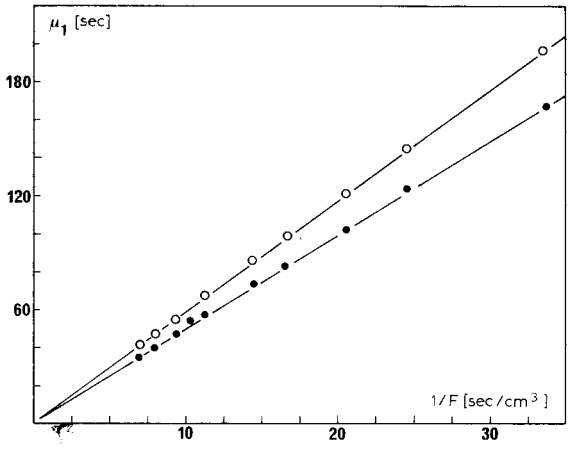

Fig. 3. Experimentally observed dependence of first moments, μ_1, on the carrier gas flow-rate, F, for packing IV at 313 (○) and 375°K (●).

From the experimental first moments, intraparticle porosities were calculated applying eqns. 1 and 3. At $T_1 = 313$ K the results for the four packings yielded a mean value of $\varepsilon = 0.333$ and a 95% confidence interval of $0.286 < \varepsilon < 0.380$. The evaluation at $T_2 = 375$°K gave a mean value of $\varepsilon = 0.302$ and a 95% confidence interval of $0.248 < \varepsilon < 0.355$. These values are in good agreement with the values obtained from other determination methods, namely $\varepsilon = 0.305$ from pycnometry and $\varepsilon = 0.289$ from the relationship $\varepsilon = V_t\sigma_a$, with the total macropore volume V_t measured by mercury porosimetry.

Fig. 4 presents a linearized plot of the experimental second moments as a function of interstitial gas velocity. During the runs the interstitial carrier gas velocity was varied between 0.3 and 2.0 cm/sec. Within this interval eqn. 10

$$\mu_2'/(2z/u) = \delta_1 + (E_A/\alpha)(1 + \delta_0)^2 \cdot \frac{1}{u^2} \tag{10}$$

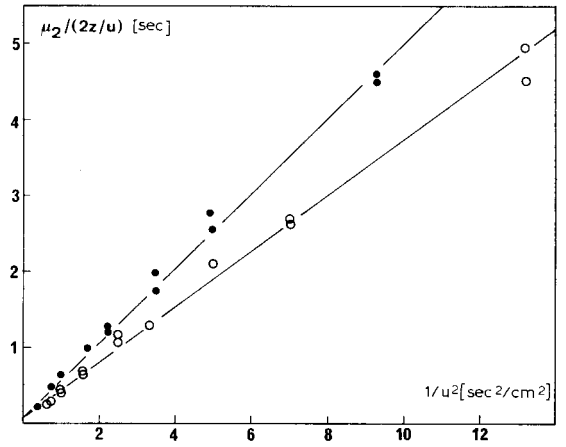

Fig. 4. Dependence of second moments on the interstitial carrier gas velocity, u, for packing IV at 313 (○) and 375°K (●).

TABLE II

AXIAL DISPERSION COEFFICIENTS AND RECIPROCAL TORTUOSITIES OF THE DIFFERENT MOLECULAR SIEVE PACKINGS (*Cf.*, TABLE I)

Packing	$T_1 = 313$ *K*		$T_2 = 375$ *K*	
	E_A *(cm²/sec)*	η	E_A *(cm²/sec)*	η
I	0.094	0.95	0.127	0.93
II	0.085	1.22	0.124	1.29
III	0.073	0.85	0.095	0.81
IV	0.069	0.79	0.096	0.80

(which is equivalent to eqn. 2) was accurate enough to account for the experimental observations. This was concluded from a statistical test for lack of fit which comprised the comparison of the residual sum of squares of the mathematical model with the experimental error. Applying eqn. 2, the axial dispersion coefficients given in Table II were calculated. The corresponding reciprocal packing tortuosity factors, η, calculated with eqn. 11

$$\eta = E_A/D_{AB}\alpha \tag{11}$$

are also listed in Table II. The molecular diffusion coefficients, D_{AB}, required for the calculation of η were obtained by the Chapman–Enskog relation[17]. The relatively large value of η obtained for packing II can be ascribed to packing inhomogeneities as is indicated by the low interparticle porosity, α, measured for this packing (*cf.*, Table I). The temperature dependence of the axial dispersion coefficients, E_A, presented in Table II is well described by a proportionality of $T^{1.7}$ and indicates that the dispersion mechanism is close to a molecular one. A linear regression analysis employing eqn. 2 yielded the following values for the axial intercepts δ_1 for the four packings at $T = 313$ K (values in parentheses are 95% confidence limits): packing I, $\delta_1 = 0.146$ (0.09–0.20); packing II, $\delta_1 = 0.049$ (0.01–0.08); packing III, $\delta_1 = 0.048$ (−0.03–0.13); packing IV, $\delta_1 = 0.119$ (0.03–0.21). The determined axial intercepts, δ_1, do not depend on particle size as the theory predicts. Thus, the investigated experimental conditions (Reynolds number range, $N_{Re} = 2uR/\nu \leqslant 3$; column to particle diameter ratio range, $3 < d_p/d_c < 33$) are not suitable for a reliable determination of the effective intraparticle diffusion coefficient.

Comparison of measurements in columns with porous and non-porous packing materials of similar mean particle sizes

In order to find the reason for the behaviour observed with the packings of different particle sizes and to obtain some idea about the sensitivity of the PGC method for the determination of the intraparticle diffusivity, comparative measurements were carried out with packings of molecular sieve particles and non-porous glass beads of similar mesh sizes. Experiments were run at 313°K with four different carrier/tracer gas pairs in the carrier gas velocity range from 0.7 to 10 cm/sec. In the subsequent notation, He/Ar means that He was the carrier and Ar the tracer gas. The axial dispersion coefficients, E_A, for the porous and non-porous packings were de-

TABLE III

AXIAL DISPERSION COEFFICIENTS AND RECIPROCAL TORTUOSITIES OBTAINED WITH NON-POROUS AND POROUS PARTICLE PACKINGS

	Mesh size 400–430 μm				*Mesh size 1000–1070 μm*			
Gas pair	*Glass bead packing (α = 0.385)*		*Molecular sieve packing (α = 0.458)*		*Glass bead packing (α = 0.413)*		*Molecular sieve packing (α = 0.376)*	
	E_A *(cm²/sec)*	η	E_A *(cm²/sec)*	η	E_A *(cm²/sec)*	η	E_A *(cm²/sec)*	η
N_2/He	0.176	0.59	0.226	0.64	0.205	0.64	0.361	1.23
N_2/Ar	0.037	0.46	0.053	0.55	0.047	0.54	0.057	0.72
He/Ar	0.192	0.61	0.215	0.58	0.224	0.66	0.259	0.84
He/N_2	0.197	0.66	0.215	0.61	0.221	0.69	0.258	0.89

termined by a linear regression analysis with eqn. 2. The values obtained are summarized in Table III together with the reciprocal tortuosity factors calculated with eqn. 11. With all of the four gas pairs used the larger porous particle packing displays a higher dispersion than the corresponding non-porous packing. The comparison with the dispersion behaviour of the glass bead packings of different mesh sizes shows that the different dispersion behaviour of the two molecular sieve fractions cannot be exclusively due to the influence of the ratio of column to particle diameter. It seems that intraparticle diffusion is contributing to axial dispersion in the larger molecular sieve particle packing. The evaluation of molecular sieve intraparticle porosity from experimental runs with the packing of mesh size 1000–1070 μm yielded the following ε values with the different gas pairs employed: N_2/He, 0.395; N_2/Ar, 0.313; He/Ar, 0.338; He/N_2, 0.347. The ε values obtained with argon as tracer gas gave a slightly larger porosity if He was the carrier gas instead of N_2. On the other hand the largest porosity is obtained when He is the tracer gas. Helium is capable of penetrating into the cavities of the molecular sieve, whereas the accessibility for N_2 (critical diameter 3 Å) and in particular Ar (critical diameter 3.84 Å) is strongly limited. The different accessibility affects the concentration distribution and the dispersion behaviour. The axial dispersion behaviour of the packing with the smaller molecular sieve particles is very similar to the one consisting of equally sized non-porous glass beads. For the latter there is no intraparticle diffusion contribution to the axial dispersion and, consistently, the intraparticle porosity, ε, from first moment results with He as tracer gas, does not exceed those obtained with Ar and N_2: N_2/He, $\varepsilon = 0.344$; N_2/Ar, $\varepsilon = 0.265$; He/Ar, $\varepsilon = 0.337$; He/N_2, $\varepsilon = 0.343$.

A more detailed analysis of the regression results obtained with eqn. 2 indicated that the assumption of a constant axial dispersion coefficient was valid only in the lower carrier gas velocity range investigated. This behaviour is illustrated in Fig. 5 which shows the deviation of the experimental and calculated second moment results, $[\mu_2'/(2z/u)_{\text{expt}} - \mu_2'/(2z/u)_{\text{calc}}]$, as a function of the carrier gas velocity for the experiments conducted with the molecular sieve packing of mesh size 1000–1070 μm. A similar tendency was also observed for the other experiments carried out at carrier gas velocities up to 10 cm/sec. The introduction of a velocity-dependent axial dispersion coefficient according to eqn. 13 into eqn. 2 did not improve the quality of the fitting of the experimental results in the higher carrier gas velocity range as a comparison of the

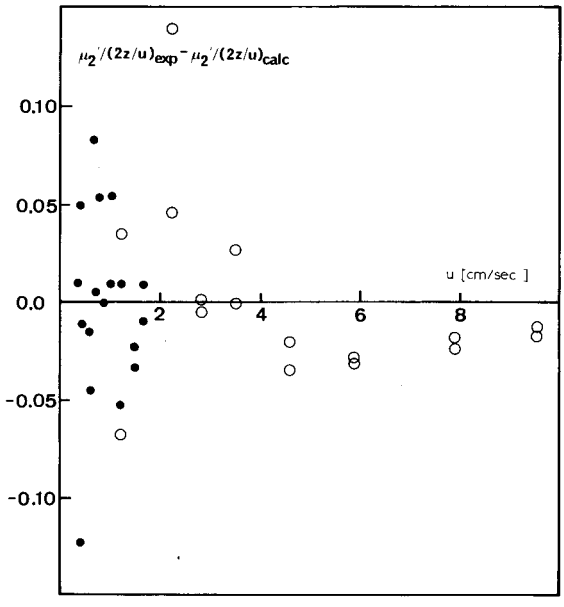

Fig. 5. Deviation between experimentally determined second moments and second moments calculated with eqn. 10 as a function of the interstitial carrier gas velocity, u, for the molecular sieve packing of mesh size 1000–1070 μm. ●, N_2/Ar, $0.3 < u < 2.0$ cm/sec; ○, N_2/Ar, $0.7 < u < 10.0$ cm/sec.

residual sum of squares obtained for both models indicated. Consequently no statistically significant axial intercept, δ_1, could be extracted for carrier gas velocities up to 10 cm/sec.

A definite conclusion concerning the influence of the intraparticle diffusion resistance on the tracer elution curve comes from a time domain regression analysis. Haynes[8] has derived eqn. 12 for the dispersion of a tracer pulse in a non-porous particle packing

$$E^* = \frac{1}{2}\left(\frac{\alpha N_1}{\pi t^{*3}}\right)^{0.5} \exp\left[-\frac{(t^* - \alpha)^2 N_1}{4\alpha t^*}\right] \tag{12}$$

where $t^* = tv/z$, $v = u\alpha$ and $N_1 = vz/E_A$; E^* is the dimensionless residence time distribution function, v the empty column-based carrier gas velocity, z the packing length, N_1 the axial Péclet number computed with the packing length and t the time. Haynes[8] showed that for $N_1 > 100$ one observes a Gaussian distribution for the tracer elution curve in non-porous packings. Furthermore, he pointed out that porous and non-porous particle packings display an identical dispersion behaviour if the diffusion is rapid in both pore systems. For packings of porous particles one has to take into account both the interparticle and the intraparticle porosity in computing t^*. Eqn. 12 was applied to the experimental results obtained at 313°K for both the porous and the non-porous particle packings of mesh size 1000–1070 μm with the gas pair He/Ar. The parameters v/z and N_1 were determined by a non-linear regression analysis. Eqn. 12 fitted the results of both packing types equally well. By comparing

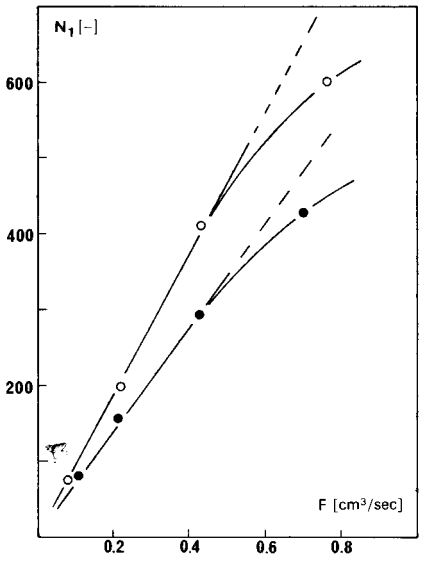

Fig. 6. Dependence of axial Péclet number, N_1, on carrier gas flow-rate, F, for glass bead packing (○) and molecular sieve packing (●) of mesh size 1000–1070 μm.

the values of v/z for the porous and non-porous packings, an intraparticle porosity of $\varepsilon = 0.314$ is estimated for the molecular sieve particles. This value agrees favourably with the value of 0.338 obtained from the first moment analysis.

Fig. 6 presents the dependence of the axial Péclet number on the carrier gas flow-rate for both packing types of mesh size 1000–1070 μm. For both the porous and the non-porous packing one obtains, in the lower flow-rate range ($F < 0.4$ cm^3/sec), a linear relationship between the axial Péclet number and the carrier gas flow-rate. At higher carrier gas flow-rates the curves for both packing types depart from linearity, indicating a velocity-dependent axial dispersion coefficient. It is also seen that the porous molecular sieve particle packing displays a larger axial dispersion coefficient.

Edwards and Richardson[18] studied the gas dispersion in packed beds of non-porous particles over a wide range of particle sizes and Reynolds numbers. They correlated the observed axial dispersion coefficient with the normal gas diffusion coefficient and a velocity-dependent term according to eqn. 13:

$$E_A = 0.73\, D_{AB} + \frac{uR}{1 + \dfrac{9.7\, D_{AB}}{2uR}} \tag{13}$$

Employing eqn. 13 one can estimate a critical carrier gas flow-rate of about 0.4 cm^3/sec for which the eddy diffusion contribution to the axial dispersion is less than 1 %. This finding is in accordance with the results shown in Fig. 6 which indicate a velocity dependence of the axial dispersion at flow-rates larger than about 0.4 cm^3/sec. Table IV shows a comparison of the experimentally determined and calculated second moments for both packing types. The second moments were calculated from the determined axial Péclet numbers with the assumption of a Gaussian distri-

TABLE IV

COMPARISON OF EXPERIMENTAL AND CALCULATED SECOND MOMENTS OBTAINED FOR NON-POROUS AND POROUS PACKINGS OF MESH SIZE 1000–1070 μm

Glass bead packing			*Molecular sieve packing*		
F (cm^3/sec)	$\mu'_{2,calc}$ (sec^2)	$\mu'_{2,exptl}$ (sec^2)	F (cm^3/sec)	$\mu'_{2,calc}$ (sec^2)	$\mu'_{2,exptl}$ (sec^2)
0.08	97.4	97.07	0.11	91.69	95.15
0.22	5.48	5.46	0.21	13.16	13.93
0.43	0.67	0.65	0.42	1.78	1.71
0.76	0.16	0.14	0.69	0.45	0.42

bution for the tracer concentration at the column end. The results listed in Table IV confirm that eqn. 12 describes the concentration distribution at the exit of both packed beds fairly well.

A comparison of the experimental runs with the porous molecular sieve particles and the non-porous glass beads indicates that under the given experimental conditions the intraparticle diffusion resistance in the molecular sieve particles could not be isolated in a significant way from axial dispersion influences. In order to investigate the influence of external mass transfer limitations on the determination of the effective intraparticle diffusivity, D_e, molecular sieve particles were used in an experimental set up corresponding closely to the single pellet string reactor (S.P.S.R.)[19]. With the S.P.S.R. external mass transfer influences should not play a major part since higher Reynolds numbers can be achieved in this arrangement. In addition, different correlations[13–16] are available from the literature to estimate the fluid-particle mass transfer coefficients in the Reynolds number range $N_{Re} > 3$. The experimental conditions and results of the S.P.S.R. runs are summarized in Table V. An estimation of the contribution of external mass transfer with the correlations given in ref. 13 indicated that the contribution of δ_e to δ_1 was less than 5% for the S.P.S.R. runs reported. Thus, the intraparticle diffusivity, D_e, was calculated employing eqn. 4 with $\delta_i = \delta_1$. On the basis of this D_e value which has to be considered as a physical property of the molecular sieve, an expected contribution, $\delta_{i,PS}$, of the intraparticle

TABLE V

EXPERIMENTAL CONDITIONS AND RESULTS OF THE "SINGLE PELLET STRING REACTOR" (S.P.S.R.) RUNS

Experimental conditions	*Results*
Carrier gas, He; tracer gas, Ar	$E_A = 0.365$ cm²/sec
Carrier gas velocity, u 2.5–9.0 cm/sec	$\eta = 0.785$
Reynolds number range, N_{Re} = 3–10	$D_e = 0.018$ cm²/sec
($N_{Re} = 2Ru/\nu$)	(0.012–0.024)
Pressure 1 bar	
Packing length 40 cm	
d_c/d_p 1.97	
Mean particle size 0.294 cm	
Particle shape spherical	

TABLE VI

EXPECTED CONTRIBUTION, $\delta_{i,PS}$ OF INTRAPARTICLE DIFFUSION RESISTANCE TO THE INTERCEPT, δ_1, FOR MOLECULAR SIEVE PACKINGS

Packing mesh size (μm)	$\delta_{i,PS} \times 10^3$ *(sec)*	$\delta_{1,exptl}$ *(sec)*	*95% confidence interval for* δ_1
1870–2000	4.87	0.146	0.09–0.20
1000–1070	2.51	0.049	0.01–0.08
400– 430	0.29	0.048	−0.03–0.13
150– 200	0.05	0.119	0.03–0.21

diffusion resistance could be calculated for the four packings of mesh sizes between 150 and 2000 μm, using eqn. 6. The results of these calculations are given in Table VI, together with the experimental regression results and their 95% confidence limits.

With the exception of mesh size fraction 400–430 μm, the experimental intercepts, $\delta_{1,exptl}$, differed significantly from zero. The calculated contributions, $\delta_{i,PS}$, based on D_e from the S.P.S.R. runs, are not included in the 95% confidence intervals of $\delta_{1,exptl}$ for the remaining three packings. Since the carrier gas velocity range in these experiments corresponded to Reynolds numbers for which the usual relations for evaluating external mass transfer rate parameters are no longer valid, the Sherwood numbers, N_{Sh}, for external mass transfer

$$k_f = N_{Sh} D_{AB}/2R \tag{14}$$

were roughly estimated from the experimental results summarized in refs. 20 and 21. The estimated values for the Sherwood number are listed in Table VII together with the corresponding range of the Péclet number, N_{Pe}, defined as:

$$N_{Pe} = 2uR/D_{AB} \tag{15}$$

From the estimated Sherwood numbers the external mass transfer resistances, δ_e, were calculated employing eqns. 5 and 14. The rough estimation of the Sherwood numbers led to δ_e values which are more than an order of magnitude larger than the calculated $\delta_{i,PS}$ from Table VI. Furthermore, these δ_e values are well within the confi-

TABLE VII

ESTIMATES OF EXTERNAL MASS TRANSFER CONTRIBUTIONS TO THE INTERCEPT δ_1 FOR MOLECULAR SIEVE PACKINGS

Packing mesh size (μm)	*Péclet number,* N_{Pe}	*Sherwood number,* N_{Sh}	δ_e *(sec)*
1870–2000	0.5 –2.4	0.02	0.15
1000–1070	0.4 –2.0	0.01	0.08
400– 430	0.16–0.80	0.005	0.04
150– 200	0.07–0.33	0.001	0.03

dence intervals of the experimental $\delta_{1,\text{expti}}$ intercepts. This result supports the assumption that external mass transfer resistances were masking the intraparticle diffusion resistances in the molecular sieve particle packings of mesh size up to 2000 μm.

Determination of intraparticle diffusivity on single pellets in a diffusion cell

In order to obtain some information about the reliability of the intraparticle diffusion coefficient determined with the PGC method, comparative diffusivity measurements were conducted on single molecular sieve pellets employing the steady state counter-diffusion[22] and the dynamic pulse-response methods[23]. The single pellets were pressed from crushed molecular sieve particles of diameters less than 100 μm. The diffusion cell employed and the experimental procedure were the same as described elsewhere[24]. Three pressed pellets of different porosities, $\varepsilon = 0.435$, 0.356 and 0.325, were investigated. Fig. 2 presents the differential macropore size distributions of the commercial particles and of the pressed single pellet with $\varepsilon = 0.435$. The pore size distribution of the pressed pellet is shifted to larger pores; however, it shows the same characteristics as the one for the commercial particles.

Steady state counter-diffusion measurements were carried out with different counter-diffusing gas pairs. When using the gas pair A/B the concentration of gas B in the stream of gas A leaving the cell chamber was measured. The effective intraparticle diffusion coefficient, D_e, was computed from the measured diffusion flux N_A using eqn. 16

$$N_A = \frac{D_e P}{R_g T L \beta} \ln\left(\frac{1 - \beta y_{AL}}{1 - \beta y_{A0}}\right) \tag{16}$$

with

$$\beta = 1 + N_B/N_A = 1 - (M_A/M_B)^{0.5} \tag{17}$$

where P is the pressure, L the length of the cylindrical pellet, R_g the gas constant, y_{A0} and y_{AL} the mole fractions of A at the pellet ends and M_A, M_B the molecular weights of components A and B, respectively. The diffusivity results obtained with the steady-state counter-diffusion measurements are summarized in Table VIII. Employing eqn. 18

$$\bar{r} = \frac{1}{V_t} \int_0^{V_t} r \mathrm{d}V \tag{18}$$

on the measured pore size distribution shown in Fig. 2 one can calculate an average macropore radius, $\bar{r}$, of 1950 Å for the commercial particles and a value of 4200 Å for the pressed pellet with $\varepsilon = 0.435$.

In cylindrical pores of this radius a transition region diffusion mechanism is most probable under the conditions given. The transition region diffusion coefficients, D_c, were calculated with eqn. 19

$$1/D_c = 1/D_{KA} + 1/D_{AB} \tag{19}$$

TABLE VIII

DIFFUSIVITY RESULTS OBTAINED WITH STEADY STATE COUNTER-DIFFUSION AND DYNAMIC PULSE RESPONSE MEASUREMENTS ON SINGLE MOLECULAR SIEVE PELLETS

Conditions		*Diffusion coefficient (cm^2/sec)*	
Pellet	*Gas pair*	*Steady state counter-diffusion*	*Dynamic pulse response*
$\varepsilon = 0.435$	He/Ar	$D_{e,Ar} = 0.049$	$D_{e,Ar} = 0.054$ (0.036–0.073)
$\varepsilon = 0.435$	He/N_2	$D_{e,N_2} = 0.059$	$D_{e,N_2} = 0.057$ (0.046–0.068)
$\varepsilon = 0.435$	N_2/Ar	$D_{e,Ar} = 0.031$	
$\varepsilon = 0.356$	He/Ar	$D_{e,Ar} = 0.040$	$D_{e,Ar} = 0.040$ (0.034–0.046)
$\varepsilon = 0.356$	He/N_2	$D_{e,N_2} = 0.046$	$D_{e,N_2} = 0.046$ (0.038–0.053)
$\varepsilon = 0.325$	N_2/Ar	$D_{e,Ar} = 0.020$	

for the pressed pellet and the commercial IG2-4Å particles using a mean pore radius, $\bar{r}$, of 4200 Å and 1950 Å, respectively. The Knudsen diffusion coefficient D_{KA} in eqn. 19 is given by eqn. 20

$$D_{KA} = 9.7 \cdot 10^{-5}\, \bar{r}\, (T/M_A)^{0.5} \tag{20}$$

whereas the molecular diffusion coefficient is obtained from the Chapman–Enskog formula[17]. Employing eqn. 21

$$\psi = D_c \varepsilon / D_e \tag{21}$$

one obtains the following values for the tortuosity factors, ψ, depending on the gas pair: He/Ar, $\psi = 4.2$; He/N_2, $\psi = 3.7$; N_2/Ar, $\psi = 2.5$. The tortuosity factor, which should be a physical property of the porous material, depends on the employed gas pair. A similar trend is also observed when the "parallel path pore" model[25] is utilized to evaluate the tortuosity. The tortuosity factors obtained by employing this model are: He/Ar, $\psi = 4.7$; He/N_2, $\psi = 3.6$; N_2/Ar, $\psi = 2.1$. The smaller tortuosity factor resulting for the gas pair N_2/Ar as compared with He/Ar is consistent with the results obtained in the gas chromatographic column arrangement, where a larger intraparticle porosity was found with the gas pair He/Ar than with N_2/Ar. The steady state diffusion results with molecular sieve pellets of different porosities given in Table VIII indicate that the assumption of a constant, but gas pair-dependent tortuosity factor is reasonable in the investigated porosity range $0.325 < \varepsilon < 0.436$.

The pellets with porosities of $\varepsilon = 0.435$ and 0.356 were also investigated by the dynamic pulse response method described by Dogu and Smith[23]. For the first normalized moment, $\mu_{1,corr}$, of the pellet itself, *i.e.*, the net diffusion time without any dead volume contributions, these authors derived eqn. 22:

$$\mu_{1,corr} = \frac{L^2 \varepsilon}{6 D_e} \cdot \frac{(3QD_e/L + F_2)}{(QD_e/L + F_2)} \tag{22}$$

Here Q is the area of the end face of the pellet and F_2 the carrier gas flow-rate on the

pellet side which is connected to the detector. Eqn. 22 was applied to the experimentally determined first moments after these were corrected for dead volume contributions. The intraparticle diffusion coefficients, D_e, were obtained by a non-linear regression analysis of eqn. 22. The diffusivity results obtained at 313°K and 100 kPa are given in Table VIII together with their 95% confidence limits as obtained from the non-linear regression analysis. A comparison of these values with the diffusivities measured by the steady state method indicates that the dynamic results are not significantly different.

From the diffusion cell results obtained with He/Ar one can estimate an effective intraparticle diffusivity, $D_e = 0.022$, for the commercial molecular sieve particles. This value is calculated from eqn. 20 with the tortuosity factor $\psi = 4.2$ obtained for this gas pair and the structure parameters ($\varepsilon = 0.305$, $\bar{r} = 1950$ Å) measured for the commercial IG2-4Å pellets. It is comparable to the intraparticle diffusivity determined with the PGC method in the S.P.S.R. arrangement ($D_e = 0.018$; 95% confidence limits 0.012–0.024). These results confirm that the macropore diffusivity of molecular sieve particles can reliably be determined by the PGC method if an S.P.S.R. arrangement is employed and the tracer gas used has a critical diameter which excludes penetration into the micropores.

CONCLUSIONS

The present investigation has shown that for reliable determination of intraparticle diffusion coefficients by the pulse gas chromatographic method there are definite limits with respect to the ratio of column to particle size. The frequently postulated simplifying assumption of a negligible external mass transfer resistance becomes doubtful with decreasing particle size. In addition, the mass transfer resistance term, δ_1, in the Kubin–Kucera model tends to become very small with decreasing particle size, leading to values which are experimentally difficult to detect. Pulse gas chromatography measurements carried out in an experimental arrangement with a column to particle diameter ratio corresponding to a "single pellet string reactor" yielded an effective intraparticle diffusivity which is comparable to the values obtained by steady-state counter-diffusion and dynamic pulse response measurements on single pressed pellets in a diffusion cell.

ACKNOWLEDGEMENT

The Swiss National Science Foundation is acknowledged for financing this work.

REFERENCES

1 R. L. Cerro and J. M. Smith, *AIChE J.*, 16 (1970) 1035.
2 Yi Hua Ma and C. Mancel, *AIChE J.*, 18 (1972) 1149.
3 W. R. Mac Donald and H. W. Habgood, *Can. J. Chem. Eng.*, 50 (1972) 462.
4 H. W. Haynes, Jr. and P. N. Sharma, *AIChE J.*, 19 (1973) 1043.
5 N. Hashimoto and J. M. Smith, *Ind. Eng. Chem., Fundam.*, 13 (1974) 115.
6 P. N. Sharma and H. W. Haynes, Jr., *Advan. Chem. Ser.*, 133 (1974) 205.
7 S. K. Gangwal, R. R. Hudgins and P. L. Silveston, *Can. J. Chem. Eng.*, 56 (1978) 554.

8 H. W. Haynes, Jr., *Chem. Eng. Sci.*, 30 (1975) 955.
9 M. Kubin, *Collect. Czech. Chem. Commun.*, 30 (1965) 1104.
10 M. Kubin, *Collect. Czech. Chem. Commun.*, 30 (1965) 2900.
11 E. Kucera, *J. Chromatogr.*, 19 (1965) 237.
12 P. Schneider and J. M. Smith, *AIChE J.*, 14 (1968) 762.
13 N. Wakao and T. Funazkri, *Chem. Eng. Sci.*, 33 (1978) 1375.
14 L. J. Petrovic and G. Thodos, *Ind. Eng. Chem. Fundam.*, 7 (1968) 274.
15 W. E. Ranz and W. R. Marshall, *Chem. Eng. (Prague)*, 48 (1952) 173.
16 P. N. Dwivedi and S. N. Upadhyay, *Ind. Eng. Chem., Proc. Des.*, 16 (1977) 157.
17 J. O. Hirschfelder, C. F. Curtiss and R. B. Bird, *Molecular Theory of Gases and Liquids*, Wiley, New York, 1954.
18 M. F. Edwards and J. F. Richardson, *Chem. Eng. Sci.*, 24 (1969) 1741.
19 D. S. Scott, W. Lee and J. Pappa, *Chem. Eng. Sci.*, 29 (1974) 2155.
20 H. Martin, *Chem. Eng. Sci.*, 33 (1978) 913.
21 P. A. Nelson and T. R. Galloway, *Chem. Eng. Sci.*, 30 (1975) 1.
22 E. Wicke and R. Kallenbach, *Kolloid-Z.Z. Polym.*, 17 (1941) 135.
23 G. Dogu and J. M. Smith, *AIChE J.*, 21 (1975) 58.
24 M. New, A. Baiker and W. Richarz, *Chem.-Ing.-Tech.*, 51 (1979) 972.
25 M. F. L. Johnson and W. E. Steward, *J. Catal.*, 4 (1965) 248.

Journal of Chromatography, 238 (1982) 29–39
Elsevier Scientific Publishing Company, Amsterdam — Printed in The Netherlands

CHROM. 14,560

RESOLUTION OF α-METHYL-α-AMINO ACID DERIVATIVES BY GAS CHROMATOGRAPHY ON OPTICALLY ACTIVE DIAMIDE STATIONARY PHASES

SHU-CHENG CHANG*, R. CHARLES and E. GIL-AV*
Department of Organic Chemistry, The Weizmann Institute of Science, Rehovot (Israel)
(Received November 19th, 1981)

SUMMARY

The resolution of α-methyl-α-amino acids derivatized as either N-trifluoroacetyl (TFA) isopropyl esters or N-TFA-*tert.*-butylamides was investigated on chiral diamide stationary phases R′′′CONHCH(R′′)CONHR′, where R′′ = methyl, isobutyl, phenyl, benzyl. The alanine phase (I) is the only solvent which shows chiral recognition for a relatively wide range of the N-TFA isopropyl esters. On the other hand, the N-TFA-*tert.*-butylamides, including that of isovaline, are well resolved on all phases studied. In particular, the phenylalanine phase (IV) shows high resolution factors and is recommended for enantiomeric analysis of the α-methyl-α-amino acids via their N-TFA-*tert.*-butylamides. Similarities and differences between the behaviour of α-methyl and α-H-amino acid derivatives are discussed.

INTRODUCTION

In recent years more and more instances of the presence of α-methyl-α-amino acids in nature have been reported. In particular, α-aminoisobutyric acid and isovaline have been found in a series of lipophilic polypeptidic antibiotics[1–4], and α-methylserine has been identified in amecitin[5]. The replacement of the α-hydrogen in α-amino acids by a methyl group may significantly change various properties, such as hydrophobicity and reactivity towards chemical reagents and enzymes. These effects may evidently fulfill certain purposes in nature.

Investigation of the pharmacological properties of α-methyl-α-amino acids has resulted in the observation that these compounds can act as inhibitors of enzymes. For instance, α-methyl-L-tyrosine methyl ester[6] and α-methyl-3,4-dihydroxy-L-phenylalanine (α-methyl-L-DOPA)[7] inhibit the action of monoamino oxidase and aromatic amino acid decarboxylase, respectively. The introduction of L-DOPA as an antihypertensive drug[8] has resulted from this work.

Other areas in which α-methylamino acids have become important are research on the origin of life and the study of meteorites. In fact, these compounds are formed in experiments simulating primitive Earth conditions[9], and have further been identified in chondritic meteorites, *e.g.*, the Murchison meteorite[10].

* Present address: Chun Shan Institute of Science and Technology, P.O. Box 1–4, Lung-Tan, Taiwan.

0021-9673/82/0000–0000/$02.75

For the study of the above topics, a knowledge of the configuration and/or optical purity of the pertinent α-methyl-α-amino acids is often essential. The present research had as its objective the development of relevant, improved methods of analytical resolution by gas chromatography.

For the enantiomeric analysis of isovaline in meteorite extracts, some authors developed procedures of gas chromatographic resolution based on the use of diastereomers, such as N-pentafluoropropionyl esters of 2-*n*-pentyl[11], 2-*n*-hexyl[11] or 3-methyl-2-butyl alcohol[12], on symmetric stationary phases. Better results were obtained with N-trifluoroacetyl (TFA)-isovaline-L-leucine isopropyl ester on chiral N-docosanoyl-L-valine *tert.*-butylamide[13].

In our laboratory the separation of enantiomeric α-methyl-α-amino acid derivatives was studied. Several years ago, the resolution and the order of emergence of a series of α-methyl-α-amino acid esters on carbonylbis-(N-L-valine isopropyl ester) were reported[14]. Subsequently[15], it was found that the monoamide, N-lauroyl-(*S*)-α-(1-naphthyl)ethylamide, shows chiral recognition for certain of the α-methyl-α-amino acid esters resolved on the former phase (r = 1.008–1.026, at 100°C), but not for isovaline or α-methylleucine.

The present work is concerned with the behaviour of both N-TFA esters and N-TFA *tert.*-butylamides of α-methyl-α-amino acids on different diamide phases, of a type introduced previously[16–18]. The purpose of this research was both to improve the available procedures for analytical resolution, as well as to study the effect of the α-methyl group on chiral recognition by diamides.

MATERIALS

The racemic α-methyl derivatives of α-aminobutyric acid, valine, norvaline, leucine, norleucine and phenylalanine were synthesized in our laboratory[14,19] from the corresponding ketones[20] by reaction with ammonium carbonate and sodium cyanide, followed by hydrolysis of the hydantoins formed. α-Methylaspartic acid was a gift from Dr. P. E. Hare, Geophysical Laboratory, Carnegie Institution of Washington, Washington, DC, U.S.A.

Samples enriched in L-isovaline and D-α-methylvaline were also available in our laboratory[14,19] from the enzymatic hydrolysis[21] with Acylase I of the corresponding racemic N-TFA-α-methyl-α-amino acids.

For the preparation of the N-TFA isopropyl esters[14] and the N-TFA *tert.*-butylamides[22], previously described procedures[15,21,22] were used. It should, however, be mentioned that, since the α-methylamino acids are resistant to racemization, it is not necessary to maintain carefully the mild conditions recommended for derivatization of α-H-amino acids.

The phases examined were N-lauroyl *tert.*-butyl amide derivatives of L-alanine (I), L-leucine (II), D-phenylglycine (III) and L-phenylalanine (IV), the properties of which have been described previously[23], as well as the novel chiral solvent N-docosanoyl-L-leucine *tert.*-butylamide (V)[24].

Chromatographic conditions

The solvents were coated by the plug method on stainless-steel capillary columns [100 ft. × 0.02 in. I.D. (for I, II and V) or 150 ft. × 0.02 in. I.D. (for III and

IV)]. Chromatography was carried out with a helium flow of 3 ml/min and a flame-ionization detector. Temperatures employed are given in the tables and figures.

RESULTS AND DISCUSSION

Previously, we had attempted to separate enantiomeric N-TFA isopropyl esters of α-methyl-α-amino acids on several diamide phases derived from L-valine. However, only in one case, *viz.* on N-docosanoyl-L-valine-2-(2-methyl)heptadecylamide (VI)[25], success was achieved. Chiral recognition was, indeed, found, but was limited to the N-TFA isopropyl ester of α-methylvaline, and did not extend to either isovaline, or the α-methyl derivatives of norvaline, leucine and norleucine. On the other hand, on the polymeric phase Chirasil–Val, the N-TFA *n*-propyl ester of isovaline was well resolved[12].

These sporadic results prompted us to study the topic more systematically, and in this article we report the behaviour of the N-TFA isopropyl esters and the N-TFA *tert.*-butyl amides of α-methyl-α-amino acids on a number of diamide stationary phases derived from amino acids other than valine[23,24].

N-TFA isopropyl esters of α-methyl-α-amino acids

N-Lauroyl-α-amino acid *tert.*-butylamides with a relatively bulky R″ group, such as isobutyl (II), phenyl (III) and benzyl (IV), did not behave differently from the valine phase VI: only the α-methylvaline ester could be separated into its enantiomers

TABLE I

SEPARATION OF ENANTIOMERS OF N-TFA ISOPROPYL ESTERS OF α-METHYLAMINO ACIDS ON N-LAUROYL-L-ALANINE *tert.*-BUTYLAMIDE (I) AND N-DOCOSANOYL-L-LEUCINE *tert.*-BUTYLAMIDE (V)

For chromatographic conditions see Experimental section.

Phase		*T* (°C)	*Configuration*	*Amino acid N-TFA isopropyl ester*							
				α-*Me-valine*		α-*Me-norvaline*		α-*Me-leucine*		α-*Me-norleucine*	
				*r**	$r_{L/D}$**	*r**	$r_{L/D}$**	*r**	$r_{L/D}$**	*r**	$r_{L/D}$**
I	N-Lauroyl L-alanine *tert.*-butylamide	80	D	35.28	1.063	28.22	1.034	37.14	1.018	54.02	1.033
			L	37.66		29.40		37.82		55.78	
		90	D	22.54	1.052	18.86	1.021	24.00	1.014	33.96	1.030
			L	23.72		19.26		24.36		34.96	
		100	D	15.14	1.046	13.04	1.020	16.44	1.000	22.46	1.018
			L	15.84		13.30		16.44		22.86	
		120	D	7.64	1.026	4.64	1.000	8.24	1.000	11.16	1.000
			L	7.84		4.64		8.24		11.16	
V	N-Docosanoyl L-leucine *tert.*-butylamide	100	D	12.40	1.087	9.26	1.000				
			L	13.48		9.26					

* r = Corrected retention time (min)

** $r_{L/D}$ = Resolution factor = ratio of the corrected retention time of the enantiomer eluting last over that of the enantiomer eluting first, calculated with r values expressed to the second decimal place.

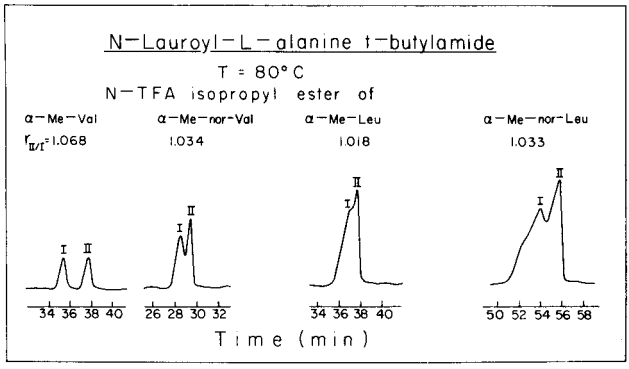

Fig. 1. Chromatogram of N-TFA isopropyl esters of some D,L-α-methylamino acids on phase I.

with resolution factors similar as on VI [r = 1.066 (IV), 1.056 (III) and 1.046 (II) at 130°C, while for VI at 80°C r = 1.086 had been reported[25]].

On the other hand, when the α-alkyl substituent of the solvent is methyl (phase derived from alanine, I), the range of chiral recognition is widened. As can be seen in Table I, all the amino acids listed were resolved at 90°C and below. However, when the temperature was raised to 120°C, only the enantiomers of α-methylvaline were separated. The chromatograms (at 80°C, Fig. I) show baseline separation for α-methylvaline, while for the other amino acids under the experimental conditions only partial peak resolution could be obtained. Another drawback of phase I is that no chiral recognition for the isovaline ester was found.

Attempts to separate the enantiomers of α-methylaspartic acid and of α-methylphenylalanine, as their N-TFA isopropyl esters, on phases I, II and IV were unsuccessful.

The order of emergence has not as yet been established experimentally. The result for the isovaline ester on Chirasil–Val, reported in the literature[12], indicates that the L-isomer in analogy should appear after the D-isomer, *i.e.* as in the corresponding α-H-α-amino acids.

N-TFA tert.-butylamides of α-methyl-α-amino acids

Recently, it was found that N-TFA *tert.*-butylamides[22] and N-TFA isopropylamides[26] of the α-H-α-amino acids are in certain cases more effectively resolved on diamide phases than the corresponding N-TFA isopropyl esters. Application of this approach to α-methyl-α-amino acids is described in the present section.

The chromatographic data listed in Table II (see also Figs. 2 and 3), show that this strategy was effective. In Table III, the resolution factors of the N-TFA isopropyl esters and the N-TFA *tert.*-butylamides on I are compared. When the difference in temperature is taken into account, it is apparent that chiral recognition for the diamide derivatives is definitely better. Also, α-methylphenylalanine, and even isovaline, were resolved on all the phases tried (Table II). However, in general, resolution factors, although sufficient for analytical purposes, remain markedly below those of the corresponding α-H-α-amino acid derivatives[22].

The close similarity of α-methyl- and α-H-α-amino acids permits the assumption that corresponding interactions with solvents are similar. Diastereomeric solute–

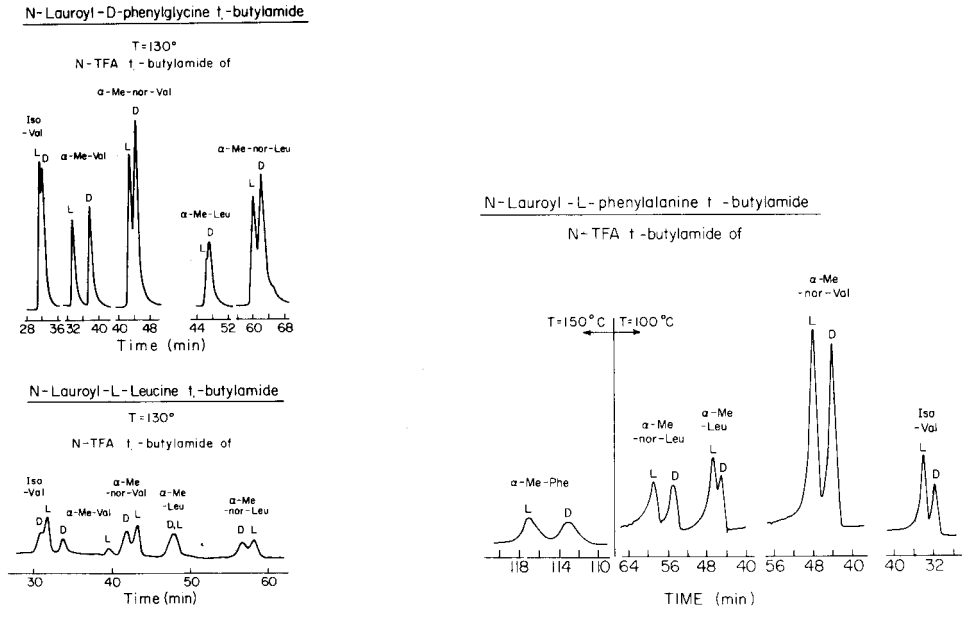

Fig. 2. Chromatogram of N-TFA *tert.*-butylamides of L-enriched isovaline, D-enriched α-Me-Val and D,L-α-Me-nor-Val, α-Me-leu and α-Me-nor-Leu, on phases II and III.

Fig. 3. Chromatogram of N-TFA *tert.*-butylamides of L-enriched isovaline and D,L-α-Me-nor-Val, α-Me-Leu, α-Me-Nor-Leu and α-Me-Phe, on phase IV.

solvent complexes, considered to be responsible for resolution, have been discussed previously[16–18,22–25]. Models of such associations involving, respectively, N-TFA esters and N-TFA *tert.*-butyl amides of α-methyl-α-amino acids, are represented in Fig. 4.

For steric reasons, it might be expected that the α-methyl group will weaken hydrogen bonding with the stationary phases. Indeed, considerably lower retention is found throguhout for the derivatives of the α-methyl- as compared with those of the α-H-α-amino acids. Thus, on phase I, the retention time of the N-TFA *tert.*-butylamide of D-valine was 75 min (140°C), as against 22 min (130°C) for the D-α-methylvaline (Table II), and that of the N-TFA isopropyl ester of D-leucine was 15.7 min (130°C), as against 8.24 min (120°C) for D-α-methylleucine (Table I). Looser association should result in a reduction of the concentration of the selective complexes formed in the stationary phase, as well as in larger distances between the associating molecules. Both of these circumstances will reduce the capacity for chiral recognition, in agreement with the findings for the two classes of derivatives investigated.

Chiral differentiation of the enantiomeric solutes in the stereoselective association complexes should be more difficult in the case of the α-methyl-α-amino acid derivatives, because they have a lesser degree of asymmetry, *i.e.*, a relatively smaller difference in the size of the substituent (R *vs.* methyl, as compared with R *vs.* H, for the α-H-α-amino acids). Isovaline, in which the alkyl substituents at the asymmetric carbon differ only by one methylene group, illustrates this effect particularly clearly,

TABLE II

SEPARATION OF ENANTIOMERS OF N-TFA *tert.*-BUTYLAMIDES OF α-METHYL-α-AMINO ACIDS ON N-LAUROYL-L-ALANINE *tert.*-BUTYLAMIDE (I), N-LAUROYL-L-LEUCINE *tert.*-BUTYLAMIDE (II), N-LAUROYL-D-PHENYLGLYCINE *tert.*-BUTYLAMIDE (III), N-LAUROYL-L-PHENYLALINE *tert.*-BUTYLAMIDE (IV) AND N-DOCOSANOYL-L-LEUCINE *tert.*-BUTYLAMIDE (V) AS STATIONARY PHASES

For chromatographic conditions, see Experimental section, for definition of r and $r_{L/D}$, see Table I.

Phase	*T(°C)*	*Configuration*	*N-TFA tert.-butylamide*													
			Isovaline		*α-Methylvaline*		*α-Methylnorvaline*		*α-Methylleucine*		*α-Methylnorleucine*		*α-Methylphenylalanine*			
			r	$r_{L/D}$★	r	$r_{L/D}$★	r	$r_{L/D}$★	r	$r_{L/D}$★	r	$r_{L/D}$★	*T(°C)*	*Configuration*	r	$r_{L/D}$★
I	110	D	37.10	1.016	37.60	1.122	49.90	1.033	58.30	1.022	71.80	1.032				
		L	37.70		42.20		51.54		59.60		74.10					
	120	D	24.60	1.000	25.40	1.098	32.30	1.018	39.00	1.000	47.00	1.017				
		L	24.60		27.90		32.90		39.00		47.80					
	130	D	21.80	1.000	22.30	1.078	28.30	1.014	33.80	1.000	40.00	1.010	140	D	122.00	1.026 (shoulder)
		L	21.80		24.04		28.70		33.80		40.40			L	125.20	
II	130	D	30.90	1.029	33.60	1.176	41.60	1.034	47.80	1.000	56.60	1.027				
		L	31.80		39.50		43.00		47.80		58.10					
	140	D	22.20	1.018	26.20	1.137	29.14	1.026	37.20	1.000	43.80	1.018	170	D	98.40	1.024
		L	22.60		29.80		29.90		37.20		44.60			L	100.80	

III**	110	L D	82.28 85.20	1.036	–	–	–	–	121.40 125.00	1.030	–	–			–	
	130	L D	31.40 32.30	1.026	35.36 38.00	1.075	42.80 44.40	1.037	46.60 47.40	1.017	60.20 62.28	1.035				
IV	100	D L	30.32 32.48	1.071	39.00 53.00	1.359	42.00 46.00	1.095	45.00 46.60	1.036	54.80 58.88	1.074				
	110	D L	19.80 21.00	1.061	25.00 31.80	1.272	27.40 29.20	1.066	35.00 36.12	1.032	42.20 44.80	1.062				
	120	D L	16.00 16.80	1.050	21.20 25.60	1.208	21.80 22.90	1.054	30.60 31.00	1.013	24.60 26.00	1.057				
	130	D L	13.00 13.60	1.046	13.40 15.60	1.164	17.80 18.60	1.045	19.20 19.20	1.000	22.60 23.20	1.027	150	D L	113.00 117.00	1.035
V	100	D L	19.20 20.70	1.078												
	110	D L	15.10 15.95	1.056												
	120	D L	10.87 11.13	1.024												

* The order of emergence ($r_{L/D} > 1$) determined with optically enriched mixutres for isovaline (L > D) and for α-Me-valine (D > L) was by extrapolation assumed to be valid also for the other α-Me-amino acids.

** III being a D phase, the order of emergence is reversed. Separation factors listed are $r_{D/L}$.

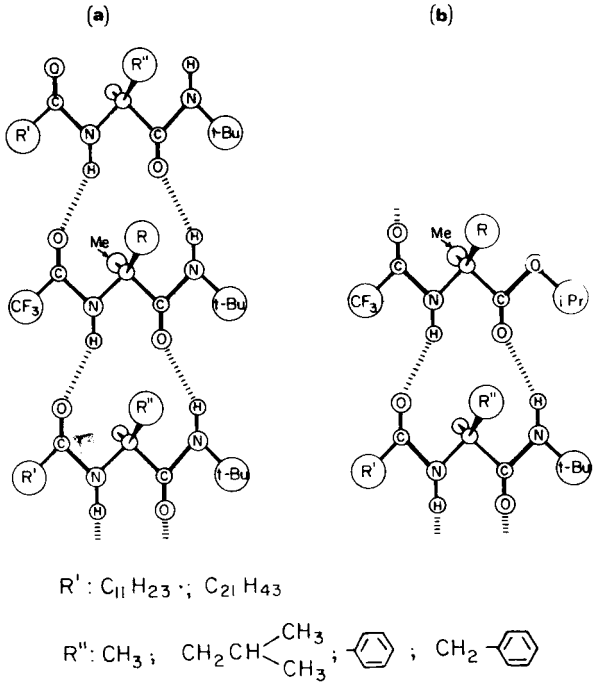

Fig. 4. Schmatic representation of hydrogen-bonded associates assumed to be responsible for resolution by diamide phases. (a) Solvent–solute–solvent complex with parallel orientation of the solvent molecules and an intercalated N-TFA *tert.*-butylamide of an L-α-methyl-α-amino acid[22]. To represent the corresponding diastereomeric complexes with D-solutes, the relative position of Me and R have to be inverted. (b) Solvent–solute complex with an N-TFA isopropyl ester of an α-methyl-α-amino acid; in diastereomeric association complexes with D-solutes the relative positions of the Me and R groups are inverted.

TABLE III

COMPARISON OF THE RESOLUTION FACTORS OF N-TFA ISOPROPYL ESTERS AND N-TFA-*tert.*-BUTYLAMIDES OF α-METHYL-α-AMINO ACIDS ON N-LAUROYL-L-ALANINE *tert.*-BUTYLAMIDE (I)

Column: 100 ft. × 0.02 in.

Amino acid	*N-TFA tert.-Butylamide*	*N-TFA Isopropyl ester*
	$r_{L/D}$★ *at 110 °C*	$r_{L/D}$★ *at 80 °C*
α-Methylvaline	1.122	1.068
α-Methylnorvaline	1.033	1.034
α-Methylleucine	1.022	1.018
α-Methylnorleucine	1.032	1.033

★ For $r_{L/D}$, see Table I.

and it is, indeed, the most difficult compound to resolve in the series studied (also its N-TFA ester is not separated on I, see above). It should be mentioned that the nature of the R substituent of the solute also has more subtle effects, which cannot be understood without a more detailed knowledge of the conformation of the solute–solvent association complexes. Thus, α-methylvaline, in which R is branched at its β-position, gives the highest $r_{II/I}$ value observed in this research (1.359, Table II). On the other hand, α-methylleucine, with the R group branched in the γ-position, is as difficult to resolve as isovaline. The same influence of substitution is indicated by the behaviour of the N-TFA esters (Table I)*.

The increase in the $r_{L/D}$ values for the diamide derivatives of the α-methyl-α-amino acids, as compared with the N-TFA isopropyl esters, is ascribed to the difference in the mode of interaction with the stationary phases. With reference to Fig. 4, it is seen that the N-TFA *tert.*-butylamide derivatives, which are capable of forming four hydrogen bonds, can intercalate between two solvent molecules (complex a). On the other hand, association of N-TFA esters with a second solvent molecule would be rather loose, as only one hydrogen bond is available for that purpose (complex b). The resulting lesser restriction of the solutes would appear to be related to the relatively lower chiral differentiation in the latter case.

The order of emergence (L after the D isomer on the L-phases) has been experimentally determined on only two enriched mixtures (isovaline and α-methylvaline, Table II). By extrapolation, and by analogy with the same consistent elution sequence found for the α-H-α-amino acid derivatives, it is provisionally assumed that, for the α-methyl-α-amino acids derivatives, also, $r_{L/D}$ on the L-phases is larger than unity, throughout. These results are in agreement with the above assumption of analogous stereoselective solute–solvent association for both types of amino acids.

As was seen for the N-TFA esters, discussed in the preceding sections, the nature of the substituent R″ in the diamide solvent is observed to play (Table II) an important role in determining the magnitude of the resolution factors. In the series I–IV of the diamides R‴CONHCH(R″)CONHR′ with the same R‴ and R′ groups, chiral recognition improves as R″ increases, except in the case of the D-phenylglycine derivative III, where the proximity of the phenyl to the chiral centre creates a special situation. For R″ = benzyl, the highest $r_{L/D}$ values were obtained throughout, and the corresponding diamide IV is the best phase found, thus far, for the enantiomeric analysis of the α-methyl-α-amino acids. It is recalled that for the N-TFA isopropyl esters, the best results were, however, obtained on the diamide with the smallest R″ group (I).

As was found for the α-H-α-amino acids, lengthening of the R‴ chain reduces to some extent the resolution factors (V, as compared with II), but has the advantage of permitting the range of column working temperatures to be widened.

APPLICATIONS

The determination of the configuration of isovaline in natural substances is of topical interest. Recently, Brueckner and co-workers[12] definitely established the D-

* In contrast, for the N-TFA esters of the α-H-α-amino acid derivatives, the effects of branching of R in the β- and γ-positions are reversed[23].

configuration of isovaline in polypeptidic antibiotics, using gas chromatographic procedures expecially developed for that purpose. Previously the opposite assignment had been made for this α-methyl-α-amino acid in antiamoebins[27] and emericidins[28]. Apparently, the erreneous conclusion was reached by the assumption that chiral recognition of α-methyl-α-amino acids is as easy as that of the α-H analogues. The new derivatives and chiral phases introduced in the present research will supplement and improve the enantiomeric analysis of isovaline, as well as of other α-methyl-α-amino acids. Furthermore, the data discussed above show clearly that, besides certain similarities, there are also marked differences between the α-methyl and α-H-α-amino acids in their interaction with chiral diamide stationary phases.

Brueckner and co-workers[12] have already pointed out the special diffuclties involved in the determination of the configuration of α-methyl-α-amino acids, such as the inapplicability[29] of the Clough–Lutz–Jirgenson rule. Also, it has been found[14] that, in this series, assignment through enzymatic hydrolysis of the N-acyl esters cannot be effected in all cases, because of resistance to attack by Acylase I. Experience has shown that the order of emergence of solutes on the chiral phases studied so far can be correlated in a consistent way with the configuration. In particular, on the diamides[16–18,22–25] no exception has yet been found to the rule that derivatives of α-H-α-amino acids elute in the order L-after the D-isomer on L-phases. Furthermore, it should be added that measurements[14,19] for five optically enriched N-TFA esters of α-methyl-α-amino acids gave throughout the same sequence of elution ($r_{L/D} > 1$) on carbonylbis-(N-L-valine isopropyl ester). There are, therefore, good reasons to conclude that the order of emergence of derivatives of α-methyl-α-amino acids on diamide stationary phases promises to become a useful tool for the determination of the configuration in this series.

ACKNOWLEDGEMENT

S.-C. C. is indebted to the Chung-Shan Institute of Science and Technology, Taiwan, R.O.C., for the grant of a scholarship.

REFERENCES

1 T. Ooka, Y. Shimojima, T. Akimoto, I. Takeda, S. Senoh and J. Abe, *Agr. Biol. Chem.*, 30 (1966) 700.
2 R. C. Pandey, H. Meng, J. C. Cook and K. L. Rinehart, *J. Amer. Chem. Soc.*, 99 (1977) 5203.
3 G. Jung, N. Dubischar and D. Leibfritz, *Eur. J. Biochem.*, 54 (1975) 395.
4 G. Irmscher and G. Jung, *Eur. J. Biochem.*, 80 (1977) 165.
5 E. H. Flynn, J. W. Hinman, E. L. Caron and D. O. Woolf, Jr., *J. Amer. Chem. Soc.*, 75 (1953) 5867.
6 T. H. Svensson and B. Waldeck, *Psychopharmacologia*, 18 (1970) 357.
7 J. A. Oates, L. Gillespie, S. Udenfriend and A. Sjoerdsma, *Science*, 131 (1960) 1890.
8 L. Gillespie, Jr., *Ann. N.Y. Acad. Sci.*, 88 (1960) 1011.
9 M. S. Chadha, J. Lawless, J. Flores and C. Ponnamperuma, in R. Buvet and C. Ponnamperuma (Editors), *Molecular Evolution I, Proceedings of the International Conference on the Origin of Life, Pont-a-Mousson, France, April 20–25, 1970*, North-Holland, Amsterdam, 1971, p. 143.
10 K. A. Kvenvolden, J. G. Lawless and C. Ponnamperuma, *Proc. Nat. Acad. Sci. U.S.*, 68 (1971) 486.
11 G. E. Pollock, *Anal. Chem.*, 44 (1972) 2368.
12 H. Brueckner, G. J. Nicholson, G. Jung, K. Kruse and W. A. Koenig, *Chromatographia*, 13 (1980) 209.
13 J. J. Flores, W. A. Bonner and M. A. Van Dort, *J. Chromatogr.*, 132 (1977) 152.
14 N. Frydman, T. Tamari, B. Feibush and E. Gil-Av, *Proc. Isr. Chem. Soc. 42nd Meeting, Dec. 1972*, p. 11.

15 S. Weinstein, B. Feibush and E. Gil-Av, *J. Chromatogr.*, 126 (1976) 97.
16 B. Feibush, *Chem. Commun.*, (1971) 544.
17 R. Charles, U. Beitler, B. Feibush and E. Gil-Av, *J. Chromatogr.*, 112 (1975) 121.
18. U. Beitler and B. Feibush, *J. Chromatogr.*, 123 (1976) 149.
19 A. Schwartz, *Ph. D. Thesis*, Weizmann Institute of Science, Rehovot, Israel, 1977.
20 H. T. Bucherer and V. A. Lieb, *J. Prakt. Chem.*, 141 (1934) 5.
21 J. P. Greenstein, M. Winitz, *Chemistry of the Amino Acids*, Wiley, New York, 1961, p. 2572.
22 S.-C. Chang, R. Charles and E. Gil-Av, *J. Chromatogr.*, 202 (1980) 247.
23 S.-C. Chang, R. Charles and E. Gil-Av, *J. Chromatogr.*, 235 (1982) 87.
24 R. Charles and E. Gil-Av, unpublished data.
25 R. Charles and E. Gil-Av, *J. Chromatogr.*, 195 (1980) 317.
26 N. Ôi, M. Horiba and H. Kitahara, *J. Chromatogr.*, 202 (1980) 299.
27 R. C. Pandey, J. C. Cook and K. L. Rinehart, *J. Antibiot.*, 31 (1978) 241.
28 R. C. Pandey, J. C. Cook and K. L. Rinehart, *J. Amer. Chem. Soc.*, 99 (1977) 5205.
29 M. Winitz, S. M. Birnbaum and J. P. Greenstein, *J. Amer. Chem. Soc.*, 77 (1955) 716.

Journal of Chromatography, 238 (1982) 41–50
Elsevier Scientific Publishing Company, Amsterdam — Printed in The Netherlands

CHROM. 14,601

COMPARATIVE GAS CHROMATOGRAPHIC SEPARATION OF SIMPLE DIASTEREOMERIC AMIDES AND CARBAMATES USING ISOTROPIC AND CHOLESTERIC LIQUID CRYSTAL PHASES

PHILIP E. SONNET* and ROBERT R. HEATH
Insect Attractants, Behavior, and Basic Biology Research Laboratory, Agricultural Research Service, USDA, Gainesville, FL 32604 (U.S.A.)
(Received October 6th, 1981)

SUMMARY

A series of diasteromeric amides and carbamates have been prepared, and comparisons are made between the gas–liquid chromatographic separations obtained with several stationary phases in capillary columns. These are: SE-54 as a non-polar phase, polyethylene glycol polar phase, and a liquid crystal phase, cholesteryl *para*-chlorocinnamate (CpCC). For the compounds studied, the CpCC column provided greater separation factors than the other two columns. Since the elution order of pairs of diasteromers was the same on all three columns, the enhanced separation with CpCC suggests greater sensitivity of the ordered mesophase to the shape of the solution conformers of solute molecules.

INTRODUCTION

Application of liquid crystals as stationary phases for the gas–liquid chromatographic (GLC) separation of insect sex pheromones and related aliphatics has generally resulted in resolution of these compounds superior to that achieved on polar and non-polar isotropic phases[1–3]. The ordered character of the liquid phase is eminently suited to discriminating these substrates, many of which are aliphatics bearing one or two olefinic links and a chain-terminating oxygenated functionality. An occasional structure has a methyl branch. These materials tend to occur in nature as complicated mixtures whose exact composition is crucial for eliciting insect sexual behavior[4].

We have also found that capillary columns that have been coated with the liquid crystal, cholesteryl cinnamate, were particularly valuable in connection with the synthesis of a series of diasteromeric amides[5]. Because of current interest in asymmetric organic synthesis[6–9], rapid chromatographic analysis of diastereomeric intermediates to determine configurational purity (and absolute configuration) is also important in chromatography. We wish to extend our observations of cinnamate ester liquid crystal columns to commonly employed diastereomeric derivatives, and describe here the preparation, configurational analysis, and chromatographic properties of a series of diastereomeric pairs of amides and carbamates. Comparisons are

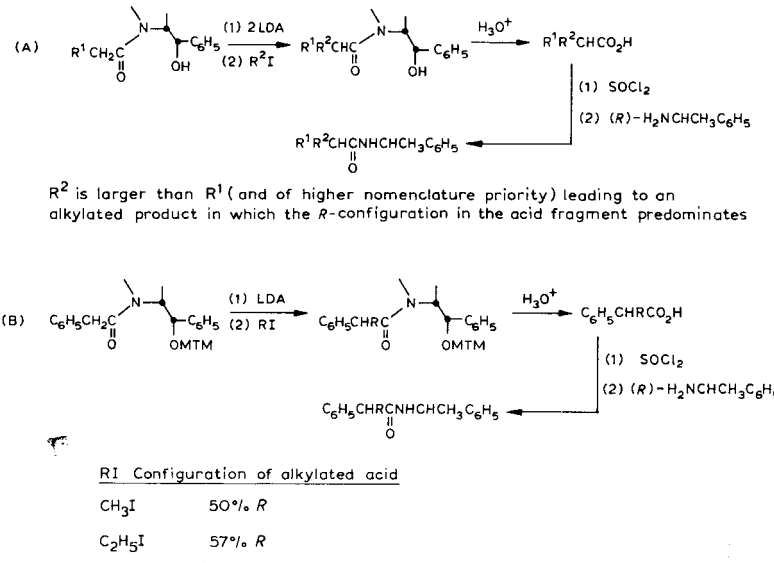

Fig. 1. Syntheses of configurationally biased amides I–XIII from (1)-ephedine. LDA = Lithium diisopropylamide, MTM = methyl thiomethyl.

made between the separations obtained with the following stationary phases: SE-54 as a non-polar phase, Carbowax 20M as a polar phase, and cholesteryl *para*-chlorocinnamate (CpCC) as a typical cholesteric liquid crystal phase[10]★.

EXPERIMENTAL

Capillary columns

The SE-54 fused-silica column was 15 m × 0.25 mm I.D. and was purchased from J. W. Scientific (Rancho Cordoba, CA, U.S.A.). The Carbowax 20M fused-silica column was 15 m × 0.20 mm I.D. and was obtained from Hewlett-Packard (Avondale, PA, U.S.A.). The CpCC columns were 20 m × 0.20 mm I.D. and were prepared in our laboratories from etched soft glass coated by the static method. Column A was prepared with a 0.25% (w/v) CpCC in methylene chloride, and column B was prepared with 0.10% (w/v) solution. Each column was conditioned for 2 h at 200°C prior to use.

All work was done on a Varian 3700 or Varian 1400 instrument with a user-designed all-glass capillary system. The carrier was helium and the linear flow velocity was 18 cm/sec. The inlet split ratio was *ca.* 100:1 and detector make-up flow was 30 ml of nitrogen/min.

The amides I–XI (Table I) were prepared as follows. Amides derived from (1)-ephedrine were alkylated in the manner recently described for (S)-prolinol and (1)-ephedrine (Fig. 1A)[5,11,12]. The resulting amides were hydrolyzed producing acids of known configurational bias (see Appendix). The acids then were converted via acid

★ Mention of a commercial or proprietary product does not constitute an endorsement by the USDA.

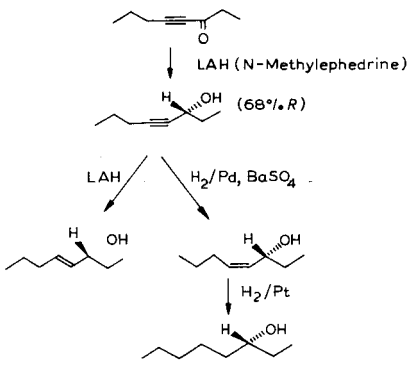

Fig. 2. Synthesis of the *R*-enriched carbinols for carbamates XV–XVIII.

halides to amides of (*R*)-α-methylbenzylamine*.

Alkylation of phenylacetamides of chiral β-aminoalcohols such as (1)-ephedrine (Fig. 1B) have not been discussed, therefore, the assignment of configurations for amides XII and XIII (Table I) was based on high-performance liquid chromatography (HPLC) elution order[13] and ^{1}H nuclear magnetic resonance (NMR) analysis of the purified diastereomers (Table II).

The urethanes XIV–XXI (Table I) were prepared from the appropriate secondary carbinol by sequential treatment with phosgene-triethylamine in ether, and (*R*)-α-methylbenzylamine-triethylamine. Samples of (*R*)- and (*S*)-2-octanols (Aldrich) were employed to prepare XIV. The related 3-octanols that were used to make carbamates XV–XVIII were synthesized as shown in Fig. 2. The 5-octyn-3-one was prepared by standard methods from 1-pentyne and propionaldehyde. Reduction of that ketone with lithium aluminum hydride (LAH) modified with (1)-N-methylephedrine produced 5-octyn-3-ol with an enantiomeric excess of 36% R (ref. 14). The ratio of enantiomers was determined by esterification with (*S*)-α-methoxy trifluoromethylphenyl acetyl chloride (MTPA-chloride)[15,16]. Samples of the *R*-enriched alkynol were reduced with $Ni(OAc)_2/NaBH_4$ (ref. 17) to give the predominantly *cis*-alkenol and with LAH to give the *trans*-alkenol. Finally, hydrogenation of the alkenols over Pt in propionic acid yielded the *R*-enriched saturated 3-octanol. Carbamate XIX was prepared as a mixture of four diastereomers from commercial 4-methyl-3-heptanol. The phenyl carbamates XX and XXI were synthesized from the racemic carbinols, and configuration assignment was based on HPLC elution order and, in the case of XXI, ^{1}H NMR evaluation of the purified diastereomers[13].

RESULTS AND DISCUSSION

Investigations by Dewar and Schroeder[18–20] using packed columns and various azoxybiphenyl derivatives for stationary liquid phases indicated the utility of ordered phases for the separation of simple benzenoid derivatives. Their observations

* Commercial (*R*)-α-methylbenzylamine (Aldrich, Milwaukee, WI, U.S.A.) was ≥92% enantiomeric excess (ee) as judged by the diastereomeric amides formed with (*S*)-MTPA-chloride, and was employed without further purification.

TABLE I

GAS–LIQUID CHROMATOGRAPHIC DATA FOR DIASTEREOMERIC AMIDES AND CARBAMATES

Column temperatures were as follows for A:SE-54; 170°C for I-XI; 190°C for XII and XIII; Carbowax 20M, 160°C for I–XI; 180°C for XII and XIII; CpCC column A; 145°C. Column temperatures were as follows for B: SE-54; 200°C for XIV–XIX; 210°C for XX and XXI; Carbowax 20M; 170°C for XIV–XIX; 190°C for XX and XXI; CpCC column B; 145°C for XIV and XV; 155°C for XIX; 160°C for XVI–XVIII, XX, and XXI.

I–XIII 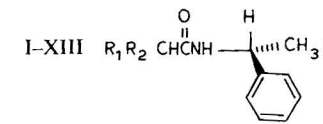 ; XIV–XXII the corresponding carbamates

Compound; R_1,R_2	*SE-54*			*Carbowax 20M*			*CpCC (column A)*		
	k' (R,R)	*k'(S,R)*	α	*k'(R,R)*	*k'(S,R)*	α	*k'(R,R)*	*k'(S,R)*	α
I; CH_3, C_2H_5	3.03	3.09	1.021	4.36	4.44	1.018	6.93	7.18	1.036
II; I-N-methyl	4.95	4.95	1.000				3.05	3.09	1.013
III; CH_3, *iso*-C_3H_7	3.91	4.06	1.040	4.64	4.86	1.046	7.76	8.26	1.064
IV; CH_3, *n*-C_3H_7	4.18	4.44	1.060	5.07	5.36	1.056	8.50	9.13	1.071
V; IV-N-methyl	6.82	6.75	1.019				4.18	5.17	1.059
VI; CH_3, *n*-C_4H_9	5.97	6.31	1.058	6.79	7.25	1.068	12.95	14.24	1.100
VII; C_2H_5, *iso*-C_3H_7	5.06	5.16	1.018	4.39	4.53	1.033	10.18	10.63	1.044
VIII; C_2H_5, *n*-C_3H_7	5.50	5.68	1.034	4.93	5.14	1.044	11.50	12.08	1.050
IX; C_2H_5, *n*-C_4H_9	7.81	8.18	1.048	6.50	6.86	1.055	17.11	18.21	1.065
X; *n*-C_4H_9, *n*-C_5H_{11}							7.47	7.60	1.017
XI; *n*-C_5H_{11}, *n*-C_6H_{13}	5.47	5.47	1.000				15.62	15.79	1.011
XII; CH_3, C_6H_5	6.76	7.35	1.088	6.93	7.93	1.144	7.00	8.00	1.143
XIII; C_2H_5, C_6H_5	8.47	9.29	1.097	7.57	8.64	1.141	8.70	9.90	1.138
XIV; CH_3, *n*-C_6H_{13}	4.13	4.33	1.048	4.65	4.96	1.066	16.36	17.86	1.09
XV; C_2H_5, *n*-C_5H_{11}	3.87	4.03	1.043	2.00	2.08	1.039	10.71	11.5	1.07
XVI; C_2H_5, *n*-$C_3H_7C{\equiv}C$–	4.63	4.80	1.036	8.92	9.23	1.037	10.21	10.57	1.04
XVII; C_2H_5, *n*-$C_3H_7CH{=}CH$– (*Z*)	3.60	3.73	1.037	4.12	4.38	1.065	6.28	6.64	1.06
XVIII; C_2H_5, *n*-$C_3H_7CH{=}CH$– (*E*)	3.93	4.07	1.034	5.08	5.27	1.038	7.82	8.18	1.05

XIX; C_2H_5, n-$C_3H_7CH(CH_3)$–	3.40	3.50	1.029	(3.31,	3.46	3.58)	1.047 1.033	(12.52, 13.20	12.99 13.50)	1.038 1.017 1.027
XX; CH_3, C_6H_5	4.43	4.57	1.030	7.96		8.31	1.044	20.10	21.8	1.08
XXI, CF_3, C_6H_5	2.73	2.67	1.025	4.31		4.31	1.000	8.89	8.43	1.07

TABLE II

^{1}H NMR DATA FOR PHENYL SUBSTITUTED ACID AND CARBINOL DERIVATIVES

^{1}H NMR data were obtained in dilute C^2HCl_3 solution with a Nicolet 300 MHz spectrometer. Shifts are reported in ppm downfield from $(CH_3)_4Si$. Values of $\Delta\delta$ are obtained from δ_1–δ_2. HPLC collections were made with a 250 mm × 18 mm I.D. column of Biosil-A, 2–10 μm, employing hexane–ethyl acetate (9:1) at a flow-rate of 9.9 ml/min. Carbamate XX was not resolved by HPLC and collections of material during peak elution were employed to establish relative rates of elution of the diastereomers on LC *versus* GLC.

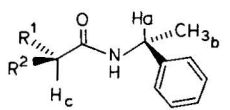

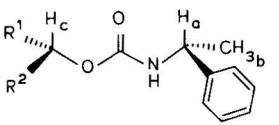

Compound	*Elution order***	R^1	R^2	M_p(°C)	δ_a	δ_b	δ_c	$\Delta\delta_a$	$\Delta\delta_b$	$\Delta\delta_c$
XII	1 (*S*,*R*)*	C_6H_5	CH_3	132–134	5.09	1.35	3.53			
	2 (*R*,*R*)*	CH_3	C_6H_5	111–114	5.08	1.39	3.57	0.01	−0.04	−0.04
XIII	1 (*S*,*R*)	C_6H_5	C_2H_5	116–119	5.09	1.35	3.21			
	2 (*R*,*R*)	C_2H_5	C_6H_5	66–68	5.09	1.41	3.24	0.00	−0.06	−0.03
XXI	1 (*R*,*R*)	C_6H_5	CF_3	73–74	4.84	1.54	6.07			
	2 (*S*,*R*)	CF_3	C_6H_5	132–135	4.82	1.48	6.05	0.02	0.06	0.02

* δ $C_6H_5CHCH_3C{=}O$ for XII-1 = 1.51; XII-2 = 1.51.

** The first configuration designator represents the acid residue. The second designator represents the (unvaried) chiral auxiliary.

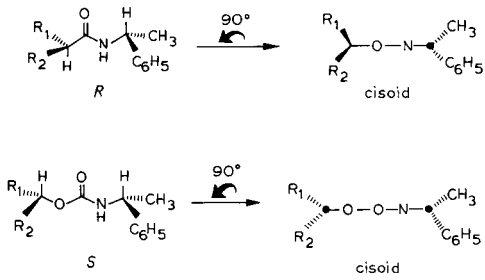

Fig. 3. Solution conformers of diastereomeric amides and carbamates[13]. R_1 and R_2 are saturated alkyl groups with R_2 longer than R_1.

suggested that the more rod-shaped molecule of a set of isomeric molecules would be preferentially dissolved (partitioned) by the ordered phase. This seemed consistent with the separations of olefins[1-3]; the *cis*-isomers which are "kinked" tend to elute first, and the separation for *cis–trans* pairs increases as the site of the double bond is shifted toward the middle of the chain.

Lochmüller and Souter[21] have investigated optically active liquid crystal phases for the separation of enantiomers. Although this polyamide ("ureide") phase provided excellent separation of chiral amides, the low mesophase transition temperature has precluded more extensive use of the phase. More recently Frank *et al.*[22] have described an optically active isotropic, hence temperature-stable, phase that provided excellent separations of enantiomeric amino acid derivatives. The diastereomeric pairs listed in Tables I and II were, in fact, analyzed with a chirasil-val column (25 m × 0.20 mm I.D.) obtained from Applied Science Labs., and the separations were always less than those obtained on CpCC columns. The performance of the chirasil-val column was intermediate to that of the two columns with isotropic phases in most cases. Thus we were led to make a comparison of the CpCC column with conventional isotropic phases, namely SE-54 and Carbowax 20M with a view to examining elution orders as well as relative separations.

The chromatographic elution orders of diasteromeric amides, carbamates, and esters have been discussed in terms of solution conformations such as those depicted in Fig. 3[23-29]. Briefly, the carbonyl-containing functional group serves to create a plane between the asymmetric centers, and these centers extend alkyl (aryl) groups to either side of that plane. Those diastereomers which feature the largest group on each asymmetric center to the same side of the plane have been referred to as *cisoid* in Fig. 3. An explanation based on a combination of steric bulk and hydrophobicity has been advanced to explain HPLC elution orders for diastereomeric carbamates[13], namely the *cisoid* diastereomer of a carbamate (S^*_{alcohol}, R^*_{amine}) can make easier approach to the stationary phase doing so from that planar face having the smaller alkyl (aryl) residues exposed. This model is tempered by the degree of repulsion (hydropobicity) experienced by these substituents, and in extreme cases the usual elution order is reversed. This situation for amides is quite analogous; asymmetric centers are separated by one less atom and *cisoid* corresponds to an *R*R** diastereomer. Although substantive criticism has been offered by way of demonstrated exceptions[30,31], for simple (otherwise unfunctionalized) substrates such as ours the model described[13] was quite adequate and elution orders followed the proposed model for HPLC elution.

The elution orders were exactly reversed in gas chromatography from that in HPLC with the *transoid* diastereomers being retained longest. More to the point, elution orders were the same for all three liquid phases indication that the mechanisms of separation for isotropic and ordered phases were perhaps quite similar. Methylation of the amide nitrogen (see II *vs.* I, and V *vs.* IV in Table I) produced a dramatic reduction in separations (α) on all GLC columns. A similar reduction in HPLC α was observed for N-methylated (as opposed to N–H) carbamates for which a higher content of the 180° rotamer about the N–C bond was suggested[13]. Such a rotamer would contribute in an opposite sense to those factors crucial to α in HPLC since the substituents on the amine asymmetric center would now be deployed on the alternative sides of the carbonyl. If one takes GLC resolutions of diastereomers to be a matter of relative solution energies of preferred solution conformations, then the N-methylated derivatives would on the same grounds as just described for HPLC separations become (solution) energetically more equivalent. Although capacity factors (k') for II and V (Table I) are greater than for their unmethylated counterparts on SE-54, they are dramatically reduced by a factor of >2 on the CpCC column, *i.e.*, solution energies have been greatly reduced for both pairs of diastereomers. Hydrogen bonding involving the N–H of amides and carbamates is an obvious suspect cause for larger k' values, but further investigation would be required to determine the existence of specific solute–solvent interactions involving the relatively apolar cholesterol ester solvent.

The trifluoromethyl substituted diastereomeric carbamates XXI were both eluted much more rapidly on all GLC columns than their methyl counterparts. The elution orders were the same with the *cisoid* isomer being retained more. This striking inversion of elution order on substituting CF_3 for CH_3 was first noted in reference to HPLC resolution[13] and was ascribed to the considerable hydrophobicity of a CF_3 group. Although the group is small, repulsion from Si-OH of the stationary phase causes both the observed inversion of elution order and smaller k' values of both diastereomers. The same observation is made with GLC elution order/k' values, and the phenomenon here would therefore need to be considered in terms of solution energetics as part of a more thorough investigation.

As part of this study we examined the diastereomers of the carbamate of 4-methyl-3-heptanol. This alcohol is the major component of the aggregation pheromone of the large European elm bark beetle, *Scolytus scolytus* (F.)[32,33], and is a minor component of the pheromonal complex of the small European elm bark beetle, *Scolytus multistriatus* (Marsham)[34]. Analyses of the MTPA esters[15,16] of the commercial alcohol had been performed on a Carbowax 20M glass column to provide separation into three peaks. (The (−)-*threo* and (−)-*erythro* derivatives of (−)-MTPA coincided. The four esters were only separated into two peaks (*ca.* 1:1 by CpCC. The carbamate XIX, however, was separated albeit incompletely into the four diastereomers by the CpCC column (Fig. 4).

In conclusion we can summarize the data in the following manner. For the compounds studied, the CpCC column provided the greatest separation factors Tables I and II). Since the elution order of pairs of diastereomers was the same on all three columns, the previously described models seem applicable to this cholesteric phase although the enhanced α with CpCC suggests greater sensitivity of this phase to the shape of the solution conformers of substrate molecules.

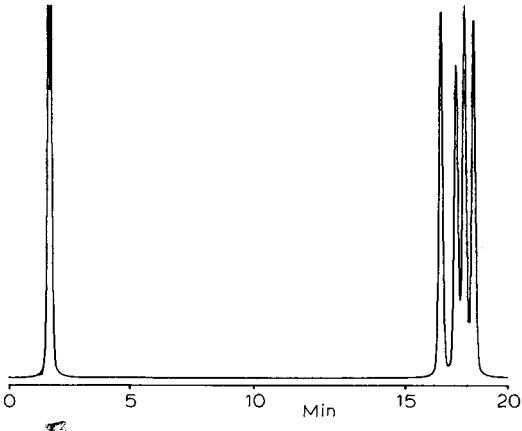

Fig. 4. Separation of diastereomeric carbamates of 4-methyl 3-heptanol, XIX on 15 m × 0.02 I.D. CpCC (column B) at 155°C, carrier gas (helium) at 18 cm/sec.

One should note also that the operating temperatures for several separations reported here were well above the meso-phase transition for CpCC. Thus the reported α values are not maximal. By reducing film thickness of liquid crystal phases, the chromatographer has a variable that permits lower operating temperatures in order to further enhance a given separation[32,33].

APPENDIX

Amides of (*S*)-prolinol and (1)-ephedrine are deprotonated by non-nucleophilic bases such as lithium diisopropylamide to produce enolate ions[5,11,12]. The example in Fig. 1A depicts the enolate (presumably *Z*, ref. 12) derived from (1)-ephedrine propionamide after reaction with more than 2 equivalents of the base. Although the detailed structure of these intermediate anions is still under investigation[12], the observation made by several independent laboratories is that the new center is created in this instance with strong *R* preference. When the hydroxyl group of the amino-alcohol is etherified bond formation between enolate and alkyl halide occurs mainly from the other face of the double bond and, for a reaction involving a propionamide with ethyl iodide, results in a strong *S* bias in the new center. Using this reaction and its predictable stereochemical consequences we were able to obtain products of known configurational bias.

In order to obtain amides XII and XIII, (1)-ephedrine was treated with phenylacetyl chloride. The resulting phenylacetamide was then allowed to react with (1) NaH, and (2) methyl thiomethyl chloride in order to convert the ephedrine hydroxyl

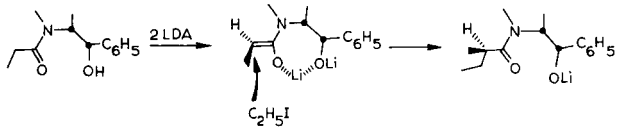

Fig. A1.

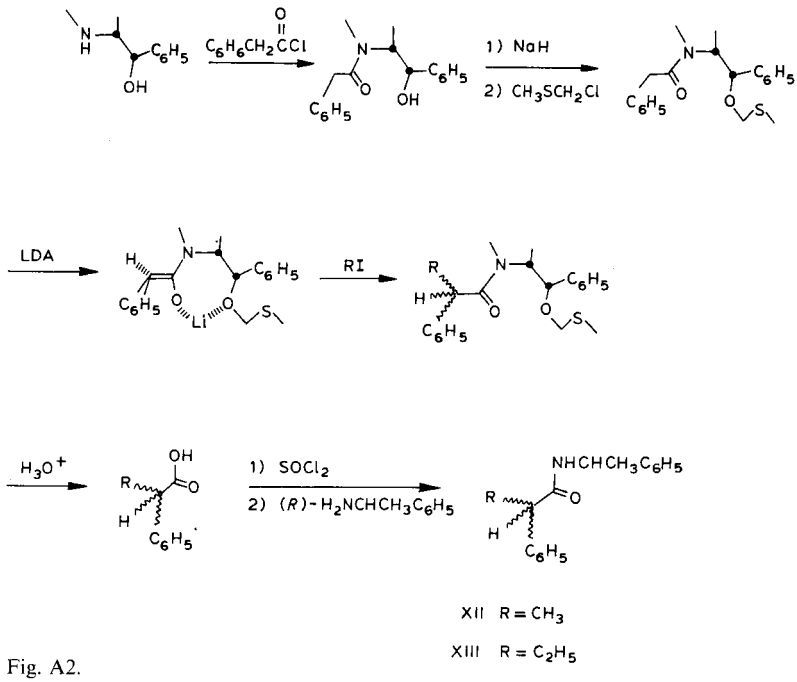

XII R = CH_3

XIII R = C_2H_5

Fig. A2.

group to a methyl thiomethyl ether (Fig. A2). This amide then served as the substrate for production of XII and XIII. The deprotonation by lithium diisopropylamide was followed by reaction either with methyliodide (→ → XII) or ethyliodide (→ → XIII). The methylation product was a 1:1 ratio of diastereomers while ethylation produced a 2:1 ratio that was shown subsequently to be *R*-predominant. As was the case for amides I–XI, the alkylated ephedrine amides were hydrolyzed (1 *N* HCl, 90°, 2–4 h), and the resulting acids where then converted to amides of (*R*)-α-methylbenzylamine. The diastereomer ratios obtained were independent of the temperature employed for deprotonation; alkylation was conducted at −78°C.

The ^{1}H NMR data in Table I of the text are consistent with the relative shift data presented for closely analogous compounds[13]. Briefly, the principal solution conformers of amides and carbamates such as those described are as indicated by the structures associated with Table I. Aryl groups on the acid-based center of asymmetry in opposition to a methyl group on the other center will shield that methyl group. Thus for XII, the CH_3 signal (absorption b) of the first-eluted (HPLC) diastereomer is shielded by 0.04 ppm relative to that of the later eluting diastereomer. A shift difference of 0.06 ppm is observed for the XIII pair. These observations in conjunction with HPLC elution order[13] and mechanistic rationalization for XIII (as per amides I–XI) led to our configuration assignments.

For urethans, or carbamates, XIV–XXI the assignment of configuration follows from the many asymmetric reductions of conjugated alkynones provided in the literature (*e.g.*, ref. 14); however, the configuration assignments for the phenyl carbamates XX and XXI were based on expected HPLC elution[13]. In addition, the ^{1}H NMR data for the purified diastereomers of XXI (Table I) were rationalized as they

had been for the phenyl-substituted amides XII and XIII. The second-eluted (HPLC) diastereomer would be expected to have the *S,R*-configuration[13] and is the diastereomer in which the CH_3 signal "b" is shifted upfield (by 0.06 ppm) by virtue of opposition to a phenyl substituent as R_1.

All new compounds were characterized by ^1H NMR and mass spectrometry.

ACKNOWLEDGEMENTS

The authors express their appreciation to Mr. Thomas Proveaux for the mass spectral data and to Ms. Barbara Dueben for technical assistance.

REFERENCES

1 R. Lester, *J. Chromatogr.*, 156 (1978) 55.
2 R. Lester and D. R. Hall, *J. Chromatogr.*, 190 (1980) 35.
3 R. R. Heath, J. R. Jordan, P. E. Sonnet and J. H. Tumlinson, *J. High Resolut. Chromatogr. Chromatogr. Commun.*, 2 (1979) 712.
4 J. M. Brand, J. Chr. Young and R. M. Silverstein, in W. Herz, H. Grisebach and G. W. Kirby (Editors), *Progress in the Chemistry of Organic Natural Products*, Vol. 37, Springer, New York, 1979, pp. 1–190.
5 P. E. Sonnet and R. R. Heath, *J. Org. Chem.*, 45 (1980) 3137.
6 D. Valentine, Jr. and J. W. Scott, *Synth.*, (1978) 329.
7 H. B. Kagan and J. C. Fiaud, in E. L. Eliel and N. L. Allinger (Editors), *Topics in Stereochemistry*, Vol. 10, Wiley, New York, 1978, pp. 175–286.
8 J. W. Apsimon and R. P. Seguin, *Tetrahedron*, 35 (1979) 2797.
9 P. A. Bartlett, *Tetrahedron*, 36 (1980) 3.
10 R. R. Heath and R. E. Doolittle, in preparation.
11 M. Larchevegue, E. Ignatova and T. Cuvigny, *J. Organometal. Chem.*, 177 (1979) 5.
12 D. A. Evans and J. M. Takacs, *Tetrahedron Lett.*, (1980) 4233.
13 W. H. Pirkle and J. R. Hauske, *J. Org. Chem.*, 42 (1977) 1839 and ref. cited.
14 J.-P. Vigneron and V. Bloy, *Tetrahedron Lett.*, (1979) 2683.
15 G. R. Sullivan, J. A. Dale and H. S. Mosher, *J. Org. Chem.*, 38 (1973) 2143.
16 J. A. Dale and H. S. Mosher, *J. Amer. Chem. Soc.*, 95 (1973) 512.
17 C. A. Brown and V. K. Ahuja, *J. Org. Chem.*, 38 (1973) 2226.
18 M. J. S. Dewar and J. P. Schroeder, *J. Amer. Chem. Soc.*, 86 (1964) 5235.
19 M. J. S. Dewar and J. P. Schroeder, *J. Org. Chem.*, 30 (1965) 2296, 3485.
20 M. J. S. Dewar, *J. Org. Chem.*, 32 (1967) 1692.
21 C. H. Lochmüller and R. W. Souter, *J. Chromatogr.*, 87 (1973) 243; 88 (1974) 41.
22 H. Frank, G. J. Nicholson and E. Bayer, *J. Chromatogr. Sci.*, 15 (1977) 174.
23 H. C. Rose, R. L. Stern and B. L. Karger, *Anal. Chem.*, 38 (1966) 469.
24 B. L. Karger, R. L. Stern, W. Keane, B. Halpern and J. W. Westley, *Anal. Chem.*, 39 (1967) 228.
25 J. W. Westley, B. Halpern and B. L. Karger, *Anal. Chem.*, 40 (1968) 2046.
26 B. Feibush, *Anal. Chem.*, 43 (1971) 1098.
27 G. Helmchen, R. Ott and K. Sauber, *Tetrahedron Lett.*, (1972) 3873.
28 G. Helmchen, H. Völter and W. Schüle, *Tetrahedron Lett.*, (1977) 1417.
29 E. Gil-Av and D. Nurok, *Aadvan. Chromatogr.*, 10 (1975) 99.
30 B. J. Bergot, R. J. Anderson, D. A. Schooley and C. A. Nenrick, *J. Chromatogr.*, 155 (1978) 97.
31 B. J. Bergot, F. C. Baker, E. Lee and D. A. Schooley, *J. Amer. Chem. Soc.*, 101 (1979) 7432.
32 R. R. Heath, J. R. Jordan and P. E. Sonnet, *J. High Resolut. Chromatogr. Chromatogr. Commun.*, 4 (1981) 328.
33 M. M. Blight, L. J. Wadhams and M. J. Wenham, *Insect Biochem.*, 9 (1979) 525.
34 G. T. Pearce, W. E. Gore, R. M. Silverstein, J. W. Peacock, R. A. Cuthbert, G. N. Lanier and J. B. Simeone, *J. Chem. Ecol.*, 1 (1975) 115.

Journal of Chromatography, 238 (1982) 51–57
Elsevier Scientific Publishing Company, Amsterdam — Printed in The Netherlands

CHROM. 14,538

HOCHLEISTUNGS-GASCHROMATOGRAPHIE AN FLÜSSIGKRISTALL-GLASKAPILLAREN

V. TRENNUNG VON ISOMEREN *n*-TRIDECENEN UND *n*-TETRADECENEN

LADISLAV SOJÁK*
Chemisches Institut, Comenius Universität, Mlynská dolina CH-2, 816 50 Bratislava (Tschechoslowakei)
GUNTER KRAUS
Martin-Luther-Universität Halle-Wittenberg, Sektion Chemie, 4020 Halle (Saale) (D.D.R)
und
PAVEL FARKAŠ und IVAN OSTROVSKÝ
Chemisches Institut, Comenius Universität, Mlynská dolina CH-2, 816 50 Bratislava (Tschechoslowakei)
(Eingegangen am 13. November 1981)

SUMMARY

High-resolution gas chromatography with liquid crystal glass capillaries. V. Separation of isomeric n-tridecenes and n-tetradecenes

The separation of isomeric *n*-tridecenes and tetradecenes was investigated on high-performance glass capillaries with nematic 4-*n*-pentyl-acetophenone (O-4-*n*-pentyloxybenzoyloxime).

The reproducibility of retention indices of *n*-alkenes in contrast to alkylbenzenes show only a small dependence on the film thickness of stationary phase.

The influence of the effect of alternation on the resolution of neighboring positional isomers could be confirmed.

EINLEITUNG

Trennungen von isomeren C_{10}–C_{13}-*n*-Alkenen an Flüssigkristall-Glaskapillaren mit nematischer, smektischer und cholesterinischer Mesophase wurden bereits beschrieben[1–3]. Dabei konnten bessere und schnellere Trennungen der Isomerengemische erzielt werden als an üblichen stationären Phasen. Die spezifische Selektivität von Flüssigkristallen für die Trennung dieser Isomere steht in Übereinstimmung mit der Verschiebung der Doppelbindung von der Mitte zum Ende des Moleküls und der damit verbundenen Vergrösserung ihres Länge–Breite Verhältnisses sowie der in der gleichen Richtung verlaufenden Elutionsfolge. Die Regelmässigkeit der Retention der Lageisomere wird zusätzlich durch den Alternationseffekt beeinflusst[4].

0021-9673/82/0000–0000/$02.75

Die Selektivität für isomere *n*-Alkene ist in den untersuchten Mesophasen ähnlich, sodass wir uns für die Messungen auf eine nematische Phase beschränkten. Zum Vergleich mit vorangegangenen Untersuchungen an 4-*n*-Pentylacetophenon-(O-4-*n*-octyloxybenzoyloxim) (OBO)[1] wurde ein homologer Oximester 4-*n*-Pentylacetophenon-(O-4-*n*-pentyloxybenzoyloxim) (PBO) eingesetzt. Darüberhinaus sollten die Trennbedingungen optimiert und die Reproduzierbarkeit der Retentionsdaten untersucht werden.

EXPERIMENTELLES

Als Substrate wurden Modellmischungen aller isomeren *n*-Alkene C_{13} und C_{14} zusammen mit den entsprechenden *n*-Alkanen eingesetzt.

Die Messungen wurden mit einem Perkin-Elmer F 11 Gaschromatographen mit Flammenionisationsdetektor durchgeführt, als Trägergas diente Wasserstoff (35 cm/sec).

Zur Optimierung und Messung der Reproduzierbarkeit der Retentionsdaten wurden 7 Glaskapillaren mit unterschiedlichen Schichtdicken dynamisch belegt (0.2–20% stationäre Phase in Chloroform).

Das Retentionsverhalten wurde an einer 62-m langen Glaskapillare (0.25 mm I.D. und 2.5% stationäre Phase in Chloroform) untersucht. Sie bestand aus weichem Na-Ca-Glas (Typ Unihost; Kavalier, Teplice, Tschechoslowakei) und wurde nach Ätzung mit Chlorwasserstoffgas mit Stickstoff bei 160°C aktiviert.

Die Effektivität dieser Säule für *trans*-2-Tetradecen bei 74°C und einem Kapazitätverhältnis von $k = 16.2$, $n = 180{,}000$ theoretische und $N = 160{,}000$ effektive Böden. Als stationäre Phase diente PBO[5] mit einem nematischen Bereich von 63–94°C (unterkühlbar bis 27°C):

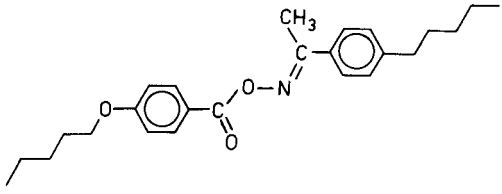

Die zum Vergleich verwendete Glaskapillare mit nematischer Phase (OBO) wurde bereits beschrieben[1]. Die Korrelation mit üblichen stationären Phasen erfolgte an einer Squalan-Glaskapillare (50 m, 0.25 mm I.D., desaktiviert mit Dimethyldichlorsilan). Die Effektivität dieser Säule betrug $n = 210{,}000$ theoretische und $N = 180{,}000$ effektive Böden für *trans*-2-Tridecen bei 90°C und einem Kapazitätsverhältnis von $k = 14.5$. Als Trägergas wurde ebenfalls Wasserstoff (33 cm/sec) verwendet.

ERGEBNISSE UND DISKUSSION

Die Trennungen der isomeren *n*-Tridecene und *n*-Tetradecene an PBO und Squalan zeigen Fig. 1 und 2. Die berechneten Retentions indices wurden in Tabelle I zusammengestellt.

Die Reproduzierbarkeit der Retentionsindices für *n*-Alkene wurde an 7 Glas-

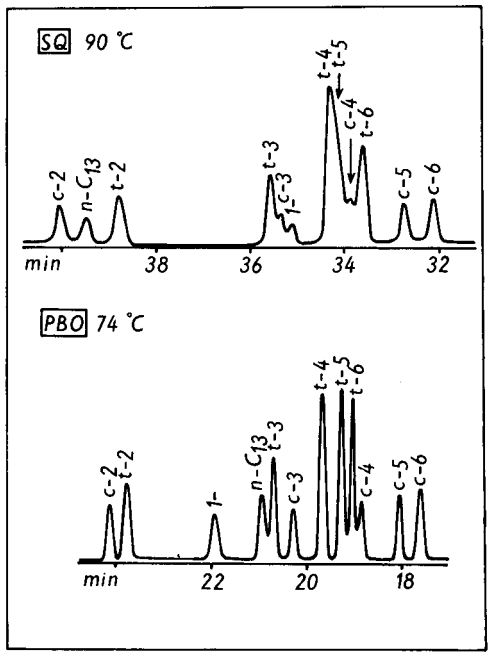

Fig. 1. Trennung von isomeren *n*-Tridecenen an PBO und Squalan (SQ). *c-* = *cis*-, *t-* = *trans*-Isomere *n*-C_{13} = *n*-Tridecan.

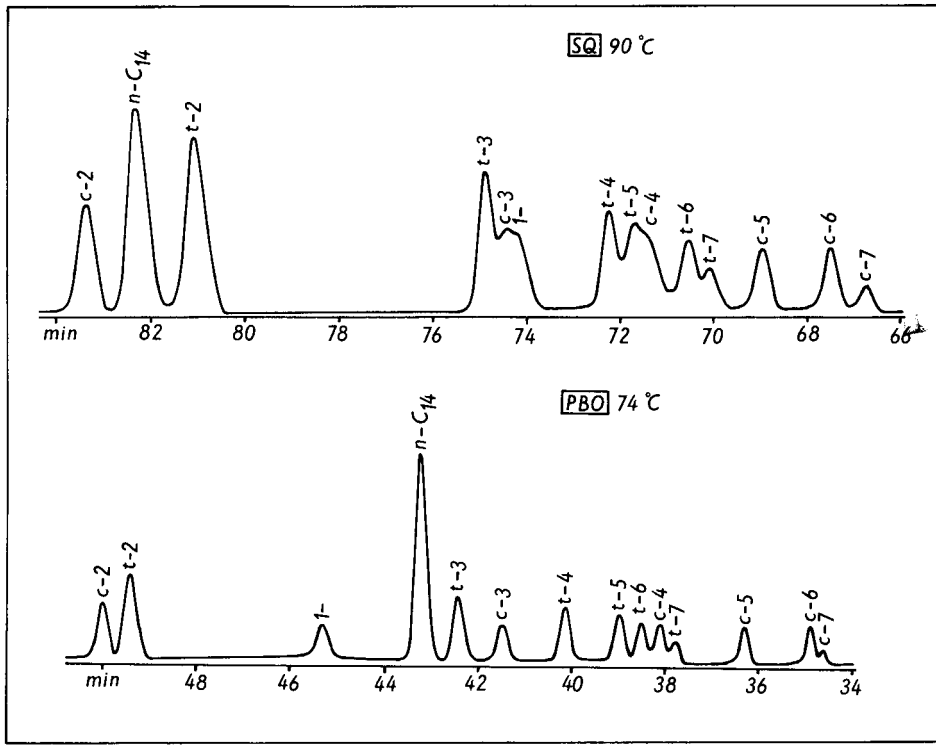

Fig. 2. Trennung von isomeren *n*-Tetradecenen an PBO und Squalan. *c-* = *cis*-, *t-* = *trans*-Isomere. *n*-C_{14} = *n*-Tetradecan.

TABELLE I

RETENTIONSINDICES DER *n*-TRIDECENE UND *n*-TETRADECENE AN PBO UND SQUALAN BEI 74°C UND DIE d*I*/d*T*-WERTE FÜR DEN BEREICH 65–74°C

n-Alkene	*PBO*		*Squalan*	
	I_{74}	dI/dT	I_{74}	$10.dI/dT$
cis-6-Tridecen	1275.2	0.49	1270.1	0.73
cis-5-Tridecen	1278.7	0.46	1272.8	0.70
cis-4-Trridecen	1285.0	0.42	1276.5	0.68
cis-3-Tridecen	1295.3	0.32	1283.5	0.43
cis-2-Tridecen	1319.8	0.02	1301.5	0.38
trans-6-Tridecen	1286.4	0.29	1276.8	0.45
trans-5-Tridecen	1288.1	0.23	1279.0	0.39
trans-4-Tridecen	1291.0	0.21	1279.9	0.25
trans-3-Tridecen	1298.4	0.19	1285.6	−0.05
trans-2-Tridecen	1317.8	0.09	1297.7	0.00
1-Tridecen	1306.4	0.10	1288.7	0.23
cis-7-Tetradecen	1369.9	0.43	1365.5	0.93
cis-6-Tetradecen	1371.0	0.48	1367.4	0.90
cis-5-Tetradecen	1376.4	0.38	1370.9	0.87
cis-4-Tetradecen	1383.0	0.30	1376.8	0.70
cis-3-Tetradecen	1394.7	0.34	1383.4	0.43
cis-2-Tetradecen	1419.5	0.09	1401.6	0.43
trans-7-Tetradecen	1381.7	0.21	1373.6	0.63
trans-6-Tetradecen	1384.4	0.19	1375.0	0.60
trans-5-Tetradecen	1386.0	0.20	1377.8	0.50
trans-4-Tetradecen	1390.0	0.10	1379.1	0.37
trans-3-Tetradecen	1397.5	0.16	1385.2	0.10
trans-2-Tetradecen	1417.9	0.09	1397.7	0.03
1-Tetradecen	1406.3	0.13	1383.4	0.27

kapillaren mit verschiedenen Filmdicken untersucht[6]. Am Beispiel von *cis*-3-Tridecen in Fig. 3 ist zu erkennen, dass die Retentionsindices von *n*-Alkenen praktisch unabhängig vom Kapazitätsverhältnis k (Filmdicke) sind, was auf einen ähnlichen Retentionsmechanismus wie bei den *n*-Alkanen schliessen lässt. Für *n*-Pentylbenzen dagegen wurde eine grosse Abhängigkeit im Bereich kleiner k-Werte gefunden.

Die Chromatogramme zeigen, dass an PBO unter den geschriebenen Versuchsbedingungen alle isomeren *n*-Alkene C_{13} und C_{14} sowei die entsprechenden *n*-Alkane getrennt werden. Im Vergleich mit vorher untersuchten Mesophasen [OBO, 5-n-Heptyl-2-(4-n-nonyloxyphenyl)-pyrimidin (NPP), Cholesterylbutyrat(CHOB)] konnten an PBO bei ähnlicher Auflösung um das 2–3 fache verkürzte Analysenzeiten erzielt werden. Ursache dafür ist hauptsächlich die optimale Filmdicke der stationären Phase und nicht ihre chemische Struktur, was durch einen Vergleich der α-Werte von benachbarte Lageisomeren *n*-Alkenen an PBO und OBO gezeigt werden kann (Tabelle II).

Der Vergleich mit Squalan zeigt die Vorteile der Flüssigkristallkapillare, jedoch ist in Fig. 4 zu erkennen, dass *cis*-7-/*cis*-6-Tetradecen an Squalan besser getrennt werden. Dieser Resultat lässt sich auf der Basis der Alternationseffekts erklären[4]. *cis*-Isomere mit geradzahliger C-Zahl und der Doppelbindung zwischen un-

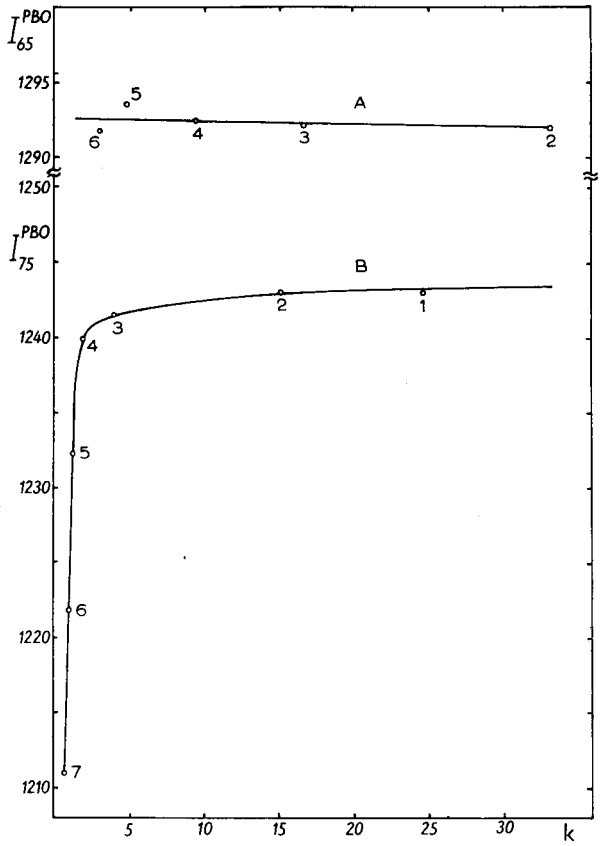

Fig. 3. Abhängigkeit der Retentionsindices von *cis*-3-Tridecen (A) bei 65°C und *n*-Pentylbenzen (B) bei 75°C vom Kapazitätsverhältnis an PBO. Glaskapillaren mit unterschiedlichen Schichtdicken dynamisch belegt: 1 = 20%, 2 = 10%, 3 = 5%, 4 = 2.5%, 5 = 0.8%, 6 = 0.4%, 7 = 0.2% PBO in chloroform.

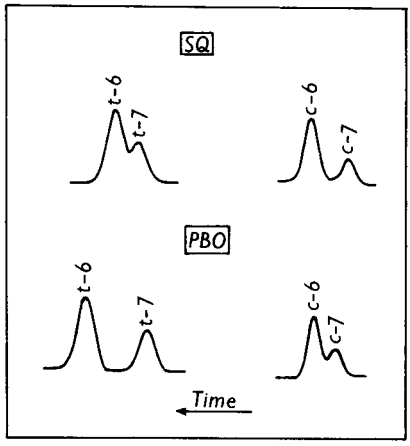

Fig. 4. Vergleich der Trennungen von *cis*-7-/*cis*-6- und *trans*-7-/*trans*-6-Tetradecenen an PBO und Squalan bei 74 C.

TABELLE II

VERGLEICH DER α-WERTE VON BENACHBARTE LAGEISOMEREN *n*-ALKENEN AN PBO, OBO UND SQUALAN (SQ) BEI 74°C

	α_{74}^{OBO}	α_{74}^{PBO}	α_{74}^{SQ}
n-Tridecene			
cis-5-/*cis*-6-	1.028	1.028	1.024
cis-4-/*cis*-5-	1.051	1.050	1.032
cis-3-/*cis*-4-	1.083	1.085	1.061
cis-2-/*cis*-3-	1.211	1.213	1.126
trans-5-/*trans*-6-	1.015	1.013	1.019
trans-4-/*trans*-5-	1.024	1.023	1.007
trans-3-/*trans*-4-	1.057	1.060	1.049
trans-2-/*trans*-3-	1.166	1.165	1.143
n-Tetradecene			
cis-6-/*cis*-7-	–	1.009	1.016
cis-5-/*cis*-6-	–	1.044	1.030
cis-4-/*cis*-5-	–	1.053	1.049
cis-3-/*cis*-4-	–	1.096	1.057
cis-2-/*cis*-3-	–	1.215	1.165
trans-6-/*trans*-7-	–	1.021	1.011
trans-5-/*trans*-6-	–	1.013	1.023
trans-4-/*trans*-5-	–	1.032	1.011
trans-3-/*trans*-4-	–	1.061	1.052
trans-2-/*trans*-3-	–	1.174	1.111

geradzahligen Kohlenstoffketten besitzen eine linearare Struktur und werden daher stärker festgehalten als benachbarte Lageisomere, wodurch sich die Elution des *cis*-7-Tetradecens näher zum *cis*-6-Tetradecen verschiebt.

Bei den entsprechenden *trans*-Isomeren ist die Trennung an PBO besser als an Squalan, da das *trans*-6-Isomere aufgrund seiner linearen Struktur wesentlich später eluiert (geradzahlige C-Zahl und Doppelbindung zwischen geradzahligen Kohlenstoffketten) und damit eine bessere Trennung der Isomere bewirkt wird. Somit zeigen die Ergebnisse, dass der Alternationseffekt die Auflösung positiv oder negativ beeinflussen kann in Abhängigkeit davon, ob lineare Isomere nach oder vor benachbarten Isomeren eluieren. Dieses Resultat ist auch durch Vergleich der α-Werte an Squalan, PBO und OBO in Tabelle II zu erkennen.

SCHLUSSFOLGERUNGEN

Die Trennung aller isomeren *n*-Tridecene und *n*-Tetradecene sowie der korrespondierenden *n*-Alkane an Flüssigkristallkapillaren konnte durch Optimierung der Filmdicke und der Säulentemperatur verbessert werden.

Die Retentionsindices von *n*-Alkenen sind an dieser Trennphase unabhängig von der Filmdicke.

Die positive und negative Beeinflussung der Auflösung benachbarter Lageisomere durch den Alternationseffekt konnte durch Vergleich mit Squalan gezeigt werden.

DANK

Die Autoren danken Herrn Dr. W. Weissflog (Halle) für die Überlassung der stationären Phase.

LITERATUR

1 L. Soják, G. Kraus, I. Ostrovský, E. Královičová und J. Krupčík, *J. Chromatogr.*, 206 (1981) 463.
2 L. Soják, G. Kraus, I. Ostrovský, E. Královičová und J. Krupčík, *J. Chromatogr.*, 206 (1981) 475.
3 L. Soják, G. Kraus, I. Ostrovský, E. Královičová und P. Farkaš, *J. Chromatogr.*, 219 (1981) 225.
4 L. Soják, G. Kraus, I. Ostrovský, und E. Královičová, *J. Chromatogr.*, 234 (1982) 347.
5 W. Weissflog, H. Schubert, S. König, D. Demus und L. Vogel, *J. Prakt. Chem.*, 319 (1977) 507.
6 L. Soják, V. G. Berezkin und J. Janák, *J. Chromatogr.*, 209 (1981) 15.

Journal of Chromatography, 238 (1982) 59–68
Elsevier Scientific Publishing Company, Amsterdam — Printed in The Netherlands

CHROM. 14,555

TRANSITION METAL ION EXCHANGE IN MIXED AMMONIUM–SODIUM X AND Y ZEOLITES

PHILIP FLETCHER and RODNEY P. TOWNSEND*
Department of Chemistry, The City University, Northampton Square, London EC1V OHB (Great Britain)
(Received November 16th, 1981)

SUMMARY

Ion-exchange characteristics of hydrated Cu^{2+}, Co^{2+}, Ni^{2+}, Mn^{2+} and Zn^{2+} ions in synthetic faujasites (X and Y) were examined at 25°C and at a total solution normality of 0.1 g equiv. dm^{-3}.

The original zeolites were samples of X and Y containing both ammonium and sodium ions. Evidence was found confirming earlier observations of significant irreversible binding of transition metals into the zeolites. Sodium ions which could not be removed by repeated exchange of the zeolite with ammonium chloride solution were removed with relative ease by the transition metals, especially copper.

INTRODUCTION

There have been to date several systematic studies on transition metal ion exchange in synthetic zeolites[1–5]. Where comparisons are possible, agreement between sets of experimental and thermodynamic data is not always good, especially in the case of zeolite X[1–3].

It is well known that acid solutions can partly hydrolyse and dealuminate a zeolite[6]. In addition, basic copper salts (under given pH conditions) can especially readily precipitate within the zeolite structure[7,8]. The work described in this paper was originally intended to complement earlier studies[1–3], on X and Y by initially using the ammonium, rather than the sodium, forms of these zeolites. However, it was found[9] not to be possible to prepare homoionic ammonium X and Y by exchange even at elevated temperatures, and the study therefore devolved to a set of ternary exchange studies, involving the ions Na^+, NH_4^+, and a particular transition metal ion. As such, the ease of removal of sodium ions from the type I, I′ and II′ sites in X and Y was found to be strongly dependent on the identity of the incoming transition metal ion.

EXPERIMENTAL

Materials

Synthetic sodium zeolites were supplied by Union Carbide. All metal salts were

0021-9673/82/0000–0000/$02.75

TABLE I

CHEMICAL ANALYSIS OF AMMONIUM–SODIUM ZEOLITES

Zeolite component	*NH_4–Na–X*		*NH_4–Na–Y*	
	%	*mol/100 g*	*%*	*mol/100 g*
SiO_2	38.41	0.6402	50.57	0.8428
Al_2O_3	24.42	0.2394	18.10	0.1766
Fe_2O_3	0.08	0.0005	0.26	0.00163
$(NH_4)_2O$	8.99	0.1728	8.49	0.1633
Na_2O	3.85	0.0628	0.916	0.0148
H_2O	24.02	1.334	22.067	1.226
Total (%)	99.77		100.41	

of AnalaR grade. Equilibrium measurements were made using chloride salts of the transition metals except in the case of copper, where the nitrate was used[10].

Analyses

Zeolite phase. Samples of zeolite were analysed chemically using methods previously described[5].

Solution phase. Sodium was determined by flame photometry in all cases. Transition metals were determined at high concentrations (*i.e.* > 0.005 mol dm^{-3}) by EDTA, and at low concentrations using either atomic absorption spectroscopy or colorimetry.

Preparation of exchanged forms of zeolites

Both zeolites were treated initially with 0.5 mol dm^{-3} solutions of sodium chloride to ensure that the starting materials were homoionic.

Ammonium-exchanged forms of the zeolites were prepared by exhaustive exchange of sodium zeolites at 70°C using 0.5 mol cm^{-3} ammonium chloride solution. The resulting zeolites were washed, then dried at 50°C. All zeolites were equilibrated over saturated sodium chloride solution in desiccators for two weeks prior to chemical analyses.

Complete removal of sodium ion was not achieved with either zeolite (Table I). Conditions could not be found which significantly improved the level of ammonium exchange in X unless the concentration of ammonium salt in solution was raised[9] to a level at which salt imbibition[11] occurs. However, it was observed that the maximum level of ammonium exchange in Y varied with temperature, being 70% at 25°C and *ca.* 90% at 70°C. This is consistent with the recently reported observations of Herman and Bulko[12]. Consequently the starting materials which were used for transition metal exchange contained sodium exchange levels of 27% and 10% for X and Y, respectively.

Maximally exchanged transition metal forms of X and Y were prepared by exhaustively exchanging 3-g samples of the NH_4–Na-zeolite samples with solutions containing 0.2 mol dm^{-3} of transition metal salt. Equilibration over saturated sodium chloride solution took place prior to any analyses. In the case of manganese

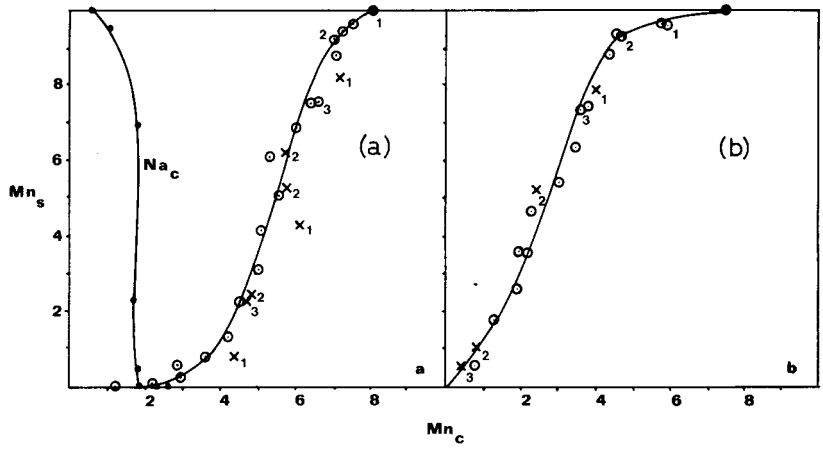

Fig. 1. Exchange isotherms for manganese in (a) X and (b) Y. ○, Forward isotherm points; ×, reverse points; ●, residual sodium content of zeolite.

zeolites this gave rise to a brown coloration in the crystals which has been observed previously in mordenite[5]. Consequently the vapour equilibrium stage was omitted. for manganese-containing zeolites.

Equilibrium studies

All isotherms were constructed at a total solution normality of 0.1 g equiv. dm^{-3} and at a temperature of 25°C. Forward and reverse isotherm points were determined by the procedures previously described[5,10,13]. This involved reverse points being constructed from previously measured forward equilibrium points. Certain systems were found to be ternary in nature due to removal by the transition metal ions of both ammonium and sodium ions from the zeolite. It is emphasised that where ternary exchange took place, the resulting isotherms (Figs. 1–5) are not meant to represent systematic studies of the ternary equilibria, but only a measure of the

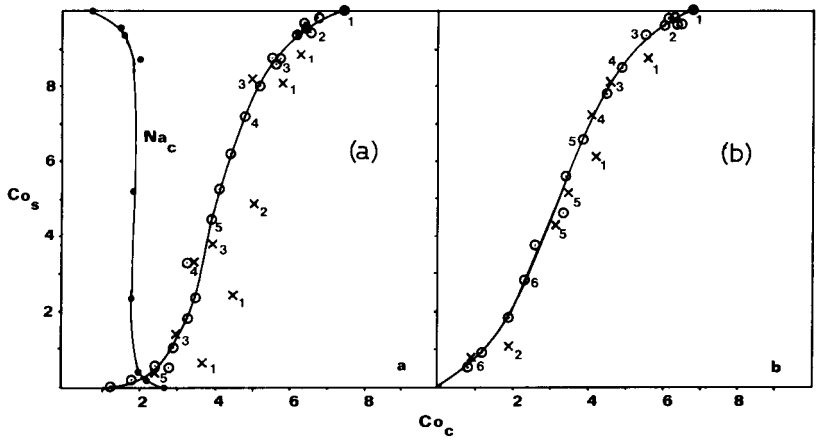

Fig. 2. Exchange isotherms for cobalt in (a) X and (b) Y. Symbols as in Fig. 1.

TABLE II

CHEMICAL ANALYSIS OF X ZEOLITES

Zeolite component	*Co–X*		*Ni–X*		*Cu–X*		*Zn–X*		*Mn–X*	
	%	*mol/100 g*	*%*	*mol/100 g*	*%*	*mol/100 g*	*%*	*mol/100 g*	*%*	*mol/100 g*
SiO_2	35.32	0.5886	34.00	0.582	33.55	0.5592	34.33	0.5722	36.02	0.602
Al_2O_3	22.45	0.220	22.16	0.2172	21.33	0.2091	21.8	0.2137	22.9	0.2245
Fe_2O_3	0.07	0.0004	0.07	0.0004	0.07	0.0004	0.07	0.0004	0.07	0.0004
MO	12.38	0.1650	11.56	0.162	13.11	0.01652	14.22	0.1746	12.98	0.1828
$(NH_4)_2O$	0.98	0.0188	1.9	0.0367	0.0	0.0	1.47	0.0282	1.25	0.024
Na_2O	1.10	0.0177	2.19	0.0353	0.0	0.0	0.703	0.0113	0.73	0.0118
H_2O	28.29	1.571	27.33	1.516	31.96	1.7756	27.64	1.535	26.02	1.446
Total (%)	100.59		99.21		100.02		100.23		99.97	

TABLE III

CHEMICAL ANALYSIS OF Y ZEOLITES

Zeolite component	*Co–Y*		*Ni–Y*		*Cu–Y*		*Zn–Y*		*Mn–Y*	
	%	*mol/100 g*	*%*	*mol/100 g*	*%*	*mol/100 g*	*%*	*mol/100 g*	*%*	*mol/100 g*
SiO_3	46.39	0.7732	46.82	0.7803	46.21	0.7702	45.64	0.7606	49.31	0.8215
Al_2O_3	16.61	0.1483	16.75	0.1642	16.54	0.1622	16.38	0.1620	17.64	0.1729
Fe_2O_3	0.25	0.00157	0.25	0.00157	0.25	0.00157	0.25	0.00157	0.25	0.00157
MO	7.38	0.1010	8.496	0.1133	9.39	0.1183	10.27	0.1267	9.29	0.1297
$(NH_4)_2O$	1.72	0.0331	1.936	0.0372	0.0	0.0	1.41	0.0271	0.646	0.0315
Na_2O	0.679	0.0109	0.798	0.0130	0.0	0.0	0.710	0.0113	0.738	0.0119
H_2O	27.25	1.514	25.13	1.396	27.86	1.548	25.91	1.439	21.454	1.1918
Total (%)	100.28		100.19		100.25		100.57		99.33	

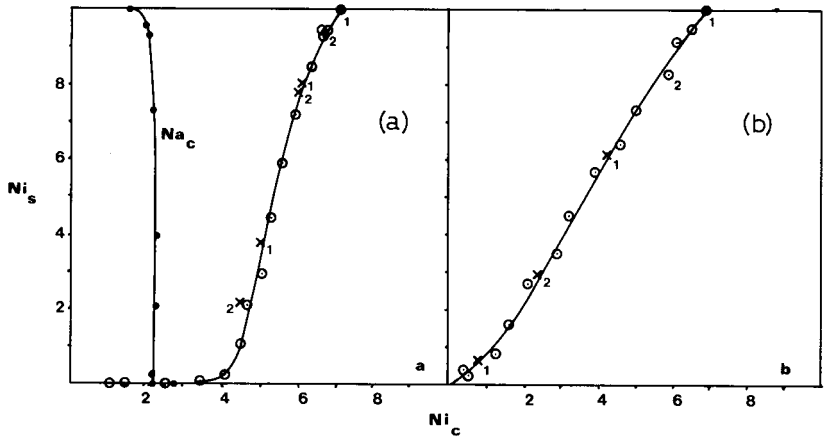

Fig. 3. Exchange isotherms for nickel in (a) X and (b) Y. Symbols as in Fig. 1.

sodium removal that took place with increasing transition metal ion loadings.

In order to confirm that crystallinity of all zeolite samples was retained throughout the exchange procedures, samples of both original and final materials were subjected to powder X-ray analyses.

RESULTS

Chemical analysis data for all the exchanged zeolites are given in Tables I–III. Ion-exchange isotherms for each transition-metal ion in X and Y, respectively, are represented in Figs. 1–5. Reverse isotherm points, which were obtained using the "wet method" described in detail elsewhere[5,10], are related to their corresponding forward points by numbers. In only two cases (manganese and nickel in Y, Figs. 1a and 3a, respectively) did the systems appear to be reversible. In the majority of cases, the isotherms were clearly not reversible, or reversibility could not be proved un-

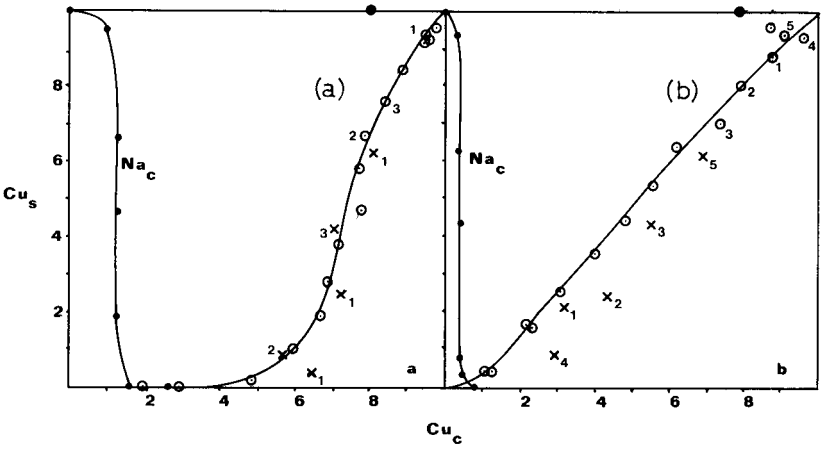

Fig. 4. Exchange isotherms for copper in (a) X and (b) Y. Symbols as in Fig. 1.

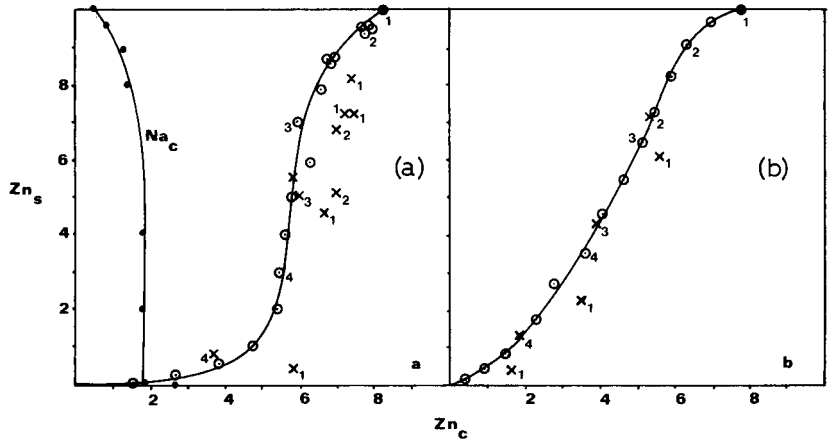

Fig. 5. Exchange isotherms for zinc in (a) X and (b) Y. Symbols as in Fig. 1.

ambiguously. Therefore, no attempt was made to calculate standard free energies for these systems. ΔG^{θ} values for the apparently reversible Mn $\rightleftharpoons$ NH_4–Y and Ni $\rightleftharpoons$ NH_4–Y exchanges were calculated to be 5.14 and 2.33 kJ (equiv.)$^{-1}$, respectively. Comparing data for any transition-metal ion in Figs. 1–5 shows that in general irreversibility was much more marked in X than in Y.

DISCUSSION

Isotherm characteristics

The characteristic feature common to all exchange isotherms (Figs. 1–5) is the sigmoidal shape. The partial irreversibility, which was observed in most cases, is generally especially obvious at high levels of exchange for the transition metal. The sodium contents of the zeolites as a function of transition metal ion loadings are also shown in Figs. 1–5. For zeolite X, reversibility apparently occurred throughout the region where the sodium content decreases very little with increasing transition metal content (*i.e.* in the middle part of the isotherm). In this region transition metals must be predominantly exchanging with ammonium ions that are in sites accessible to the ammonium ion at 25°C.

A consideration of the sodium content of the original NH_4–Na–X sample gives some insight into the nature of the transition metal exchanges. It is probable that in zeolite X *ca.* 10% of the exchangeable component consisted of sodium ions residing in the SII sites in the main channels[9]. In support of this it has been shown that certain ions may be exhaustively exchanged into the main channels of synthetic faujasites without complete removal of the sodium ions originally resident in those sites[14]. In contrast it is likely that the NH_4–Na–Y sample contained sodium ions in the sodalite cages and hexagonal prisms only[9,12].

Inspection of the isotherms for zeolite X (Figs. 1–5) shows that even at low levels of transition metal ion loadings exchange involved removal of sodium that was not removed by ammonium ions even at 70°C. The initial exchange in of Cu^{2+}, Co^{2+}, Zn^{2+}, and Mn^{2+} ions apparently involves removal of the amount of sodium that is

expected to reside in the main channels[9,14], indicating, as expected, that ion exchange is confined to these sites. At higher levels of exchange, transition metals appear to remove sodium ions from within the sodalite units and hexagonal prisms. This may occur either by the transition metal ions passing through the oxygen windows and entering those sites, or by migration of the sodium ions out of their original sites, without the entering transition metal ions moving into the vacated sites. The process of penetration of transition metals into the SI, SI′ and SII′ sites requires substantial removal of the hydration shell of the divalent ion. Having once passed through however, the ions are in an environment in which coordination to lattice oxygens is possible. Evidence has been given for the presence of Cu^{2+} in the SI and SII′ sites in X[15]. In the case of Ni^{2+} exchange in X the level of sodium removed indicates that the nickel may be confined to the main channels. This is entirely consistent with the conclusions of Maes and Cremers[1] who used as the starting material homoionic Na–X.

In contrast to zeolite X, ion exchange of transition metals in Y induces removal of sodium ions only in the case of Cu^{2+}. The fact that sodium is removed from Y at low levels of Cu^{2+} occupancy (Fig. 4) suggests penetration of Cu^{2+} into the network of smaller cavities, even at low copper content[16].

The irreversibility observed in the cases of Co^{2+} and Zn^{2+} exchange in Y may not be an intrinsic property of these systems, but rather merely due to exchange also occurring with ammonium ions that had been forced into the zeolite at elevated temperatures (70°C; see preparative procedures) and which reside in sites that are not freely accessible to ammonium ions at 25°C. This again suggests that for these metal ions exchange is predominantly confined to the main channels at 25°C, with penetration into the small cavities occurring at higher transition metal loadings.

Maximum levels of exchange

The maximum levels of exchange obtained for Mn^{2+}, Co^{2+}, Ni^{2+}, Cu^{2+} and Zn^{2+} ions in mixed NH_4–Na–X were 81%, 75%, 71%, 79% and 82%, respectively (Table II). Zeolites containing manganese and zinc appear to be the only ones where stoichiometric exchange is observed. The limit observed after exhaustive re-exchange in Cu–X is totally inconsistent with the isotherm shape (Fig. 4), being lower than the value of 100% exchange that would be deduced by extrapolating the forward isotherm. Although the apparent exchange level was less than 100%, total analysis of Cu–X (Table II), nevertheless indicated complete removal of Na^+ and NH_4^+ from the zeolite. This observation has been reported previously[1,10]. The exchange involving cobalt in X was similar (*i.e.* non-stoichiometric) but occurred to a lesser extent. In contrast, analysis of Ni–X showed *more* equivalents of nickel in the zeolite than the total equivalents of sodium and ammonium that had been removed during exchange. This suggests that some precipitation of basic nickel salts into the zeolite framework had taken place.

Table III shows that stoichiometric exchange was observed with most of the transition metals in zeolite Y. Copper(II) is the one exception to this, low levels of copper in the zeolite again being observed on exhaustively re-exchanging a sample of NH_4–Na–Y.

The low levels of copper and cobalt in the zeolites after exhaustive exchange may be attributed to the acidic nature of the transition metal ion solutions. Uyt-

TABLE IV

IRREVERSIBLY BOUND TRANSITION METAL IN X AND Y

Transition metal ion, M	*Equivalent fraction M_C, irreversibly bound in*	
	Zeolite X	*Zeolite Y*
Mn^{2+}	0.003	0.001
Co^{2+}	0.048	0.004
Ni^{2+}	0.101	0.002
Cu^{2+}	0.213	0.038
Zn^{2+}	0.005	0.002

terhoeven[17] has suggested a mechanism for the reduction in the exchange capacity of a zeolite upon exchange with H_3O^+. Hydrogen ions are considered to be directly incorporated into the zeolite[17] with consequent reduction of the exchange capacity, without removal of the aluminiums from the structure. It then follows that the less acidic cobalt(II)[5] should exhibit this phenomenon to a lesser extent than copper(II), as is observed.

In order to assess whether or not the transition metals were irreversibly bound into the zeolite structures (as has been observed in the case of transition metals into pure Na–X and Na–Y[1,18]) samples of transition metal exchanged zeolites were next exhaustively re-exchanged with first ammonium nitrate (0.5 mol dm^{-3}) and then sodium nitrate (0.5 mol dm^{-3}) solutions.

The resulting samples were analysed for transition metal ion content. The results are shown in Table IV, where it is seen that copper(II) is irreversibly bound into both zeolite X and Y. Nickel(II) and cobalt(II) are also bound to a considerable extent in zeolite X although only trace amounts of these two metals remained in Y. The observed irreversible binding of nickel into X throws some doubt onto the apparent reversibility of the isotherm (Fig. 3).

Although the Mn–X (Fig. 1) and the Zn–X and Zn–Y (Fig. 5) isotherms appear to be partially irreversible, analysis indicated that stoichiometric exchange occurred (Tables II and III). In addition, there was no indication of irreversible binding of these metals into either zeolite (Table IV). This is, however, consistent with the fact that Mn^{2+} and Zn^{2+} show a less acidic reaction in solution than do Co^{2+}, Ni^{2+} or Cu^{2+} and are less susceptible to hydrolysis and precipitation[5].

It seems apparent that, as with Na–X and Na–Y[1], exchange of transition metals into NH_4–X and NH_4–Y not only involves stoichiometric exchange but also hydrolysis and precipitation problems. Some disruption of the lattice structure may also have occurred[17], but no direct evidence bearing on the matter was found in this work. It is, however, significant that in this study uncertainties regarding both reversibility and maximum levels of exchange were far more evident with X than Y, since zeolite Y has a much greater stability towards acid hydrolysis[6].

Final remarks

From the isotherms, the general selectivity sequence for NH_4–X is seen to be $Co < Mn < Zn < Ni \approx Cu$, although this sequence changes at low transition metal ion loadings. The selectivity trend for zeolite Y is not so clear, but careful analysis

shows it to be Mn < Co < Cu ≈ Zn ≈ Ni. Unfortunately the ambiguities over maximum levels of exchange and the apparent irreversibilities make a detailed analysis of selectivity data inappropriate. However, greater selectivity is exhibited for a given transition metal ion by X than by Y. This is in conformity with simple dielectric theory[10,13] and also with the trends observed by previous workers using sodium X and Y. In many previous studies[1–3] the reversibility and stoichiometry of exchange were not tested in detail. Consequently it is difficult to assess whether or not the differences in exchange characteristics that have been observed for the same equilibria[1–3,17] are due to the problems of hydrolysis and precipitation that have been emphasized in this paper. Indeed the variability in measured ΔG^{θ} values for the transition metal exchanges in X in previously reported studies[1–3,16] may well be ascribed to the ambiguities in the maximum level of exchange.

A general principle is that stoichiometric reversible exchange of transition metals in zeolites is most likely when transition metal ions of low acidity exchange into zeolites having a high Si:Al ratio. Thus Barrer and Townsend[5] examined transition metal ion exchange in synthetic mordenite and complete reversibility and stoichiometry was observed. Conversely, it would therefore be expected that transition metals exchanging into zeolite A should exhibit serious non-stoichiometry of exchange, together with irreversible binding of these metal ions within the structure[19,20]. Gal *et al.*[4] have measured the exchange of Co^{2+}, Ni^{2+}, Zn^{2+} and Cd^{2+} ions in Na–A. Their analytical data for the transition metal exchanged zeolites show a lower cobalt content in the zeolite than would be expected from the observed aluminium and sodium content, whereas Ni–A contained more nickel than expected. Their analyses of Zn–A showed that near-stoichiometric exchange had taken place. These results conform well with the results and conclusions in this present study on faujasites.

ACKNOWLEDGEMENTS

We acknowledge the support and interest of British Gas throughout this programme, and one of us (P.F.) thanks British Gas for a Scholarship.

REFERENCES

1 A. Maes and A. Cremers, *J. Chem. Soc., Farad. Trans. I*, 71 (1975) 265.
2 I. J. Gal and P. Radovanov, *J. Chem. Soc., Farad. Trans. I*, 71 (1975) 1671.
3 G. Gallei, D. Eisenbach and A. Ahmed, *J. Catal.*, 33 (1974) 62.
4 I. J. Gal, O. Janković, S. Malcić, P. Radovanov and M. Todorović, *Trans. Faraday Soc.*, 67 (1971) 999.
5 R. M. Barrer and R. P. Townsend, *J. Chem. Soc., Farad. Trans. I*, 72 (1976) 662.
6 C. V. McDaniel and P. K. Maher, in *Zeolite Chemistry and Catalysis*, ACS Monograph, No. 171, 1976, p. 283.
7 K. G. Ione, N. N. Bobrov, G. K. Boreskov and L. A. Vostrikova, *Dokl. Akad. Nauk. SSSR*, 210 (1973) 388.
8 N. G. Maksimov, K. G. Ione, V. F. Anufrienko, P. N. Kuznetsov, N. N. Bobrov and K. G. Boreskov, *Dokl. Akad. Nauk SSSR*, 217 (1974) 135.
9 P. Fletcher and R. P. Townsend, *J. Chem. Soc., Farad. Trans. I*, 78 (1982) in press.
10 P. Fletcher and R. P. Townsend in L. V. C. Rees (Editor) *Proc. 5th Int. Conference on Zeolites, Naples, June 1980*, Heyden & Son, London, 1980, p. 311.
11 R. M. Barrer and A. J. Walker, *Trans. Faraday Soc.*, 60 (1964) 171.
12 R. G. Herman and J. B. Bulko, in W. H. Flank (Editor) *Adsorption and Ion Exchange With Synthetic*

Zeolites, ACS Symposium Series No. 135, American Chemical Society, Washington, DC, 1980, p. 177.
13 P. Fletcher and R. P. Townsend, *J. Chem. Soc., Farad. Trans. I*, 77 (1981) 497.
14 M. L. Costenoble, W. J. Mortier and J. B. Uytterhoeven, *J. Phys. Chem.*, 77 (1973) 2880.
15 W. De Wilde, R. A. Schoonheydt and J. B. Uytterhoeven in *Fourth Int. Conference on Molecular Sieves*, ACS Symposium Series No. 40, American Chemical Society, Washington, DC, 1977, p. 132.
16 F. H. Cano, J. Marti and J. Soria, *Advan. Chem. Ser.*, 121 (1973) 230.
17 J. B. Uytterhoeven, L. G. Christner and W. K. Hall, *J. Phys. Chem.*, 69 (1965) 2117.
18 P. P. Lai and L. V. C. Rees, *J. Chem. Soc., Farad. Trans. I*, 72 (1976) 2650.
19 L. B. McCusker and K. Seff, *J. Phys. Chem.*, 85 (1981) 405.
20 H. S. Lee and K. Seff, *J. Phys. Chem.*, 85 (1981) 379.

Journal of Chromatography, 238 (1982) 69–74
Elsevier Scientific Publishing Company, Amsterdam — Printed in The Netherlands

CHROM. 14,530

REACTIVE POLYMERS

XLI. EFFECT OF THE CONTENT AND DISTRIBUTION OF POLAR GROUPS ON THE POLARITY OF GLYCIDYLMETHACRYLATE POLYMERIC SORBENTS

J. LUKÁŠ*, F. ŠVEC and J. KÁLAL
Institute of Macromolecular Chemistry, Czechoslovak Academy of Sciences, 162 06 Prague 6 (Czechoslovakia)
and
B. JEŽEK
The J. Heyrovský Institute of Physical Chemistry and Electrochemistry, Czechoslovak Academy of Sciences, 118 40 Prague 1 (Czechoslovakia)

(Received November 9th, 1981)

SUMMARY

Photoelectron spectroscopy has revealed that the distribution of polar groups (carboxylic and epoxy groups) in macroporous copolymers based on glycidylmethacrylate (GMA)–ethylene dimethacrylate (EDMA) is not uniform, but that their concentration increases starting from the surface towards the centre of the globules. Heat treatment of these copolymers gives rise to conformational changes, which in turn cause an increase in the concentration of polar groups on the surface of the globules, and thus also a rise in polarity.

Differences between the modified Rohrschneider constants on the copolymers GMA–EDMA and methyl methacrylate (MMA)–EDMA were used in order to evaluate the participation of epoxy groups in the overall polarity of glycidylmethacrylate polymeric sorbents.

INTRODUCTION

Sorbents based on macroporous copolymers GMA–EDMA are polymeric beads which consist of more or less regular agglomerates of so-called globules[1]. Their physical and specific chromatographic properties[2] which can be modified by polymer-analogous reactions[3] or heat treatment[4] have been reported in the literature.

The polarity of GMA sorbents has been expressed using the modified Rohrschneider method[2–5]. The modification consists in the replacement of a standard stationary phase (squalane) with a non-polar adsorbent Carbopack B, the porosity and specific surface of which are close to the values of these copolymers. A similar

0021-9673/82/0000–0000/$02.75

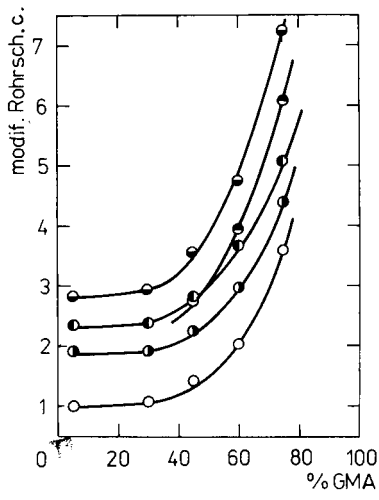

Fig. 1. Effect of GMA content on the polarity of GMA–EDMA copolymers expressed through the modified Rohrschneider constants. ○, x' values (benzene); ◐, y' values (ethanol); ◑, z' values (methyl ethyl ketone); ◒, u' values (nitromethane); ◓, s' values (pyridine).

procedure was employed by Lindsay Smith *et al.*[6] in order to modify the McReynolds constants in the characterization of the selectivity of aromatic copolymers.

In this paper, the relationships existing between the concentration of polar groups, their distribution in the surface layer of the globules and the polarity of sorbents are elucidated using photoelectron spectroscopy (XPS).

EXPERIMENTAL

Photoelectron spectroscopy

Measurements were performed with an ESCA 3 Mark II photoelectron spectrometer (VG Scientific, Great Britain) using Al-K_α (1486.6 eV) radiation. Copolymer samples were ground in an agate dish and deposited in thin layers on double-sided Scotch tape on a holder. The signal intensities of electrons, from levels C_{1s}, O_{1s}, O_{2s}, were determined at $1 \cdot 10^{-6}$ Pa and at angles between the planes of the samples surface and the electron escape into the inlet slit of the analyser (Θ) 20, 40, 60 and 80°.

Gas chromatography

The values of the modified Rohrschneider constants for the basic series of copolymers GMA–EDMA (Fig. 1) were taken from an earlier paper[2]; the same procedure was also employed in the determination of these constants for the samples of the MMA–EDMA copolymers.

RESULTS AND DISCUSSION

In an earlier paper[2] we determined the polarity of the basic series of the polymeric sorbents GMA–EDMA. Fig. 1 shows that the GMA content has a decisive influence on the polarity of the copolymers. Up to a GMA content of *ca.* 40% the

TABLE I

O/C MOLAR RATIO IN GMA–EDMA COPOLYMERS DETERMINED AT VARIOUS ANGLES OF ELECTRON ESCAPE (Θ)

Θ (°)	*Composition of GMA–EDMA copolymers (%, w/w)*				
	5:95	*30:70*	*45:55*	*60:40*	*75:25*
20	0.354	0.364	0.359	0.369	0.368
40	0.377	0.373	0.370	0.382	0.384
60	0.379	0.376	0.380	0.385	0.388
80	0.382	0.373	0.381	0.390	0.383
Theoretical*	0.401	0.408	0.413	0.417	0.421

* Calculated stoichiometrically from the composition of copolymers.

polarity does not vary very much, and a steep rise appears only beyond this value. Such a non-linear dependence could be explained by using XPS spectra of these copolymers recorded at various angles between the plane of the sample and the electron escape (Θ) into the slit of the analyser. The copolymer particles were used in the XPS measurements in a pulverized state. It was found microscopically that only the particular agglomerates of the globules can be separated by rubbing, but that no destruction of globules takes place. Because of the small dimensions of the globules (68–80 nm) the deposited layer of the pulverized copolymer can be regarded as sufficiently smooth for the XPS measurements. The spectra provided information on the composition of the surface layer of the globules approximately to a depth of 18 nm[7]. This depth represents roughly 20–25 % of the diameter of the globule. Table I shows the theoretical molar oxygen: carbon ratios determined at various Θ angles for copolymers having various GMA–EDMA compositions. The results indicate that the oxygen content on the surface of the globules is always lower compared with the theoretical results obtained from the stoichiometric composition of the copolymers and that it increases with increasing angle Θ (and hence with the depth of the recorded spectrum). This means that there exists a concentration of oxygen in the direction from the surface to the centre of the globules. Some decrease in O/C should be assigned at the expense of the so-called contamination carbon deposited on the sample surface in the course of the measurement. However, the overall effect cannot be attributed merely to the effect of this carbon, as the existence of the concentration gradient of oxygen in the globules can be proved also be determination of the intensities of signals of oxygen electrons from the 1*s* and 2*s* levels. For the individual copolymers this ratio varies between 16.8 and 21.4, while theoretically it should correspond to the ratio of the effective cross-sections of the given lines multiplied by factors depending on the kinetic energy of the electrons (mean free path of the electrons, + transmission of the analyser), amounting to 25.9. The determined lower values compared with the theoretical ones indicate a relatively stronger O_{2s} electron signal which, owing to their higher kinetic energy and hence also a longer mean free electron path, comes from a greater depth.

The composition heterogeneity of the individual globules is closely connected with the physicochemical properties of both copolymerizing monomers. It has been

TABLE II

O/C MOLAR RATIO IN THE INITIAL AND THERMALLY TREATED GMA–EDMA COPOLYMERS DETERMINED AT VARIOUS ANGLES OF ELECTRON ESCAPE (Θ)

GMA–EDMA (%, *w/w*)	*Heat treatment*		Θ (°)			
	(°C)	(h)	20	40	60	80
45:55*	–	–	0.359	0.370	0.380	0.381
45:55	280	1	0.391	0.395	0.393	0.389
45:55	250	4	0.384	0.392	0.389	0.380
60:40*	–	–	0.369	0.382	0.385	0.390
60:40	250	2	0.387	0.396	0.379	0.379
60:40	260	2	0.398	0.403	0.397	0.393

* Initial copolymers.

demonstrated[8] that the double bond of GMA is more reactive and thus polymerizes more quickly. Thus, at the very beginning of polymerization at a low GMA concentration in the polymerization mixture the polymer molecules formed are richer in GMA and form a nucleus which later gives rise to a globule. These nuclei continuously increase in volume owing to the proceeding copolymerization in which GMA is more quickly removed from the system and the mixture of monomers becomes richer in EDMA. In the final stage it is mainly EDMA that remains, and the surface layer of the globules consists predominantly of a polymer rich in EDMA. If the GMA content in the mixture is higher than 40% (w/w), no such marked loss of GMA occurs in the mixture, because reactivity parameters of the two monomers do not differ much from each other and the globules become more homogeneous. The higher content of GMA units appears also on the surface, which in the case where the copolymers are utilized in chromatography facilitates interactions between polar groups and molecules of the sorbents. A further rise in the GMA content will be reflected in an essential rise in polarity.

The heat treatment of the GMA–EDMA copolymers in which the basic mono-

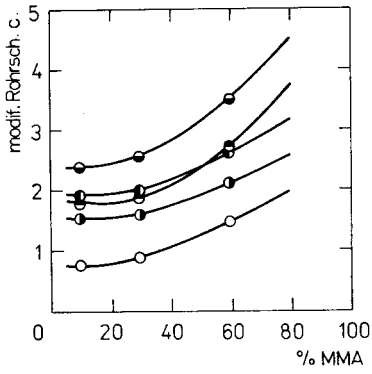

Fig. 2. Effect of MMA content on the polarity of MMA–EDMA copolymers expressed through the modified Rohrschneider constants. Sorbates denoted as in Fig. 1.

TABLE III

INCREMENTS OF MODIFIED ROHRSCHNEIDER CONSTANTS EXPRESSING THE PARTICIPATION OF EPOXY GROUPS OF GLYCIDYL-METHACRYLATE UNITS ($-\overline{CH-CH_2}O$) IN THE COPOLYMER IN SPECIFIC INTERACTIONS WITH MOLECULES OF THE SORBATES

GMA content in the copolymer (% w/w)	$\Delta(\Delta I)_{x'} \cdot 10^{-2}$ (%)		$\Delta(\Delta I)_{y'} \cdot 10^{-2}$ (%)		$\Delta(\Delta I)_{z'} \cdot 10^{-2}$ (%)		$\Delta(\Delta I)_{u'} \cdot 10^{-2}$ (%)		$\Delta(\Delta I)_{s'} \cdot 10^{-2}$ (%)	
10	0.22	(22.2)	0.42	(18.1)	0.33	(17.7)	0.44	(15.6)	–	–
20	0.23	(22.5)	0.44	(18.8)	0.33	(17.6)	0.46	(16.0)	–	–
30	0.22	(21.0)	0.46	(19.3)	0.34	(17.9)	0.47	(16.0)	–	–
40	0.26	(22.2)	0.46	(17.7)	0.37	(18.0)	0.48	(15.0)	–	–
50	0.48	(32.7)	0.86	(28.7)	0.71	(29.8)	1.01	(26.2)	0.99	(32.7)
60	0.94	(46.8)	1.47	(40.8)	1.25	(42.7)	1.93	(39.4)	1.80	(46.2)
70	1.73	(59.2)	2.05	(46.1)	1.88	(49.9)	3.07	(48.0)	2.78	(52.5)

mers (GMA in the first place) are split off yielded sorbents which surprisingly possessed a higher polarity[4]. Table II clearly demonstrates that the oxygen concentration in the surface layer of the globules is higher in the thermally treated samples than in the initial ones, and even that it increases towards the surface (lower values at $\Theta = 20°$ are probably affected by the contamination carbon). This means that, during heat treatment, migration of the copolymer chains gives rise to conformational changes leading to a rise in polarity. The results of measurements by the XPS method demonstrate that the polarities of sorbents based on GMA–EDMA are determined not only by the content of carboxylic and epoxy groups, but also by the orientation of these groups inside the globules.

For comparison, we determined the effect of the MMA content in a series of MMA–EDMA copolymers on their polarity. It can be seen from Fig. 2 that with increasing MMA content no pronounced discontinuity appears in the dependence as is the case with GMA. Bearing in mind that the glycidylmethacrylate unit in the copolymer differs from the methyl methacrylate unit only in the epoxy end group ($-\overline{CH}-\overline{CH_2O}$), it is obvious that this epoxy group is the cause underlying the much higher polarity of copolymers of the GMA type. From the differences between values of the modified Rohrschneider constants of GMA and MMA copolymers (by using the graphic displays in Figs. 1 and 2), it is possible to obtain increments for the individual contents of monomers which represent the participation of epoxy end-groups in specific interactions with the individual types of molecules of the sorbates (Table III). Also, these results confirm that the effect of epoxy groups on polarity becomes markedly apparent at a GMA content in the copolymer of $>40\%$ (w/w). The participation of epoxy groups in the overall polarity suggests that their interaction is strongest with sorbates containing free π-electrons (benzene–x', pyridine–s'). On the contrary, in specific interactions of GMA copolymers with nitromethane (u'), which are the strongest (*cf.* Fig. 1), the epoxy groups alone participate to a smaller extent.

REFERENCES

1 Z. Pelzbauer, J. Lukáš, F. Švec and J. Kálal, *J. Chromatogr.*, 171 (1979) 101.
2 J. Lukáš, F. Švec and J. Kálal, *J. Chromatogr.*, 153 (1978) 15.
3 J. Lukáš, F. Švec, E. Votavová and J. Kálal, *J. Chromatogr.*, 153 (1978) 373.
4 J. Lukáš, E. Votavová, F. Švec, J. Kálal and M. Popl, *J. Chromatogr.*, 194 (1980) 297.
5 J. Lukáš, *J. Chromatogr.*, 190 (1980) 13.
6 J. R. Lindsay Smith, A. H. H. Tameesh and D. J. Waddington, *J. Chromatogr.*, 151 (1978) 21.
7 P. Cadman, G. Gossedge and J. D. Scott, *J. Electron Spectrosc. Relat. Phenom.*, 13 (1978) 1.
8 D. Horák, F. Švec, C. M. A. Ribeiro and J. Kálal, *Angew. Makromol. Chem.*, 87 (1980) 127.

Journal of Chromatography, 238 (1982) 75–87
Elsevier Scientific Publishing Company, Amsterdam — Printed in The Netherlands

CHROM. 14,603

RETENTIONSVERHALTEN DER HAUPTKOMPONENTEN DER LAVENDEL- UND LAVANDINÖLE AN VERSCHIEDENEN STATIONÄREN PHASEN IN ABHÄNGIGKEIT VON DER SÄULENTEMPERATUR

R. BENECKE* und H. THIEME
Sektion Biowissenschaften der Karl-Marx-Universität Leipzig, Brüderstr. 34, 7010 Leipzig (D.D.R.)
und
Sz. NYIREDY
Institut für Pharmakognosie der Semmelweis Medizinischen Universität Budapest, Üllöi út 26, 1085 Budapest (Ungarn)
(Eingegangen am 9. Dezember 1981)

SUMMARY

Effect of the column temperature on the retention behaviour of major components of lavender and lavandin oils on various stationary phases

For the gas chromatographic characterization of lavender and lavandin oils the retention indices of 17 major components were determined on OV-101, QF-1 and Carbowax 1500 columns at different column temperatures as well as during temperature programming. The difference in temperature dependence of the retention indices caused a change in the sequence of the peaks of some substances when the column temperature was varied. The magnitude of the temperature coefficient appeared to be correlated not only with the molecular structure but also with the interaction between the polarity of substance and stationary phase.

EINLEITUNG

Lavendel- und Lavandinöle sind in ihrer Zusammensetzung sehr ähnlich; wertbestimmende Komponente ist Linalylacetat. Beide Öle lassen sich auf Grund der unterschiedlichen Konzentrationen an Campher und 1,8-Cineol gaschromatographisch (GC) differenzieren[1].

Im Zusammenhang mit der Auswahl einer geeigneten stationären Phase für die GC-Bestimmung des Gehalts an Linalylacetat, Campher und 1,8-Cineol im officinellen Lavendelöl prüften wir unter Verwendung gepackter Trennsäulen eine Reihe von Trennflüssigkeiten unterschiedlicher Polarität, die z.T. auch in der Literatur zur Analyse von Lavendelöl vorgeschlagen werden[1]. In der vorliegenden Arbeit soll über das Retentionsverhalten von 17 Hauptkomponenten vergleichsweise an OV-101, QF-1 und Carbowax 1500 berichtet werden. Aus den McReynolds-Konstanten[2] bzw. der Retentionspolarität[3] dieser Phasen ist ersichtlich, dass sie einen weiten Polaritäts-

0021-9673/82/0000–0000/$02.75

bereich überspannen. Zur Charakterisierung und Identifizierung der Substanzen wurden die Retentionsindices sowohl isotherm bei unterschiedlichen Säulentemperaturen als auch bei temperaturprogrammierter Arbeitsweise bestimmt, da sich letztere für die qualitative und quantitative Analyse der ätherischen Öle auf Grund der grossen Siedepunkts-, Polaritäts- und Konzentrationsbereiche ihrer Komponenten notwendig macht.

Die Beobachtung, dass einige Substanzpaare in Abhängigkeit von der Säulentemperatur in unterschiedlicher Weise voneinander getrennt wurden und es dabei z.T. zu einer Änderung iher Elutionsreihenfolge kam, sollte an Hand der Temperaturabhängigkeit der Retentionsindices erklärt und für die Charakterisierung der Komponenten genutzt werden, was uns besonders für die Bestimmung des Camphers interessierte.

EXPERIMENTELLES

Die Untersuchungen erfolgten an einem Hochtemperatur-Gaschromatographen GC-HF-18.3 (VEB Chromatron, D.D.R.) bei folgenden Bedingungen: Säule, Rasotherm-Glas, 2 m × 3 mm I.D.; Füllung, Chromosorb W-AW-DMCS (80–100 mesh), imprägniert mit jeweils 10% stationärer Phase; Trägergas, Argon, optimale Strömungsgeschwindigkeit bei 30–40 ml/min; Detektor, Flammenionisationsdetektor.

Zur Bestimmung der Retentionsindices wurden Säulentemperatur und Probenmenge so gewählt, dass symmetrische Peaks mit angemessenen Retentionszeiten resultierten und letztere nicht von der Probenmenge beeinflusst wurden. Alle Arbeitsbedingungen wurden so weit wie möglich konstant gehalten. Die Messung der Retentionszeiten erfolgte manuell mit elektronischer Stoppuhr. Zur Ermittlung der Nettoretentionszeit wurde die Totzeit an Hand dreier aufeinanderfolgender *n*-Alkane errechnet[4]. Die Berechnung der Retentionsindices aus den Retentionszeiten erfolgte nach Kováts[5]. Die Reproduzierbarkeit betrug ±2–3 Indexeinheiten an den polaren Phasen und ±1 Indexeinheit an OV-101. Die Retentionsindices für die temperaturprogrammierten Analysen wurden mit Hilfe der Retentionstemperaturen berechnet[6]. Der Messfehler wird auf ±7–10 Indexeinheiten geschätzt.

An jeder stationären Phase wurden die Retentionsindices für 3–4 unterschiedliche Temperaturen bestimmt. Die in den Tabellen I–III angegebenen Werte wurden aus drei bis fünf Bestimmungen gemittelt.

ERGEBNISSE UND DISKUSSION

Von den eingesetzten Trennflüssigkeiten unterschiedlicher Polarität erwies sich unter den gegebenen Arbeitsbedingungen nur QF-1 als geeignete Phase zur optimalen Trennung der für die Bewertung der Öle interessierenden Komponenten. Wie Fig. 1 zeigt, werden bei temperaturprogrammierter Arbeitsweise sowohl Linalylacetat und Campher von den Alkoholen Linalool, Lavandulol, Borneol usw. als auch 1,8-Cineol von den Terpenkohlenwasserstoffen gut getrennt. Polare Phasen, wie Carbowax 1500 und Carbowax 20M, führten dagegen weder zu einer vollständigen Trennung von Linalylacetat und Linalool noch zur Abtrennung des 1,8-Cineols von *cis*-Ocimen. Mit OV-101 und ähnlich apolaren Phasen (SE-30, DC-200) war zwar die Bestim-

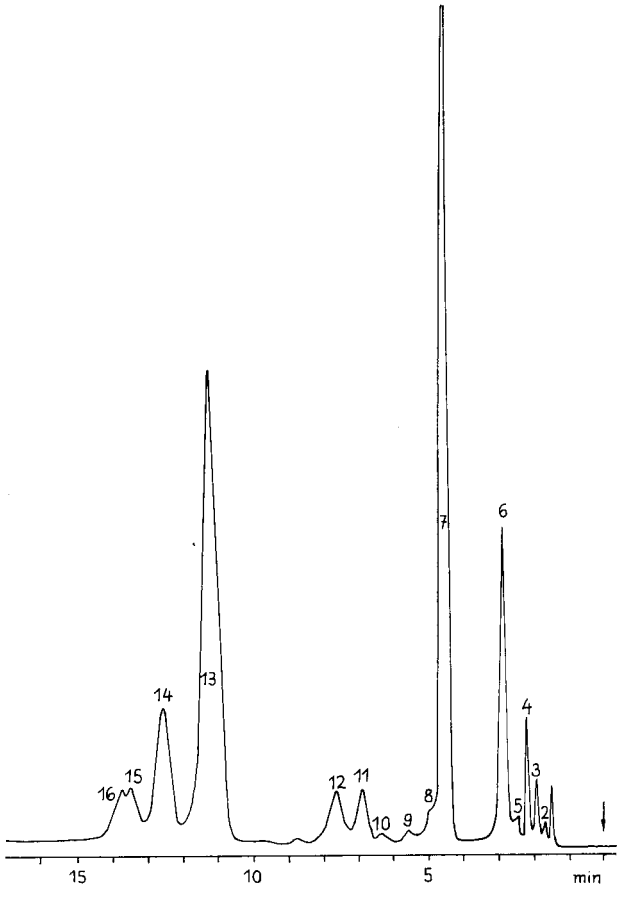

Fig. 1. Chromatogramm von Lavandinöl (Grosso) an QF-1. Temperatur: T_0 = 90°C; Heizrate 1.5°/min; Argon: 40 ml/min; Papiervorschub: 1 cm/min. Peak Nr.: 1 = α-Pinen; 2 = Camphen; 3 = β-Pinen; 4 = Limonen, *cis*-Ocimen; 5 = *trans*-Ocimen, *p*-Cymen; 6 = 1,8-Cineol; 7 = Linalool; 8–10 = unbekannt; 11 = Lavandulol, Terpinenol-(4); 12 = Borneol, α-Terpineol; 13 = Linalylacetat; 14 = Campher; 15 = Lavandulylacetat; 16 = Caryophyllen.

mung von Linalylacetat und Campher möglich, jedoch keine Trennung des 1,8-Cineols von Limonen und *cis*-Ocimen.

In den Tabellen I–III werden 17 Komponenten durch ihre Retentionsindices bei verschiedenen Temperaturen und bei Temperaturprogrammierung vergleichsweise an QF-1 (mittelpolar), Carbowax 1500 (polar) und OV-101 (apolar) charakterisiert.

In Zusammenhang mit der Bestimmung des Camphers an QF-1 beobachteten wir, dass in Abhängigkeit von der Temperatur Campher, Caryophyllen und Lavandulylacetat in unterschiedlicher Weise voneinander getrennt werden (Fig. 2). Während bei 95°C eine Bestimmung des Camphers möglich ist, wird dieser bei 120°C zusammen mit Lavandulylacetat und bei 155°C zusammen mit Caryophyllen eluiert. Ein solcher Platzwechsel des Camphers in Bezug auf andere Komponenten in Ab-

TABELLE I

RETENTIONSINDICES DER KOMPONENTEN AN QF-1

Komponente	*Retentionsindex (I)*							$I^{\star}_{TGC}$
	90°C	*100°C*	*120°C*	*130°C*	*150°C*	*160°C*	*180°C*	
α-Pinen	976	983	997	1004				975
Camphen	1010	1017	1031	1037				1009
β-Pinen	1041	1048	1063	1069				1038
Limonen	1072	1078	1089	1095				1075
cis-Ocimen	1075	1076	1078	1079				1075
trans-Ocimen	1104	1105	1107	1108				1107
p-Cymen	1109	1114	1124	1129				1107
1,8-Cineol	1130	1137	1150	1156				1134
Linalool			1239	1242	1248	1251		1228
Terpinenol-(4)			1350	1357	1368	1374		1335
Lavandulol			1351	1356	1365	1369		1335
Borneol			1376	1387	1407	1418		1364
α-Terpineol			1380	1386	1397	1403		1364
Linalylacetat					1452	1455	1461	1441
Lavandulylacetat					1506	1510	1517	1498
Campher					1540	1555	1586	1480!
Caryophyllen					1556	1567	1588	1519

⋆ Retentionsindex bei Temperaturprogrammierung (I_{TGC}): T_0 = 90°C; Heizrate 1.5°C/min.

TABELLE II

RETENTIONSINDICES DER KOMPONENTEN AN CARBOWAX 1500

Komponente	*Retentionsindex (I)*							$I^{\star}_{TGC}$
	120°C	*130°C*	*140°C*	*150°C*	*160°C*	*170°C*	*180°C*	
α-Pinen	1057	1065	1072	1079				1037
Camphen	1110	1117	1124	1131				1090
β-Pinen	1150	1158	1167	1175				1129
Limonen	1230	1236	1242	1249				1215
cis-Ocimen	1241	1242	1243	1245				1240
trans-Ocimen	1264	1265	1268	1270				1260
1,8-Cineol	1258	1266	1273	1281				1240!
p-Cymen	1299	1305	1311	1318				1287
Linalool				1564	1561	1557	1553	1574
Linalylacetat				1582	1582	1583	1582	1582
Campher				1593	1605	1617	1630	1555!
Lavandulylacetat				1632	1631	1630	1628	1635
Terpinenol-(4)				1643	1647	1651	1654	1635
Caryophyllen				1642	1655	1668	1681	1613!
Lavandulol				1709	1705	1702	1698	1712
α-Terpineol				1730	1734	1738	1741	1730
Borneol				1736	1744	1751	1758	1730

⋆ Retentionsindex bei Temperaturprogrammierung (I_{TGC}): T_0 = 90°C; Heizrate 4°C/min.

TABELLE III

RETENTIONSINDICES DER KOMPONENTEN AN OV-101

Komponente	*Retentionsindex (I)*					$I^{\star}_{TGC}$
	130°C	*140°C*	*150°C*	*160°C*	*170°C*	
α-Pinen	952	956	960	965		941
Camphen	968	974	979	984		958
β-Pinen	993	999	1004	1009		982
p-Cymen	1026	1029	1032	1036		1017
cis-Ocimen	1027	1028	1029	1030		1026
Limonen	1036	1040	1045	1049		1026
1,8-Cineol	1039	1045	1050	1055		1026
trans-Ocimen	1040	1041	1042	1043		1037
Linalool		1092	1093	1095	1097	1087
Campher		1153	1159	1166	1173	1133
Lavandulol		1159	1161	1163	1165	1153
Borneol		1171	1178	1184	1191	1153
Terpinenol-(4)		1180	1186	1192	1197	1165
α-Terpineol		1190	1195	1201	1206	1177
Linalylacetat		1243	1244	1245	1246	1240
Lavandulylacetat		1273	1274	1275	1276	1271
Caryophyllen		1427	1434	1442	1449	1422

* Retentionsindex bei Temperaturprogrammierung (I_{TGC}): T_0 = 100°C; Heizrate 2°C/min.

hängigkeit von der Temperatur war uns bereits auf Chromatogrammen von Lavandinölen in einer Arbeit von Bruns[7] aufgefallen. Auch bei Untersuchungen über das Retentionsverhalten von Sesquiterpenkohlenwasserstoffen erwähnen Andersen und Falcone[8] bei einigen dieser Verbindungen, u.a. Caryophyllen, einen Positionswechsel mit Temperaturänderung an Carbowax 20M. Peakverschiebungen infolge Änderung der Analysentemperatur sind dann zu beobachten, wenn die Temperaturabhängigkeit der Retentionsdaten zweier oder mehrerer Substanzen sehr unterschiedlich ist, d.h. im vorliegenden Fall von Campher und Caryophyllen im Vergleich zu Lavandulylacetat. Sie lassen sich praktisch zur Identifizierung bestimmter Peaks im Chromatogramm eines komplexen Gemisches benutzen[9,10].

Die Temperaturabhängigkeit der Retentionsindices der untersuchten Substanzen, die in dem vermessenen Temperaturbereich bei allen drei Phasen linear verlief, ist in den Fig. 3–5 graphisch dargestellt. Aus den Darstellungen lässt sich die für das jeweilige Trennproblem geeignete Analysentemperatur abschätzen bzw. die zu erwartende Reihenfolge oder Coelution der Peaks bei einer bestimmten Säulentemperatur entnehmen. So wird nach Fig. 3 verständlich, dass bei temperaturprogrammierter Analyse des Lavendelöls (T_0 = 90°C; Heizrate 1.5°C/min) Campher vor Lavandulylacetat eluiert wird und die Peaks von *cis*-Ocimen und Limonen sowie von *trans*-Ocimen und *p*-Cymen zusammenfallen (vgl. Fig. 1, Tabelle I). Wie aus Fig. 3 hervorgeht, zeigen bei der Analyse an QF-1 auch andere Substanzpaare auf Grund des unterschiedlichen Anstiegs ihrer Geraden Überschneidungen, die jedoch ohne Bedeutung waren, da die Substanzen im Gemisch wegen ihrer sehr dicht aufeinanderfolgenden Retentionszeiten praktisch bei allen Temperaturen coeluiert wurden (z.B. α-Terpineol–Borneol, Terpinenol-(4)–Lavandulol).

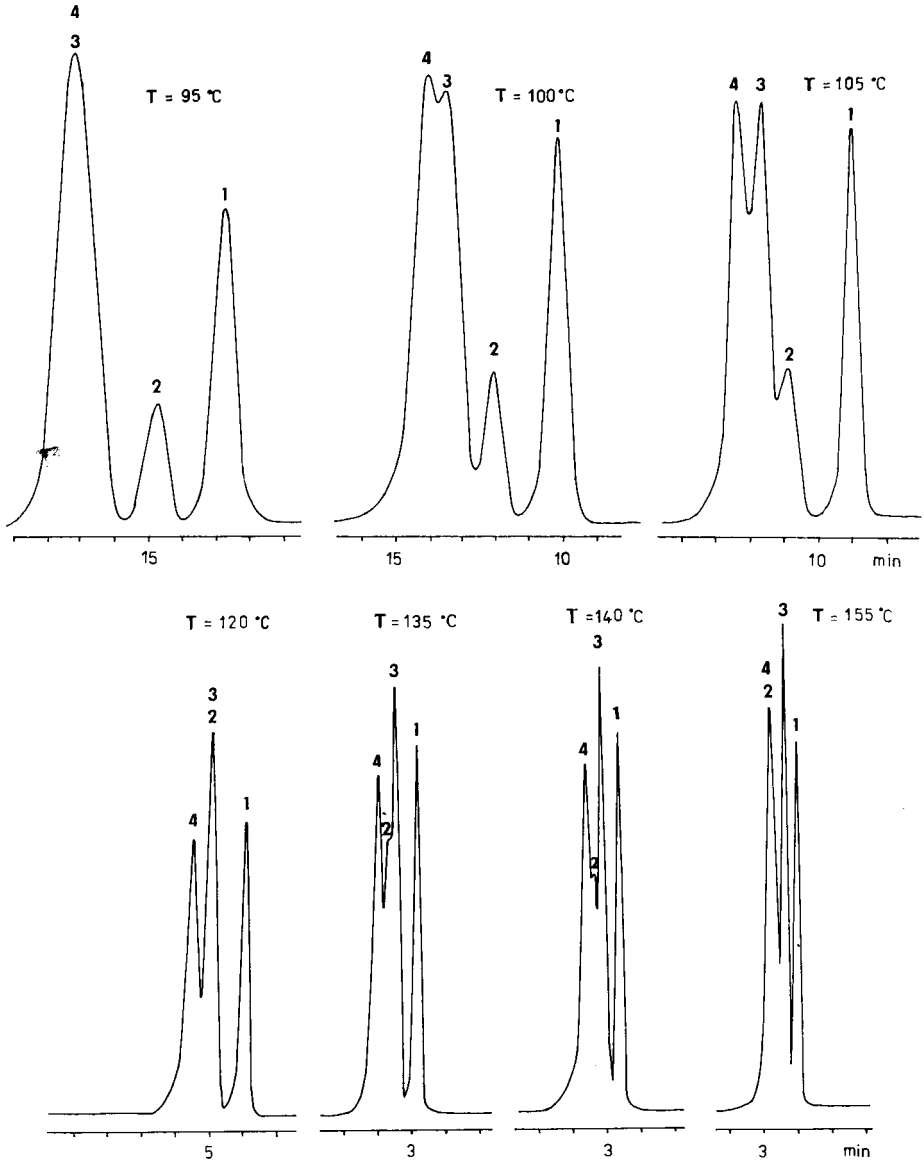

Fig. 2. Trennung von Linalylacetat (1), Campher (2), Lavandulylacetat (3) und Caryophyllen (4) an QF-1 in Abhängigkeit von der Säulentemperatur.

In Tabelle IV wird die Temperaturabhängigkeit der Retentionsindices durch die Temperaturkoeffizienten, angegeben als Indexdifferenz bei Erhöhung der Säulentemperatur um 10°C ($\partial\ I/10°C$), für alle Komponenten an den drei stationären Phasen verglichen. Die Substanzen werden nach ihrer chemischen Polarität in zwei Gruppen unterteilt (apolare und polare Komponenten). Zum Vergleich sind ihre ΔI-Werte angegeben, die die GC-Polarität[5,11–14] dieser Verbindungen ausdrücken und

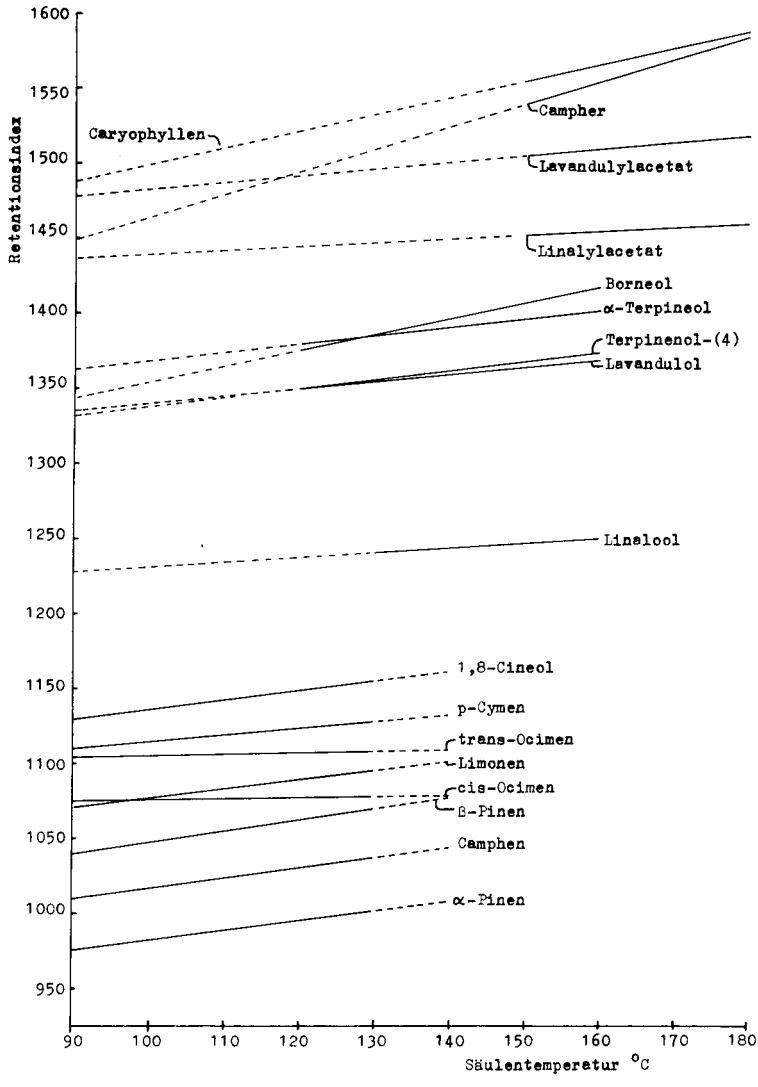

Fig. 3. Retentionsindices an QF-1, aufgetragen gegen die Säulentemperatur (—, Temperaturbereich, in welchem die Werte bestimmt wurden).

hier als Differenz zwischen den an Carbowax 1500 und OV-101 bei 150°C gemessenen Retentionsindices definiert sind. Bei Betrachtung der Gruppe A lässt sich feststellen, dass die Temperaturkoeffizienten aller apolaren Komponenten mit steigender Polarität der Trennphase grösser werden. Diesbezüglich vergleichbare Ergebnisse finden wir auch bei Luisetti und Yunes[14] sowie Andersen und Falcone[8] für eine Reihe von Mono- und Sesquiterpenkohlenwasserstoffen. Die mittelpolaren bis polaren Substanzen der Gruppe B dagegen zeigen ihre maximalen Werte an der mittelpolaren QF-1-Phase. Bezüglich der niedrigsten Werte verhalten sich die Verbindungen dieser

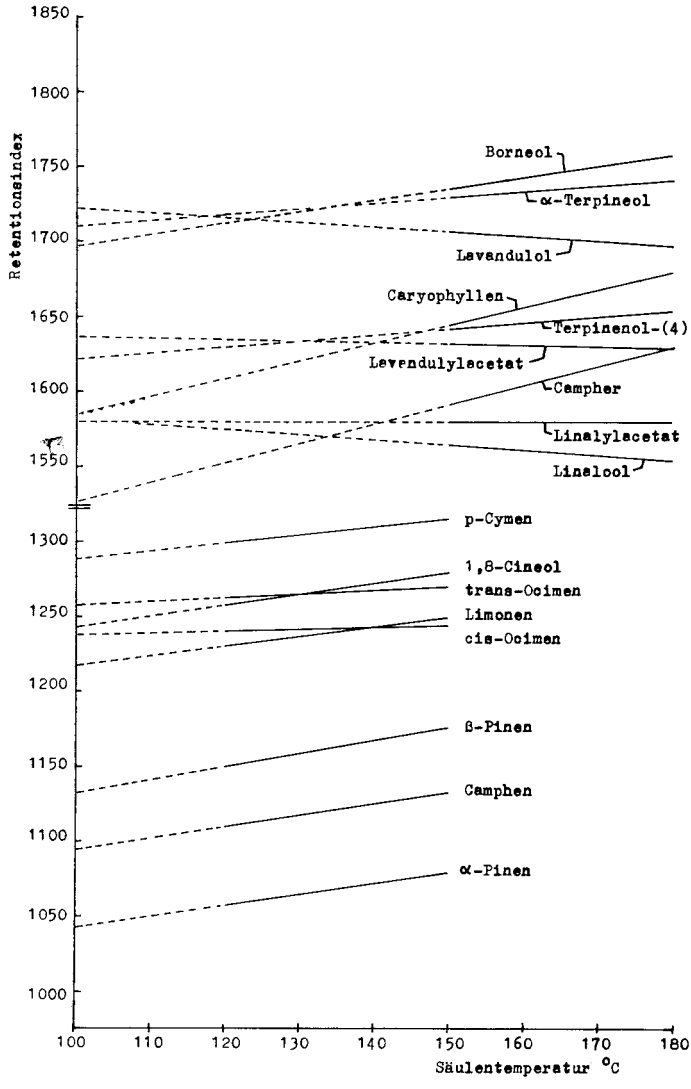

Fig. 4. Retentionsindices an Carbowax 1500, aufgetragen gegen die Säulentemperatur (—, Temperaturbereich, in welchem die Werte bestimmt wurden).

Gruppe nicht einheitlich; z.B. wurden diese für Borneol und Campher an OV-101, für α-Terpineol und Terpinenol-(4) dagegen an Carbowax 1500 gefunden.

Breckler und Betts[15], die eine Reihe von Komponenten ätherischer Öle an Hand ihrer relativen Retentionszeiten und deren Änderung mit der Temperatur charakterisieren und klassifizieren, vermuten, dass die Temperaturabhängigkeit der Retentionsdaten in Beziehung zur Polaritätsgleichheit zwischen Substanz und stationärer Phase steht. Andererseits wird von verschiedenen Autoren[9,10,16–18] die Grösse des Temperaturkoeffizienten aus der Struktur der Verbindung hergeleitet, d.h. als Funktion der Molekülabmessungen und unabhängig von der Polarität betrachtet.

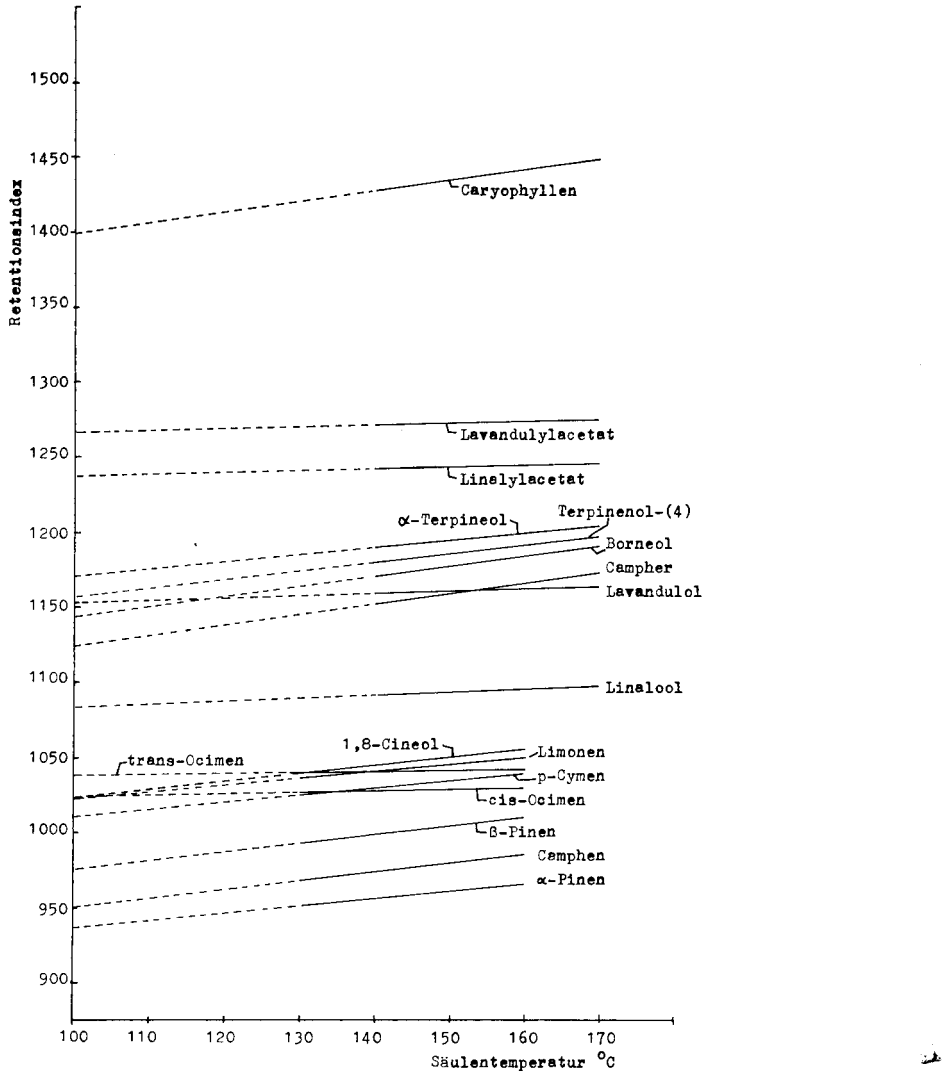

Fig. 5. Retentionsindices an OV-101, aufgetragen gegen die Säulentemperatur (–, Temperaturbereich, in welchem die Werte bestimmt wurden).

Ein Zusammenhang zwischen Temperaturabhängigkeit der Retentionsindices und dem "quadratischen Mittelwert des Molekülradius", der von Altenburg[18] als Mass zur Charakterisierung der Grösse und Form bestimmter Moleküle (verzweigte Alkane, Alkylbenzene) formuliert wird, kann jedoch für die von uns untersuchten Verbindungen nicht diskutiert werden, da eine solche Berechnung bei vorliegenden Strukturen nicht anwendbar ist. Auch mit anderen topologischen Indices zur Charakterisierung von Molekülform und -grösse, wie Wiener Zahl[19] und Konnektivitätsindex[20,21], die zur Berechnung von Retentionsdaten benutzt werden[22], ergeben sich

TABELLE IV

TEMPERATURKOEFFIZIENTEN DER RETENTIONSINDICES

Komponente	*Struktur*	*AI**	*∂I/10°C*		
			OV-101	*QF-1*	*Carbowax 1500*
A. Apolare Komponenten					
α-Pinen		119	+4.3	+ 7.0	+ 7.3
β-Pinen	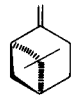	171	+5.3	+ 7.0	+ 8.3
Camphen		152	+5.3	+ 6.8	+ 7.0
1,8-Cineol	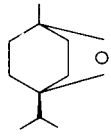	231	+5.3	+ 6.5	+ 7.7
Limonen	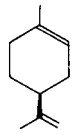	204	+4.3	+ 5.8	+ 6.3
p-Cymen	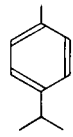	286	+3.3	+ 5.0	+ 6.3
cis-Ocimen	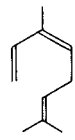	216	+1.0	+ 1.0	+ 1.3
trans-Ocimen	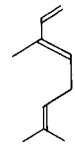	228	+1.0	+ 1.0	+ 2.0
Caryophyllen	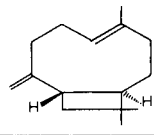	208	+7.3	+10.7	+13.0

TABELLE IV (*Fortsetzung*)

Komponente	*Struktur*	*ΔI**	*∂I/10° C*		
			OV-101	*QF-1*	*Carbowax 1500*
B. Polare Komponenten					
Linalylacetat	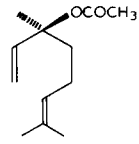	338	+1.0	+ 3.0	0
Lavandulylacetat	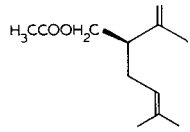	358	+1.0	+ 3.7	− 1.0
Linalool	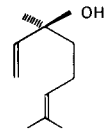	471	+1.7	+ 3.0	− 3.7
Lavandulol	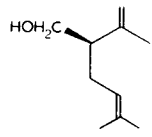	548	+2.0	+ 4.5	− 3.7
α-Terpineol	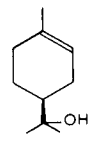	535	+5.3	+ 5.8	+ 3.7
Terpinenol-(4)	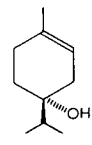	457	+5.7	+ 6.0	+ 3.7
Borneol	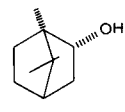	558	+6.7	+10.5	+ 7.3
Campher	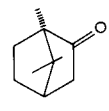	434	+6.7	+15.3	+12.3

* $\Delta I = I^{PEG} - I^{OV\text{-}101}$ bei 150°C.

an Hand unserer wenigen Verbindungen und der ungenügend präzisen Werte keine Korrelationen zur Grösse des Temperaturkoeffizienten.

Sicherlich lässt sich weder mit einfachen molekülgeometrischen Parametern noch an Hand polarer Wechselwirkungen allein die Kompliziertheit des Zusammenhangs von Retentionsverhalten und Temperatur erklären. Dennoch werden in Tabelle IV Beziehungen zwischen Temperaturkoeffizient und Struktur der Verbindungen ersichtlich. In der Gruppe A beispielsweise zeigten die apolaren mono- und bicyclischen Monoterpene an allen drei stationären Phasen wenig unterschiedliche Werte. Auffallend niedrig waren die Werte der beiden offenkettigen Monoterpene *cis*- und *trans*-Ocimen. Vergleichsweise zu allen Monoterpenen dieser Gruppe wies der Sesquiterpenkohlenwasserstoff Caryophyllen besonders an QF-1 und Carbowax 1500 signifikant höhere Werte auf. Ohne Ausnahme zeigten alle Komponenten dieser Gruppe mit Anstieg der Temperatur eine Vergrösserung der Retentionsindices, was wiederum vergleichbar mit dem Retentionsverhalten der von Andersen und Falcone[8] untersuchten apolaren Sesquiterpenkohlenwasserstoffen ist.

Ähnliche Zusammenhänge zwischen Struktur und Temperaturverhalten liessen sich bei den polaren Substanzen finden, z.B. zeigten α-Terpineol und Terpinenol-(4), sowie Linalool und Lavandulol nahezu identische Temperaturkoeffizienten. Auch in dieser Gruppe lagen die Werte der acyclischen Verbindungen relativ niedrig und waren an OV-101 grössenordnungsmässig mit denen von *cis*- und *trans*-Ocimen vergleichbar. Auffällig war, dass an Carbowax 1500 sowohl Linalool und Lavandulol als auch deren weniger polare Ester negative Temperaturkoeffizienten aufwiesen, was bei Vergleich mit der Literatur[5,11,13] insbesondere für Alkohole an polaren Trennphasen charakteristisch zu sein scheint. An OV-101 und QF-1 dagegen waren die Werte wie die aller übrigen untersuchten Verbindungen positiv. Die Temperaturkoeffizienten von Campher und Borneol unterschieden sich an der apolaren Phase OV-101 nur unwesentlich von denen der monocyclischen Terpenalkohole (Terpinenol-(4), α-Terpineol) und liessen sich auch mit denen der strukturell ähnlichen unpolaren Verbindungen (z.B. β-Pinen, Camphen) vergleichen. Nicht aus der Struktur erklärbar sind dagegen die grossen Werte für Campher an den polaren Trennflüssigkeiten, insbesondere an QF-1, im Vergleich zu denen strukturell ähnlicher apolarer Verbindungen (z.B. Camphen). Auch die Unterschiede zwischen Borneol und Campher an diesen Phasen lassen sich nicht aus dem Molekülbau herleiten, so dass man annehmen muss, dass hier neben Molekülgrösse und -form Wechselwirkungskräfte zwischen Polarität von Substanz und stationärer Phase und damit die Selektivität der Trennflüssigkeit Einfluss auf die Temperaturabhängigkeit der Retentionsindices nehmen.

DANK

Frau C. Lehmann danken wir für ihre Unterstützung bei den experimentellen Arbeiten.

ZUSAMMENFASSUNG

Zur gaschromatographischen Charakterisierung von Lavendel- und Lavandinölen wurden für 17 Hauptkomponenten vergleichsweise an OV-101, QF-1 und Car-

bowax 1500 mit gepackten Säulen die Retentionsindices bei verschiedenen Säulentemperaturen sowie bei Temperaturprogrammierung bestimmt. Die unterschiedliche Temperaturabhängigkeit der Retentionsindices führt bei einigen Substanzen mit der Änderung der Säulentemperatur zu einer Vertauschung ihrer Elutionsreihenfolge. Die Grösse des Temperaturkoeffizienten scheint in Zusammenhang sowohl mit der Molekülstruktur als auch der Wechselwirkung zwischen Polarität von Substanz und stationärer Phase zu stehen.

LITERATUR

1 R. Benecke, H. Thieme und J. Brotka, *Zentralbl. Pharm., Pharmakother. Laboratoriumsdiagn.*, 120 (1981) 245.
2 W. O. McReynolds, *J. Chromatogr. Sci.*, 8 (1970) 685.
3 G. Tarján, Á. Kiss, G. Kocsis, S. Mészáros und J. M. Takács, *J. Chromatogr.*, 119 (1976) 327.
4 R. Kaiser, *Chromatographia*, 2 (1969) 219.
5 E. Kováts, *Helv. Chim. Acta*, 41 (1958) 1915.
6 H. van den Dool und P. Dec. Kratz, *J. Chromatogr.*, 11 (1963) 463.
7 K. Bruns, *Seifen, Öle, Fette, Wachse*, 105 (1979) 291.
8 N. H. Andersen ünd M. S. Falcone, *J. Chromatogr.*, 44 (1969) 52.
9 N. C. Saha und G. D. Mitra, *Technology (Sindri, India)*, 5 (1968) 212.
10 L. S. Ettre, *Chromatographia*, 7 (1974) 141.
11 A. Wehrli und E. Kováts, *Helv. Chim. Acta*, 42 (1959) 2709.
12 R. ter Heide, *Fresenius' Z. Anal. Chem.*, 236 (1968) 215.
13 R. ter Heide, *J. Chromatogr.*, 129 (1976) 143.
14 R. U. Luisetti und R. A. Yunes, *J. Chromatogr. Sci.*, 9 (1971) 624.
15 P. N. Breckler und T. J. Betts, *J. Chromatogr.*, 53 (1970) 163.
16 D. A. Tourres, *J. Chromatogr.*, 30 (1967) 357.
17 R. A. Hively und R. E. Hinton, *J. Gas Chromatogr.*, 6 (1968) 203.
18 K. Altenburg, in H. G. Struppe (Herausgeber), *Gas-Chromatographie 1968*, Akademie-Verlag, Berlin, 1968, S. 1.
19 H. Wiener, *J. Amer. Chem. Soc.*, 69 (1947) 17.
20 M. Randič, *J. Amer. Chem. Soc.*, 97 (1975) 6609.
21 K. Altenburg, *Z. Phys. Chem.*, 260 (1980) 389.
22 D. Bonchev, Ov. Mekenjahn, G. Protič und N. Trinajstič, *J. Chromatogr.*, 176 (1979) 149.

Journal of Chromatography, 238 (1982) 89–95
Elsevier Scientific Publishing Company, Amsterdam — Printed in The Netherlands

CHROM. 14,602

MIXED SOLVENTS IN GAS–LIQUID CHROMATOGRAPHY

ACTIVITY COEFFICIENTS FOR TETRACHLOROMETHANE IN SQUALANE–DINONYL PHTHALATE MIXTURES AT 303°K

ANTHONY J. ASHWORTH* and GARETH J. PRICE
School of Chemistry, University of Bath, Claverton Down, Bath BA2 7AY (Great Britain)
(Received December 10th, 1981)

SUMMARY

Activity and partition coefficients for tetrachloromethane at infinite dilution in squalane–dinonyl phthalate solvent mixtures have been determined at 303°K by the extrapolation of measurements made using a vacuum microbalance technique. The deviation from solution ideality shown in the mixed solvents is greater than that shown in the separate solvents. This results in the activity and partition coefficients in the mixed solvents lying outside the range delineated by the coefficients for the separate solvents for a large part of the mixed solvent composition. The partition coefficients can be accounted for to within 0.2% by conventional solution theory but values predicted by the Purnell–Andrade relation differ by as much as 7%.

INTRODUCTION

The activity coefficients at infinite dilution for several C_6 and related hydrocarbons in squalane (SQ) and dinonyl phthalate (DNP) solvent mixtures have been reported previously[1,2] and used to demonstrate the deviation of the systems from the simple relation proposed by Purnell and Vargas de Andrade[3] to predict the solute partition coefficient for mixed solvents in gas–liquid chromatography (GLC). It was further demonstrated that the experimentally determined partition coefficients for the mixed solvent systems could be accounted for, to within 1%, by a relation derived from basic solution theory.

It was decided to investigate further the ability of these relations to express mixed solvent behaviour by examining the solubility of tetrachloromethane in the same solvent mixture. It was thought that the simple symmetrical and therefore non-polar nature of the tetrachloromethane molecule would make it a very suitable solute for this purpose. Moreover, by extrapolation of their static vapour absorption results Freeguard and Stock[4] estimated the activity coefficient at inifinite dilution at 30°C for tetrachloromethane to be 0.522 in squalane and 0.600 in dinonyl phthalate, showing the negative deviation from ideal solution behaviour to be very similar in the separate solvents.

0021-9673/82/0000–0000/$02.75

TABLE I

ABSORPTION OF TETRACHLOROMETHANE (A) IN SQUALANE (B)–DNP (C) MIXTURES AT 303°K

$n_B:n_C$ = Solvent mole ratio; other symbols, see text.

$n_B:n_C$ = 1:0			$n_B:n_C$ = 3:1			$n_B:n_C$ = 1:1			$n_B:n_C$ = 1:3			$n_B:n_C$ = 0:1		
x_A	P_A (mmHg)	γ_A	x_A	P_A (mmHg)	γ_A	x_A	P_A (mmHg)	γ_A	x_A	P_A (mmHg)	γ_A	x_A	P_A (mmHg)	γ_A
0.0641	5.095	0.5659	0.0495	3.795	0.5495	0.0578	4.430	0.5496	0.0593	4.670	0.5642	0.0543	4.590	0.6058
0.1114	9.150	0.5883	0.0971	7.590	0.5599	0.1020	7.985	0.5611	0.1084	8.765	0.5791	0.1078	9.450	0.6278
0.1689	14.370	0.6091	0.1414	11.430	0.5787	0.1511	12.270	0.5814	0.1564	13.040	0.5984	0.1573	14.210	0.6468
0.2163	18.935	0.6266	0.1925	15.990	0.5948	0.2064	17.265	0.5988	0.2080	17.915	0.6163	0.2067	19.180	0.6640
0.2534	22.725	0.6418	0.2490	21.510	0.6181	0.2515	21.730	0.6182	0.2693	24.180	0.6423	0.2555	24.430	0.6840
0.2997	27.650	0.6599	0.2996	26.705	0.6376	0.3041	27.180	0.6394	0.3212	29.875	0.6649	0.3057	30.140	0.7050
0.3420	32.510	0.6796	0.3523	32.575	0.6610	0.3550	32.920	0.6629	0.3680	35.270	0.6852	0.3502	35.450	0.7236
0.3899	38.190	0.7000	0.3930	33.320	0.6787	0.3921	37.270	0.6794	0.4157	41.230	0.7086	0.3969	41.410	0.7454

EXPERIMENTAL

Absorption isotherms were determined at 303.04 ± 0.01 °K using a Sartorius Model 4102 electronic vacuum microbalance in conjunction with a Texas Instruments quartz Bourdon gauge. (A nominal temperature of 303°K is used throughout this report.) The apparatus, the techniques and the materials were as described previously[1], except for the tetrachloromethane which was supplied by BDH (Poole, Great Britain) as "specially pure for spectroscopy".

Squalane–dinonyl phthalate mixtures were prepared for nominal mole ratios of 3:1, 1:1 and 1:3. The actual ratios were 3.011:1, 1:0.999 and 1:2.989.

RESULTS

The absorption isotherms are presented in Table I in the form of the mole fraction of solute absorbed x_A in the involatile solvent mixture at a solute vapour pressure p_A. The activity coefficient γ_A of the solute in the solvent mixture was then calculated from these measurements using a second virial coefficient B_{AA} and a molar volume $V_A^\bullet$ for the tetrachloromethane of -1423 and 97.667 $cm^3\ mol^{-1}$, respectively (see eqns. 2 and 3 of ref. 1). The second virial coefficient was obtained by extrapolation of experimentally determined values[5] to 303.04°K by plotting ln B_{AA} against ln T. The molar volume was determined from the specific volume measurements of Wood and Gray[6].

TABLE II

ACTIVITY COEFFICIENTS γ_A^∞ AND PARTITION COEFFICIENTS K_R FOR TETRACHLOROMETHANE IN SQUALANE (B)–DNP (C) MIXTURES AT 303°K

$n_B:n_C$ = solvent mole ratio.

	$n_B:n_C$				
	1:0	*3:1*	*1:1*	*1:3*	*0:1*
γ_A^∞	0.5447	0.5262	0.5241	0.5384	0.5838
K_R	466.2	504.8	531.1	543.2	527.8

The activity coefficients at infinite dilution shown in Table II were determined by regarding the SQ–DNP solvent mixture as a single component and fitting the absorption results for an individual isotherm to the conventional Flory–Huggins expression for the solute activity coefficient in a binary system (see eqn 1 of ref. 2). Effectively, the same values at infinite dilution can be found by a simple linear extrapolation of the logarithm of the activity coefficients plotted against solute mole fraction as shown in ref. 1. The partition coefficients for the solute between the solvent and the vapour phase at infinite dilution given in Table II were calculated using the standard relation

$$K_R = RT/(p_A^\bullet \gamma_{\kappa,A}^\infty V_L)$$
$$= [RT/(p_A^\bullet \gamma_A^\infty V_L)] \exp\{[V_A^\bullet - B_{AA} + (B_{AA}{}^2 p_A^\bullet/2RT)]p_A^\bullet/RT\} \quad (1)$$

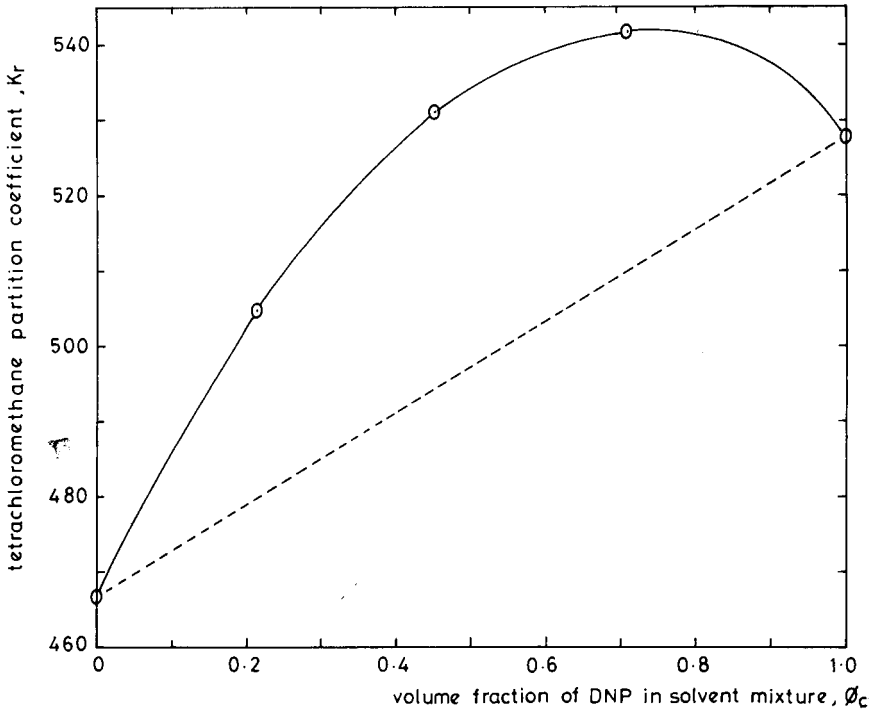

Fig. 1. Plot of the tetrachloromethane partition coefficient at infinite dilution, K_R, at 303 K *vs.* the volume fraction of DNP in the SQ–DNP solvent mixture. The full curve is given by eqn. 3 with $\chi_{BC} = 0.306$. The dashed line is given by the Purnell–Andrade relation, eqn. 2.

In equation 1 $p_A^\bullet$ is the vapour pressure of the pure solute and $\gamma_{K,A}^\infty$ is the uncorrected activity coefficient at infinite dilution (*i.e.* $\lim_{x_A, p_A \to 0} [p_A/(p_A^\bullet x_A)]$). The molar volume V_L of the SQ–DNP mixture is taken as a linear function of the mole fraction composition using the molar volumes of the separate solvents[7]. It has been established by density measurements that there is effectively a zero volume of mixing between these solvents[8]. The vapour pressure of the tetrachloromethane at 303.04 °K, $p_A^\bullet = 141.1$ mmHg, was calculated from the constants for the Antoine equation determined by Boublik and Aim[9].

DISCUSSION

The activity coefficients at infinite dilution determined for tetrachloromethane in squalane and dinonyl phthalate as separate solvents shown in Table II are 1.3% and 2.7% smaller, respectively, than those reported by Freeguard and Stock[4]. The difference is probably a result of the greater experimental error present in the Freeguard and Stock results where measurements of vapour absorption using a quartz spring balance and a mercury manometer were extrapolated to infinite dilution. Measurements by this technique are subject to increasing errors as the concentration of the solute in the solvent decreases, giving small spring extensions and small differences in manometer heights[10,11].

Fig. 1 shows the deviation of the partition coefficients in the SQ–DNP solvent mixtures from those predicted using the linear relation of Purnell and Andrade,

$$K_R = \varphi_B K_{R(B)} + \varphi_C K_{R(C)} \quad (2)$$

The partition coefficient at infinite dilution in the (B + C) solvent mixture, K_R, is related linearly to the partition coefficients at infinite dilution in the separate solvents $K_{R(B)} + K_{R(C)}$ through the volume fractions in the mixed solvent, φ_B and φ_C. The full curve in Fig. 1 is that given by the relation derived from conventional Flory–Huggins theory[2],

$$\ln K_R = \varphi_B \ln K_{R(B)} + \varphi_C \ln K_{R(C)} + \varphi_B \varphi_C \chi_{BC} \quad (3)$$

The parameter $\chi_{BC} = 0.306$ accounting for the interaction between the solvent molecules was obtained by analysis of all five isotherms in Table I in terms of the Flory–Huggins expression for a ternary system as explained in ref. 2. The Flory–Huggins based relation can account to within 0.2% for the experimentally derived mixed solvent partition coefficients, whereas the values derived from the Purnell–Andrade relation, described by the dashed line in Fig. 1, show a deviation as great as 7%. It is interesting to note that for over more than half of the composition range the partition coefficients for the mixed solvents lie outside the range delineated by the partition coefficients for the two separate solvents.

It has been realised for some time that the dinonyl phthalate supplied commercially for chromatographic analysis and purported to be the *bis*(3,5,5-trimethylhexyl) isomer is impure[8,10,12]. In spite of this, excellent agreement has been found between static[11] and GLC[8] determinations of the activity and partition coefficients at infinite dilution of several C_6 and related hydrocarbons in DNP supplied commercially. Moreover, a comparison of static[1,2] and GLC[8] derived infinite dilution activity and partition coefficients for hexane in three mixtures of SQ–DNP agree on average within 0.5%. Laub and Purnell[13] proposed that systems which are described by eqn. 2 be termed "diachoric" and point out that the presence of isomers of DNP in no way affects the validity of the diachoric relation. The same may be said for the use of eqn. 3, as it has been shown that each SQ + DNP solvent mixture can be treated as a single solvent[1,2], and that the solubility of each of the solutes studied can be accounted for in terms of the Flory–Huggins equation for a binary system.

The possibility of the coefficients for the mixed solvents having values outside the range delineated by the values for the two separate solvents is more strikingly shown when the activity coefficients are examined. Fig. 2 shows the activity coefficients determined at infinite dilution plotted as a function of solvent composition. The full curve is that given by the Flory–Huggins expression for a ternary system with interaction parameters given in Table III. The interaction parameters were determined from analysis of the five combined isotherms in Table I according to eqn. 5 and 6 of ref. 2. The value of the interaction parameter for the mixed solvents per unit molar volume of the solute $\chi_{BC}/V_A^\bullet$ of 3.13 mol dm^{-3} lies between that found with benzene as the solute[2] (3.80 mol dm^{-3}) and that for pentane, hexane, heptane and cyclohexane as solutes[2] (2.70 ± 0.06 mol dm^{-3}). The dashed line gives the activity coefficients in the mixed solvents according to the Purnell–Andrade relation expressed in

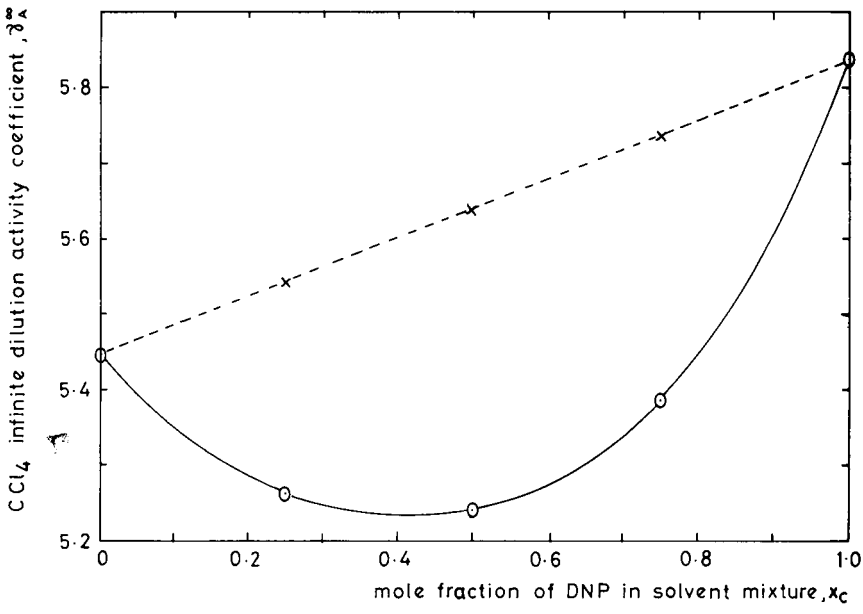

Fig. 2. Plot of the tetrachloromethane activity coefficient at infinite dilution, γ_A^∞, at 303°K *vs.* the mole fraction of DNP in the SQ–DNP solvent mixture. The full curve is given by the Flory–Huggins expression for a ternary system (eqn. 5 and 6 of ref. 2) using interaction parameters given in Table III. The dashed curve is given by the Purnell–Andrade relation expressed in terms of activity coefficients (eqn. 13 of ref. 1).

terms of activity coefficients (see eqn. 13, ref. 1). Since the relation for the partition coefficients (eqn. 2) is linear with respect to composition and K_R is inversely proportional to the reciprocal of γ_A^∞ (eqn. 1), it is surprising that the relation produces what is almost a linear plot for the solute activity coefficient with solvent mole fraction. This is a result, however, of the small difference between the activity coefficients for the tetrachloromethane in the separate solvents. The activity coefficients for tetrachloromethane in the mixed solvents lie outside the range given by the activity coefficients in the separate solvents for more than 80% of mixed solvent composition when expressed as a mole fraction. There is with this particular system a greater deviation from ideality with the mixed solvents than is shown by the separate solvents. Hence the use of an empirical relation based on the assumption of a linear relation between the partition coefficients for the separate solvents could well lead to a misleading conclusion.

TABLE III

INTERACTION PARAMETERS DETERMINED FROM ANALYSIS OF THE COMBINED ISOTHERMS (THREE TERNARY AND TWO BINARY) IN TABLE I FOR TETRACHLOROMETHANE (A) IN SQUALANE (B)–DNP (C) MIXTURES AT 303 K

V_A^* = solute molar volume.

χ_{AB}^0	χ_{AB}'	χ_{AC}^0	χ_{AC}'	χ_{BC}	χ_{BC}/V_A^* (*mol dm*$^{-3}$)
0.273	−0.028	0.202	0.097	0.306	3.13

REFERENCES

1 A. J. Ashworth and D. M. Hooker, *J. Chromatogr.*, 131 (1977) 399.
2 A. J. Ashworth and D. M. Hooker, *J. Chromatogr.*, 174 (1979) 307.
3 J. H. Purnell and J. M. Vargas de Andrade, *J. Amer. Chem. Soc.*, 97 (1975) 3585.
4 G. F. Freeguard and R. Stock, *Trans. Farad. Soc.*, 59 (1963) 1655.
5 J. H. Dymond and E. B. Smith, *2nd Virial Coefficients of Pure Gases and Mixtures*, Oxford University Press, Oxford, 1980, p. 17.
6 S. E. Wood and J. A. Gray, *J. Amer. Chem. Soc.*, 74 (1952) 3729.
7 A. J. Ashworth and D. M. Hooker, *J. Chem. Soc., Farad. Trans. I*, 72 (1976) 2240.
8 M. W. P. Harbison, R. J. Laub, D. E. Martire, J. H. Purnell and P. S. Williams, *J. Phys. Chem.*, 83 (1979) 1262.
9 T. Boublik and K. Aim, *Collect. Czech. Chem. Comm.*, 37 (1972) 3513.
10 A. J. Ashworth, in T. Gast and E. Robens (Editors), *Progress in Vacuum Microbalance Techniques*, Vol. 1, Heyden and Son, London, 1972, p. 313.
11 A. J. Ashworth, *J. Chem. Soc., Farad. Trans. I*, 69 (1973) 459.
12 M. F. Grenier-Loustalot, J. Bonastre and P. Grenier, *Analusis*, 6 (1978) 207.
13 R. J. Laub and J. H. Purnell, *J. Amer. Chem. Soc.*, 98 (1978) 30.

Journal of Chromatography, 238 (1982) 97–102
Elsevier Scientific Publishing Company, Amsterdam — Printed in The Netherlands

CHROM. 14,598

SELECTIVE EFFECTS OF MOBILE AND STATIONARY PHASES IN REVERSED-PHASE HIGH-PERFORMANCE LIQUID CHROMATOGRAPHY OF ECDYSTEROIDS

I. D. WILSON*, C. R. BIELBY and E. D. MORGAN
Department of Chemistry, University of Keele, Keele, Staffordshire ST5 5BG (Great Britain)
(Received December 1st, 1981)

SUMMARY

Observation of a number of different solvent systems and reversed-phase packing materials used for the chromatography of ecdysteroids has shown that order of elution and degree of separation between compounds of the series can be varied with useful limits by choice of the appropriate stationary and mobile phase. The effect on retention properties of substituent hydroxyl groups varies considerably with their position in the molecule.

INTRODUCTION

The ecdysteroids are a group of steroidal compounds interesting in themselves, as the moulting hormones of insects and crustaceans. Attention has been focused on their separation by chromatography recently, by the discovery of several minor ecdysteroids among the metabolites of ecdysone in the ovaries and embryos of a number of insects[1,2]. They are interesting for chromatographic studies in another sense, because they all have the same rigid 5β-cholestane skeleton, with a 7-ene-6-one chromophore and a variety of substituent hydroxyl groups, with occasionally an alkyl or lactone substituent. Over fifty such compounds are known[3]. A number of compounds are therefore available to study the effect on chromatographic properties of small alterations in structure.

In the course of our studies with these compounds we have (in common with others, *e.g.* Lafont's group in France) observed that order of elution and degree of separation of some members of the class varied unexpectedly with both packing material (stationary phase) and organic modifier in the solvent (mobile phase), in reversed-phase high-performance liquid chromatography (RP-HPLC). We have examined these effects more closely, because they may be used to advantage to achieve difficult separations and here describe the chief points of interest. We have also observed the effect of extra substituent hydroxyl groups on retention properties within the series. The twelve ecdysteroids used in this study are illustrated in Fig. 1.

* Present address: Hoechst UK Ltd., Walton Manor, Milton Keynes, Bucks. MK7 7AJ, Great Britain.

0021-9673/82/0000–0000/$02.75

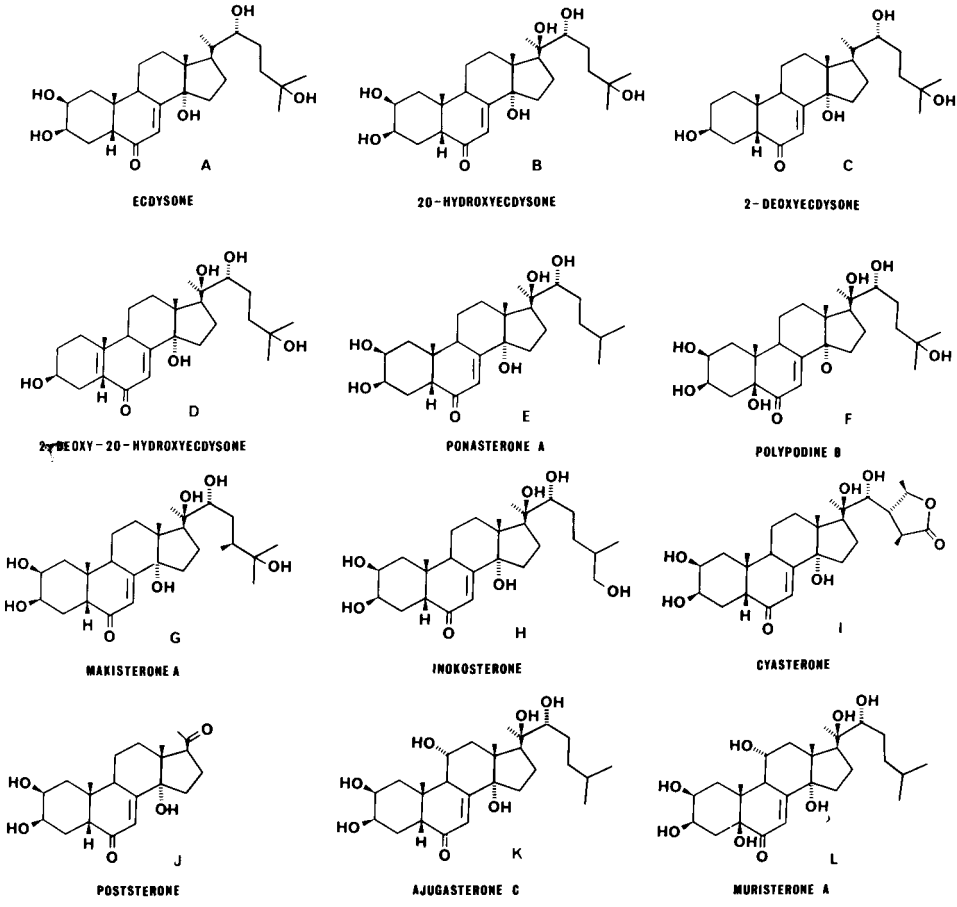

Fig. 1. Structures of the ecdysteroids used in this study.

EXPERIMENTAL

Chromatography was performed on 150 × 3 mm I.D. stainless-steel columns slurry packed with either 5 μm ODS Spherisorb (Phase Separations, Great Britain), or 5 μm ODS Nucleosil (HPLC Technology, Great Britain). Mobile phase was pumped using an LDC Constametric III pump (LDC, Stone, Great Britain), at 1 ml min^{-1}. Eluent was monitored at 254 nm using an LC3-UV detector (Pye Unicam, Cambridge, Great Britain). Samples were introduced onto the column via a Rheodyne Model 7120 loop injector (Magnus Scientific, Great Britain) using a syringe. The mobile phase was degassed before use and chromatography performed at ambient temperature.

Ecdysteroids were used as solutions in methanol, and were gifts from various sources.

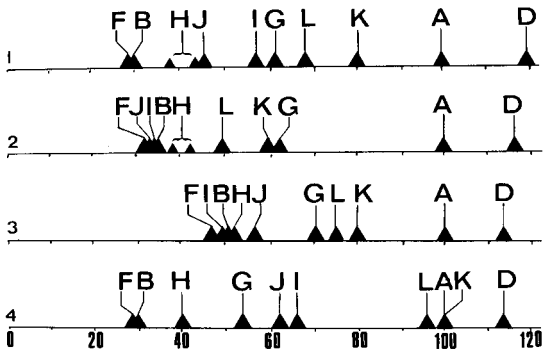

Fig. 2. Diagramatic representation of differences in selectivity observed between ODS Nucleosil and ODS Spherisorb, using methanol–water and acetonitrile–water solvent systems. 1 = ODS Spherisorb acetonitrile water (15:85); 2 = ODS Spherisorb methanol–water (35:65); 3 = ODS Nucleosil methanol–water (50:50); 4 = ODS Nucleosil acetonitrile–water (20:80). Retention is measured relative to ecdysone (A) which is given a value of 100 units. Compounds A–L as in Fig. 1.

RESULTS AND DISCUSSION

Selective effects of the stationary phase

These observations have been made using water–methanol as the mobile phase for simplicity of comparison. However, as seen in the text section, changing the organic component can alter the elution order on a given stationary phase.

Among the group of twelve familiar ecdysteroids (see Fig. 1), for six of them, 2-deoxy-20-hydroxyecdysone, 20-hydroxyecdysone, inokosterone, makisterone A, polypodine B, and ponasterone A (all containing the C-20, C-22 diol), elution order was unchanged in chromatography on ODS Nucleosil or ODS Spherisorb.

Small differences in the degree of separation of particular pairs are observed (Fig. 2). For example, 20-hydroxyecdysone and inokosterone are better resolved on ODS Spherisorb than on ODS Nucleosil, while for 20-hydroxyecdysone and polypodine B the reverse is true. Inokosterone consists of a mixture of 25-*R* and 25-*S* isomers which are resolved on ODS Spherisorb but not by ODS Nucleosil.

Much greater differences between ODS Nucleosil and ODS Spherisorb were noted when the two 11α-hydroxyecdysteroids were chromatographed. Ajugasterone C and muristerone A eluted before makisterone A on ODS Spherisorb, but after it on ODS Nucleosil. Although this pair is better retained on ODS Nucleosil, the separation is only half as efficient. The separation of posterone and cyasterone is poor on ODS Spherisorb, and close to 20-hydroxyecdysone. By contrast, on ODS Nucleosil, separation is much better, cyasterone eluting before 20-hydroxyecdysone. ODS Spherisorb and ODS Nucleosil require different quantities of methanol in the mobile phase for similar retention. The ODS Nucleosil requires more methanol, because it has a higher carbon loading (16% as compared with 8% for Spherisorb). Unfortunately pore volume and specific surface area as well as carbon loading, differ between Spherisorb and Nucleosil, preventing any conclusion being drawn on what factors govern differences of retention.

It is nevertheless possible, by the judicious selection of ODS Spherisorb or ODS Nucleosil, to obtain most required separations of pairs of ecdysteroids. Further examples of the use of different stationary phases for ecdysteroid separations are given by Lafont *et al.*[4] and Dinan *et al.*[5].

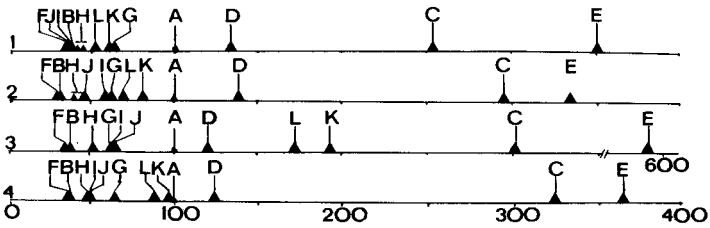

Fig. 3. Diagramatic representation of changes in selectivity seen with four different organic modifiers with ODS Spherisorb. 1 = Methanol–water (35:65); 2 = acetonitrile–water (15:85); 3 = tetrahydrofuran–water (10:90); 4 = dioxan–water (20:80). Retention is measured relative to ecdysone (A) which is given a value of 100 units.

Selective effects of mobile phase composition

It is well known from other studies that changes in the mobile phase can produce unexpected differences in relative retention in RP-HPLC. For example, changing the organic modifier in the chromatography of a large number of organic compounds, even on a silica surface highly covered with *n*-octyl groups, greatly influenced separation[6]. In another study, small amounts of organic ethers, added as a third component to the mobile phase significantly altered the resolution of some steroidal hormones[7].

Replacing methanol by acetonitrile causes changes in retention on both ODS Nucleosil and ODS Spherisorb, so that on ODS Spherisorb cyasterone and poststerone are better resolved and eluted after 20-hydroxyecdysone. Ajugasterone C and muristerone A which elute before makisterone A with methanol, now elute after it, but the resolution is unchanged (Fig. 3). On ODS Nucleosil, the positions of poststerone and cyasterone relative to makisterone A are reversed on changing between acetonitrile–water and methanol–water. Other improved separations on changing to acetonitrile can be seen in Fig. 3, including a better separation of inokosterone and 20-hydroxyecdysone.

Using tetrahydrofuran as organic modifier, the most notable change is in the retention of the two 11-hydroxysterols, ajugasterone C and muristerone A, which are retained considerably longer, relative to ecdysone, and though having more hydroxyl groups than ecdysone, elute after it. The relative retention of ponasterone A is also increased to six times that of ecdysone. This emphasized the importance of the C-25 hydroxyl group in ecdysteroids in conferring polar character and affecting chromatographic behaviour. Cyasterone and poststerone, though at the extremes of variation of chemical structure, have similar chromatographic properties, but perversely, the separation of this pair is not much affected by change of solvent.

An example of the marked difference of behaviour of ecdysteroids between tetrahydrofuran–water and acetonitrile–water is illustrated in Fig. 4.

Dioxan also has its effect on separation or relative retention compared with methanol, expecially for the 11-hydroxyecdysteroids which are strongly affected by each change of organic modifier.

Effect of substituent groups

The retention volumes of ecdysteroids relative to ecdysone on 5 μm ODS Spherisorb using methanol–water shows clearly that the number of hydroxyl groups per molecule is less important than their position. The three pentahydroxy-ecdysteroids, ecdysone, 2-deoxy-20-hydroxyecdysone and ponasterone A, display large

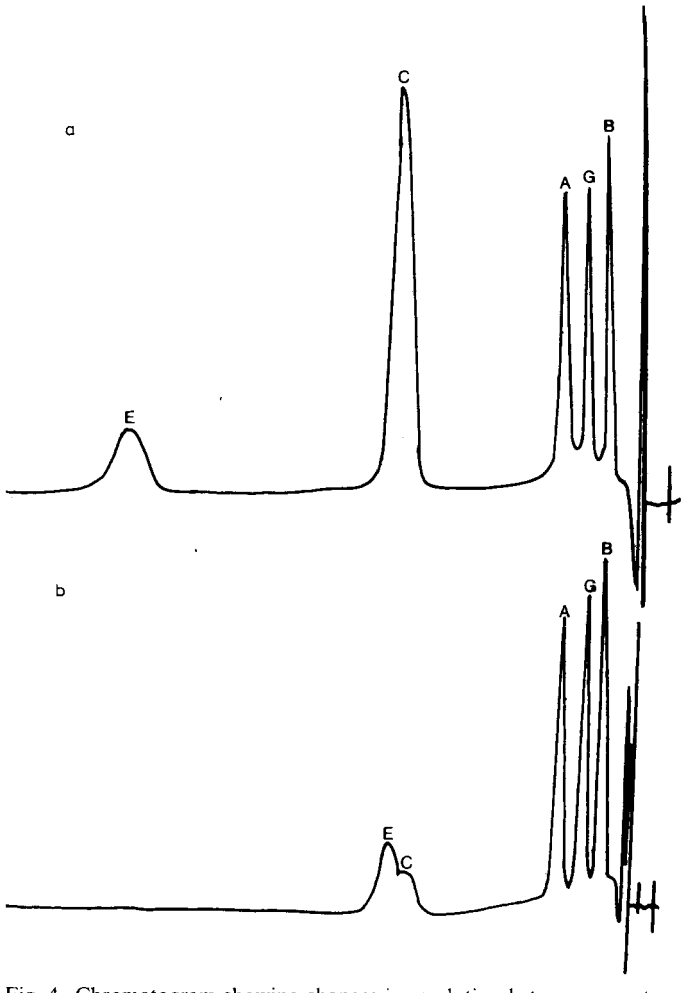

Fig. 4. Chromatogram showing changes in resolution between ponasterone A (E) and 2-deoxyecdysone (C) with acetonitrile (b) and tetrahydrofuran (a) based solvent systems.

differences in retention. The effect of an hydroxy at C-25 is much greater than at C-2 and this in turn is greater than that at C-20. The combined effect of hydroxyls at C-2 and C-20 in methanol–water is about the same as one at C-25. In the same way, addition of an α-OH at C-11 to ponasterone A to give ajugasterone C produces a large decrease in retention. Comparing ajugasterone C and 20-hydroxyecdysone (each with six OH groups), the hydroxyl at C-11α has a much smaller effect on retention than that at C-25. An hydroxyl at C-5β (polypodine B) has a negligible effect on retention, indeed the separation of polypodine B and 20-hydroxyecdysone is one of the most difficult to achieve in the group. The polarity of the 5β-OH may be reduced through hydrogen bonding to the adjacent carbonyl group. The effect of the C-5β-OH is much greater when comparing ajugasterone C and muristerone A.

Evidently, the effect of hydroxyl groups on ecdysteroid retention is not simply one of polarity, but steric effects are important. On ODS Spherisorb, in methanol–water the eluotropic effect of some of the hydroxyls decreases in the order: 25 > 26 > 2β > 20 > 11α > 5β. But it must be added that the effect of an added hydroxyl

groups depends also upon those already present. As Bush[8] has pointed out, it is not enough for a polar group in an organic compound to be able to associate with solvent molecules, there must be room around the group to fit in several molecules of solvent if it is to interact strongly with the lattice of the solvent.

The effect of an extra methyl group attached to the side chain is surprisingly large. Makisterone A has a retention volume about 50% greater than 20-hydroxyecdysone. Shortening the side chain to only two carbon atoms (poststerone) seems to produce a balance of polar and non-polar effects so that its retention is not very different from 20-hydroxyecdysone. Conversion of the end of the chain to a lactone (as in cyasterone) also produces little change.

CONCLUSIONS

The selective effects of different stationary phases may lie in the efficiency of covering of the silica surface, the proportion of residual silanol groups and in the pore size. We cannot, in the present state of knowledge, study these factors separately. Moreover, the selectivity of a column may change slightly with age and batch from the manufacturer. Stationary phases have to be chosen by trial and error. The collection of data here is helpful in making a choice for the ecdysteroids. As yet, not many studies have been made on effects of mobile phase and since it is evident that other effects than partition influence retention on reversed phases, no predictive powers are available in this respect either. The data displayed here can be used to aid the choice of suitable stationary and mobile phases for the RP-HPLC of ecdysteroids. In general, acetonitrile–water seems to be the best mobile phase, since it gives the best spread of retention values. Lafont *et al.*[4] recommended acetonitrile–water systems as in their hands these mixtures gave least peak tailing.

Two practical examples of the use of this data are illustrative. We have been able to choose a system that altered the retention of muristerone A to remove impurities, and also to separate mixtures of 2-deoxyecdysone and ponasterone A, which are very difficult to separate by thin layer chromatography, or by HPLC with some common mobile phases.

ACKNOWLEDGEMENTS

We wish to thank Drs. V. Vecchietti, J. A. Beisler, B. Danielli, D. H. S. Horn, J. Jizba and Professors Chou Wei-shan, G. Ferrarri and K. Nakanishi for samples of ecdysteroids.

REFERENCES

1 L. N. Dinan and H. H. Rees, *J. Insect Physiol.*, 27 (1981) 51.
2 R. Lafont, J.-L. Pennetier, M. Andrianjafintrimo, J. Claret, J. F. Modde and C. Blais, *J. Chromatogr.*, 236 (1982) 137.
3 C. Hetru and D. H. S. Horn, in J. A. Hoffman (Editor), *Progress in Ecdysone Research*, Elsevier/North-Holland, Amsterdam, 1980, p. 13.
4 R. Lafont, G. Sommé-Martin, B. Mauchamp, B. F. Maume and J. P. Delbecque, in J. A. Hoffmann (Editor), *Progress in Ecdysone Research*, Elsevier/North-Holland, Amsterdam, 1980, p. 45.
5 L. N. Dinan, P. L. Donnahey, H. H. Rees and T. W. Goodwin, *J. Chromatogr.*, 205 (1981) 139.
6 N. Tanaka, H. Goodell and B. L. Karger, *J. Chromatogr.*, 158 (1978) 233.
7 G. J.-L. Lee, R. M. K. Carlson and S. Kushinsky, *J. Chromatogr.*, 212 (1981) 108.
8 I. E. Bush, *The chromatography of sterols*, Pergamon, Oxford, 1961.

Journal of Chromatography, 238 (1982) 103–112
Elsevier Scientific Publishing Company, Amsterdam — Printed in The Netherlands

CHROM. 14,576

ATMOSPHERIC MICROWAVE-INDUCED PLASMA DETECTOR FOR THE GAS CHROMATOGRAPHIC ANALYSIS OF LOW-MOLECULAR-WEIGHT SULFUR GASES

J. L. GENNA*, W. D. McANINCH and R. A. REICH
Aluminum Company of America, Alcoa Laboratories, Alcoa Center, PA 15069 (U.S.A.)
(Received September 21st, 1981)

SUMMARY

New methodology has been developed for the analysis of low-molecular-weight sulfur compounds such as SO_2, COS and H_2S. The method employs gas chromatographic separation with specific element detection using emission spectroscopy. The emission spectroscopic source is a helium microwave-induced atmospheric plasma which is interfaced directly to the gas chromatographic column. Utilizing the vacuum ultraviolet sulfur emission line at 182.04 nm, detection limits of COS, H_2S and SO_2 are 50, 100 and 100 ppb*, respectively. Because of its specificity, other matrix components eluting with the peaks of interest have virtually no effect on the detectability of the sulfur species.

INTRODUCTION

The analysis of low-molecular-weight sulfur compounds such as SO_2, COS and H_2S has become increasingly important for both environmental monitoring and process control. Gas chromatography (GC) provides an acceptable means of isolating each sulfur compound from the others as well as from the diluent matrix. Until recently, however, GC analysis on these gaseous sulfur compounds has proven to be a difficult and time-consuming method due to the lack of adequate GC detectors. This is particularly true when determinations are required at the low ppm or ppb* concentration levels. In general, most conventional detectors, including flame ionization (FID), thermal conductivity (TCD) and electron capture, either do not have adequate sensitivity or are adversely affected by the diluent matrix due to their lack of specificity. If separation is not totally achieved between the diluent, such as air and the compounds of interest, the large excess of diluent can easily obscure the chromatographic peaks of interest. Flame photometric detectors (FPDs) provide good sensitivity and specificity for sulfur analysis but can suffer from non-linearity, are compound dependent, and can be somewhat cumbersome to use. In addition, the lack of versatility of FPDs, when compared to FIDs or TCDs, makes it incompatible to

* Throughout this article, the American billion (10^9) is meant.

0021-9673/82/0000–0000/$02.75

many other applications, thus making it necessary to have a GC system dedicated to sulfur analysis or require time-consuming detector changes on a single GC unit.

The utilization of atomic emission spectroscopy as an element-specific detector for GC offers an attractive alternative to both conventional detectors and FPDs for low-molecular-weight sulfur compounds. Several emission sources exist that are or may be adaptable to interfacing with a gas chromatograph. Among these sources are the inductively coupled plasma (ICP), the d.c. arc plasma and the microwave-induced plasma (MIP). The MIP has to date received the greatest attention for element-specific GC detection. McCormack *et al.*[1] first described a low-pressure microwave plasma employed for the analysis of compounds eluting from a gas chromatograph. The detection of sulfur compounds utilizing the low-pressure MIP has also been described[2–4].

Recently attention has been drawn to the use of an atmospheric microwave plasma as an atomic emission source for gas chromatographic detection. Since Beenakker described the construction and use of a microwave cavity able to support both a helium and argon plasma at atmospheric pressure[5,6], an increasing amount of work is taking place to apply it to a wide range of GC problems[7–10].

The atmospheric microwave plasma possesses several important advantages over other atomic emission sources: (1) the atmospheric pressure MIP is extremely well suited for gaseous analysis; (2) the small quartz plasma tube is easily interfaced with GC columns while both d.c. and ICP sources require somewhat elaborate plumbing arrangements to assure the integrity of the eluted peak; (3) in addition, the MIP is extremely stable, easily tuned and relatively inexpensive to construct and operate.

The work described here is aimed at utilizing atomic emission spectroscopic detection for the analysis of low molecular weight sulfur-containing gases. A helium atmospheric MIP was chosen as the emission source. The GC microwave-cavity interface is described. This study was restricted to the analysis of H_2S, COS and SO_2 in air, although sulfur compounds such as CS_2 and small-chain mercaptans should be equally applicable. Generally detection limits have been found to be in the fractional ppm to ppb range. Because the most sensitive emission lines for sulfur appear in the vacuum ultraviolet, a study of the emission spectra between 170.0 and 200.0 nm was undertaken in order to characterize the discharge in this region. Since other elements of interest, such as phosphorus and carbon, emit strongly in this region, a characterization such as this can be extremely useful for other applications not discussed here.

EXPERIMENTAL

Gas chromatographic system

A Fisher/Victoreen series 4400 gas chromatograph was equipped with a 6 ft. × 1/8 in. O.D. Teflon (FEP) Chromosil 310 column (Supelco, Bellefonte, PA, U.S.A.). Helium was employed as the carrier gas at a flow-rate of 12 ml/min. All separations were carried out at a constant temperature of 50°C. Standard injection volumes were 1.0 ml utilizing Pressure-Lok gas syringes (Supelco).

Standard gas mixtures were made from commercially obtained cylinders of 0.5% H_2S and COS, and 0.5% SO_2 (Linde Division, S. Plainfield, NJ, U.S.A.). Utilizing 500-ml round-bottom flasks equipped with side-arms to which septums could be attached, the appropriate amounts of each gas were delivered into the vessel

through the septum. Prior to introduction of gas samples, the vessels were purged with nitrogen. To assure rapid mixing, *ca.* twenty 1/8-in. acrylic mixing balls were placed in the flask which was then vigorously shaken. Standard concentrations as low as 0.10 ppm were successfully prepared utilizing this procedure. Samples to be analyzed were injected without dilution or any other sample handling.

Microwave plasma detector system

A schematic diagram of the microwave plasma detector system is shown in Fig. 1. The microwave cavity was an all-copper Beenakker-type cavity[5,6]. The cavity was equipped with a type N coaxial cable connector. The original cavity tuning screws described by Beenakker were removed and not used at any time. The microwave power supply was the Model MPG 4M microwave generator supplied by Ophthos, Rockville, MD, U.S.A. The generator was equipped with both forward and reflected power meters and operated at a frequency of 2450 MHz.

Tuning was accomplished by a coaxial/stub stretcher Model SL-03N (Microlab/FXR, Livingston, NJ, U.S.A.) attached between the microwave cavity and coaxial line leading to the cavity. In addition a microwave circulator CT3487-N (UTE Microwave, Asbury Park, NJ, U.S.A.) and termination TB-7MN (Microlab/FXR) were placed in the coaxial line just prior to the microwave cavity. The termination was continually cooled by a small 3-in. fan. The combination of circulator and termination acted to reduce or eliminate reflected power from reaching the generator which can cause both damage and instability in the generator. At powers less than 70 W the circulator proved to be nearly 100% efficient in eliminating reflected power to the generator. At powers in excess of 70 W a minimal amount of reflected power could be observed at the generator. At the typical operating power of 100 W, reflected power was only 4 W. This could be reduced to zero but only at the expense of plasma stability.

The plasma tube assembly was simply a 1.3 mm I.D. × 6 mm O.D. quartz tube which was inserted in the microwave cavity at its center. The entire plasma cavity was

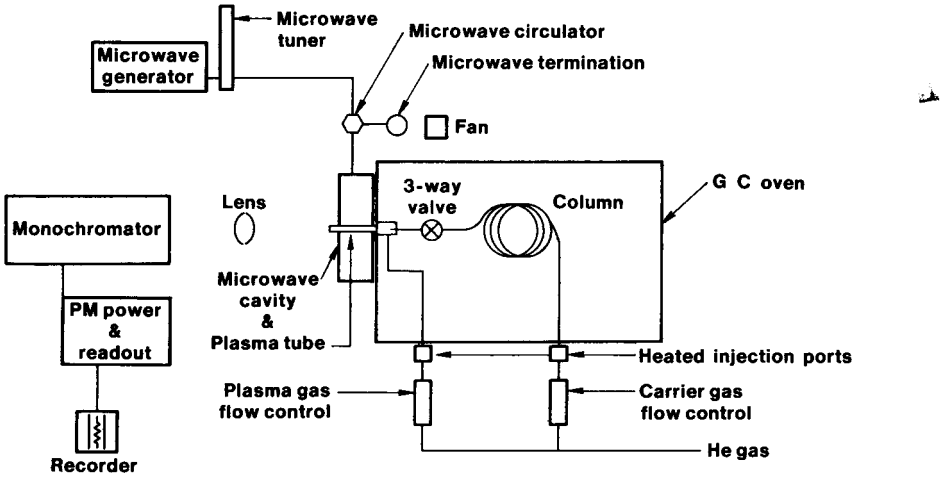

Fig. 1. Schematic diagram of GC atmospheric microwave plasma detector.

attached directly to the GC oven side wall with a series of four nut-and-bolt assemblies. The quartz plasma tube when inserted into the cavity would extend into the GC oven through an access hole provided in the GC oven wall. The plasma discharge was operated in helium at a total flow-rate of 50 ml/min. This helium was supplied to the discharge via two routes; *ca.* 12 ml/min was supplied by the carrier gas of the column, and the remainder through a secondary injection port on the gas chromatograph. This port was sealed off from use except for providing the plasma support gas. A 1/8-in. stainless-steel line was silver-soldered into a hole drilled into a 1/4-in. Swagelok union. This line was then attached to the rear of the injection port while the plasma tube was placed into one end of the Swagelok union. This provided control of the plasma support gas by rotometers already supplied with the gas chromatograph. In addition all lines servicing the plasma were maintained within the GC oven providing easy access and preheating of gases which might contact the GC effluent.

A three-way electrically actuated switching valve with a 1/8 in. bore was mounted between the plasma tube and GC column (1-43-90; General Valve Corporation, East Hanover, NJ, U.S.A.). The valve was actuated by the operator and provided dumping of any column effluent prior to reaching the microwave discharge. This was important when large injections were employed where the solvent eluting from the column caused plasma instability or extinction.

Optical system

The optical system used to monitor the emission from the plasma consisted of 0.25-m Ebert monochromator Model 82-410 (Jarrell-Ash, Waltham, MA, U.S.A.) and a 15-mm diameter, 25-mm focal length fused-silica lens. An optical bench was constructed from a 1/4-in. aluminum plate to which all optical components were mounted. This was then attached directly to the GC wall by an angle iron (Fig. 2). This provided excellent stability of alignment between the microwave plasma and other optical components.

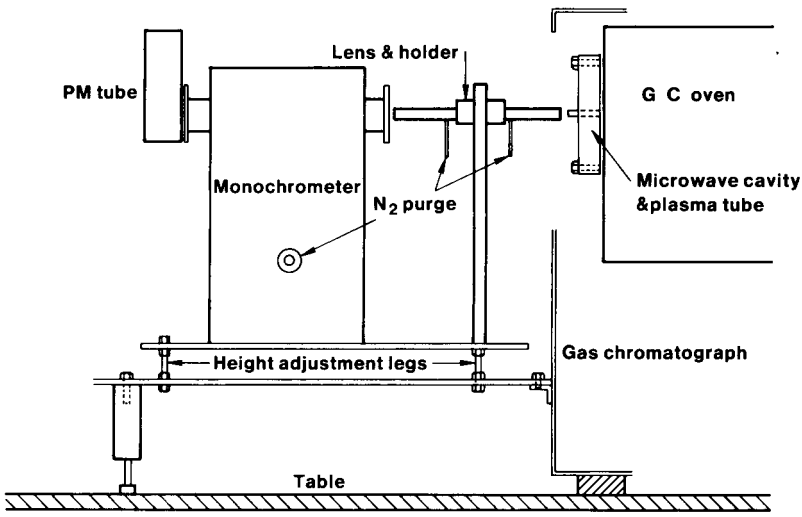

Fig. 2. Optical emission detector arrangement showing nitrogen purge.

The monochromator was equipped with a dual grating. The grating utilized in this work has 2360 grooves/mm, 300.0 nm blaze angle, and the system provided a linear dispersion of 1.65 nm/mm. Both entrance and exit slits were 150 μm. A standard RCA 1P28 photomultiplier (PM) tube operating at -750 V was used. Both photomultiplier power and readout were supplied by a Model 124 digital photometer (Pacific Photometric Instruments, Emeryville, CA, U.S.A.). A Model 1202 Linear recorder (Linear Instrument Corporation, Hackensack, NJ, U.S.A.) was used to record all chromatographic peaks.

Because nearly all of the sensitive sulfur emission lines are located in the vacuum ultraviolet, the optical system was modified to incorporate nitrogen puring of both the optical path and monochromator. Glass tubes, equipped with 1/3-in. side-arms, were mounted on either side of the lens directly onto the lens holder. These tubes extended to the entrance slit of the monochromator on one side and to within 5 mm of the plasma tube on the opposite side. Nitrogen was introduced through the side-arms. In addition, the glass tubes were blackened to minimize light loss or light scattering from overhead lights.

The monochromator was purged by drilling and tapping a 1/4-in. hole in its top and mounting a 1/4-in. pipe-to-Swagelok adaptor to it. A nitrogen bleed was provided by a line attached at this point. A period of *ca.* 24 h was given to purge the system completely and then a bleed of 200–400 ml/min of nitrogen was maintained at all times. For convenience, liquid nitrogen was used.

RESULTS AND DISCUSSION

Spectral characteristics

The spectral characteristics of the atmospheric pressure helium MIP have not been widely documented to date. Considerably more work has been directed towards development of methodology for adapting the MIP as a GC detector than towards examining it phenomenologically. Tanabe *et al.*[12] have developed a wavelength table for emission lines of non-metallic elements for a helium atmospheric MIP. However, this study does not extend below 190 nm.

With the primary concern of our investigation aimed at developing a sensitive tool for the quantitation of low molecular weight sulfur compounds, the spectral region below 190 nm was of interest. In this region three of the most sensitive sulfur emission lines exist at 180.73, 182.04 and 182.63 nm.

The effect of possible nitrogen entrainment into the discharge was of concern. Nitrogen band systems are known to extend into the vacuum ultraviolet, in particular the Far Ultraviolet System and the Lyman–Birge–Hopfield System, arising from N_2^+ and the neutral molecule N_2, respectively.

Fig. 3 shows a wavelength scan between 170.0 and 200.0 nm which was taken while a constant bleed of 10 ppm COS in N_2 was maintained to the plasma. It is interesting to note that a nearly identical spectrum was obtained when no sample was added except for the absence of the sulfur peaks. The majority of the spectrum between 183.0 and 200.0 nm was attributed to nitrogen bands most likely being the N_2^+ band system. It is fair to assume that the nitrogen flushing of the optical path just in front of the discharge tube was causing an appreciable amount of N_2 entrainment into the plasma. In addition to nitrogen band structure, the carbon emission

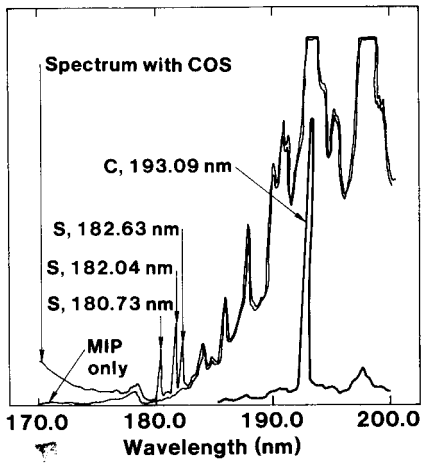

Fig. 3. Wavelength scan between 170.0 and 200.0 nm during continuous bleed of 10 ppm COS into plasma and with no COS bleed. Carbon emission line shown at 193.09 nm on a reduced scale.

line at 193.09 nm was identified and is shown in Fig. 3, where the scale has been substantially reduced. The presence of carbon was attributed to hydrocarbon impurities in the helium gas supply.

Of the three prominent sulfur emission lines, the 182.04-nm line was chosen for the balance of the analytical work due to its slightly better sensitivity than either the 180.73 nm or the 182.63 nm line.

Operational characteristics of the MIP

Several variables were considered important in obtaining both a stable and reproducible plasma and in interfacing the MIP to the gas chromatograph. Among the variables studied were power to the plasma, total helium flow-rate to the plasma, tuning variability of the plasma cavity, and plasma tube size.

Previous experience with atmospheric microwave plasmas has shown that ignition and tuning of the cavity can sometimes be difficult with seemingly large variations in day-to-day performance. In an attempt to alleviate this difficulty several additional components were added to the tuning circuit which had previously consisted of a single coaxial stub stretcher tuner. In addition to the tuner a microwave circulator and termination were added to the circuit. The circulator acts as a shunt for power which is being reflected back towards the generator due to impedance mismatching between the microwave cavity and generator. The circulator allows power to flow from the generator to the cavity but reflected power is deverted to a dummy load termination where it is dissipated as heat. The addition of these components had two significant effects on the operation of the plasma. First the tuning and ignition of the discharge were greatly simplified. Once the tuning position on the coaxial stub stretcher was found, no further tuning was required. This was due to the fact that, prior to plasma ignition, a small impedance mismatch occurred which normally requires retuning, however, with the additional circuit components this mismatch was removed. The second important effect was the reproducible plasma conditions obtained from day to day. With the tuning performance improved, plasma conditions

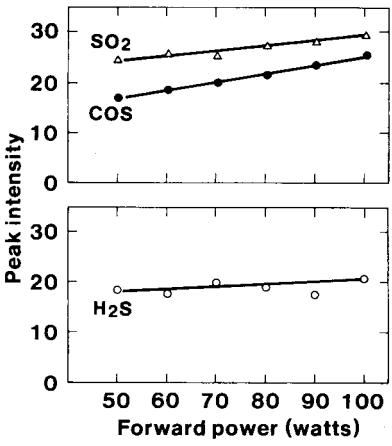

Fig. 4. Relative peak intensity *versus* forward microwave power applied to plasma for COS, H_2S and SO_2 at 100 ppm each in nitrogen.

were stable with reproducibility better than 98 % and background drifts during an 8-h period of operation being less than 1 %.

The choice of the plasma tube inside diameter was based on the need for the GC effluent to contact the plasma to the largest degree possible. It was found that with quartz tubes of 1–1.5 mm the plasma would fill the entire tube cavity at powers ranging from 60 to 100 W. Larger plasma tube cavities produced a noticeable localization of the discharge, with the plasma growing to fill the cavity only at powers exceeding 100 W.

The work reported here was carried out with a quartz plasma tube of 1.3 mm I.D. The ability of the plasma to fill the quartz tube at relatively low powers produced a remarkable low dependence on power input *versus* analytical performance of the system for the low molecular weight sulfur gases studied. Fig. 4 shows the variation of peak height *versus* power for COS, SO_2 and H_2S. Peak height was found to be an acceptable measure of response in most cases due to the sharp narrow bands ob-

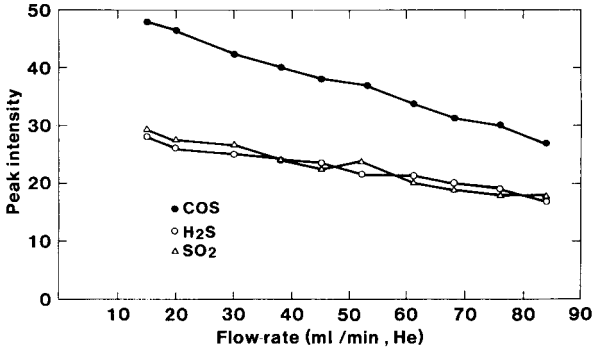

Fig. 5. Relative peak intensity *versus* helium flow-rate to plasma for COS, H_2S and SO_2 at 100 ppm each in nitrogen.

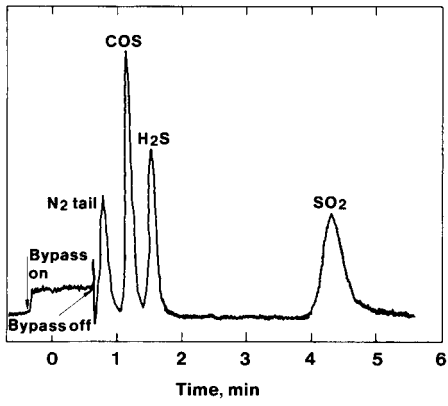

Fig. 6. Chromatogram of 5 ppm each of COS, H_2S and SO_2 in nitrogen. Operating conditions: 1 ml injection; column temperature, 60°C; column flow-rate, 15 ml/min He; total flow-rate to plasma, 60 ml/min He; forward microwave power, 100 W; reflected power, 4 W; sulfur emission line, 182.04 nm.

served. All analytical quantitations however were based on peak area. Although there seemed to be little gained by operating at higher powers, it was also found that the discharge was more stable at higher powers when the introduction of a large sample volume was necessary. In addition, plasma ignition was significantly easier at powers above 70 W. A general operating power of 100 W was maintained.

Total helium flow-rate to the discharge had a greater effect on detector response than power as can be seen in Fig. 5, where the relative peak intensity is shown *versus* total flow-rate. The combination of helium column carrier gas and plasma support gas comprised the total helium flow-rate to the plasma. The plasma can be maintained over a wide range of flow-rates, although at flow-rates less than 25–30 ml/min the discharge exhibited some instability. A flow-rate of 50 ml/min was chosen in order to provide good sensitivity while maintaining excellent plasma stability.

A typical chromatogram of a 5 ppm mixture of COS, H_2S and SO_2 is shown in Fig. 6. It was found that when sample volumes greater than 0.1 cc were utilized there was a tendency for the matrix gas, in this case nitrogen, to extinguish the plasma. In

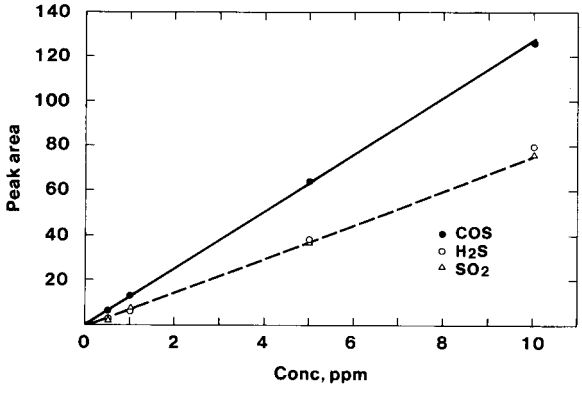

Fig. 7. Calibration curves for COS, H_2S and SO_2. Operating parameters same as Fig. 6. .

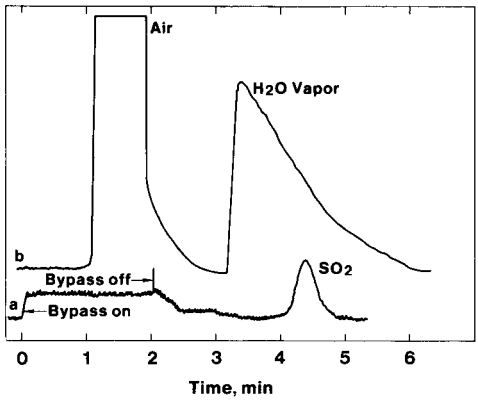

Fig. 8. (a) Chromatogram of atmospheric SO_2 with significant water vapor content using MIP detection. Operating parameters: 1 ml injection; column temperature, 60°C; column flow-rate, 15 ml/min He; total flow-rate to plasma, 60 ml/min He; forward microwave powers, 100 W; reflected power, 4 W; sulfur emission line, 182.04 nm. (b) Chromatogram of SO_2 analysis under identical chromatographic conditions with a TCD.

addition, the matrix gas was of significant concentration to produce large background changes in the spectrum which could imitate a true sulfur compound being eluted.

To solve this problem a bypass valve was placed between the column and the MIP discharge tube similar to that reported by Quimby *et al.*[9]. Prior to injecting a sample the valve was activated causing effluent from the column to bypass the MIP. Because the helium flow-rate to the plasma was also slightly diminished, the observed background increased. Enough time was allowed for the solvent to elute from the column, at which time the valve was deactivated allowing the effluent from the column to pass into the MIP. Due to the proximity of the trailing edge of the N_2 peak to the COS peak, the valve was deactivated slightly before total elution of N_2 had

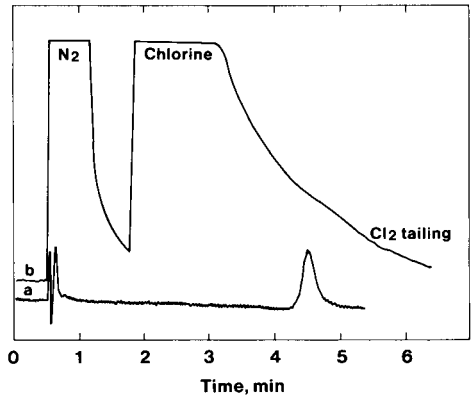

Fig. 9. (a) Chromatogram of SO_2 containing large amounts of N_2 and Cl_2. Operating parameters same as Fig. 6, 0.1-ml sample injection used and bypass valve not employed. (b) Chromatogram of SO_2 under identical conditions using a TCD.

taken place. In this case a false peak resulted from the small amount of N_2 still eluting which caused a background shift in the plasma. This, however, had no effect on our ability to resolve or quantitate COS or H_2S.

Typical calibration curves for COS, H_2S and SO_2 are shown in Fig. 7. Detection limits were determined based on the equivalent concentration at a signal-to-noise ratio of 2. The detection limits for COS, H_2S and SO_2 were 50, 100 and 100 ppb, respectively, Linear dynamic ranges, assuming the detection limits as the lowest quantitative concentration, were 2.5 for COS and 3.5 for both H_2S and SO_2.

To demonstrate the specificity of the atmospheric microwave plasma as a GC detector, a series of determinations were run for SO_2 in air samples. All samples contained large amounts of water vapor. An attempt was made to use a thermal conductivity detector but as can be seen in Fig. 8b, the water vapor eluting from the column obscures the SO_2 peak. Fig. 8a shows an identical analysis utilizing the MIP as the detector. Since only emission from sulfur is observed, the SO_2 peak is completely unaffected by the water vapor, although in reality they are eluted together.

A similar application involved the determination of SO_2 in a gas which contained large amounts of chlorine. Once again an analysis failed to detect SO_2 when a TCD was employed because of the large tailing peak due to chlorine (Fig. 9). The MIP detector was not responsive to the chlorine gas and essentially no problem was encountered in performing this analysis.

In conclusion, a system using an atmospheric microwave plasma detector for GC can be extremely useful for the determination of low molecular weight sulfur compounds. This is especially true when concentrations are low and large solvent peaks obscure the sulfur peaks of interest when conventional GC detection is used.

REFERENCES

1 A. J. McCormack, S. C. Tong and W. D. Cooke, *Anal. Chem.*, 37 (1965) 1470.
2 W. Braun, N. C. Peterson, A. M. Bass and M. J. Kurylo, *J. Chromatogr.*, 55 (1971) 237.
3 C. A. Bache and D. J. Lisk, *Anal. Chem.*, 39 (1967) 786.
4 W. R. McLean, D. L. Stanton and G. E. Penketh, *Analyst (London)*, 98 (1973) 432.
5 C. I. M. Beenakker, *Spectrochim. Acta, Part B*, 31 (1976) 483.
6 C. I. M. Beenakker, *Spectrochim. Acta, Part B*, 32 (1977) 173.
7 S. P. Wasik and F. P. Schwarz, *J. Chromatogr. Sci.*, 18 (1980) 660.
8 B. D. Quimby, P. C. Uden and R. M. Barnes, *Anal. Chem.*, 50 (1978) 2112.
9 B. D. Quimby, M. F. Delaney, P. C. Uden and R. M. Barnes, *Anal. Chem.*, 51 (1979) 875.
10 B. D. Quimby, M. F. Delaney, P. C. Uden and R. M. Barnes, *Anal. Chem.*, 52 (1980) 259.
11 S. R. Eltebracht, C. M. Fairless and S. E. Manahan, *Anal. Chem.*, 50 (1978) 1649.
12 K. Tanabe, H. Haraguchi and K. Fuwa, *Spectrochim. Acta*, 36B (1981) 119.

Journal of Chromatography, 238 (1982) 113–120
Elsevier Scientific Publishing Company, Amsterdam – Printed in The Netherlands

CHROM. 14,570

UNIVERSAL, MULTI-CHANNEL ULTRAVIOLET DETECTION IN THE PURITY ANALYSIS OF 2-ETHYL-3-(4-HYDROXYBENZOYL)INDOLIZINE BY HIGH-PERFORMANCE LIQUID CHROMATOGRAPHY

B. F. H. DRENTH*, R. T. GHIJSEN and R. A. DE ZEEUW
Laboratory for Pharmaceutical and Analytical Chemistry, Department of Toxicology, State University, Ant. Deusinglaan 2, 9713 AW Groningen (The Netherlands)
(Received November 23rd, 1981)

SUMMARY

The use of a multi-channel UV–visible detector coupled with high-performance liquid chromatography in purity analysis is described. A discussion of some advantages and disadvantages in comparison with a conventional (single-wavelength) UV detector is given. Detection and identification limits for a particular contaminant of 2-ethyl-3-(4-hydroxybenzoyl)indolizine are determined. Sensitivities for both detectors with regard to the same contaminant are derived from the calibration curves.

INTRODUCTION

During our studies[1,2] on butoprozine, {4-[3-(dibutylamino)propoxy]phenyl-{(2-ethyl-3-indolizinyl)methanone, a new drug with anti-anginal properties, we found that a number of impurities could occur in the parent drug when no special precautions were taken during its synthesis.

When ^{13}C-labelled butoprozine was needed for drug metabolism studies, we again paid special attention to the purity, with emphasis, on the immediate butoprozine precursor in the synthetic route[3], 2-ethyl-3-(4-hydroxybenzoyl)indolizine (EHBI, I) since in large scale synthesis almost all impurities in butoprozine result from impurities in EHBI. These latter impurities can be separated more easily than the butoprozine impurities. In addition to the known impurities, other contaminants might be expected as the synthesis of the [^{13}C]material was not a normal large scale production.

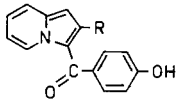

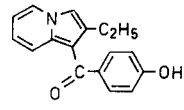

	R
II	CH_3
I	CH_2CH_3

III

0021-9673/82/0000–0000/$02.75

In our laboratory both thin-layer chromatography (TLC) and high-performance liquid chromatography (HPLC) are used routinely in purity control. Some compounds may go undetected when using column separation systems because of strong interaction between solute and stationary phase, so that these compounds are not eluted from the column. In TLC this is not a problem; compounds that interact strongly with the stationary phase appear as a spot at or near the start of the chromatogram. In addition, detection in general is more universal in TLC. Despite the disadvantages of HPLC in these respects, we have found this technique very useful in purity control because it allows the detection of trace amounts in the presence of a large amount of another substance. This can also apply when the substances are very similar.

In this paper we will describe some advantages and limitations of a multi-channel UV–visible detector as compared to a conventional UV detector in purity control by means of HPLC.

EXPERIMENTAL

Chemicals and reagents

[^{12}C]- and [^{13}C]EHBI were gifts from Labaz (Brussels, Belgium). Methanol was analytical grade (pro analysis) and obtained from E. Merck (Darmstadt, G.F.R.). Distilled water was used.

High-performance liquid chromatography

A M 6000 pump (Waters Assoc.) was used with a Model SF 770 variable-wavelength UV detector (Schoeffel), operated at 240, 280 or 380 nm, or with a HP 8450 A (Hewlett-Packard) multi-channel UV–visible detector equipped with a Model 178.32 QS quartz cell (Hellma) with 8-μl volume. Injections were made with a WISP 710 B autoinjector (Waters) using an injection volume of 25 or 100 μl.

In all experiments a stainless-steel column (150 × 4.6 mm I.D.) was used. The column was packed with Hypersil-ODS (mean particle size 5 μm, Chrompack) using a slurry in carbon tetrachloride–methanol (8:2). The mobile phase consisted of methanol–water (65:35, v/v). Before mixing the components were filtered through a 0.45-μm membrane filter (Schleicher and Schüll). The flow-rate was 1 ml/min.

The multi-channel detector measured an absorption spectrum (200–800 nm) every 7 sec. These spectra were stored on a tape cartridge using a dual tape drive Model HP 9875 A (Hewlett-Packard). Plotting of the chromatograms was done using a Model 9825 desk top computer (Hewlett-Packard) and a Model 9872 A plotter (Hewlett-Packard). The plotting program was obtained from Hewlett-Packard, but we adapted it in several ways to meet our requirements. Details have been given elsewhere[4].

RESULTS AND DISCUSSION

Detection

From results of other experiments we expected EHBI to be contaminated with the isomeric 1-(4-hydroxybenzoyl)-2-ethylindolizine (III) and with 2-methyl-3-(4-hydroxybenzoyl)indolizine (II). Small amounts of II and III could be separated from

each other and from large amounts of I by HPLC, but not by TLC, for which numerous systems were tried. The chromatograms at different wavelengths are given in Fig. 1; the small peaks b and c are caused by III and II respectively, while I gives d. Peak a was found to be composed of several compounds (see below).

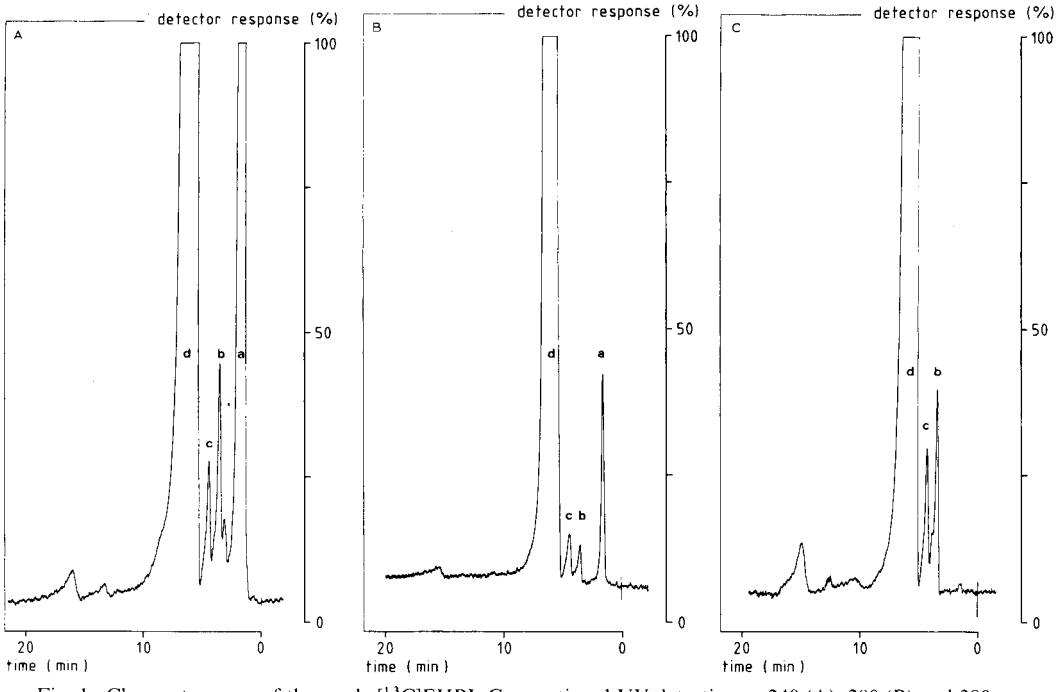

Fig. 1. Chromatograms of the crude [^{13}C]EHBI. Conventional UV detection at 240 (A), 280 (B) and 380 nm (C). Code: b = III; c = II; d = I.

As can be seen from Fig. 1, the selectivity of the conventional detector results in different chromatograms, depending on the wavelength selected. The fast eluting compounds in peak a are detected at 240 nm but not at 380 nm. Each individual wavelength required a new injection of the sample. In this way some information could be obtained on the presence of unknown compounds.

A detector that can cover a large range of wavelength, however, would provide more information, which in addition would be available much faster as only a single injection is needed. In this respect the multi-channel detector offers substantial advantages: in 1 sec the whole wavelength range between 200 and 800 nm is measured. This rapid measurement of the spectrum avoids the use of stop-flow conditions[5]. In cases where samples of unknown composition have to be analyzed, the stop-flow technique is useless anyhow for practical reasons: after every small time interval the flow has to be stopped in order to obtain an absorption spectrum. The amount of information produced by the multichannel detector is so large that data storage is necessary. After the chromatographic run the stored data can then be processed.

In Fig. 2 the absorbance–wavelength–time surface is shown, reconstructed from spectra taken with a 7-sec interval. Such a surface ("three-dimensional chromatogram") shows the presence of UV–visible active contaminants at a glance, together

with preliminary structural information. In the rear of the three-dimensional chromatogram EHBI causes the large mountain (d). The other ridges are due to contaminants. Although absorbances larger than 0.150 have not been plotted because of clarity, full spectral information is available on the tape; the UV–visible spectrum for each contaminant can be obtained. As there are small differences in the spectra between II and III the small ridges in front of I can readily be identified.

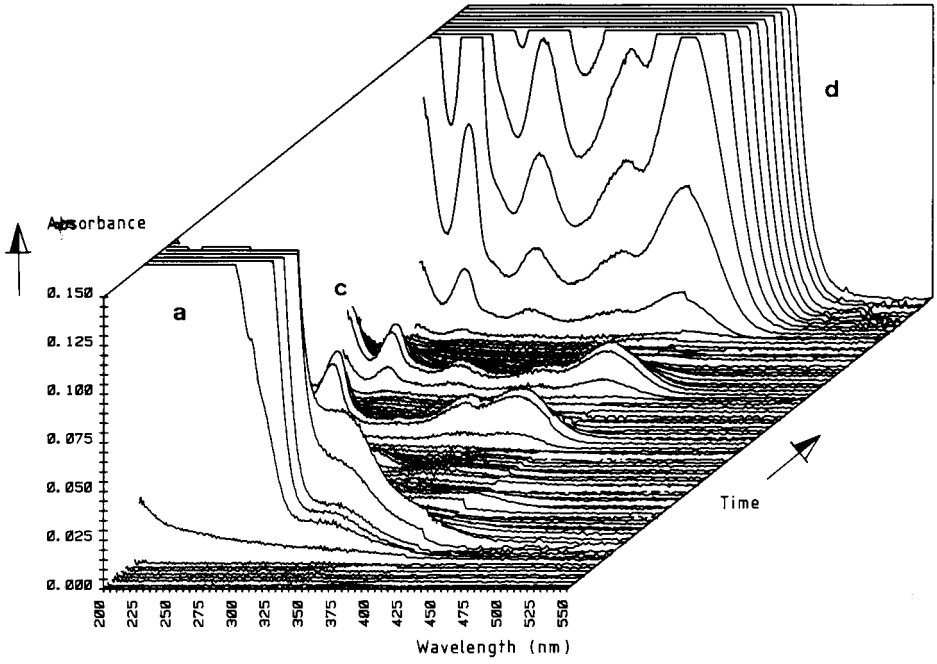

Fig. 2. Chromatogram of the crude [^{13}C]EHBI. Multi-channel UV detection.

The contaminants eluting in and just after the void volume show such a large absorbance that the surface behind cannot be observed. In order to obtain this information it is not necessary to repeat the measurement using more suitable conditions. The same data can be used to plot a new surface while omitting the interfering spectra (Fig. 3). An alternative is to plot the spectra in the reverse direction. In this way we can take a look at the rear of the front ridge (Fig. 4). It is obvious from this Figure that several compounds with different spectral properties are present.

Finally, in Fig. 5 the results obtained with material that has been purified by preparative HPLC[6] are shown. The amount injected was the same as in Fig. 2, so the much higher purity is readily seen.

Detection limits

As a basis we have taken the treatise on detection limits by Boumans[7]. This means that in the following discussion the net measures (net signal magnitudes) are used to make decisions. With the aid of a calibration line the minimum detectable amounts or concentrations are then calculated using these limiting signal magnitudes.

When we have to determine whether compounds other than the main com-

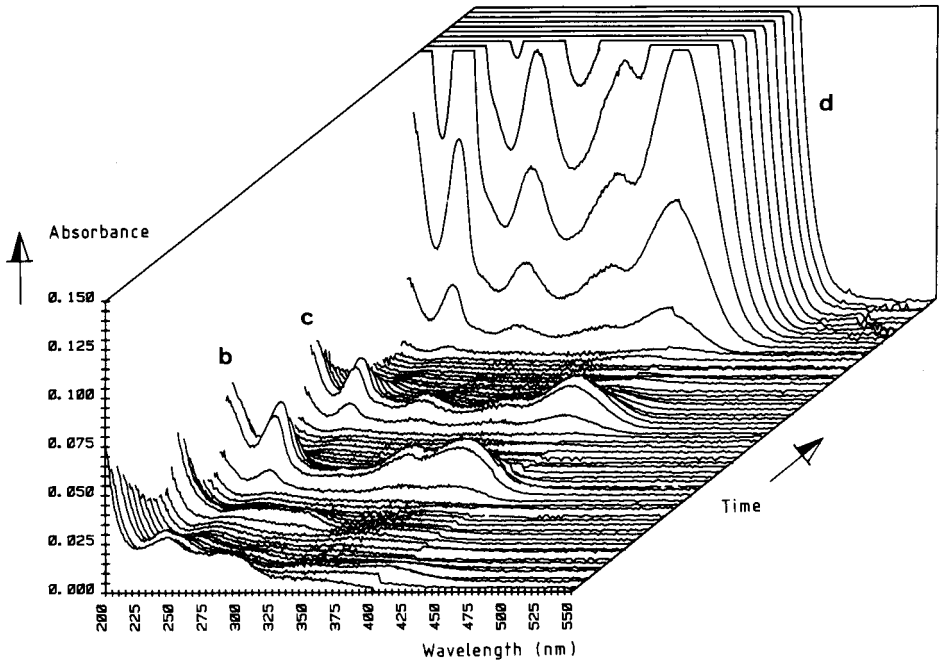

Fig. 3. The same chromatographic run as used in Fig. 2, but for a better view of the peaks eluting just after the front the first spectra have been omitted.

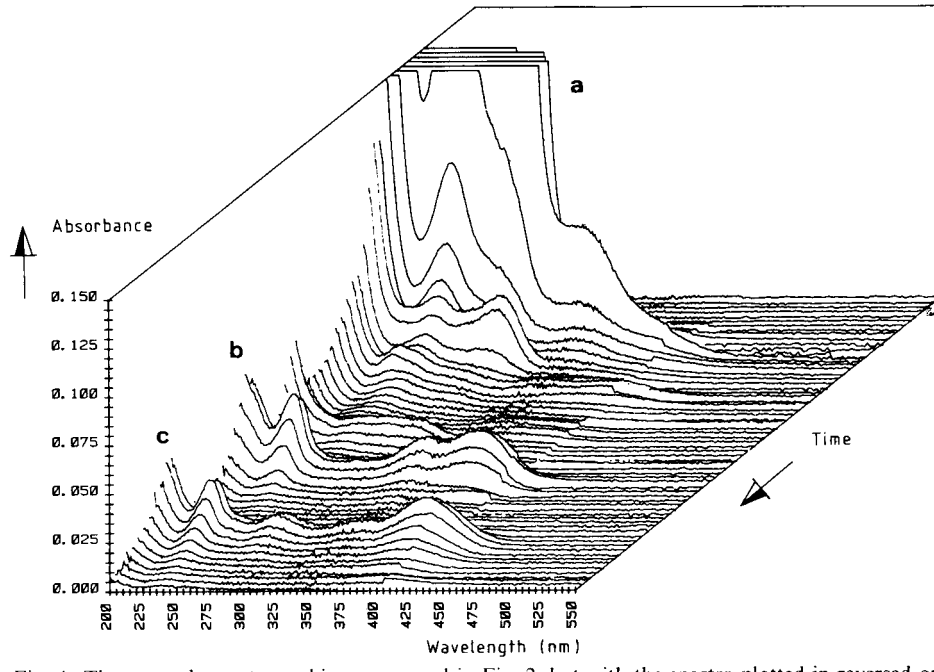

Fig. 4. The same chromatographic run as used in Fig. 2, but with the spectra plotted in reversed order (note the time axis), omitting the spectra resulting from EHBI.

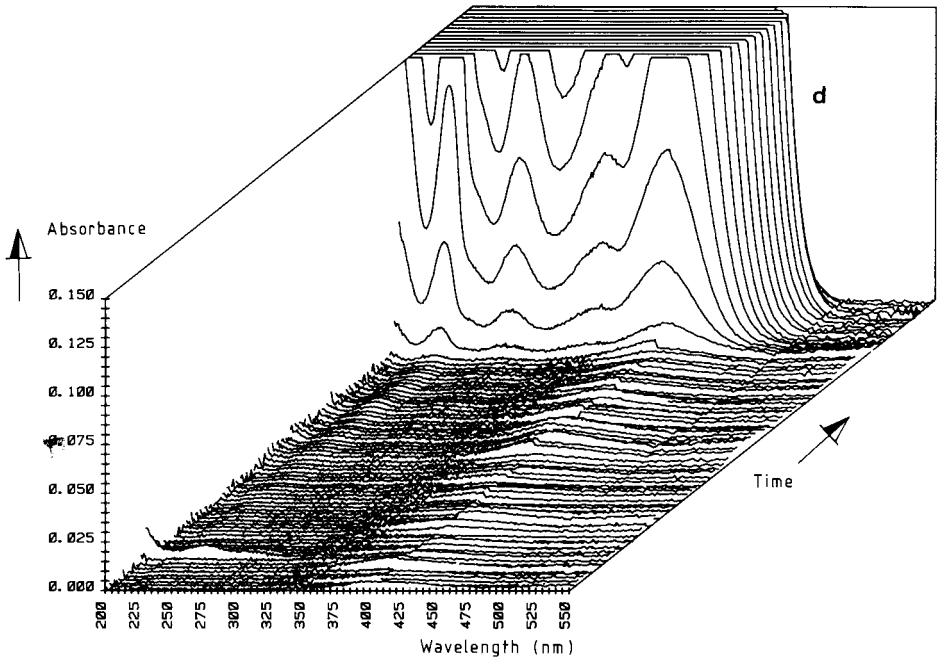

Fig. 5. Chromatogram of the purified [^{13}C]EHBI. Conditions as in Fig. 2.

pound are present, all we can do is to examine the chromatogram and decide if signals are present that cannot be attributed to the background or main compound. Such a decision requires a limiting signal, L_D, to be chosen. This is the smallest signal that is not attributed to background. The detection limit L_D is chosen in such a way that the risk, α, of fiding a background signal larger than L_D is small. If the background signals are normally distributed

$$L_D = k\sigma_B$$

where σ_B is the standard deviation related to the background signal distribution and k is the standard normal deviate. In general, the background fluctuations will be well known for isocratic elution: a reliable estimate, s_B, for σ_B is obtained from a large number of background measurements: $s_B \approx \sigma_B$. From a table of a (single sided) normal distribution it can be found that $L_D = 2.3\ \sigma_B$ for risk $\alpha = 1\%$. The detection limit depends on the background fluctuations only. The magnitude of these fluctuations vary somewhat over the wavelength range from 200 to 800 nm.

For unknown contaminants only a decision "detected" or "not detected" can be made. When contaminants are known and a calibration line is available, the limiting concentration or limiting amount can be calculated. However, for a sample giving a mean signal L_D the risk that a signal smaller than L_D will be produced is 50%. If a lower risk (β risk) for attributing a true signal to background is wanted, a larger limiting signal, L_I, must be chosen. For the identification limit L_I, we state

$$L_I = L_D + k\sigma_I$$

where σ_I is the standard deviation of the true signal distribution with mean L_I. As σ_I is usually estimated from a small number of observations the Student distribution has to be used:

$$L_I = L_D + t \cdot s_I$$

For compound II we determined the calibration function in the low mass range (0.5–40 ng) as

$$R = 0.225 \times 10^{-3} \times M - 0.029 \times 10^{-3}$$

where R = response, *i.e.*, the peak height (a.u.), and M = mass (ng) using the conventional detector (at 233 nm with time constant 0.5 sec).

For the multi-channel detector the calibration function found (at 233 nm with 1-sec interval) is:

$$R = 0.220 \times 10^{-3} \times M - 0.207 \times 10^{-3}$$

In both cases the same column, eluent and injection volume (100 μl) were used, so the same factors representing the dilution in the column[8] are included in the overall sensitivities.

Using these calibration curves the amounts (ng) corresponding to L_D and L_I can be calculated (risk α = 1%, risk β = 5%, t = 1.7):

	L_D	L_I
conventional:	0.000067 a.u. (0.4 ng)	0.000116 a.u. (0.6 ng)
multi-channel:	0.000383 a.u. (2.6 ng)	0.000667 a.u. (4.0 ng)

From the equations of the calibration curves it can be seen that the sensitivities (slopes of the lines) are almost equal. The noise level for the multi-channel detector, however, is much higher as can be seen from the values of L_D.

Although II could no longer be detected in the ^{13}C-material obtained after purification by preparative HPLC when using the multi-channel detector (Fig. 5), traces of II could be shown to be still present in the purified material when the conventional detector was used.

CONCLUSIONS

The multi-channel detector is exteremely useful for the screening of unknown compounds. An impression of the purity of a compound can be obtained in a short time as far UV–visible active contaminants are concerned. Although the multi-channel detector has a higher noise level than the conventional detector, this will be compensated to a large extent because the wavelength giving the highest sensitivity can be found easily with the former. In cases where the properties of contaminants are known, we prefer the use of a conventional detector tuned to the relevant contaminant because lower levels can be detected.

ACKNOWLEDGEMENT

We gratefully acknowledge Labaz S.A. for various gifts of materials and facilities.

REFERENCES

1 B. F. H. Drenth and R. A. de Zeeuw, *J. Chromatogr.*, 191 (1980) 109–114.
2 F. Overzet, B. F. H. Drenth and R. A. de Zeeuw, *High Resolut. Chromatogr. Chromatogr. Commun.*, 4 (1981) 448–453.
3 J. Gubin, G. Rosseels, M. Peiren, M. Prost, M. Descamps, J. Richard, J. Bauthier and R. Charlier, *Eur. J. Med. Chem.*, 12 (1977) 345–350.
4 R. T. Ghijsen, B. F. H. Drenth, F. Overzet and R. A. de Zeeuw, *J. High Resolut. Chromatogr. Chromatogr. Commun.*, submitted for publication.
5 A. M. Krstulovic, R. A. Hartwick, P. R. Brown and K. Lohse, *J. Chromatogr.*, 158 (1978) 365–376.
6 B. F. H. Drenth, A. J. G. Wormeester and R. A. de Zeeuw, in preparation.
7 W. J. M. Boumans, *Spectrochim. Acta, Part. B*, 33 (1978) 625–634.
8 B. L. Karger, M. Martin and G. Guiochon, *Anal. Chem.*, 46 (1974) 1640–1647.

Journal of Chromatography, 238 (1982) 121–132
Elsevier Scientific Publishing Company, Amsterdam — Printed in The Netherlands

CHROM. 14,600

GAS CHROMATOGRAPHIC DIFFERENTIATION AND ESTIMATION OF SOME SULFUR AND NITROGEN MUSTARDS USING A MULTIDETECTOR TECHNIQUE

SAMUEL SASS* and RALPH J. STEGER
Research Division, Chemical Systems Laboratory, Aberdeen Proving Ground, MD 21010 (U.S.A.)
(Received October 28th, 1981)

SUMMARY

A simultaneous multidetector system for gas chromatography was designed and applied to a series of sulfur and nitrogen mustard compounds. It was found possible to detect and estimate species even when very proximate in retention time. Up to four detectors could be operative at the same time with a single injection of nanograms to micrograms of sample. Parathion was selected as a compound sensitive to all the detectors.

INTRODUCTION

Some sulfur and nitrogen mustards have been found to be relatively persistent and a few have even been considered or even applied as chemotherapeutic agents because of their cytotoxicity. The need existed for a trace analytical system that could be used to identify and estimate these species as residues from a wide variety of media, both physical and biological. Among these compounds were bis(2-chloroethyl)sulfide (H), bis(2-chloroethyl)ethylamine (HN-1), bis(2-chloroethyl)methylamine (HN-2), tris(2-chloroethyl)amine (HN-3), bis(2-chloroethylthio)ethane (Q) and bis(2-chloroethylthioethyl)ether (T). Also of interest in the past were mixtures such as H and Q (HQ) and H and T (HT). At a time when no single method had been available with the capability of differentiating between the mustards at the low milligram to nanogram range, gas chromatography (GC) was shown to be highly effective for this purpose[1]. In this investigative work, beginning circa 1965, the electron-capture detector (ECD) which had become generally available for GC, was evaluated and thence employed in our laboratories for both identification and trace quantitative estimation of these compounds.

Since that time a number of investigators have reported on the application of GC to the analysis of mustard "gas" [bis(2-chloroethyl)sulfide] and related compounds[2–5].

With the advent of the flame photometric detector (FPD) for phosphorus and sulfur[6], plus the Coulson[7,8] and then the Hall[9] nitrogen detector, the concept of GC with multidetector finish became one of potential practical application. For this pur-

0021-9673/82/0000–0000/$02.75

pose, we had originally equipped an F&M Scientific (now Hewlett-Packard) Model 5750 gas chromatograph having a flame ionization detector (FID) and an ECD, with a Microtech photometric head having phosphorus (526-nm) and sulfur (394-nm) filters and an electrometer. This equipment thus gave the capability for determining the mustards with the identical GC column, but sampled separately for different detectors. The added advantage observed by combining selectivity of detection with proximity of retention times brought us to the point of specifying design of equipment that would produce simultaneous recordings or printouts relating the retention time found with the respective detectors and even the relative quantity of compound as represented by integrated peak areas. An obvious additional benefit, especially when the amount of available sample might be limited, is the fact that at least three detector outputs could be obtained with only a single injection of solution or of air sample. The request for bid thus included our specifications to best meet, within the then state of the art, our requirements. We selected parathion of certified purity as the test compound for acceptance of instrument. This report describes our application of the multidetector concept to the determination of trace quantities of some mustards, and parathion as a representative of a phosphorus pesticide.

EXPERIMENTAL

Equipment and materials

The gas chromatograph which most closely approximated our specifications was the Tracor Microtek MT 220 which at that time was the sole licensee for flame photometry, the Coulson nitrogen detector and later the Hall, on a commercial basis. The design of the basic instrument was such that phosphorus and sulfur were detectable simultaneously on a dual head flame photometer[6]. Four ports were available for injection and the instrument was capable of holding four different columns. According to our design, each column could be connected to a separate detector or the output from any single column could be split two or three ways for separate and simultaneous detection such as by ECD (pulsed or d.c. mode), FID and FPD in the combined P and S mode, or a three-way combination that could include the Coulson or Hall nitrogen detector. Four recordings could be obtained simultaneously by means of two dual needle recorders. The peaks could be quantitated by means of ball and disc integrators or measured separately using electronic integrators. Included in the instrumentation capability was a teletypewriter which served for data handling as well as programming. Microweighing was done on a Cahn Electrobalance and injections were performed using Hamilton microliter and gas-tight syringes. The column coatings and supports were obtained from Applied Science Labs., State College, PA, U.S.A. Solvents used were of CP grade except for the nanograde hexane used in determinations that involved the ECD.

Sample standards

The sulfur and nitrogen mustards used as standards were available samples further purified where necessary. This was accomplished by either fractional distillation or preparative GC as for H, Q, and T, and by fractional crystallization as for the nitrogen mustards which were stored as their hydrochlorides. The free bases of nitrogen mustard compounds are very unstable, being susceptible to *in situ* intra-

and intermolecular alkylation. HD (distilled mustard) samples were of purities no lower than 96.5% as determined by freezing point depression, alkylation titration employing thiosulfate[10], thin-layer chromatography[11] and by GC employing thermal conductivity detection (F&M Scientific, Model No. 810). Q (or sesquisulfur mustard) was 98.5% pure as determined by melting point, the alkylation titration, elemental analysis and GC. HN-1, HN-2, and HN-3 as their hydrochloride salts were 95, 97 and 97% pure, respectively, on the basis of elemental analysis, alkylation titration, and by GC after conversion to their free bases, as described later.

HQ was a mixture of H and Q (50:50, w/w). Parathion was of 95%+ purity as obtained from Shell Chemical.

Procedure

Purity determination by GC. The basic instrumentation employed in this investigation included a Tracor Model MT 220 gas chromatograph equipped with a dual head, an FPD (phosphorus and sulfur filters), an FID; the Model M5 Coulson (CCD) and later the Model 700 Hall electrolytic conductivity detector (HCD), both in the nitrogen mode; and the Tracor pulsed-mode and d.c.-mode electron capture (^{63}Ni) modules which could be alternately tied into the system. Each of the detectors were separately equipped with their own dual channel electrometers. Data handling was performed with the Infotronics CRS-208 electronic integrator, and the Hewlett-Packard Model 3380A report integrator, two Westronic M-22 dual-pen recorders of 0–1 mV range and a Teletype 33T2 teletypewriter. Switching for detector selection was accomplished by means of Cat. No. 4011, Carle valves (Carle Inst., Fullerton, CA, U.S.A.).

The arrangement of columns and valves on the modified Tracor MT-220 to allow for multidetection is shown in Fig. 1.

In our configuration with the capability for four columns, the sample could be directed to a single detector or to simultaneous multidetection. The columns could contain the same packings or allow a variety of choice. Fig. 1 illustrates the arrange-

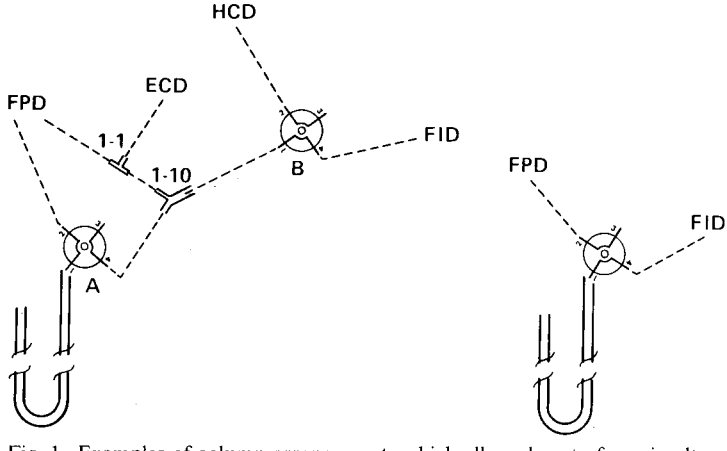

Fig. 1. Examples of column arrangements which allowed up to four simultaneous detector responses. A and B are two way valves; splitters are 1:10 and 1:1 as indicated. (Parathion gave simultaneous response for FPD-S and -P, ECD, and FID or HCD.)

ment whereby the valve off the column (valve A) allows either direct FPD or flow to a two-way splitter. The first two-way splitter directs column effluent as a one (FPD and ECD) to ten [Hall nitrogen (HCD) or FID] feed. The 1:1 splitter feeds an equal amount of effluent to FPD and ECD. Replumbing could allow a split wherein FPD might be eliminated in favor of ECD, FID and HCD or, with the elimination of ECD, to allow inclusion of FPD, FID and HCD. Column 2 of the equipment was dedicated to ECD and columns 3 and 4 were each connected via a valve that gave the capability for separate detectors and the same or different packings.

Purified samples (or samples of known purity, 90% and better) of sulfur mustards were dissolved in hexane or chloroform to obtain a concentration of about 50 mg/ml of solution.

For nitrogen mustards of known purity (90% and better) as the hydrochloride salts, weighed quantities were dissolved in chloroform (also at a concentration of about 50 mg/ml). Sufficient sodium carbonate (roughly equal to the weight of the sample) was added to a vial, followed by an amount of water approximating the quantity of chloroform. After shaking for about 30 sec, all of the nitrogen mustard as the free base was found in the chloroform layer.

Aliquots of the chloroform solutions of the sulfur and nitrogen mustards in the range of 5 μl (0.23 μl, 1.0 mg) were subjected to GC, fitted with the thermal conductivity detector (TCD). A calibration curve of peak area *versus* weight of compound (corrected for known purity) was prepared. This curve was found to be linear over the range of 0.25 to 1.0 mg of mustard.

Samples resubmitted to the determination of purity were weighed and dissolved in chloroform in the range of 50 mg/ml and then treated in the same manner as the known purity compounds used in the calibration. Aliquots (10 μl) of the chloroform were injected and the actual mustard content was extrapolated from the calibration curve. This value divided by the calculated weight of material injected times 100, gave the purity of the material being analyzed.

Using calibration based on known purity mustard, the standard deviation was of the order of 1%.

The conditions used for the purity determination, while employing an F&M Model 810 gas chromatograph, follow: bridge current (TCD): 150 mA; attenuation: $\times$ 16; sample size: 10-μl aliquot from 50 mg/ml of solution; carrier gas flow-rate: helium, 90 ml/min; detector temperature: 310°C; injection chamber temperature: 200°C; column: 6 ft., Pyrex glass, 1/4 in. O.D.; column coating: 10% QF-1; column support: Gas-Chrom Q (60–80 mesh).

Procedures for estimation of trace quantities. Conditions were established whereby each trace detector system could be calibrated separately, or together with the other detector(s) being employed. Helium was the carrier gas of choice to fit all of the detectors except the ECD. For electron capture in the conventional pulsed mode, argon–methane was used as the carrier and purge gas. For the d.c. mode, nitrogen served as the carrier and purge gas, with helium used as the carrier gas only when in the multidetector phase.

Chromatography was performed both under temperature-programmed conditions and isothermally. The former was useful for aiding in the identification of the species and for determining the most reasonable isothermal temperatures for analysis of the specific compounds.

Dual flame-ionization detection. The 6 ft., 3% QF-1 GC column employing FID or other detectors was programmed at 8°C/min from 60 to 230°C. For FID, quantities of mustards or parathion were at the concentration level of 100 μg/ml of solvent or greater and 3 μg or more of the compounds were injected for assay or calibration purposes. The elution temperatures found for the various mustards, using the 6 ft. 3% QF-1 column under temperature programming (8°C/min from 60 to 230°C), are listed in Table I.

TABLE I

ELUTION TEMPERATURES AND RETENTION TIMES OF THE MUSTARDS

Programmed at 8°C/min from 60°C. (B) = free base.

Agent	*Peak elution*	
	Temperature (°C)	*Retention time (min)*
HN-1	100	5
H	100	5
HN-2 (B)	110	6.3
HN-3 (B)	120	7.5
Q	165	13.1

Electron-capture detection. When employing the ECD in the pulsed mode (PM-ECD) calibration curves and linearity checks were made by injecting measured volumes of a variety of concentrations, *e.g.*, 1, 10, 25 and 50 ng/μl, of sulfur mustards dissolved in hexane instead of chloroform. Unknown solutions and vapor concentrations of the mustards were estimated based on these calibration curves. Calibrations were performed daily for each agent being analyzed to compensate for any sensitivity changes that might occur in the chromatographic system.

Similar calibration curves were prepared for the nitrogen mustards in hexane after conversion of the salts to the free bases. The concentration of sample subjected to chromatography was similar to that used for the sulfur mustards mentioned above. Salts of the nitrogen mustards, in the proportion of 1 mg/ml of hexane, were treated with approximately 0.05 g of sodium carbonate followed immediately with 10 ml of water and mixing. Aliquots from the hexane layer were used in the preparation of the standard solutions for calibration in the same increments as mentioned previously.

Solutions of mustards of uncertain concentration were analyzed using sample volumes from 0.5 to 30 μl, starting with the lower volume to minimize the possibility of detector overload. Similar precautions were taken with vapor samples, where volumes in a range from 0.5 to 5 ml are recommended.

A listing of the chromatographic conditions common to all of the mustards, and parathion, when using the various detectors, follows: column: 6 ft. × 2 mm I.D. Pyrex glass, packed with 3% QF-1 on 100–120 mesh Gas-Chrom Q; column temperature: programmed at 8°C/min from 60 to 230°C. Isothermal as shown in Table II; inlet temperature: 200°C; transfer temperature at valves: 210°C; detector temperature: FID 250°C, FPD 185°C, HCD solvent transfer, 220°C, furnace 875°C, d.c.-ECD 220°C, PM-ECD 250°C; carrier gas: helium at 40 ml/min for all detectors

TABLE II

RETENTION TIMES FROM DIFFERENT ISOTHERMAL COLUMN TEMPERATURES

a = 4.5 ft. 10% QF-1, b = 6 ft. 3% QF-1.

Agent	*Column temperature (isotherm) (°C)*		*Retention time (peak maximum) (sec)*	
	a	*b*	*a*	*b*
H	110	90	240	140
HN-1	120	90	240	125
HN-2	120	105	180	70
HN-3	140	110	480	330
Q	170	155	390	80
T	200		390	
Parathion	200		390	

except argon–methane at 90 ml/min for PM-ECD, and preferably nitrogen at 30 ml/min for d.c.-ECD only when the latter is not in a multi-detector phase; purge gas: HCD, helium at 40 ml/min and as make-up gas when the solvent was vented before it reached the reaction furnace; d.c.-ECD, nitrogen at 30 ml/min; PM-ECD, argon–methane (90:10) at 10 ml/min; reaction gas: HCD, hydrogen at 50 ml/min; fuel gas: FPD: hydrogen at 120 ml/min, oxygen at 20 ml/min and air at 35 ml/min; FID: hydrogen at 40 ml/min and air at 35 ml/min with helium at 20 ml/min as equilibrator gas.

RESULTS AND DISCUSSION

Tests with a variety of column substrates had indicated that the subject mustard compounds were reasonably elutable when present in microgram or larger amounts. Among the coatings tested were dodecyl phthalate, SE-30, Apiezon N, Versamid 900 and QF-1. Prior experience with relatively reactive compounds such as the mustards described here[1] and the irritant type compounds CA (bromobenzylcyanide), CN (chloroacetophenone) and CS (*o*-chlorobenzylidenemalononitrile)[12], and some pesticides[13] had indicated that the QF-1 coating yielded the sharpest peaks even at the low nanogram level. Gas-Chrom Q was the support material found to give optimum results. To preclude direct reaction with the column, metal-catalyzed decomposition or thermolability, a glass column and the on-column injection technique were utilized.

Initial studies made using a sample of unknown purity started with a semi-quantitative GC assessment (thermal conductivity) based on the ratio of agent peak area to total peak area. H, Q, T and parathion were injected as chloroform solutions, and the nitrogen mustards were run as their respective free bases after partitioning into chloroform from aqueous solution, via sodium carbonate treatment.

Experiments similar to those described above, were made employing the dual hydrogen FID but on more dilute solutions (μg to mg/ml). This study aided in the selection of optimum column conditions (temperature and flow-rate).

As with all analysis employing the ECD, especially in the case of halo com-

pounds, great care was exercised to keep the amount of each mustard agent chromatographed initially in the low (1 to 10) nanogram range. Once the degree of response was established at this low level, progressively larger samples (10 to 20 ng increments) were injected to establish the linear region of the response curves and to insure against severe detector overload. Hydrogen chloride and methylene chloride can be present as decomposition products of H, Q and T. Dilute solutions of the sulfur mustards and parathion were prepared in spectrophotometrically pure hexane. It was also found possible to determine low concentrations of the salts of the nitrogen mustards by their conversion to the free base with aqueous sodium carbonate and a simultaneous extraction into hexane. Very little loss through hydrolysis of the mustard agent was observed while using this conversion procedure.

Freshly prepared solutions of H (10 to 50 ng/ml) in 1 l of saline–water (1:10) were extracted almost immediately with 100 ml of hexane, in a separatory funnel. Aliquots of the supernatant hexane were subjected to GC, fitted with the ECD. With the original favorable increase in concentration of 10 to 1, due to solvent transfer (1000 ml reduced to 100 ml) plus the sensitivity of the detector to nanogram quantities of mustard, it appeared possible to measure residual H present in aqueous media at the level of ppt (10^{12}). This scheme should also have application to the measurement of unreacted mustards in physiological media. The rate determining step for hydrolysis of sulfur mustards (H, Q and T) is the cyclization to the ethylenesulfonium ion

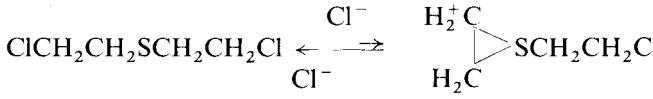

Chloride ion supresses the sulfonium ion formation thus giving a degree of stability to the mustard dissolved in the water. The rate determining step for hydrolysis of the nitrogen mustards is the hydration of the relatively stable ethyleneimonium complex

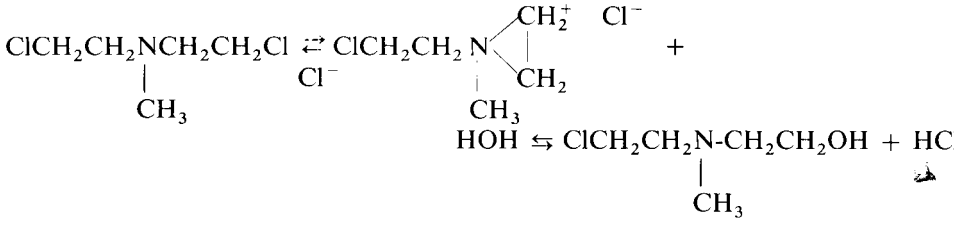

Solution concentrations were measured for all the mustard agents and parathion from 1 to 100 ng and up to micrograms (FID) employing each of the appropriate detectors. The responses observed for practical linearity are summarized in Table III.

The characteristics of the separate detectors relating to response sensitivity and thus linearity and reproducibility can vary with the state of the art in instrumentation. The multidetector arrangement that we have established using the modified Tracor MT-220, with its accompanying detectors, could be applied to equipment from other sources. The essential difference might be in the relative sensitivities, and possibly specificity, when compared to later detector systems, *i.e.*, "light pipe" for FPD[14] and

TABLE III

LINEARITY RANGE OF DETECTORS FOR APPROPRIATE COMPOUNDS

Agent	*Linearity range**					
	FPD-S (ng)	*FID (μg)*	*d.c.-ECD (ng)***	*PM-ECD (ng)*	*HCD-N (ng, 30 V)*	*FPD-P (ng)*
H	10–100	0.5–500	5–100	5–200	50–200	–
HN-1	–	0.5–500	5–100	5–100	50–200	–
HN-2	–	0.5–500	5–50	5–50	50–200	–
HN-3	–	0.5–500	5–100	5–100	50–200	–
Q	10–100	0.5–500	5–100	5–70	–	–
Parathion	10–100	0.5–500	10–100	5–100	50–200	5–100

* No attempt was made to test any of the agents for linearity in excess of the cited ranges. Wider ranges of concentrations were analyzed simply by varying the sample size.

** ECD, pulse interval of 50 μsec, d.c.-ECD (30 V).

the alkali thermionic detectors for nitrogen and phosphorus[15,16] along with electronic filter/electrometer improvements for baseline maintenance and signal-to-noise ratio advantages. The detectors available to us were evaluated for each of the mustards and for parathion using attenuation settings that would permit quantitative measurement of column effluent via three way splitting. For simplicity, "equalized" thirds of sample would be supplied to the respective detectors. The goal was to determine the sensitivity thresholds of the detectors for the respective compounds, as well as the concentrations *versus* instrument settings for near equal responses. The

TABLE IV

RESPONSE OF DETECTORS FOR MUSTARDS AND PARATHION

	HN-1	*HN-2*	*HN-3*	*H*	*Q*	*Parathion*
FPD-S						
Attenuation				32 × 10	32 × 10	32 × 10
Minimum detectable limit (ng)				2	2	2
At 10:1 signal-to-noise level (ng)				5	5	7
d.c.-ECD 30 V						
Attenuation	32 × 10	32 × 10	32 × 10	32 × 10	32 × 10	32 × 10
Minimum detectable limit, (ng)	0.2	0.2	0.3	0.3	2	0.3
At 10:1 signal-to-noise level (ng)	2	2	4	3	4	4
FID						
Attenuation	4 × 10	4 × 10	4 × 10	4 × 10	4 × 10	4 × 10
Minimum detectable limit (ng)	60	40	70	60	40	40
At 10:1 signal-to-noise level (μg)	0.5	0.5	0.7	0.5	0.5	0.5
HCD-N						
Attenuation	2 × 10	2 × 10	2 × 10			2 × 10
Minimum detectable limit (ng)	10	5	10			5
At 10:1 signal-to-noise level (ng)	40	20	40			25
FPD-P						
Attenuation						32×10^2
Minimum detectable limit (ng)						0.7
At 10:1 signal-to-noise level (ng)						5

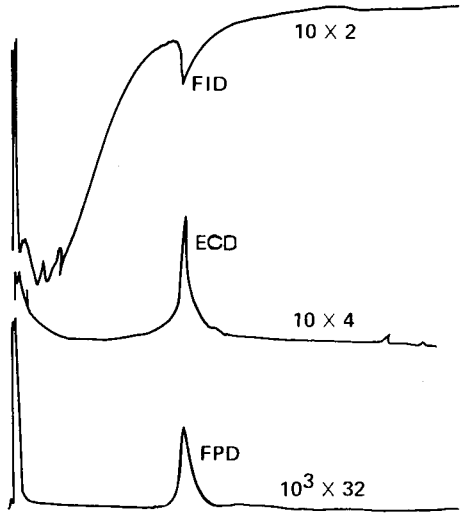

Fig. 2. Simultaneous detector response for purified H using two recorders.

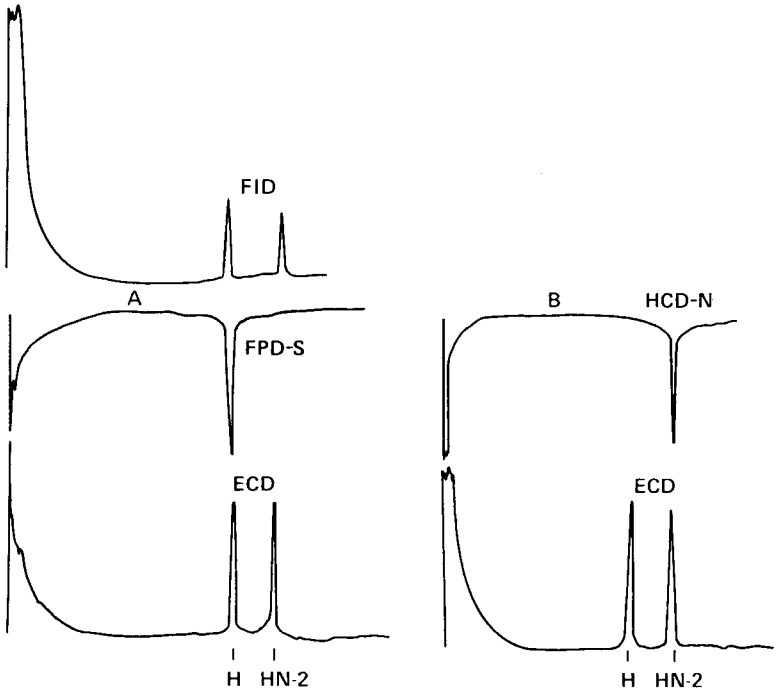

Fig. 3. Simultaneous detector response for a mixture of H and HN-2. Left: ECD, FPD-S and FID; right: ECD and HCD-N.

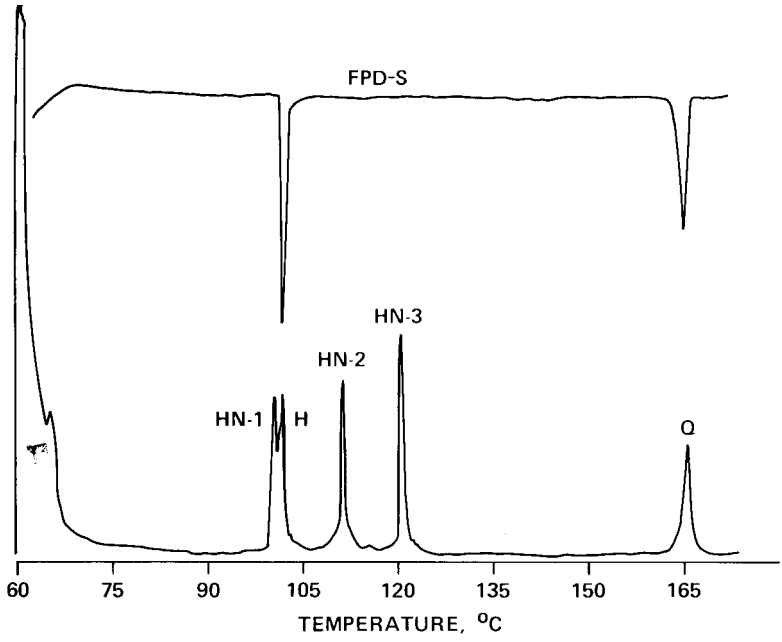

Fig. 4. Composite chromatography of the mustards employing FID and FPD-S, programmed at 8°C/min from 60°C. Similar chromatograms were obtained using other detectors. Parathion gave simultaneous responses for FPD-S and -P, ECD, and FID or HCD; and T was detectable via FPD-S, FID and ECD.

relative sensitivities of the detectors for these compounds in decreasing order are d.c.-ECD > FPD > FID > Hall nitrogen > Coulson nitrogen. Dilutions of the compounds in their respective solvents were injected into the GC column (210°C) under single, dual and multidetector configurations. With the optimum electrometer attenuations set for the respective detectors it was possible to determine the minimum detection limits for the mustards. Also estimated were the analytical limits wherein a 10:1 signal-to-noise level could be obtained. These results are shown in Table IV.

d.c.-ECD was originally selected for the multidetector approach because it could use a carrier gas more common to the other detectors. An ECD capable of operation in the constant mode has since been reported[14] as having a similar advantage. d.c.-ECD is less specific than when in the pulsed mode, and can be advantageous since it is applicable to the detection of a broader number of compounds. It should be pointed out that at least one of our four columns was dedicated to PM-ECD. With the pulsed mode detector the range could be extended by decreasing the pulse interval to 15 μsec or less, if desired. The minimum detectable quantity using an ECD for all the compounds was found to be approximately 4 ng with a signal-to-noise ratio of 10:1; similarly 5 to 7 ng for FPD-P or -S were applicable (Table IV). This would correspond to a solution concentration (assuming 30 μl as the maximum liquid sample volume) of about 160 ng/ml. Similarly, assuming a maximum vapor sample size of 5 ml, vapor concentrations as low as 1 ng/ml, or 1 mg/m^3, could be readily monitored. An average of replicate determinations (peak areas) in the 1 to 100 ng range indicated that the standard deviation for an aliquot containing 50 ng of a

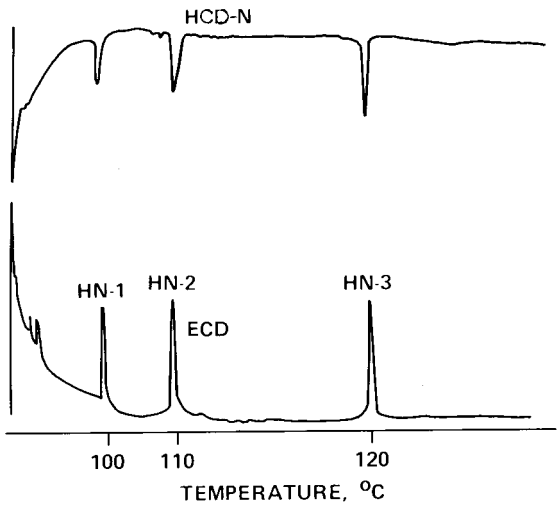

Fig. 5. Chromatogram of nitrogen mustards employing ECD and HCD.

mustard is 2.2% (± 1.1 ng). These data were obtained using solutions similar to those prepared for determining linearity.

The design of column and valves included also the requirement for venting sufficient solvent prior to the detector(s) thus allowing a near return to base line for sample analysis. The column assemblies for single, dual and simultaneous multidetection are illustrated in Fig. 1.

Sulfur mustards were injected mostly from solution in hexane but also out of chloroform. Since these compounds contain no nitrogen the valves were configured to give simultaneous readings from ECD, FID and FPD-S. The nitrogen mustards were detected via ECD, FID and HCD. Parathion was detected via ECD, FPD-P and -S, and FID or HCD. The respective combined chromatograms for the mustards are illustrated in Figs. 2–5.

Referring back to Table I it can be seen that under temperature-programmed conditions HN-1 (B) and H show an elution peak and retention time that could be superposable if in the same mixture. When determined via multidetector, HN-1 shows no FPD-S, while H shows no HCD-N. Similarly, although not shown here, a wide variety of potential break-down products or related compounds were found resolvable based on detector specificity. A few of these compounds were described in reported thin-layer chromatography studies[11].

ACKNOWLEDGEMENT

The authors are grateful to Mrs. Margaret Williamson for typing and reproducing this report.

REFERENCES

1 T. L. Fisher, M. Jaskot and S. Sass, *Def. Doc. Center*, AD 858138, EATR 4321 Chemical Systems Laboratory, Aberdeen Proving Ground, MD, 1969.

2 P. W. Albro and L. Fishbein, *J. Chromatogr.*, 46 (1970) 202.
3 R. L. Erickson, R. N. MacNair, R. H. Brown and H. D. Hogan, *Anal. Chem.*, 44 (1972) 1040.
4 A. A. Casselman, N. C. C. Gibson and R. A. B. Bannard, *J. Chromatogr.*, 78 (1973) 317–322.
5 N. C. C. Gibson, A. A. Casselman and R. A. B. Bannard, *J. Chromatogr.*, 92 (1974) 162.
6 H. W. Grice, M. L. Yates and D. J. David, *J. Chromatogr. Sci.*, 8 (1970) 90.
7 D. M. Coulson, *J. Gas Chromatogr.*, 4 ((8) (1966) 285.
8 D. M. Coulson, *Amer. Lab.*, (1969) 220.
9 R. C. Hall, *J. Chromatogr. Sci.*, 12 (1974) 152.
10 S. Sass and D. M. Hench, *Laboratory Manual*, unpublished results.
11 S. Sass and M. H. Stutz, *J. Chromatogr.*, 213 (1981) 173.
12 S. Sass, T. L. Fisher, M. J. Jaskot and J. Herban, *Anal. Chem.*, 43 (1971) 462.
13 S. Sass, T. L. Fisher and C. D. Thompson, *Def. Doc. Center*, AD 869379, EATR 4389, Chemical Systems Laboratory, Aberdeen Proving Ground, MD, 1970.
14 R. Pigliucci, W. Averill, J. E. Purcell and L. S. Ettre, *Chromatographia*, 8 (1975) 165.
15 M. J. Hartigan, J. E. Purcell, M. Novotný, M. L. McConnel and M. L. Lee, *J. Chromatogr.*, 99 (1974) 339.
16 B. Kolb and J. Bischoff, *J. Chromatogr. Sci.*, 12 (1974) 625.

Journal of Chromatography, 238 (1982) 133–139
Elsevier Scientific Publishing Company, Amsterdam — Printed in The Netherlands

CHROM. 14,553

LARGE INJECTION VOLUMES OF DERIVATIZED IODOTHYRONINES IN CAPILLARY GAS CHROMATOGRAPHY

JEFFREY A. CORKILL and ROGER W. GIESE*
Department of Medicinal Chemistry in the College of Pharmacy and Allied Health Professions, and Institute of Chemical Analysis, Northeastern University, Boston, MA 02115 (U.S.A.)
(Received November 16th, 1981)

SUMMARY

The response of some derivatized iodothyronines by capillary gas chromatography with electron-capture detection decreases with larger injection volumes under isothermal conditions (column at 265°C). However, this response is constant under temperature-programmed conditions (column initially at 200°C). These results are not influenced by the different retention times of these solutes, nor by the length or composition of the injector (glass *vs.* quartz, each silanized), but are influenced significantly by the choice of injection solvent. Collectively, these data indicate a solvent-induced loss of the derivatized iodothyronines in the fused silica column, as opposed to a loss in the injector, or a loss (or decreased sensitivity) in the electron-capture detector, with larger injection volumes. Nevertheless, the chromatographic performance, aside from the lower recovery, is acceptable even with injection volumes as large as 6 μl under isothermal conditions onto a narrow-bore capillary column, due primarily to the high flow-rate of carrier gas in the injector and column (11.5 cm^3 min^{-1}), and the characteristics of the derivatized iodothyronines in this type of analysis.

INTRODUCTION

The volume of sample injected into a gas chromatograph fitted with a capillary column is usually kept small in order to minimize the initial width of the sample on the column, thereby optimizing the efficiency of the solute peaks and minimizing the overlap of these peaks with the solvent tail[1]. However, it can be advantageous, particularly in trace analysis, to inject larger volumes. This is because the use of such volumes may enhance the recovery and convenience of the final steps in sample handling, such as redissolving or extraction/washing steps, prior to injection of the sample into the gas chromatograph.

In our work on the trace analysis of derivatized iodothyronines by capillary gas chromatography (GC), we have been evaluating the injection of large sample volumes into the instrument. For example, previously we reported that a direct sampling injection technique (which places all of the injected sample onto the column), along with temperature programming, allows a constant response to be obtained for

0021-9673/82/0000–0000/$02.75

derivatized iodothyronines even when increasing volumes up to 8 μl are injected onto a narrow-bore capillary column[2]. Nevertheless, we noted that a decreased response is obtained under isothermal conditions (involving a higher column temperature) with such larger volumes.

In this paper we more thoroughly investigate this decreased response with larger injection volumes under isothermal conditions for derivatized iodothyronines. Based on the results from several experiments, we conclude that the lower response is due to a loss of these solutes in the fused-silica column, rather than in the injector or detector of the instrument. Excluding this loss in response, we observe that this system is quite tolerant of larger injection volumes.

EXPERIMENTAL

The derivatized iodothyronines were synthesized as described previously[3]. The instrument was a Model 3740 gas chromatograph fitted with a glass direct injection insert (Varian, 15.5 cm × 0.9 mm I.D.), or a quartz insert (11 cm × 0.9 mm I.D.) each of which was silanized before installation[2]; a 15-m fused-silica capillary column (0.25 mm I.D.), either as a DB5 column (a bonded version of SE-52) or coated with a 0.25-μm film thickness of SE-52 (J and W Scientific); and a constant-current, pulse-modulated, ^{63}Ni electron-capture detector (ECD). The injector, column, and detector temperatures were 270, 265, and 320°C, respectively, for the isothermal analyses. For the analyses under temperature-programmed conditions, the same temperatures were used for the injector and detector, but the column was initially held at 200°C for 2 min, and then its temperature was raised at an actual rate of 43°C min^{-1} (from a setting of 60°C min^{-1}) to a final temperature of 275°C. The carrier and makeup gas was nitrogen with an actual flow-rate in the column of 11.5 cm^3 min^{-1} at 265°C, and flow-rates of 10 and 8.5 cm^3 min^{-1} (measured at room temperature and uncorrected) at the detector base and detector insert base, respectively. The septum purge flow-rate was 2 cm^3 min^{-1} per 5 p.s.i. column head pressure, and the head pressure was 30 p.s.i. Injections into the gas chromatograph were made with silanized 10-μl syringes, either type 1701N or 1701RN (Hamilton), fitted with a type 26S needle.

RESULTS AND DISCUSSION

Characteristics of derivatized iodothyronines

The compounds analyzed in this work are derivatized iodothyronines, and their structures are shown in Fig. 1. In the underivatized form, T_3 and T_4 are the two naturally occurring thyroid hormones, T_2 is a deiodination metabolite of these hormones, and Br_2T_2 is a synthetic analogue which has been used as an internal standard in the analysis of these substances by GC–ECD[4].

The iodothyronines are present in trace amounts in physiological samples, and they require derivatization prior to analysis by GC. Large injection volumes, therefore, can facilitate the analysis of these substances by allowing larger volumes during the steps immediately preceding injection of the sample into the gas chromatograph, for higher recoveries and more convenience.

The derivatized iodothyronines are somewhat unusual as solutes for analysis

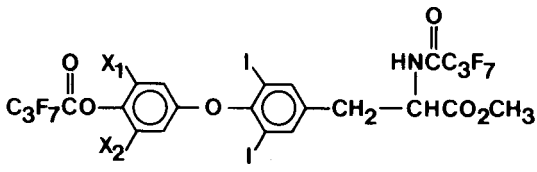

T_2 [$X_1 = X_2 = H$]
T_3 [$X_1 = H, X_2 = I$]
Br_2T_2 [$X_1 = X_2 = Br$]
T_4 [$X_1 = X_2 = I$]

Fig. 1. Structures of the derivatized thyroid hormones.

by GC, primarily because of their high molecular weights (range 600–1200) and polar composition. Consequently, they possess limited thermal stability, and their recovery is optimized by increasing the flow-rate in the column[2]. Further, the plate numbers observed for their peaks are significantly lower, *e.g.* by three- or four-fold, than the corresponding plate numbers for the peaks of simple solutes such as lindane, under the same flow-rate conditions.

Use of large injection volumes

The conditions of broad peaks, solutes with low volatility, and a high flow-rate of carrier gas potentially create a special opportunity to inject larger sample volumes even with a direct sampling technique and a narrow-bore column under isothermal conditions without a significant change in chromatographic performance. There are several reasons for this: (1) broad peaks are less susceptible on a relative basis to further broadening from injection effects; (2) the high flow-rate and accompanying high inlet pressure will act to minimize the back diffusion as well as backflashing during the injection step; and (3) the larger solvent volumes will tend to focus the solutes at the beginning of the column[5]. In regard to the first reason, we observe a peak width for T_4 of 53 sec with a sample injection volume of 0.5 μl at a flow-rate of carrier gas in the column of 11.5 cm^3 min^{-1}. In the ideal case, where the effective sample volume upon injection is the vapor volume of the sample at the injector temperature and pressure, we calculate that even a much larger injection volume (*e.g.* 4.0 μl) would require only 4.3 sec to be swept into the column. This particular circumstance, aside from the other effects noted, would add very little to the initial peak width obtained with a 0.5-μl injection volume. Also, the high retention of these compounds, relative to the elution time of the solvent peak, and the selectivity of the electron capture detector, tend to significantly displace the peaks for these compounds from the solvent tail, further minimizing the potential influence of a larger injection volume on the chromatogram.

To pursue this experimentally, we injected larger sample volumes by diluting a given amount of solute with more solvent prior to injection (constant solute mass for each of a series of injections), and we also injected increasing volumes of a given solution (increasing solute mass with each injection). In both cases, consistent with the above discussion, the band width at half height, *e.g.*, for derivatized T_4, only increased by 18% even up to an injection volume of 7.0 μl. The peak asymmetry was

constant (at a value of 2.0 for derivatized T_4) up to an injection volume of 4.0 μl, but increased two-fold for an injection volume of 6.0 μl and four-fold for 7 μl.

Unexpectedly, however, the response for these solutes decreased in each of these experiments with larger injection volumes. This is shown in terms of peak height for constant solute mass with larger injection volumes in Fig. 2, and for increasing solute mass with larger volumes in Fig. 3. For example, as seen in Fig. 2, the response falls off *ca.* two-fold when the original sample volume of 0.5 μl is diluted to 4.0 μl prior to injection.

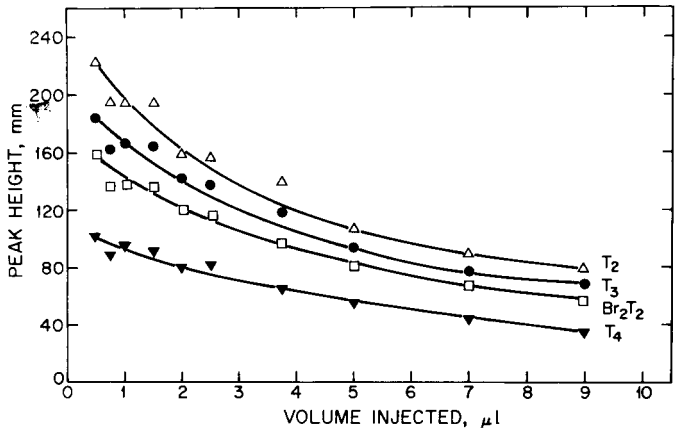

Fig. 2. Peak height for derivatized T_2, T_3, T_4 and Br_2T_2 with constant solute masses (195, 326, 310 and 301 pg, respectively) as a function of injection volume at a flow-rate of 11.5 cm^3 min^{-1}.

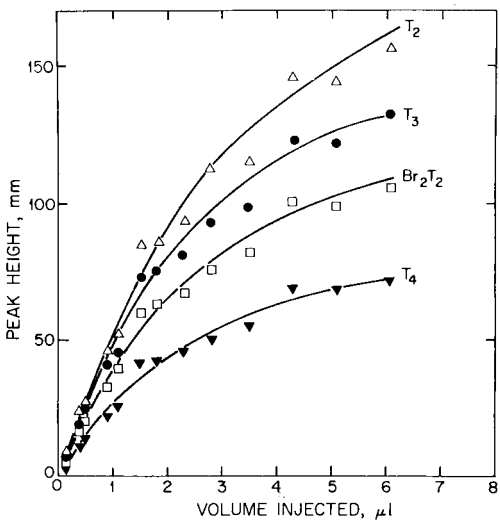

Fig. 3. Peak height for derivatized T_2, T_3, T_4 and Br_2T_2 as a function of increasing solute masses from larger injection volumes of a solution containing 78, 130, 124 and 120 pg μl^{-1}, respectively, at a flow-rate of 11.5 cm^3 min^{-1}.

Source of decreased response

The potential sources of the lower response with larger injection volumes are either a decreased recovery in the injector, column or detector; or a decreased sensitivity in the detector due to the presence of pre-eluting or co-eluting injection solvent.

The decrease in response with larger injection volumes is quite unlikely to arise in the detector from a decreased sensitivity due to the injection solvent, since a parallel decrease in the response for all of the derivatized iodothyronines is observed, in spite of their markedly different retention times, as the volume of injection solvent is increased from 1 to 9 μl. (This progressively subjects these solutes differentially to the presence of injection solvent in the detector.) For example, the coefficients of variation for the peak height ratios of derivatized T_2, T_3 and T_4 relative to Br_2T_2 as a function of injection volume, are 4.4, 2.3 and 4.4%, respectively, for the data in Fig. 2, and range from 2.0 to 4.5% for the data in Fig. 3. This also makes it extremely unlikely that a solvent-induced loss of these compounds is occurring in the detector.

The injector temperature was 270°C in this work, the same as in our previous experiments with temperature programming (2–8 min hold at 200°C, program up to 275°C) in which a constant response was obtained with increasing injection volumes[2]. Ordinarily this would rule out the injector as the source of the decreased response. However, in this gas chromatograph, the lower end of the injector is located in the column oven, so that the temperature of the injector is not uniform throughout its entire length when the temperatures of the injector compartment and column oven are different.

To fully exclude the injector as the source of decreased response with larger

TABLE I

RESPONSE OF THE DERIVATIZED IODOTHYRONINES, AS A FUNCTION OF THE INJECTION VOLUME, INJECTION SOLVENT, AND THE TEMPERATURE CONDITIONS APPLIED TO THE COLUMN

Column and injection conditions		*Derivatized iodothyronines: peak area per microliter of injection volume**			
		T_2	T_3	Br_2T_2	T_4
Temperature programmed					
Toluene	1 μl	1.00	1.00	1.00	1.00
	6 μl	0.92	1.05	1.08	0.88
Acetonitrile	1 μl	0.52	0.58	0.60	0.55
	6 μl	0.60	0.69	0.56	0.60
Isothermal					
Toluene	1 μl	0.93	1.06	0.98	0.92
	6 μl	0.38	0.54	0.52	0.54
Acetonitrile	1 μl	0.16	0.29	0.22	0.29
	6 μl	–**	0.35	0.26	0.30

* In each case, a mixture of 72, 70, 107 and 76 pg, respectively, of derivatized T_2, T_3, T_4 and Br_2T_2 was injected onto a DB5 column, in an injection volume of either 1 or 6 μl. The resulting peak areas are normalized relative to the areas obtained by injecting 1 μl of a solution of the derivatized iodothyronines under temperature-programmed conditions, as shown.

** The peak for derivatized T_2 was obscured by the solvent peak under these conditions.

injection volumes, we not only insulated and shortened it (from 15.5 to 11 cm), so that it was no longer partly exposed to the column oven, but we also changed its composition from glass to quartz (each of which was silanized). Then we repeated the injection volumes of 1 μl and 6 μl of the derivatized iodothyronines in toluene as before, using both isothermal and temperature-programmed conditions. As seen in Table I, the response is essentially constant for these compounds only with temperature programming, and essentially the same decrease in response is obtained as observed in Fig. 2 and 3 under isothermal conditions with the longer, non-insulated, silanized glass injector. Thus, the injector clearly is not the source of the decreased response under isothermal conditions.

By a process of elimination, this implicates the column as the site of the decreased response with larger injection volumes when its temperature during the injection step is 265°C. If this, indeed, is the case, then one might expect that the recovery of the derivatized iodothyronines would be influenced by the nature of the injection solvent. Thus, we compared the response with acetonitrile rather than toluene as an injection solvent, both for large and small injection volumes and under both isothermal and temperature-programmed conditions.

These results are also summarized in Table I, and were obtained with the modified injector (shortened, insulated, and composed of silanized quartz). For all injection volumes under both isothermal and temperature-programmed conditions, we see that the response is significantly lower with acetonitrile than with corresponding volumes of toluene. Other comparisons can be made as well between the results from these two solvents as a function of the temperature conditions and injection volume, but the main point for our purposes is simply that the response is markedly affected by the nature of the injection solvent.

Thus, the decreased response is related not only to the column temperature but also to the volume and type of injection solvent. These results collectively indicate that the decreased response with larger injection volumes arises from a loss of the derivatized iodothyronines in the column as opposed to losses or decreased sensitivity elsewhere in the GC–ECD. The practical significance of these results is to indicate the potential for temperature or solvent related effects on the response to complex solutes even in a deactivated, fused-silica column. Consistent with this, previously we observed that column temperatures in excess of 265°C during the injection step lead to losses of these compounds on the column[2]. We suggested that these losses were thermal rather than adsorptive in nature, and the current data now allow the elaboration that the injection solvent may be contributing to these former losses with higher temperature as well. Further, it is conceivable that the changes in response with higher flow-rates under isothermal conditions were similarly related, in part or in total, to the presence of the injection solvent in the injector or the column.

Performance with large injection volumes

The chromatogram resulting from the injection volume of 6 μl in the previous experiment involving increasing solute mass (Fig. 3) is shown in Fig. 4. Obviously, the chromatographic performance is acceptable in spite of the total injection of an unusually large volume of sample under isothermal conditions onto a narrow-bore column. Thus, this approach potentially can be utilized to facilitate the trace analysis of these compounds as discussed above. Although column lifetime potentially may be short-

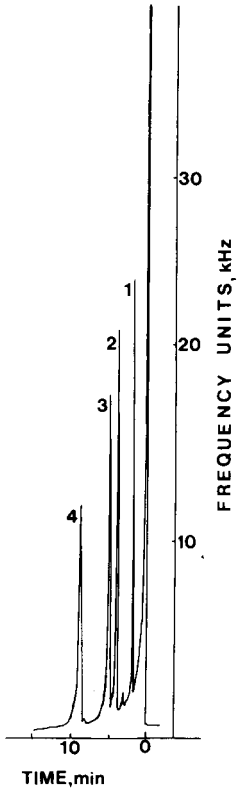

Fig. 4. Chromatogram corresponding to an injection volume of 6 μl in Fig. 3. Peaks: 1 = T_2; 2 = T_3; 3 = Br_2T_2; 4 = T_4.

ened by leaching of the liquid stationary phase by large volumes of injection solvent, bonded phases should tend to resist this problem.

ACKNOWLEDGEMENTS

We wish to acknowledge NIH for support of this work under grant AM21797, and helpful discussions with Frank J. Yang. Contribution No. 110 for the Institute of Chemical Analysis.

REFERENCES

1 W. Jennings, *Gas Chromatography with Glass Capillary Columns*, Academic Press, New York, 2nd ed., 1980.
2 J. A. Corkill and R. W. Giese, *Anal. Chem.*, 53 (1981) 1667.
3 B. A. Petersen, R. N. Hanson, R. W. Giese and B. L. Karger, *J. Chromatogr.*, 126 (1976) 503.
4 B. A. Petersen, R. W. Giese, P. R. Larsen and B. L. Karger, *Clin. Chem.*, 23 (1977) 1389.
5 F. J. Yang, A. C. Brown, III and S. P. Cram, *J. Chromatogr.*, 158 (1978) 91.

Journal of Chromatography, 238 (1982) 141–150
Elsevier Scientific Publishing Company, Amsterdam — Printed in The Netherlands

CHROM. 14,580

FRACTIONATION AND CAPILLARY GAS CHROMATOGRAPHIC–MASS SPECTROMETRIC CHARACTERIZATION OF THE NEUTRAL COMPONENTS IN MARIJUANA AND TOBACCO SMOKE CONDENSATES

MILOS NOVOTNÝ*, FRANCO MERLI*, DONALD WIESLER, MARY FENCL and TALAT SAEED

Department of Chemistry, Indiana University, Bloomington, IN 47405 (U.S.A.)

(Received November 20th, 1981)

SUMMARY

Polar and non-polar "neutral" constituents of the smoke condensates of Mexican marijuana and standard tobacco were resolved by capillary gas chromatography and structurally characterized through mass spectrometry. Comparisons of the two materials reveal substantial qualitative and quantitative differences. The cannabinoid-like substances partition into both the non-polar and polar fraction. In total, over 130 "neutral" smoke components have been characterized.

INTRODUCTION

An increasing use of marijuana in our society necessitates detailed evaluation of its health hazards. Objective pharmacological and toxicological studies of this drug are handicapped by an insufficient understanding of its chemical composition. While already the plant extracts contain a great number of constituents, the problem is further complicated by the complex processes that occur during the burning of marijuana materials.

Since marijuana is usually administered through smoking, the smoke condensate must primarily be analyzed with respect to both biological effects and chemical composition. Whereas our knowledge of the chemical aspects has been steadily increasing, the obvious complexity of marijuana smoke challenges even the best separation and identification techniques. High-resolution (capillary) gas chromatography (GC), high-performance liquid chromatography (HPLC), and GC–mass spectrometry (MS) have been extensively used in the field of tobacco smoke analysis where a similar degree of complexity is encountered.

In spite of the great resolving power of glass capillary columns, a direct analysis of the smoke extracts does not yield sufficiently detailed information. An effective search for the minor smoke components requires some form of sample enrichment and

* Present address: Instituto Superiore di Sanitá, Laboratorio di Igiene del Lavoro, Rome, Italy.

0021-9673/82/0000–0000/$02.75

fractionation. Fractionation of smoke condensates is furthermore desirable to assess various biological activities.

In recent studies[1–7], marijuana smoke condensate was fractionated to yield different classes of compounds for compound identification[1–4] and toxicological evaluation[5–7]. Much interest in this approach stems from the fact that marijuana may not always be toxicologically and pharmacologically synonymous with its major components, cannabinoids.

In the solvent partition scheme[8] used in our study, it is possible to obtain fractions according to their pH characteristics and polarities. While the previous work dealt with the analysis of polycyclic aromatics[1], acids and phenols[2,3], and basic substances[4] in marijuana smoke condensate, the present study concentrates on polar and non-polar neutral components. Tobacco smoke condensate has been used here as a "baseline material" to distinguish certain constituents from the usual products of combustion.

EXPERIMENTAL

Smoke condensates were obtained by means of a standard smoking machine[9] from either Mexican marijuana cigarettes (National Institute on Drug Abuse, Rockville, MD, U.S.A.) or standard tobacco cigarettes (Tobacco-Health Research Institute, University of Kentucky, Lexington, KY, U.S.A.). The content of major cannabinoids in marijuana, as determined by gas chromatography, was: Δ^9-tetrahydrocannabinol, 1.18%; cannabinol, 0.18%; cannabidiol plus cannabicyclol, 0.16%. The total weight of both materials was determined prior to the smoke-collection experiments. Three separate smoke collections were carried out, each involving approximately 1000 cigarettes of the starting materials, over the total period of 15 months.

Puffs of a 2-sec duration in 1-min intervals were drawn while the smoke was trapped in pure acetone using a cryogenic trap held at approximately $-60°C$. After acetone was evaporated to dryness, the residual condensate weights were determined.

A previously described[1–6] partition scheme was utilized to yield different fractions of smoke condensates; the fractionation is shown schematically in Fig. 1. Thus, both types of smoke condensate were divided into acidic, basic, polar neutral, non-polar neutral, and polynuclear aromatic fractions.

The weights of the individual fractions from the three smoke collections were determined. The same fractionation scheme has also been applied to yield fractions for pharmacological screening experiments as reported elsewhere[5,6].

An aliquot of the non-polar neutral fraction residue was redissolved in an appropriate small volume of methylene chloride solution and injected onto a 50 m × 0.25 mm I.D., glass capillary column coated with OV-101 methylsilicone fluid; the column was programmed from 50 to 270°C at 1°C/min.

An appropriate aliquot of the polar neutral residue was silylated with N-methyl-N-trimethylsilyltrifluoroacetamide (MSTFA) at 70°C for 30 min, and a 0.15-μl amount of the resulting solution was injected into the same column as described above; the column was programmed from 50 to 270°C at 1°C/min.

A Varian Model 3700 gas chromatograph was used for all GC experiments. In order to identify the individual chromatographic peaks as separated, the methylsilicone-coated glass capillary column was attached to the ion source of a Hewlett-

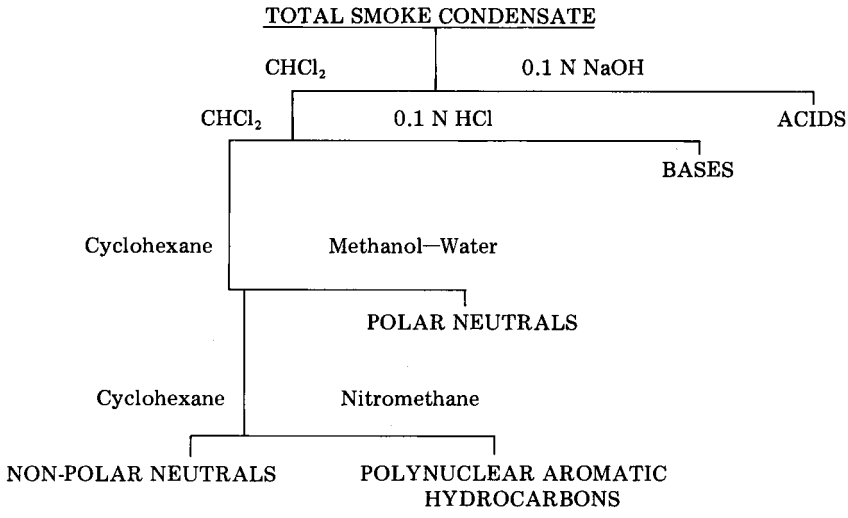

Fig. 1. The fractionation scheme used for tobacco and marijuana smoke condensates.

Packard Model 5982 combined gas chromatograph–mass spectrometer operating in the electron impact mode. The spectra were repetitively taken at appropriately selected time intervals throughout the entire chromatogram.

RESULTS AND DISCUSSION

Average yields of the individual fractions obtained through the described fractionation scheme (Fig. 1) from three smoke condensates are listed in Table I. Both the uncontrolled variations during smoke collection and losses due to evaporations of solvents cause most probably the deviations from the average weights. While in such

TABLE I

SMOKE FRACTION WEIGHT EXPRESSED AS PERCENTAGE OF THE DRY PLANT MATERIAL WEIGHT

Fraction type	*Weight (%)*	
	Tobacco	*Marijuana*
Total smoke condensate	4.97 ± 0.91	8.27 ± 1.24
Acidic	0.31 ± 0.15	0.38 ± 0.09
Basic	0.26 ± 0.06	0.23 ± 0.16
Total neutral residue	1.87 ± 0.38	3.87 ± 0.15
Polar neutral	0.87 ± 0.23	1.73 ± 0.58
Non-polar neutral	0.57 ± 0.15	0.83 ± 0.15
Polynuclear aromatic	0.20 ± 0.10	0.47 ± 0.12

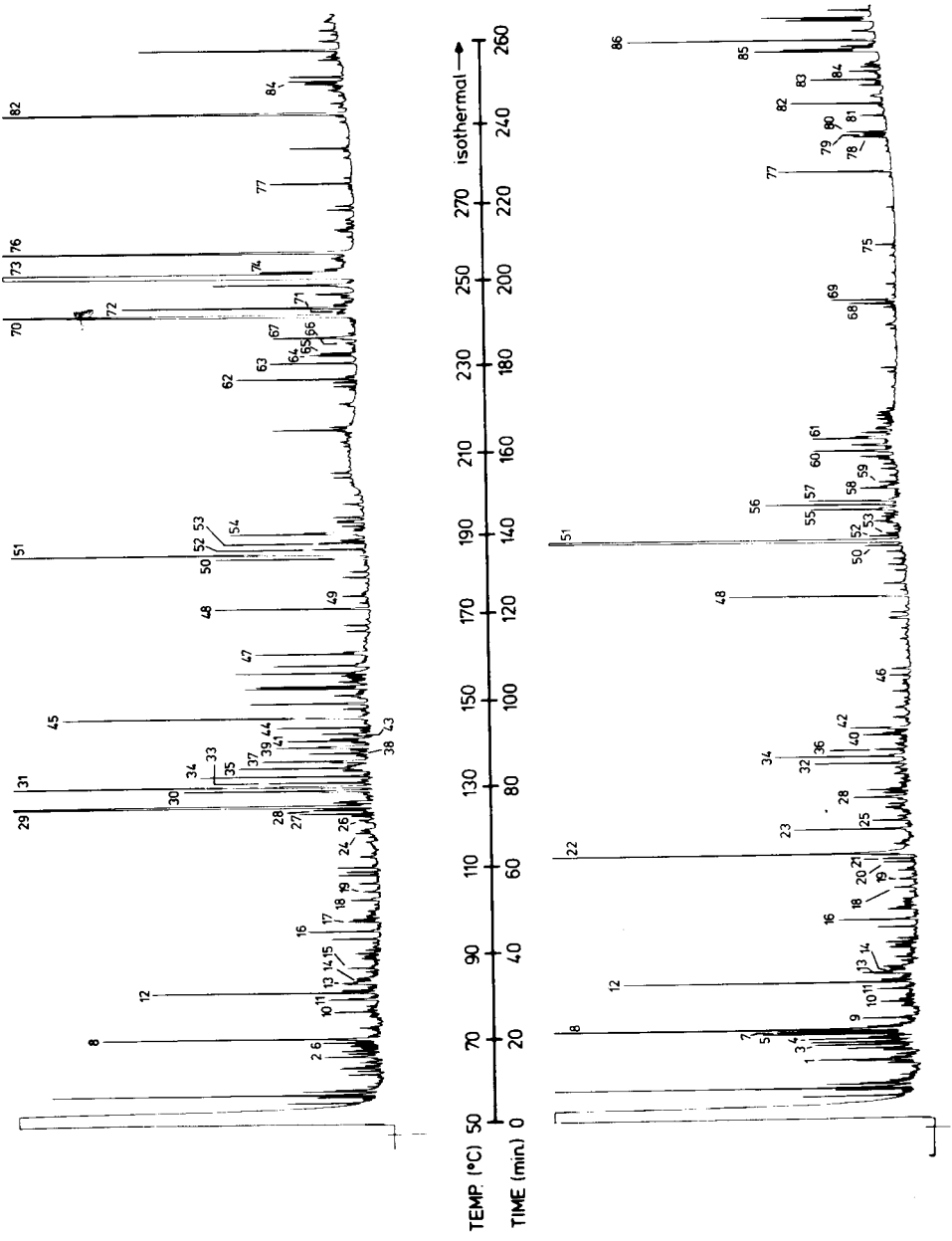

Fig. 2. Comparison of chromatograms obtained from the non-polar neutral fraction of marijuana (above) and tobacco (below) smoke condensates. For compound identifications, see Table II.

a case it is appropriate to look at the trends rather than absolute values, it is quite clear that marijuana smoke differs significantly from tobacco smoke in both the total amount of condensate and the proportion of the individual fractions.

Whereas the chemical characterization of polynuclear aromatics[1], acids and phenols[2,3], as well as an extensive analysis of the basic fraction[4] were carried out on previous occasions, the principal aim of this study was to characterize the relatively volatile portion of the neutral fraction. The polar neutral constituents are mostly non-volatile, but silylation of this sample facilitates a partial characterization of the polar neutral fraction.

In contrast to marijuana smoke, chemical data on tobacco smoke composition are relatively more abundant[10,11]. Thus, the emphasis of this communication, in relation to tobacco smoke components, is primarily in providing comparative qualitative indications.

The chromatographic profiles of the non-polar fractions for marijuana and tobacco, respectively, are compared in Fig. 2, indicating some similarities, but also both qualitative and quantitative differences. The individual components were tentatively identified through gas chromatographic and mass spectral data for both types of materials. Table II lists most major and some minor components of the analyzed mixtures. Relatively small aromatic molecules that are represented by the earlier peaks in these chromatograms appear to be rather uncharacteristic products of common combustion processes. Various hydrocarbon substances encountered throughout the chromatographic profiles are also well-recognized non-polar plant products. Some of these were found earlier[12] in marijuana plant extracts, although the burning process will undoubtedly increase the degree of mixture complexity.

Numerous terpene-like substances can be found in Table II. Because of the entirely different biosynthetic pathways that are known to occur in the cannabis plant as compared to tobacco, differences in their terpenic composition are expected. A cluster of peaks (components 55–61) that suggests C_{19} and C_{20} unsaturated cyclic compounds appears to be typical for tobacco smoke. On the other hand, most peaks eluting in the temperature range of 120–160°C represent fairly unique components of marijuana smoke. Terpenes of these and similar structures have previously been found in the unburned marijuana samples[13]; they are believed to be responsible for a characteristic odor of marijuana and its smoke.

Many cannabinoids are encountered in the later part of the marijuana chromatogram (peaks 62–76 of the upper chromatogram, Fig. 2). As expected these are totally absent in the corresponding tobacco profile. While some identifications presented here on such compounds are tentative and we have been unable to record recognizable mass spectra from some minor components, this group of compounds appears to be the best candidate for further studies in supplementing the lists of already reported compounds of a similar nature[14,15]. Some of these cannabinoids possess very interesting pharmacological properties. Further separation schemes must be designed to isolate such compounds from the complex smoke condensate matrix and major cannabinoids, Δ^9-tetrahydrocannabinol, cannabinol, and cannabidiol.

Analytical results obtained with the polar neutral fraction of the smoke condensates (Fig. 3 and Table III) reveal considerable similarity between the two materials. Just as with the "neutral" polar fraction of another product of pyrolytical

TABLE II

COMPOUNDS FOUND IN THE NON-POLAR NEUTRAL FRACTION OF MARIJUANA SMOKE CONDENSATE

Peak No.	*Molecular weight*	*Molecular formula*	*Identification*	*Present in tobacco smoke*
1	120	C_9H_{12}	An ethylmethylbenzene	+
2	120	C_9H_{12}	An ethylmethylbenzene	–
3	136	$C_{10}H_{16}$	Myrcene*	+
4	138	$C_{10}H_{18}$	An acyclic diene*	+
5	142	$C_{10}H_{22}$	Decane*	+
6	134	$C_{10}H_{14}$	A C_2 ethylbenzene	–
7	138	$C_{10}H_{18}$	A dihydrolimonene*	+
8	136	$C_{10}H_{16}$	Limonene	+
9	134	$C_{10}H_{14}$	A C_4 benzene*	+
10	132	$C_{10}H_{12}$	A C_2 styrene	+
11	154	$C_{11}H_{22}$	An undecene	+
12	156	$C_{11}H_{24}$	Undecane	+
13	130	$C_{10}H_{10}$	A methylindene or dihydronaphthalene	+
14	130	$C_{10}H_{10}$	A methylindene or dihydronaphthalene	+
15	128	$C_{10}H_8$	Naphthalene	–
16	170	$C_{12}H_{26}$	Dodecane	+
17	184	$C_{13}H_{28}$	An isomer of tridecane	–
18	142	$C_{11}H_{10}$	2-Methylnaphthalene	+
19	142	$C_{11}H_{10}$	1-Methylnaphthalene	+
20	182	$C_{13}H_{26}$	A tridecene*	+
21	182	$C_{13}H_{26}$	A tridecene*	+
22	162	$C_{10}H_{14}N_2$	Nicotine*	+
23	194	$C_{13}H_{22}O$	Solanone*	+
24	156	$C_{12}H_{12}$	An ethylnaphthalene	–
25	196	$C_{14}H_{28}$	A tetradecene*	+
26	156	$C_{12}H_{12}$	An ethylnaphthalene	–
27	204	$C_{15}H_{24}$	A sesquiterpene	–
28	196	$C_{14}H_{28}$	A tetradecene	+
29	204	$C_{15}H_{24}$	beta-Caryophyllene	–
30	204	$C_{15}H_{24}$	alpha-Bergamotene	–
31	204	$C_{15}H_{24}$	Humulene	–
32	206	$C_{15}H_{26}$	A dihydrosesquiterpene*	+
33	204	$C_{15}H_{24}$	A sesquiterpene	–
34	204	$C_{15}H_{24}$	beta-Farnesene	+
35	204	$C_{15}H_{24}$	A sesquiterpene	–
36	212	$C_{15}H_{32}$	An isomer of pentadecane*	+
37	204	$C_{15}H_{24}$	A sesquiterpene	–
38	204	$C_{15}H_{24}$	A sesquiterpene	–
39	204	$C_{15}H_{24}$	A sesquiterpene	–
40	210	$C_{15}H_{30}$	A pentadecene*	+
41	204	$C_{15}H_{24}$	Bisabolene	–
42	212	$C_{15}H_{32}$	Pentadecane	+
43	170	$C_{13}H_{14}$	A C_3 naphthalene	–
44	204	$C_{15}H_{24}$	A sesquiterpene	–
45	202	$C_{15}H_{22}$	A dehydrosesquiterpene	–
46	224	$C_{16}H_{32}$	A hexadecene*	+

TABLE II *(continued)*

Peak No.	*Molecular weight*	*Molecular formula*	*Identification*	*Present in tobacco smoke*
47	222	$C_{15}H_{26}O$	A sesquiterpene alcohol	–
48	266	$C_{19}H_{38}$	Norphytene	+
49	252	$C_{18}H_{36}$	An octadecene	–
50	264	$C_{18}H_{32}O$	A solanone-like ketone	+
51	278	$C_{20}H_{38}$	Neophytadiene	+
52	266	$C_{19}H_{38}$	A nonadecene	+
53	278	$C_{20}H_{38}$	An eicosadiene	+
54	278	$C_{20}H_{38}$	An eicosadiene	–
55	274	$C_{20}H_{34}$	An eicosatetraene*	+
56	274	$C_{20}H_{34}$	An eicosatetraene*	+
57	270	$C_{19}H_{26}O$	An androstadienone*	+
58	270	$C_{19}H_{26}O$	An androstadienone*	+
59	278	$C_{20}H_{38}$	An eicosadiene*	+
60	276	$C_{20}H_{36}$	An eicosatriene*	+
61	276	$C_{20}H_{36}$	An eicosatriene*	+
62	314	$C_{21}H_{30}O_2$	Cannabicitran	–
63	286	$C_{19}H_{26}O_2$	Tetrahydrocannabidivarol	–
64	314	$C_{21}H_{30}O_2$	Isotetrahydrocannabinol	–
65	328	$C_{22}H_{32}O_2$	Cannabidiol monomethyl ether	–
66	328	$C_{22}H_{32}O_2$	Cannabichromene monomethyl ether	–
67	314	$C_{21}H_{30}O_2$	Cannabicyclol	–
68	342	$C_{25}H_{42}$	A dihydrosesterterpene*	+
69	342	$C_{25}H_{42}$	A dihydrosesterterpene*	+
70	314	$C_{21}H_{30}O_2$	Cannabidiol	–
71	332	$C_{20}H_{28}O_4$	Cannabichromanone	–
72	314	$C_{21}H_{30}O_2$	Cannabichromene	–
73	314	$C_{21}H_{30}O_2$	Δ^9-Tetrahydrocannabinol	–
74	312	$C_{21}H_{28}O_2$	A dihydrocannabinol	–
75	352	$C_{25}H_{52}$	Pentacosane*	+
76	310	$C_{21}H_{26}O_2$	Cannabinol	–
77	380	$C_{27}H_{56}$	Heptacosane	+
78	394	$C_{28}H_{58}$	Octacosane	+
79	410	$C_{30}H_{50}$	Squalene*	+
80	410	$C_{30}H_{50}$	An isomer of squalene*	+
81	408	$C_{29}H_{60}$	An isomer of nonacosane*	+
82	408	$C_{29}H_{60}$	Nonacosane	+
83	422	$C_{30}H_{62}$	An isomer of triacontane	+
84	422	$C_{30}H_{62}$	Triacontane	+
85	436	$C_{31}H_{64}$	An isomer of hentriacontane*	+
86	436	$C_{31}H_{64}$	Hentriacontane*	+

* Present in tobacco but not marijuana

degradation, coal tar[16], the substances such as phenols and certain nitrogen-containing molecules inevitably partition into the methanol–water layer under the used fractionation conditions. The only notable differences are the expected presence of nicotine and main cannabinoids in tobacco and marijuana smoke, respectively. Isoeugenol and olivetol (peaks 27 and 35, Fig. 3), tentatively identified in this work, are the expected biosynthetic correlates of cannabinoids.

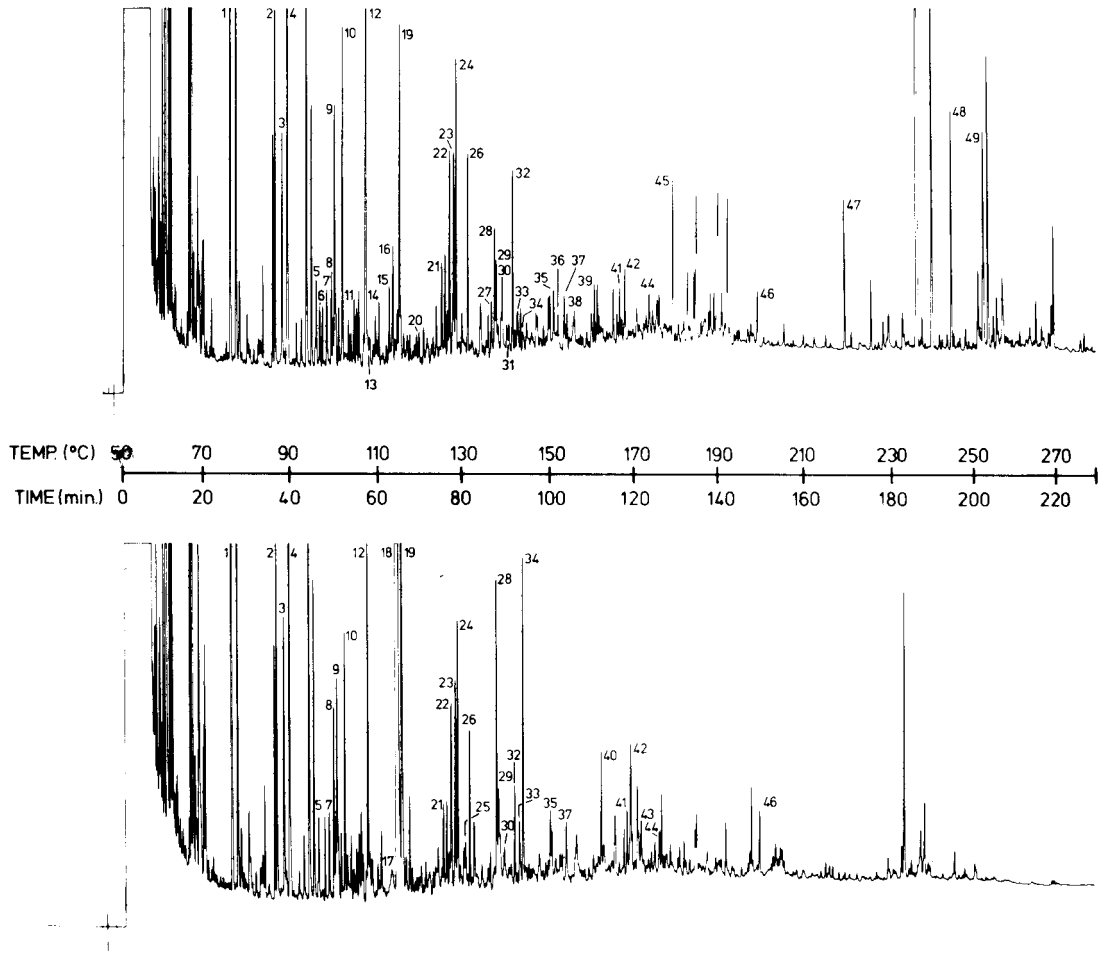

Fig. 3. Comparison of chromatograms obtained from the polar neutral fraction of marijuana (above) and tobacco (below) smoke condensates. For compound identifications, see Table III.

Inefficiency of the present partition scheme to separate completely cannabinoids into one layer was previously noted[12] with the plant materials. Again, an improved fractionation strategy is needed for isolation of minor cannabinoids from this fraction.

Various phenolic compounds were tentatively identified in both materials. Their toxicological significance resides in co-carcinogenicity, cilia toxicity and bronchial irritation; these properties have been long noted[17] in connection with tobacco smoking. The profiles of phenolic substances in tobacco and marijuana, as indicated in this work, appear to be qualitatively and quantitatively similar.

It should be pointed out that the range of compounds characterized in this study represents substances that are relatively volatile, or whose volatility can be extended by a simple chemical derivatization. Characterization of the heavier smoke constituents will remain a complicated task until liquid chromatographic techniques of very high resolution become widely applicable to these sample types.

TABLE III

COMPOUNDS FOUND IN THE POLAR NEUTRAL FRACTION OF MARIJUANA SMOKE CONDENSATE

Peak No.	*Molecular weight*	*Molecular formula*	*Identification*	*Present in tobacco smoke*
1	94	C_6H_6O	Phenol	+
2	108	C_7H_8O	*o*-Cresol	+
3	108	C_7H_8O	*p*-Cresol	+
4	108	C_7H_8O	*m*-Cresol	+
5	112	$C_5H_4O_3$	Furoic acid	+
6	122	$C_8H_{10}O$	An ethylphenol	–
7	122	$C_8H_{10}O$	A dimethylphenol	+
8	124	$C_7H_8O_2$	2-Methoxyphenol	+
9	122	$C_8H_{10}O$	A dimethylphenol	+
10	122	$C_8H_{10}O$	A dimethylphenol	+
11	110	$C_6H_{10}N_2$	A C_3 imidazole or pyrazole	–
12	120	C_8H_8O	A vinylphenol	+
13	124	$C_7H_8O_2$	A methoxyphenol	–
14	136	$C_9H_{12}O$	A C_3 phenol	–
15	136	$C_9H_{12}O$	A C_3 phenol	–
16	124	$C_7H_{12}N_2$	A C_4 imidazole or pyrazole	–
17	138	$C_8H_{10}O_2$	A methoxymethylphenol*	+
18	162	$C_{10}H_{14}N_2$	Nicotine*	+
19	110	$C_6H_6O_2$	Catechol	+
20	128	$C_5H_4O_4$	A hydroxyfuroic acid	+
21	154	$C_8H_{10}O_3$	A dimethoxyphenol	+
22	124	$C_7H_8O_2$	A methylbenzenediol	+
23	124	$C_7H_8O_2$	A methylbenzenediol	+
24	117	C_8H_7N	Indole	+
25	128	$C_5H_4O_4$	A hydroxyfuroic acid	+
26	150	$C_9H_{10}O_2$	A vinylmethoxyphenol	+
27	164	$C_{10}H_{12}O_2$	A C_1 vinylmethoxyphenol *e.g.* isoeugenol	–
28	138	$C_8H_{10}O_2$	A C_2 benzenediol	+
29	138	$C_8H_{10}O_2$	A C_2 benzenediol	+
30	142	$C_6H_6O_4$	A methylhydroxyfuroic acid	+
31	138	$C_8H_{10}O_2$	A C_2 benzenediol	–
32	131	C_9H_9N	A methylindole	+
33	168	$C_{12}H_8O$	A hydroxyacenaphthylene	+
34	136	$C_8H_8O_2$	A styrenediol	+
35	136	$C_8H_8O_2$	A styrenediol	+
36	162	$C_{11}H_{14}O$	A pentenylphenol	–
37	180	$C_{11}H_{16}O_2$	A C_4 methoxyphenol	+
38	150	$C_9H_{10}O_2$	A methylstyrenediol	+
39	154	$C_8H_{10}O_3$	A methoxymethylbenzenediol	–
40	178	$C_6H_4Cl_2O_2$	A dichlorobenzenediol*	+
41	138	$C_8H_{10}O_2$	A C_2 benzenediol	+
42	152	$C_8H_8O_3$	A styrenetriol	+
43	174	$C_{11}H_{10}O_2$	A methoxynaphthol*	+
44	138	$C_8H_{10}O_2$	A C_2 benzenediol	+
45	180	$C_{11}H_{16}O_2$	A C_5 benzenediol *e.g.* olivetol	–
46	180	$C_9H_8O_4$	A methoxydihydroxybenzofuran	+

(Continued on p. 150)

TABLE III (*continued*)

Peak No.	*Molecular weight*	*Molecular formula*	*Identification*	*Present in tobacco smoke*
47	256	$C_{16}H_{32}O_2$	Palmitic acid	–
48	314	$C_{21}H_{30}O_2$	Δ^9-Tetrahydrocannabinol	–
49	310	$C_{21}H_{26}O_2$	Cannabinol	–

* Present in tobacco but not marijuana

ACKNOWLEDGEMENTS

This work was supported by the research grant No. DA 507 from the National Institute on Drug Abuse, U.S. Public Health Service. Generous help of Ms. Carolyn Keene, Tobacco-Health Research Institute, University of Kentucky, Lexington, KY, U.S.A., with the preparation of smoke condensates is appreciated.

REFERENCES

1 M. L. Lee, M. Novotny and K. D. Bartle, *Anal. Chem.*, 48 (1976) 405.
2 M. P. Maskarinec, G. Alexander and M. Novotný, *J. Chromatogr.*, 126 (1976) 559.
3 M. P. Maskarinec, *Doctoral Thesis*, Department of Chemistry, Indiana University, Bloomington, IN, 1977.
4 F. Merli, D. Wiesler, M. P. Maskarinec, M. Novotný, D. L. Vassilaros and M. L. Lee, *Anal. Chem.*, 53 (1981) 1929.
5 J. M. Johnson, L. Lemberger, M. Novotný, R. B. Forney, W. S. Dalton and M. P. Maskarinec, submitted for publication.
6 J. M. Johnson, *Doctoral Thesis*, Department of Toxicology, Indiana University School of Medicine, Indianapolis, IN, 1981.
7 F. W. Busch, D. A. Said and E. G. Wei, *Cancer Lett.*, 6 (1979) 319.
8 M. Novotný, M. L. Lee and K. D. Bartle, *J. Chromatogr. Sci.*, 12 (1974) 606.
9 F. Seehofer and J. E. Miller, *Beitr. Tabakforsch.*, 3 (1965) 75.
10 L. Schmeltz and D. Hoffmann, *Chem. Rev.*, 77 (1977) 295.
11 J. N. Schumacher, C. R. Green, F. W. Best and M. P. Newell, *J. Agr. Food Chem.*, 25 (1977) 310.
12 M. Novotný, M. L. Lee, C. E. Low and A. Raymond, *Anal. Chem.*, 48 (1976) 24.
13 L. V. S. Hood, M. E. Dames and G. T. Barry, *Nature (London)*, 242 (1973) 402.
14 R. Mechoulam, N. K. McCallum and S. Burstein, *Chem. Rev.*, 76 (1976) 75.
15 C. E. Turner, M. A. Elsohly and E. G. Boeren, *J. Nat. Prod.*, 43 (1980) 169.
16 M. Novotný, J. W. Strand, S. L. Smith, D. Wiesler and F. J. Schwende, *Fuel*, 60 (1981) 213.
17 E. L. Wynder and D. Hoffmann, *Tobacco and Tobacco Smoke*, Academic Press, New York, 1967.

Journal of Chromatography, 238 (1982) 151–156
Elsevier Scientific Publishing Company, Amsterdam — Printed in The Netherlands

CHROM. 14,485

IDENTIFICATION OF ENDOGENOUS N-(3-INDOLEACETYL)ASPARTIC ACID IN SCOTS PINE (*PINUS SYLVESTRIS* L.) BY COMBINED GAS CHROMATOGRAPHY–MASS SPECTROMETRY, USING HIGH-PERFORMANCE LIQUID CHROMATOGRAPHY FOR QUANTIFICATION

BARBRO ANDERSSON*
Department of Organic Chemistry, University of Umeå, S-901 87 Umeå (Sweden)
and
GÖRAN SANDBERG
Department of Forest Genetics and Plant Physiology, Swedish University of Agricultural Sciences, S-901 83 Umeå (Sweden)
(Received October 13th, 1981)

SUMMARY

N-(3-indoleacetyl)aspartic acid (IAAsp), a conjugate of the phytohormone 3-indoleacetic acid (IAA), was conclusively identified by combined gas chromatography–mass spectrometry (GC–MS) in dormant shoots of Scots pine (*Pinus sylvestris* L.). A procedure based on reversed-phase liquid chromatography and fluorescense detection is described for quantitative analysis of IAAsp levels in pine tissue. The current year's shoots of dormant seven-year-old trees of Scots pine contained 60 ng/g IAAsp fresh weight. The sensitivity of this method for IAAsp, applied to this material, was 1 ng, and 200 pg for pure standard. The preceding clean-up of the extract included the use of Amberlite XAD-7, a polyacrylic ester, which transfers organic compounds from a water phase to small volumes of organic solvents, an excellent alternative to the often used buffer–organic solvent extractions.

INTRODUCTION

The substance 3-indoleacetic acid (IAA) has for many years been considered to be a natural growth-regulating compound in plants. During the past decade, this substance has been conclusively identified in a number of species[1], and recently in conifers, including Scots pine[2–5]. It is, however, obvious that the concentration of the free IAA in plant tissue depends on synthesis, degradation and conjugation of the acid. Accordingly, it is necessary to estimate these reactions before correlations between phytohormone contents and exogenous factors can be considered. This paper describes a quantification method developed for a specific part of conjugated IAA. It has been obvious for many years that the IAA molecule in many cases is conjugated rather than oxidized, and when exogenous IAA is supplied to plants it is usually converted into 1-(3-indoleacetyl)-β-D-glucose or N-(3-indoleacetyl)aspartic acid

0021-9673/82/0000–0000/$02.75

(IAAsp)[1]. Other conjugates of IAA have also been proposed, such as with inositol and with different amino acids other than aspartic acid (Asp)[6–8].

IAAsp was first reported in 1955 as a metabolite of exogenously applied IAA to pea tissue by Andreae and Good[9]. Following this paper, a number of reports dealing with the presence of IAAsp in IAA-fed[10] and unfed[11–14] tissue have been published. Paper or thin-layer chromatography with colour reagents specific to indole compounds were the usual methods and these were also used after the hydrolysis of IAAsp to free indoleacetic acid and free aspartic acid. Feung *et al.*[15] in 1976 used direct-inlet mass spectrometry (MS) for the identification of IAAsp in fed crown gall tissue but obtained mixed spectra. In 1980 IAAsp was identified in fed pine tissue by ^{1}H nuclear magnetic resonance (NMR) spectroscopy[16]. An endogenous conjugate between 4-Cl-IAA and Asp, the monomethyl ester of N-(4-Cl-3-indoleacetyl)aspartic acid, was identified in peas using mass spectrometry[17].

The hydrolysis method is often used in quantitative analysis where the amount of free IAA is correlated to that of IAAsp even though the origin of the IAA is unknown. Conjugates of IAA have different chemical properties and are also supposed to have different physiological functions in plants. It is therefore necessary to develop quantification methods for each conjugate separately. The purpose of the present study was to identify IAAsp as an endogenous substance in Scots pine, and to develop a reliable high-performance liquid chromatographic (HPLC) method for quantitative analysis of the substance.

EXPERIMENTAL

Synthesis of IAAsp

The synthesis of (±)-IAAsp was performed by the method of Mollan *et al.*[18]. The product was further purified on a 30 × 1.6 cm I.D. Sephadex G-10 column with 0.5 *M* ammonium hydrogen carbonate as eluent. The column was packed and pre-eluted with 200 ml of this eluent before use. A UV detector at 275 nm was used and the 25–75-ml fraction was collected. After evaporation, pink crystals, m.p. 190–191°C, were obtained in a yield of 37%. Final identification was made using IR, ^{1}H NMR and MS techniques, and all spectra were in agreement with those previously published[19].

Plant material

The current year's shoots of seven-year-old Scots pine (*Pinus sylvestris* L.) were collected in October 1980 at a natural stand 25 km north-east of Umeå, Sweden. The plant material was stored at −80°C until analysed.

Reagents

The following reagents were used: methanol (redistilled; analytical-reagent grade for HPLC analysis), buffer chemicals (Merck, Darmstadt, G.F.R.; analytical-reagent grade), ethanol (p.a.), diethyl ether (p.a.), butanol (p.a.), poly-N-vinylpyrrolidone (PVP, purchased as Polyclar At powder, GAF Corp., New York, NY, U.S.A.), Celite (30–80 mesh for GC, BDH), Sephadex G-10 and LH-20 (Pharmacia, Sweden), Amberlite XAD-7 (purchased as Servachrom®-XAD-7, pract, 300–1000 μm, Serva, G.F.R.). Purification and sieving of XAD-7 were performed as follows.

The synthetic resin was washed seven times with water in a beaker and the fines were discarded by decanting. Further washing was performed with methanol (seven times), the resin was dried by filtration, sieved (30–45 mesh) and finally washed with diethyl ether in a Soxhlet apparatus (2 × 12 h), and then dried in air.

Columns for clean-up

All columns were wet-packed in the respective solvents. For the combined Celite–PVP–Sephadex LH-20 column (45 × 1 cm I.D.) water was used when packed. The bottom layer of Sephadex LH-20 (19.5 cm) was eluted with water (70 ml) before the next layer of PVP (24.5 cm) was added. This was then eluted with water (50 ml) and the Celite layer (1 cm) added. The column was further eluted with 150 ml of 0.1 *M* phosphate–citrate buffer, pH 4.5, before use. The first XAD-7 column (15 × 0.5 cm I.D.) was packed in water and eluted with 20 ml of 0.1 *M* phosphate–citrate buffer, pH 4.5, before use. The second XAD-7 column, of the same size, was packed and eluted in the same way as the first, but the pH of the buffer was 2.7.

Extraction procedure (Fig. 1)

Pine shoots (each 10 g) were homogenized (Ultra Turrax) in cold methanol (200 ml) and extracted at −18°C for 18 h. After filtration, 10 ml of 0.1 *M* phosphate buffer (pH 8.0) were added and the solution was evaporated to 5–10 ml in a rotary evaporator (< 40°C). The same buffer was added to a final volume of 15 ml, the pH was corrected to 4.5 and the sample centrifuged. The extract was applied to the combined

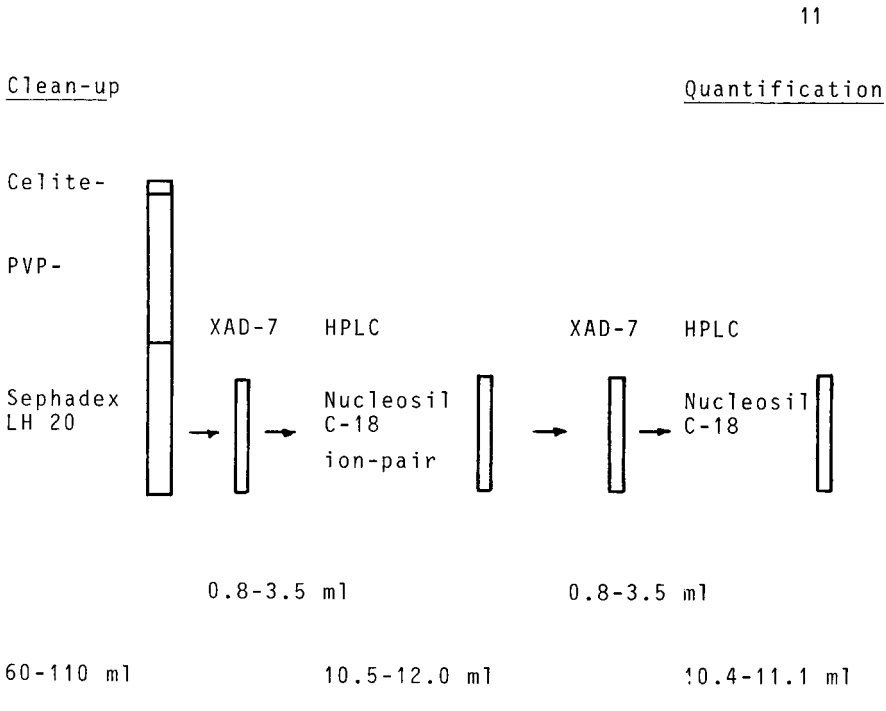

Fig. 1. Overview of the extraction procedure.

Celite–PVP–Sephadex LH-20 column. The 60–110-ml fraction was collected and applied to the XAD-7 concentrator column. The eluent was changed to ethanol, after which the 0.8–3.5-ml fraction was collected, evaporated to dryness in a stream of nitrogen (<40°C) and redissolved in 200 μl of 0.1 *M* phosphate buffer, pH 6.5, for HPLC analysis.

Equipment for HPLC and quantification of IAAsp

The HPLC system consisted of a Milton Roy Minipump connected via a Valco 50-μl loop injector to a 15 × 0.46 cm I.D. analytical column of 5-μm Nucleosil C-18 (Skandinaviska GeneTec AB, Sweden) and a Spectra-Physics SD-970 spectrofluorimetric detector with a 5-μl cuvette. The detector was adjusted to an excitation wavelength of 285 ± 5 nm. The emitted light was passed through an interference filter with a wavelength of 360 ± 10 nm. Two Nucleosil C-18 columns were used: the first in the preparative clean-up, and the second in the quantification step. The preparative column was eluted with methanol in 0.01 *M* phosphate buffer and 0.01 *M* tetrabutyl ammonium hydrogen sulphate. The methanol concentration was 25%, pH 6.5, and the flow-rate 1.5 ml/min. Fractions from four consecutive injections (10.5–12.0 ml) were collected and the methanol was evaporated with nitrogen. The 10-ml residue was adjusted to pH 2.7 and then applied to the second XAD-7 column as above. The 0.8–3.5-ml fraction was collected. After evaporation of ethanol, the extract was redissolved in 200 μl of 0.01 *M* phosphate buffer, pH 6.5, and applied to the second Nucleosil C-18 column for quantification. The eluent now consisted of methanol (25%), water (73%), and acetic acid (2%), and the flow-rate was 1.5 ml/min.

Equipment for GC–MS and identification of IAAsp

The gas chromatograph was equipped with a 25 m × 0.25 mm I.D. capillary quartz column OV-101 (Hewlett-Packard). The Grob-type injector was kept at 280°C. The column temperature was initially kept at 90°C for 1 min; it was then increased by 25°C/min to a final value of 280°C, which was held for 15 min. The gas chromatograph was connected to a Finnigan Model 4021 mass spectrometer equipped with a INCOS computer system. The temperature of the interface and the ion source was 250°C. The electron multiplier voltage was 1600 V and the spectra were recorded at 70 eV.

For the identification, fractions (10.4–11.1 ml) from four consecutive injections were combined after the second HPLC column. A few ml of butanol (azeotrope) were added and the extract was evaporated in a stream of nitrogen. The extract was then methylated with diazomethane in diethyl ether and a few drops of methanol and then purified on the second HPLC column as the IAAsp dimethyl ester. The eluent was methanol–water–acetic acid as before and the fraction (9.0–10.0 ml) was collected. After addition of butanol and evaporation, the extract was redissolved in a minimum amount (50 μl) of dichloromethane for GC–MS analysis. The retention time on GC was 9 min. Blank samples were treated in an identical way.

RESULTS AND DISCUSSION

The purification of pine extracts is very comprehensive and we started with the combined Celite–PVP–Sephadex LH-20 column used in our previous work[5,19,20],

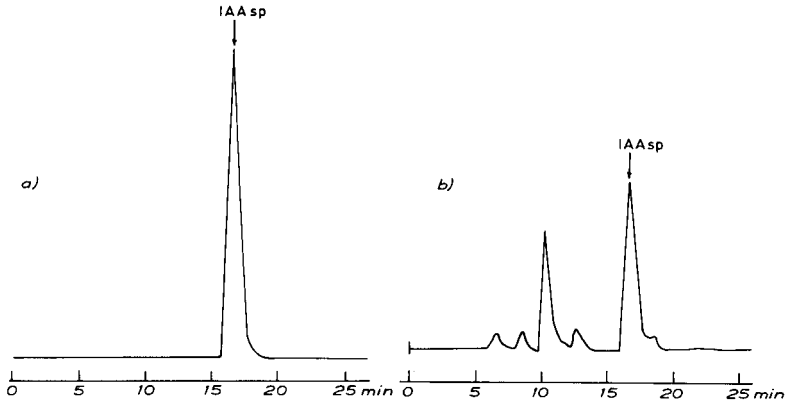

Fig. 2. HPLC chromatogram of (a) 100 ng standard IAAsp, (b) extract from 10-g pine shoots on Nucleosil C-18. Eluent: methanol–water–acetic acid (25:73:2).

where IAAsp is eluted with buffer. Extraction of this phase with organic solvents is difficult, however, since IAAsp is rather water-soluble even at low pH. For that reason we used column extraction on Amberlite XAD-7[21,22], which adsorbs organic compounds from water and releases them in a few ml of organic solvent. Ethanol was found to give high desorption efficiency and, moreover, to produce dry extracts after evaporation, since it forms an azeotrope with water. The XAD-7 column also had a favourable purification effect on the extract and, for that reason, we used two XAD-7 columns at two different pH values. The recoveries of IAAsp were quantitative at both pH values.

The identification of natural IAAsp in pine shoots was confirmed by retention time in two different HPLC systems, and by retention time as its dimethyl ester in both HPLC and GC. Final identification was afforded by combined GC–MS. All data agreed with those of the standard, and the mass spectrum also agreed with that published earlier[23].

Further HPLC clean-up was necessary before GC–MS identification since the residue of tetrabutylammonium ion from the first HPLC column resulted in a tremendous background noise in the GC analysis.

Owing to the huge amount of extractable compounds present in pine tissues, a multi-clean-up process had to be used for correct quantification of IAAsp. As can be seen in Fig. 2, a very clean extract is finally obtained. The tedious clean-up is thus worth the effort.

Today there is no doubt of the presence of IAAsp in plant tissue as a result of investigations that provide direct or indirect proof. Investigations of this type are often based on the ability of the tissue to convert applied IAA into a compound which, after hydrolysis, splits into compounds with the same chromatographic properties as indoleacetic acid and aspartic acid. However, there has been a lack of direct identification of IAAsp in unfed tissue. The present work thus provides the final proof for the presence of natural IAAsp in plant tissue.

The need for quantitative analysis of IAAsp has been still greater. Earlier indirect quantification of liberated IAA is based on the assumption that IAAsp is very

soluble in the organic phase in buffer/organic phase partitioning at low pH. We have found that this is correct for *n*-butanol. However, for diethyl ether or ethyl acetate (the solvents usually used in extraction of IAAsp) this is by no means true. The IAAsp losses can thus be very high if an unsuitable organic solvent is used. Neglecting this causes incorrect amounts of IAA after hydrolysis and thus a wrong picture is obtained of the actual amount of IAAsp present in the tissue.

The total yield of the extraction procedure is 35% and was determined in parallel where one sample was spiked with 1000 ng of standard IAAsp. It is intended to use [^{14}C]IAAsp, when available, for calculations of losses, which would afford better control of the yields in routine analyses.

ACKNOWLEDGEMENTS

We thank the staff at the National Board of Occupational Safety and Health, Umeå, for the GC–MS facilities put at our disposal. We offer our special thanks to Drs. Kurt Andersson and Arne Dunberg for the inspiring discussions we had with them and for their advice. The work was financially supported by the Swedish Council for Forestry and Agricultural Research (grants P316, P331 and P425), and the J. C. Kempe and Seth M. Kempe Memorial Foundations.

REFERENCES

1 E. A. Schneider and F. Wightman, in D. S. Letham and T. J. V. Higgins (Editors), *Phytohormones and Related Compounds —A Comprehensive Treatise*, Volume 1, Elsevier, Amsterdam, 1979, p. 29.
2 D. R. DeYoe and J. B. Zaerr, *Plant Physiol.*, 58 (1976) 299.
3 C. H. A. Little, J. K. Heald and G. Browning, *Planta*, 139 (1978) 133.
4 Å. Crozier, J. Loferski, J. B. Zaerr and R. O. Morris, *Planta*, 150 (1980) 366.
5 G. Sandberg, B. Andersson and A. Dunberg, *J. Chromatogr.*, 205 (1981) 125.
6 R. S. Bandurski, in F. Eisenberg and W. W. Wells (Editors), *Cyclitois and the Phosphoinositides*, Academic Press, New York, 1979.
7 C. S. Feung, R. H. Hamilton and R. O. Mumma, *Plant Physiol.*, 59 (1977) 91.
8 W. K. Purves, S. L. Hollenberg and T. G. Chappel, *Plant Physiol.*, 65 (1980) supplement No. 865.
9 W. A. Andreae and N. E. Good, *Plant Physiol.*, 30 (1955) 380.
10 M. H. Zenk, *Regulateurs Naturels de la Croissance Vegetale*, C.N.R.S., Paris, 1964, 241.
11 H. D. Klämbt, *Naturwissenschaften*, 47 (1960) 398.
12 G. M. Weaver and H. O. Jackson, *Can. J. Bot.*, 41 (1963) 1405.
13 H. O. Olney, *Plant Physiol.*, 43 (1968) 293.
14 L. E. Fellows and E. A. Bell, *Phytochemistry*, 10 (1971) 2083.
15 C. S. Feung, R. H. Hamilton and R. O. Mumma, *Plant Physiol.*, 58 (1976) 666.
16 J. Riov and H. E. Gottlieb, *Physiol. Plant.*, 50 (1980) 347.
17 H. Hattori and S. Marumo, *Planta*, 102 (1972) 85.
18 R. C. Mollan, D. M. X. Donnelly and M. A. Harmey, *Phytochemistry*, 11 (1972) 1485.
19 B. Andersson, N. Häggström and K. Andersson, *J. Chromatogr.*, 157 (1978) 303.
20 G. Sandberg, A. Dunberg and P.-C. Odén, *Physiol. Plant.*, 53 (1981) 219.
21 G. A. Junk, J. J. Richard, M. D. Grieser, D. Witiak, J. L. Witiak, M. D. Arguello, R. Vick, H. J. Svec, J. S. Fritz and G. V. Calder, *J. Chromatogr.*, 99 (1974) 745.
22 W. L. Budde and J. W. Eichelberger, *Organics Analysis Using Gas Chromatography Mass Spectrometry*, Ann Arbor Sci. Publ., Ann Arbor, MI, 1979, p. 39.
23 C. S. Feung, R. H. Hamilton and R. O. Mumma, *J. Agr. Food Chem.*, 23 (1975) 1120.

Journal of Chromatography, 238 (1982) 157–166
Elsevier Scientific Publishing Company, Amsterdam — Printed in The Netherlands

CHROM. 14,559

REVERSED- AND NORMAL-PHASE HIGH-PERFORMANCE LIQUID CHROMATOGRAPHY OF GIBBERELLIN METHOXYCOUMARYL ESTERS

ALAN CROZIER*
Department of Botany, The University, Glasgow G12 8QQ (Great Britain)
JOE B. ZAERR
Department of Forest Science, Oregon State University, Corvallis, OR 97331 (U.S.A.)
and
ROY O. MORRIS
Department of Agricultural Chemistry, Oregon State University, Corvallis, OR 97331 (U.S.A.)
(Received November 19th, 1981)

SUMMARY

The methoxycoumaryl esters of thirteen gibberellins were synthesized by crown ether catalysis. These derivatives are highly fluorescent (λ_{max}^{ex} 320 nm, λ_{max}^{em} 400 nm) and can be detected at the low picogram level with a spectrophotofluorimeter after reversed-phase high-performance liquid chromatography. The various gibberellin esters were readily resolved by high-performance liquid chromatography on both ODS-Hypersil and CPS-Hypersil supports. There were marked differences in the selectivity of the reversed- and normal-phase systems especially in relation to the behaviour of mono, bis and tris esters. Chemical ionization negative-ion mass spectra of the gibberellin methoxycoumaryl esters were obtained by direct-probe mass spectrometry.

INTRODUCTION

The application of high-performance liquid chromatography (HPLC) to the analysis of gibberellins (GAs) is still in its infancy. Although GAs are readily chromatographed they exhibit only low UV absorbance, and the main dilemma confronting potential users of the technique is the choice of a detector system. Although an absorbance monitor operating at *ca.* 210 nm can detect *ca.* 50 ng of GA, the UV cut-off point of most solvents restricts this level of sensitivity to a very limited range of mobile-phase conditions. The problem is compounded when analysing trace amounts of GAs in multicomponent plant extracts as many of the impurities induce a strong detector response. One course of action is to use selective GA bioassays to detect active components in HPLC eluates[1,2]. However, if chromatographic peak capacity is to be maintained many fractions have to be collected and assayed. This is time-consuming and much of the practicality of HPLC is lost. More often only small numbers of fractions are assayed, and in these circumstances resolution is clearly

0021-9673/82/0000–0000/$02.75

being traded for enhanced speed of analysis. This can be an acceptable compromise when HPLC is being used to purify unknown endogenous GA-like compounds prior to analysis by mass spectrometric techniques.

An alternative approach, that involves sacrificing detector selectivity in favour of the resolution and general flexibility of HPLC, is to convert GAs into derivatives that absorb in an accessible region of the UV spectrum. This option is feasible when either radioactive GAs are being analysed or the identity of the individual GAs in a sample are known or suspected. Reeve and Crozier[3] made use of GA benzyl esters which were synthesized by esterification of N,N′-dimethylformamide dibenzylacetal and have a λ_{max} of 256 nm. The GA benzyl esters were chromatographed on a silica gel adsorption column which readily separated several isomers because of its ability to distinguish subtle differences in the spatial relationships of the polar groupings of structurally similar molecules. Marked changes in the selectivity of the silica gel column were achieved by using different reagents to modify the mobile phase. The procedures have been used in conjunction with a radioactivity monitor to analyse [^{3}H]GA metabolites from *Phaseolus coccineus* seedlings[3–5] and lettuce hypocotyl sections[6]. A comprehensive discussion of silica gel adsorption HPLC of GA benzyl esters has also been published[3].

Although GA benzyl esters have proved useful in metabolism studies it should be noted that the ε_{max} of mono derivatives is 205 l mol^{-1} cm^{-1} and that the limit of detection at 254 nm is only 300 ng. This lack of sensitivity is a serious constraint when it comes to utilizing fully the high resolving power of HPLC to analyse sub-microgram amounts of endogenous GAs. Other derivatives do, however, offer much greater potential in this regard. Heftmann *et al.*[7] prepared *p*-nitrobenzyl GA esters (λ_{max} 265 nm, $\varepsilon_{max} > 6000$) using O-*p*-nitrobenzyl-N,N′-diisopropylurea[8]. Unfortunately when the esters were chromatographed on a preparative silver nitrate impregnated silica gel column the speed of analysis was very slow and the performance was poor (number of theoretical plates, $N = 1500$; height equivalent to a theoretical plate, $H = 3.25$ mm). As 50–200-ml peak volumes were obtained the limit of detection at A_{265} was 100 ng rather than the <10 ng that might have been anticipated if conventional HPLC techniques had been used. Morris and Zaerr[9] used 18-crown-6 according to the procedures of Durst *et al.*[10] to catalyse the conversion of GAs into GA *p*-bromophenacyl esters (λ_{max} 256 nm, ε_{max} 19,100). The limit of detection at A_{254} for mono esters eluting from reversed- and normal-phase HPLC columns was <5 ng.

This paper reports on the synthesis and HPLC of GA methoxycoumaryl esters (GACE) which are strongly fluorescent derivatives (λ_{max}^{excit} 320 nm, λ_{max}^{emiss} 400 nm) that can be detected at the low picogram level.

MATERIALS AND METHODS

Solvents were delivered at a flow-rate of 1 ml min^{-1} by an Altex Model 332 gradient liquid chromatograph. Samples were introduced off-column via an Altex Model 210 valve fitted with a 20-μl loop. A 250 × 5 mm I.D. ODS-Hypersil (5 μm) column eluted with varying ratios of either methanol or ethanol in 20 m*M* ammonium acetate buffer (pH 3.5) was used for reversed-phase HPLC, while normal-phase separations were carried out on a 250 × 5 mm I.D. CPS-Hypersil (5 μm) column eluted isocratically with various ratios of hexane and dichloromethane con-

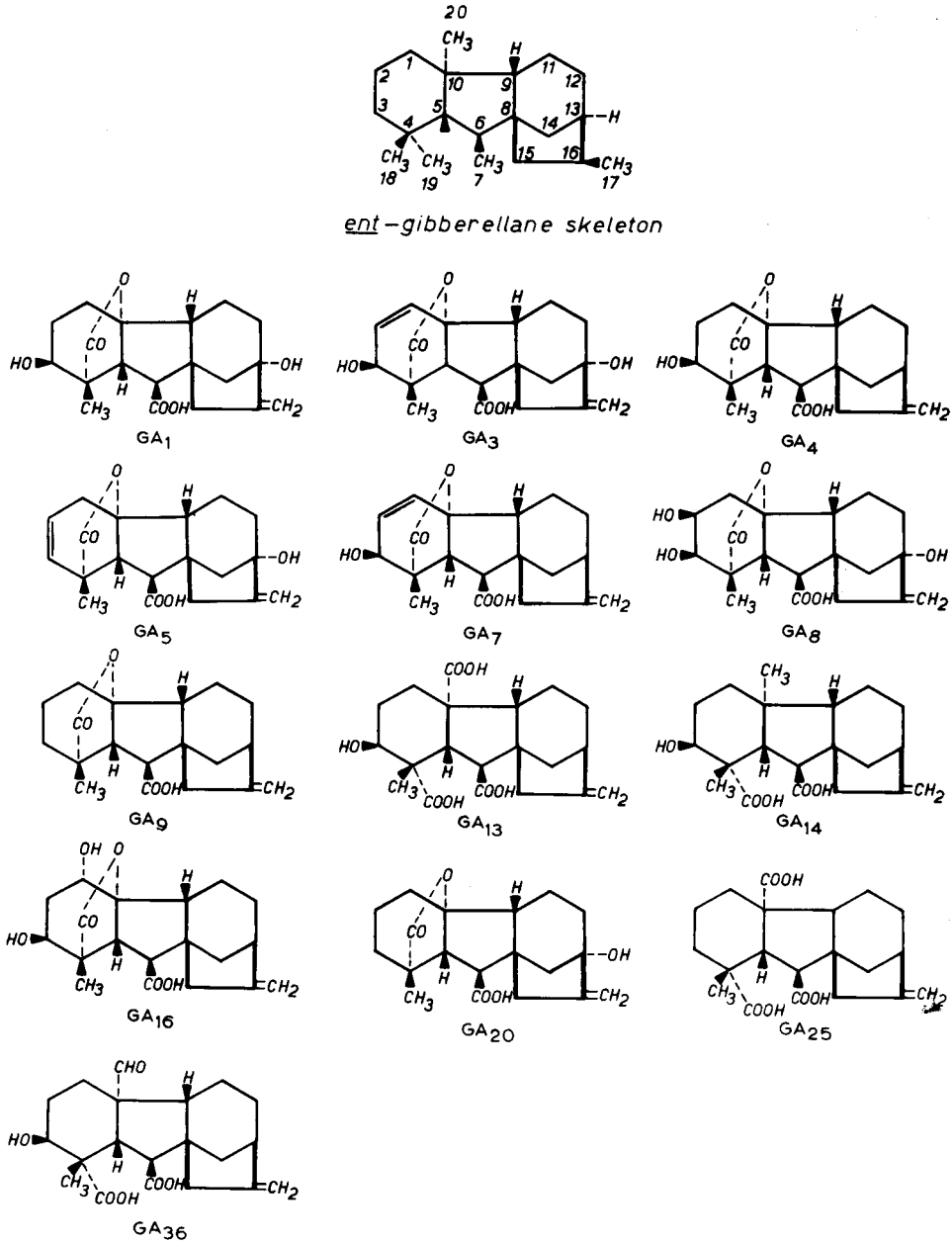

Fig. 1. Gibberellin structures.

taining 3% ethanol. Column effluent was monitored with either a Perkin-Elmer 650-10S spectrophotofluorimeter (excitation 320 nm, emission 400 nm) fitted with an 18 μl flow cell or an ISCO Model UA-5 absorbance monitor at 254 nm with an 8-μl flow cell. When radioactive samples were analysed, effluent leaving the fluorimeter was

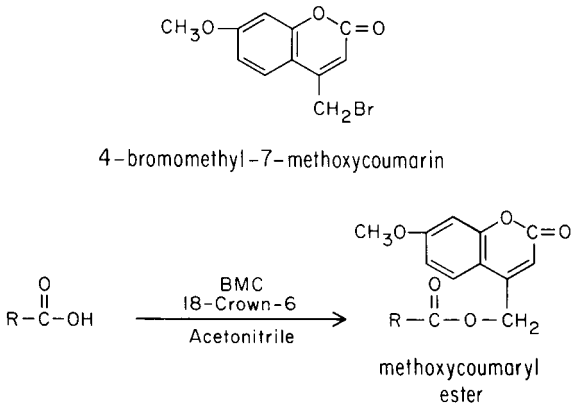

Fig. 2. Synthesis of a methoxycoumaryl ester.

directed to a Reeve Analytical (Glasgow, Great Britain) Splitter–Mixer, mixed with scintillant and passed to an on-stream radioactivity monitor[11]. A scintillant composed of 10 g of PPO, 330 ml of Triton X-100, 670 ml of distilled xylene and 150 ml of methanol was used for reversed-phase HPLC analyses. A 3:1 scintillant–eluent ratio was compatible with all methanol–ethanol concentrations from 0–100% giving 12–15% counting efficiencies for ^3H when using reagent grade chemicals. The mobile phase from the cyanopropyl column was mixed with scintillant containing 12 g of PPO, 150 g of naphthalene, 50 ml of Triton X-100 and 1 l of distilled toluene. An efficiency of 25% for ^3H was obtained with a 2:1 scintillant–eluent ratio.

Methoxycoumaryl esters of GA_1, GA_3, GA_4, GA_5, GA_7, GA_8, GA_9, [17^{3}H]GA_9 (11.2 mCi mmol^{-1}), GA_{13}, GA_{14}, GA_{16}, GA_{20}, GA_{25} and GA_{36} (see Fig. 1) were prepared according to the procedures of Dünges[12] by reaction of each of the free acids with an equimolar amount of 4-bromomethyl-7-methoxycoumarin (BMMC), a one-tenth molar equivalent of 18-crown-6 and a crystal of K_2CO_3 in 100 μl of dry acetonitrile at 60°C for 2 h. The reaction is shown in Fig. 2. The reaction mixture was taken to dryness, water was added and the GACEs were extracted into chloroform and dried prior to purification by steric exclusion[13] and reversed-phase HPLC. Electron impact and chemical ionization mass spectra of GACEs were obtained by direct insertion probe using a Finnigan 4023 mass spectrometer.

RESULTS AND DISCUSSION

The efficacy of the 18-crown-6-catalysed conversion of GAs into GACEs was determined by analysing a [^{3}H]GA_9 reaction mixture by reversed-phase HPLC using fluorescence and radioactivity monitors. The data obtained are illustrated in Fig. 3. The traces show that the GA_9 underwent complete conversion into GA_9CE, which was the predominant fluorescent component in the sample.

Although fluorimetry offers inherently high sensitivity, practical performance is very much instrument-dependent and limits of detection can vary by as much as three orders of magnitude. We assessed several commercial HPLC fluorescence monitors and obtained the best results with a Perkin-Elmer 650-10S spectrofluorimeter,

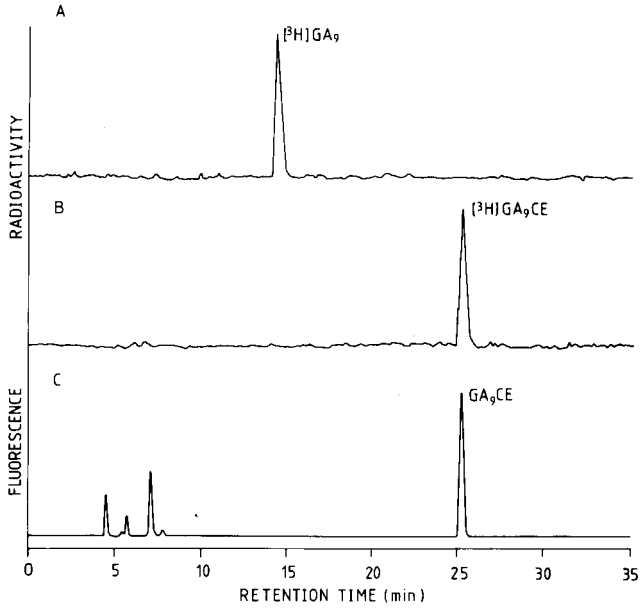

Fig. 3. Conversion of [^{3}H]GA_9 into [^{3}H]GA_9 methoxycoumaryl ester. Column, 250 × 5 mm I.D. ODS-Hypersil; mobile-phase, 30 min gradient, 60–100% methanol in 20 m*M* ammonium acetate buffer (pH 3.5); flow-rate, 1 ml min^{-1}. Samples: (A) *ca.* 15 × 10^3 dpm aliquot of [^{3}H]GA_9-BMC-18-crown-6 reaction mixture at 0 h; (B, C) *ca.* 15 × 10^3 dpm aliquot of [^{3}H]GA_9-BMC-18-crown-6-reaction mixture after 2 h at 60 C. Detectors, homogeneous radioactivity monitor and spectrofluorimeter (excitation 320 nm, emission 400 nm).

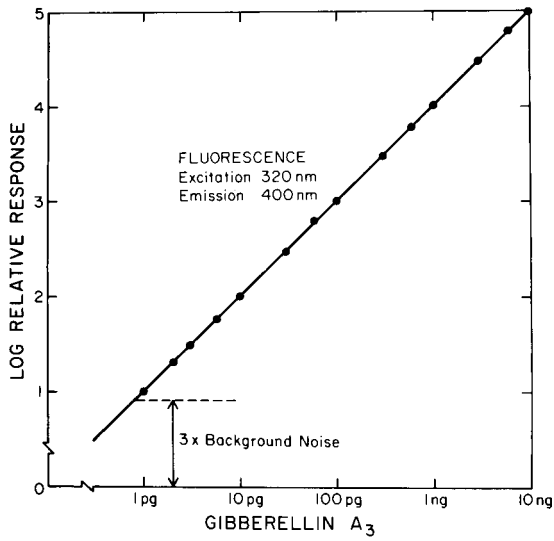

Fig. 4. Fluorescence detection limit of the methoxycoumaryl ester of GA_3 after reversed-phase HPLC. Column, 250 × 5 mm I.D. ODS-Hypersil; mobile phase, 45% ethanol in 20 m*M* ammonium acetate buffer (pH 3.5); flow-rate, 1 ml min^{-1}; sample, GA_3CE (k' = 2.3), load as indicated; detector, spectrofluorimeter (excitation 320 nm, emission 400 nm).

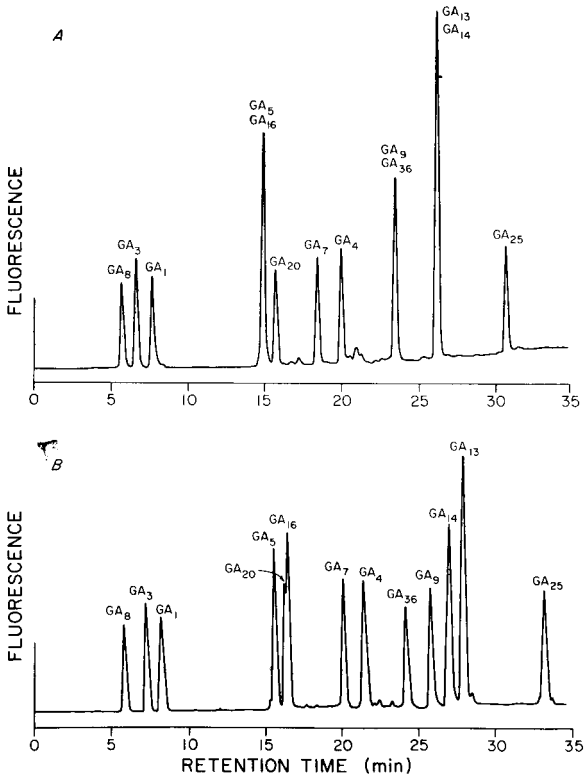

Fig. 5. Reversed-phase HPLC of gibberellin methoxycoumaryl esters. Column, 250 × 5 mm I.D. ODS-Hypersil; mobile phase, 30 min gradient (A) 60–100% methanol in 20 m*M* ammonium acetate buffer (pH 3.5), (B) 40–80% ethanol in 20 m*M* ammonium acetate buffer (pH 3.5); flow-rate, 1 ml min^{-1}; sample, methoxycoumaryl esters of GA_1, GA_3, GA_4, GA_5, GA_7, GA_8, GA_9, GA_{13}, GA_{14}, GA_{16}, GA_{20}, GA_{25} and GA_{36}; *ca.* 9.0 ng mono, 4.5 ng bis and 3.0 ng tris esters; detector, spectrofluorimeter (excitation 320 nm, emission 400 nm).

which was capable of detecting GA_3CE at the low picogram level after reversed-phase HPLC. This is shown in Fig. 4, where a log–log plot of relative response against sample size gives a line with a slope of 1.0, linear over almost four orders of magnitude. The limit of detection for GA_3, which forms a mono ester, is *ca.* 1 pg (2.8 fmol) as determined by the point at which the curve intersects the ordinate equivalent to three times the level of background noise. With bis and tris derivatives the figure is correspondingly lower.

Reversed-phase separations of a range of GACEs obtained by gradient elution from an ODS-Hypersil column are illustrated in Fig. 5. The recovery of $[^3H]GA_9CE$ was greater than 90%. The system was able to distinguish between closely related GAs. The double-bond isomers GA_1CE/GA_3CE, GA_4CE/GA_7CE and $GA_5CE/GA_{20}CE$ all separated with baseline resolution with the $\Delta^{1,2}$ and $\Delta^{2,3}$ derivatives eluting before their saturated analogs. It is of interest to note the effect of solvents on column selectivity. When a methanol–buffer mobile phase was employed $GA_{13}CE$ and $GA_{14}CE$ co-chromatographed as did GA_9CE and $GA_{36}CE$ (Fig. 5A).

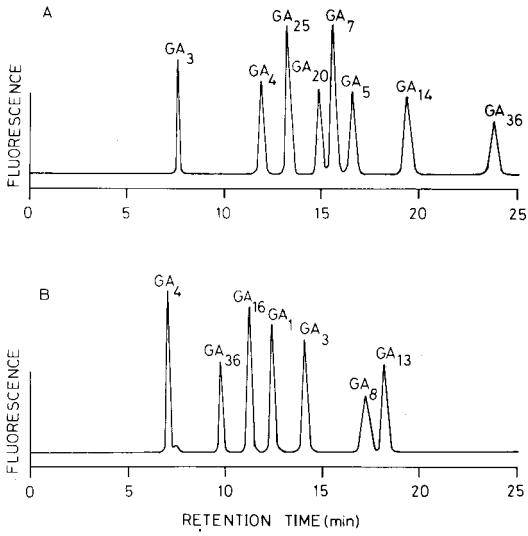

Fig. 6. Normal-phase HPLC of gibberellin methoxycoumaryl esters. Column, 250 × 5 m I.D. CPS-Hypersil; mobile phase, (A) 3% ethanol in dichloromethane–hexane (12:88) and (B) 3% ethanol in dichloromethane–hexane (20:80); flow-rate, 1 ml min^{-1}; sample, methoxycoumaryl esters of GA_1, GA_3, GA_4, GA_5, GA_7, GA_8, GA_9, GA_{13}, GA_{14}, GA_{16}, GA_{20}, GA_{25} and GA_{36} as indicated; *ca.* 3.0 ng mono, 1.5 ng bis and 1.0 ng tris esters; detector, spectrofluorimeter (excitation 320 nm, emission 400 nm).

However, when ethanol was substituted for methanol the compounds were well resolved (Fig. 5B). In general, increasing the number of free hydroxyl groups decreases retention, 13α-hydroxylation to a much greater extent than 3β-hydroxylation which, in turn, is more effective than hydroxylation at either the 1α or 2β positions. A comparison of the retention characteristics of GA_4CE, $GA_{36}CE$, $GA_{14}CE$ and $GA_{13}CE$ as well as GA_9CE and $GA_{25}CE$ shows an elution order of mono > bis > tris esters indicating that increasing the number of methoxycoumaryl functions decreases polarity. The elution of $GA_{14}CE$ and $GA_{38}CE$ implies that C-20 methyl GACEs are less strongly retained than the C-20 aldehydic counterparts.

The ODS-Hypersil column generated 9300 theoretical plates when GACEs were analysed. This compares unfavourably with a figure of 16,500 obtained when a test mixture containing biphenyl was chromatographed and monitored at A_{254}. In both instances retention volumes were more than 20 ml. This minimized extra-column effects and ensured that the differences in column performance were not a consequence of the larger flow-cell volume of the fluorimeter used to detect the GACEs. The reduced efficiency with GACEs was much more marked on Ultrasphere ODS and MicroPak MCH-5 columns and was not counteracted by increasing the molarity of the ammonium acetate buffer in the mobile phase. The symptoms may therefore reflect the effectiveness with which the various supports were end capped.

Normal-phase separations of GACEs on a CPS-Hypersil column eluted isocratically with 3% ethanol in either 12% or 20% dichloromethane in hexane are illustrated in Fig. 6. Recoveries of the [^{3}H]GA_9CE from the cyanopropyl column were *ca.* 85%. Although the effects of 3β- and 13α-hydroxylation and 1,2 and 2,3 double bonds are, as anticipated, the opposite of those observed in reversed-phase

TABLE I

METHANE CHEMICAL IONIZATION NEGATIVE-ION MASS SPECTRA OF GIBBERELLIN METHOXYCOUMARYL ESTERS

Compound	*Mol.wt.*	
GA_1CE	536	347—100% (M − 189)
GA_3CE	534	534—100% (M^-), 345—43% (M − 189), 301—7% (M − 233), 283—7% (M − 251)
GA_4CE	520	331—100% (M − 189)
GA_5CE	518	329—100% (M − 189)
GA_7CE	518	518—100% (M^-), 329—34% (M − 189), 285—5% (M − 233), 267—15% (M − 251), 265—5% (M − 253)
GA_8CE	552	363—100% (M − 189)
GA_9CE	504	315—100% (M − 189)
$GA_{13}CE$	942	565—8% (M − 377 [− 189 − 188]), 547—100% (M − 395 [− 189 − 206]), 359—54% (M − 583 [− 189 − 188 − 206 and/or − 189 − 206 − 188]), 315—5% (M − 627), 314—6% (M − 628)
$GA_{14}CE$	724	535—100% (M − 189), 347—18% (M − 377 [− 189 − 188])
$GA_{16}CE$	536	347—100% (M − 189), 329—6% (M − 207), 303—9% (M − 233)
$GA_{20}CE$	520	331—100% (M − 189)
GA_{36}	738	549—10% (M − 189), 343—100% (M − 395 [− 189 − 206])

analyses, the overal elution pattern is not a mirror image of the ODS-Hypersil profiles in Fig. 5. This is primarily due to the behaviour of bis and tris GACEs which exhibit increased capacity factors (k') with respect to their increased number of methoxycoumaryl groups. The polarity of GACEs, in this regard is, thus, the opposite of that observed on the reversed-phase support. The other noticeable difference, as indicated by the elution of $GA_{16}CE$ close to GA_1CE rather than $GA_{20}CE$, is that 1β-hydroxylation has a more marked effect on retention in the normal than the reversed-phase system. There was no reduction in the performance of the CPS-Hypersil column when GACEs were analysed as *ca.* 14,000 theoretical plates were generated with both GACEs and a test mixture containing 2,6-dinitrotoluene. The only exception was the 2β-hydroxy derivative GA_8CE which chromatographed with an efficiency of only 6100 theoretical plates. Because of increased levels of background fluorescence and/or quenching in the mobile phase the limit of detection of mono GACEs eluting from the CPS column was no better than 30 pg.

GACEs are not readily volatile and as a consequence mass spectra have to be obtained by direct-probe mass spectrometry rather than combined gas chromatography–mass spectrometry. Direct-probe electron impact and chemical ionization positive-ion spectra were of no practical value as the dominant fragment in all instances is *m/e* 191 with no other ions of significant intensity being present. However, chemical ionization negative-ion spectra proved to be of more diagnostic value (Table I). A strong molecular ion was obtained with the $\Delta^{1,2}$ GACEs, GA_3CE and GA_7CE. M − 189 arising from the loss of the methoxycoumaryl moiety was the main fragment in the spectra the other C_{19}-GA derivatives that were tested. The C_{19}-GA isomers GA_4CE and $GA_{20}CE$ yielded identical spectra. These compounds can however be readily distinguished on the basis of their HPLC retention characteristics. Spectra were obtained from the methoxycoumaryl esters of three C_{20}-GAs. M − 189 was the strongest ion produced by $GA_{14}CE$ while M − 395 was the base peak in the spectra of both $GA_{13}CE$ and $GA_{36}CE$.

The picogram limits of detection of the fluorescence monitor to GACEs enhance the overall flexibility of HPLC as an analytical tool, especially in the investigation of trace amounts of endogenous GAs in vegetative tissues. It should be noted, however, that the high sensitivity is not accompanied by any degree of detector selectivity. GAs do not exhibit native fluorescence. Thus, when plant extracts are derivatized not only endogenous GAs but also any other carboxylic acids in the sample will form methoxycoumaryl esters and so acquire fluorescent properties. As a consequence considerable purification will be required before homogeneity of detector response can be obtained and an accurate analysis achieved. Such an approach appears feasible with HPLC because of the wide array of diverse separatory mechanisms that can be employed and the ease and efficiency of sample recovery. Procedures for use in the verification of accuracy of such analyses have been proposed by Reeve and Crozier[14] and further discussed by Crozier[5,15,16].

The HPLC fluorescence procedures that have been described have the potential to quantitatively analyse endogenous GAs as their methoxycoumaryl esters only when the identity of individual GA(s) likely to be present in a sample is known or suspected and when reference compounds are available to determine HPLC retention characteristics and quantify the response of the fluorimetric detector. If estimates are to be truely quantitative a radioactive internal standard must also be available to account for sample handling losses and variability in derivatizing efficiency. With the exception of [^{3}H]GA_1 and [^{3}H]GA_4, labelled GAs suitable for use as internal markers are not currently available from commercial sources so investigators are faced with the choice of either accepting such errors or investing time in the synthesis of either ^{14}C-labelled or, more preferably, high specific activity ^{3}H-labelled GAs.

ACKNOWLEDGEMENTS

This investigation was initiated at Oregon State University, when Alan Crozier was on leave of absence, and completed at the University of Glasgow. Studies at Oregon State University were supported by grants from the Weyerhauser Company, Crown Zellerbach Corporation, Sun Studs Company, International Paper Company and St. Regis Paper Company. Research at the University of Glasgow made use of an HPLC purchased with a Royal Society Grant-in-Aid and a spectrofluorimeter acquired with funds from the Science Research Council. We wish to thank Alison Sutcliffe (University of Glasgow) for expert technical assistance and Don Griffin (Oregon State University) for obtaining the mass spectra.

REFERENCES

1 G. W. M. Barendse, P. H. van de Werken and H. Takahashi, *J. Chromatogr.*, 198 (1980) 449.
2 M. G. Jones, J. D. Metzger and J. A. D. Zeevaart, *Plant Physiology*, 65 (1980) 218.
3 D. R. Reeve and A. Crozier, in J. Hillman (Editor), *Isolation of Plant Growth Substances*, Cambridge Univ. Press, London, New York, 1978, p. 41.
4 A. Crozier and D. R. Reeve, in P. E. Pilet (Editor), *Plant Growth Regulation*, Springer, Berlin, 1977, p. 67.
5 A. Crozier, in H. W. Woolhouse (Editor), *Advan. Bot. Res.*, 9 (1981) 33.
6 L. J. Nash, R. L. Jones and J. L. Stoddart, *Planta*, 140 (1978) 143.
7 E. Heftmann, G. A. Saunders and W. F. Haddon, *J. Chromatogr.*, 156 (1978) 71.
8 D. R. Knapp and S. Kruger, *Anal. Lett.*, 8 (1975) 603.

9 R. O. Morris and J. B. Zaerr, *Anal. Lett.*, AII(i) (1978) 73.
10 D. Durst, M. Milano, E. J. Kitka, Jr., S. A. Connelly and E. Grushka, *Anal. Chem.*, 47 (1975) 1797.
11 D. R. Reeve and A. Crozier, *J. Chromatogr.*, 137 (1977) 271.
12 W. Dünges, *Anal. Chem.*, 49 (1977) 442.
13 A. Crozier, J. B. Zaerr and R. O. Morris, *J. Chromatogr.*, 198 (1980) 57.
14 D. R. Reeve and A. Crozier, in J. MacMillan (Editor), *Hormonal Regulation of Development 1. Molecular Aspects of Plant Hormones, Encyclopeadia of Plant Physiology New Series*, Vol. 9, Springer, Berlin, 1980, p. 203.
15 A. Crozier, in C. H. A. Little (Editor), *Control of Shoot Growth in Trees*, Canadian Forest Service, Fredericton, 1980, p. 325.
16 A. Crozier, in J. R. Lenton (Editor), *Gibberellins-Chemistry, Physiology and Use*, Monograph No. 5, British Plant Growth Regulator Group, Wantage, 1980, p. 17.

Journal of Chromatography, 238 (1982) 167–173
Elsevier Scientific Publishing Company, Amsterdam — Printed in The Netherlands

CHROM. 14,557

DETERMINATION OF HOST-SELECTIVE PHYTOTOXINS FROM *ALTERNARIA ALTERNATA* F. SP. *LYCOPERSICI* AS THEIR MALEYL DERIVATIVES BY HIGH-PERFORMANCE LIQUID CHROMATOGRAPHY

D. J. SILER* and D. G. GILCHRIST
Department of Plant Pathology, University of California, Davis, CA 95616 (U.S.A.)
(Received November 17th, 1981)

SUMMARY

A rapid, fully reversible, and highly reproducible procedure for separation and quantitative detection of disease-determining phytotoxic metabolites of *Alternaria alternata* f. sp. *lycopersici* as their maleyl amide derivatives by reversed-phase high-performance liquid chromatography is described. Maleyl-derivatized toxin, prepared by reaction with maleic anhydride, with an absorbance maximum at 250 nm, was detected for 0.5–10 nmoles following chromatography on a C_{18} bonded-phase column using binary gradient systems. Toxin samples, maleylated at pH 9.2 and then demaleylated at pH 3.0, showed no detectable loss of biological activity after the chromatographic separation. Quantification of the procedure was based on a trinitrophenol–aspartic acid standard. The procedure is currently being used to study kinetics of toxin production in culture and qualitative detection of phytotoxin in diseased host tissue.

INTRODUCTION

The fungal pathogen, *Alternaria alternata* f. sp. *lycopersici* has been shown to cause a stem canker disease on tomato[1]. Two fractions have been isolated from cell-free culture filtrates of the fungus which are phytotoxic and reproduce the macroscopic disease symptoms only on pathogen-susceptible tomatoes in concentrations less than 10 ng/ml. Such toxins are termed "host-selective" and are of interest as primary determinants of disease. One of these fractions (TA), characterized by high-resolution mass spectrometry (HRMS) and nuclear magnetic resonance (NMR), is reported to consist of two esters (at C-13 and C-14) of propane-1,2,3-tricarboxylic acid and 1-amino-11,15-dimethylheptadeca-2,4,5,13,14-pentol[2]. Preliminary evidence indicates that the second fraction (TB) also consists of two components with the same carbon skeleton as TA but which lack the C-5 hydroxyl and differ in stereochemistry at one or more of the chiral centers from C-11 to C-15[2].

Precise definition of the role of these host-selective toxins as the molecular basis of disease stress requires a quantitative procedure to detect the phytotoxic components in culture filtrates of the pathogen and diseased tomato tissue with concom-

0021-9673/82/0000–0000/$02.75

itant recovery of biological activity. Preparation of a toxin chromophore is required because of the lack of significant absorbance by the native toxins at wavelengths above 210 nm.

Maleic anhydride has been used for reversible modification of amino groups in proteins and peptides for enzymatic degradation, binding studies, and to increase peptide solubility[3–5]. This report describes the use of maleic anhydride as a fully reversible derivatizing reagent for aliphatic amines, and for quantitative detection of the aforementioned phytotoxins.

EXPERIMENTAL

Apparatus

The liquid chromatography system consisted of a Varian (Palo Alto, CA, U.S.A.) Model 5060 liquid chromatograph with ternary solvent delivery coupled to a Valco air-actuated injection valve fitted with a 10-μl sample loop. Column effluent was passed through a Varian UV-50 variable-wavelength detector with a 7.9-μl flow cell, connected to a Varian Model 9176 strip chart recorder. A Micro Pak MCH-10 column (30 cm × 4 mm I.D.), consisting of a monomeric C_{18} bonded onto 10-μm silica gel, with *ca.* 6000 theoretical plates was used for the reversed-phase separations. A guard column with disposable cartridges packed with the same material as the analytical column was installed between the injection valve and the analytical column.

Reagents and solvents

All reagents were analytical reagent grade. Maleic anhydride was recrystallized twice from chloroform before use. Methanol was purchased from Burdick & Jackson Labs. (Muskegon, MI, U.S.A.) and had a UV cut-off of 203 nm. Water was obtained from a Millipore (Bedford, MA, U.S.A.) Milli Q water purification system. The mobile-phase buffer was 0.05 *M* potassium phosphate adjusted to pH 3.5 or 2.7 with 0.1 *M* HCl by measurement with a pH meter, and filtered through a Gelman (Ann Arbor, MI, U.S.A.) 0.2-μm filter before use. All mobile-phase solvents were degassed before use.

Toxin purification

Phytotoxins were isolated as previously described[1,2] from cell-free culture filtrates of *A. alternaria* f. sp. *lycopersici* by treatment with barium acetate to a final concentration of 0.4 *M*, centrifugation, butanol extraction of the supernatant, exchange into water and concentration on a rotovap at 37°C, followed by gel permeation chromatography on polyacrylamide Biogel P-2 (Bio-Rad Labs, Richmond, CA, U.S.A.), which partially separates TA and TB. TA- and TB-rich fractions were detected by separation on analytical thin-layer chromatography (TLC) plates, 0.25 mm silica gel without gypsum (Sybron/Brinkmann, Westbury, NY, U.S.A.) developed in ethyl acetate–glacial acetic acid–water (6:3:1), and subsequently sprayed with ninhydrin[6]. Semi-preparative TLC with the same solvent system was used to purify TA and TB, which were located on the plates by spraying with water, extracted from the silica gel with butanol, exchanged back into water on the rotovap with separation confirmed by additional TLC and then used as HPLC standards. Equivalent prepa-

rations were characterized by NMR and HRMS as mixtures of the two isomers of TA and TB respectively[2]. Biological activity (gene-selective phytotoxin activity) of both TA and TB was confirmed by bioassay on excised tomato leaves as previously described[1]. Toxin concentration was quantified on the basis of μmoles/ml of amino group by reaction with trinitrobenzenesulfonic acid (TNBS), measurement of absorption at 340 nm, and comparison with a standard curve prepared with trinitrophenol (TNP)–aspartic acid[7].

Maleylation

Solutions containing 0.1–2 μmole/ml of toxin were treated with maleic anhydride by a method similar to that used for chemical modification of amino acids in proteins and peptides[3,4]. A 1 *M* solution of maleic anhydride in dioxane was prepared immediately before use, and 10-μl aliquots were added to a solution containing toxin in 0.1 *M* sodium carbonate, pH 9.2, at room temperature. The progress of the reaction was monitored by loss of ninhydrin positive reaction through spot testing on a silica gel TLC plate[6]. The pH was maintained above 9.0 by dropwise addition of 0.1 *M* sodium hydroxide, and was more than 90% complete in less than 5 min. Alternatively, maleic anhydride crystals were added slowly over a period of 5 min to a solution containing toxin buffered at pH 9.2 with 0.1 *M* sodium carbonate. At least a 10:1 molar excess of maleic anhydride to toxin was used in both cases to ensure complete derivatization. The maleylation reaction is specific for amino groups under the conditions used, and more extensive treatment with maleic anhydride is required for maleylation of hydroxyl groups[3,4]. Before HPLC analysis, the maleylation mixtures were adjusted to pH 6–7 by addition of hydrochloric acid or dilution with the mobile-phase buffer. HPLC analysis confirmed that derivatized TA, TB, or a mixture of the two were stable for at least a month at pH 6–7 when stored at 4°C.

HPLC analysis

HPLC analysis was performed at 24–26°C and the detector wavelength was 250 nm. The molar extinction coefficient for the maleylamino group has been reported to be 3360 at 250 nm[4]. Fractions for bioassay or rechromatography were collected directly from the detector flow-cell exit line in correspondence with the detector response. The methanol was removed by evaporation under a stream of gaseous nitrogen, and the maleyl groups removed by incubation of an aqueous solution of maleylated toxin at pH 3.0–3.5 for 20–24 h at 37°C. Demaleylation also was achieved by incubation of maleylated toxin for 20–24 h at 37°C in the methanol–phosphate buffer mixture in which the peaks eluted from the column. The half-life for maleylated amines has been reported[3] to be 11 h at 37°C at pH 3.5.

RESULTS AND DISCUSSION

The choice of derivatizing reagent to permit efficient detection of the toxins was limited because of the need to study the biological activity of the phytotoxins after HPLC separation. The following were considered essential requirements: mild reaction conditions during derivatization with respect to temperature and pH in order to prevent cleavage of the ester bond in the toxin molecules; relatively inexpensive mobile-phase solvents which could easily be removed or which would not interfere

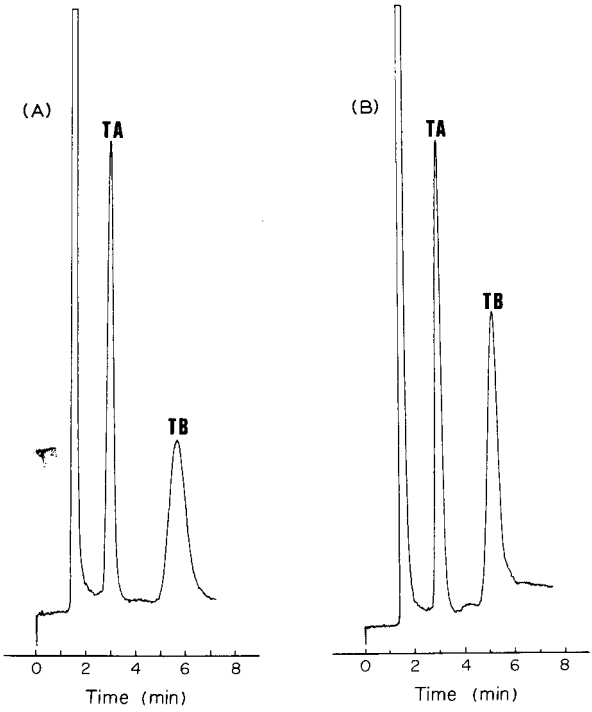

Fig. 1. HPLC separation of phytotoxic fractions TA and TB isolated from *A. alternata* f. sp. *lycopersici*. Conditions: mobile phase, (A) methanol–0.05 *M* potassium phosphate buffer (pH 3.5) (60:40) isocratic, (B) gradient (10 min) from 60:40 to 70:30 methanol–0.05 *M* potassium phosphate buffer pH 3.5; flow-rate 2 ml/min; UV detection at 250 nm, 0.05 a.u.f.s.; sample size 10 μl, 8 nmole of toxin injected.

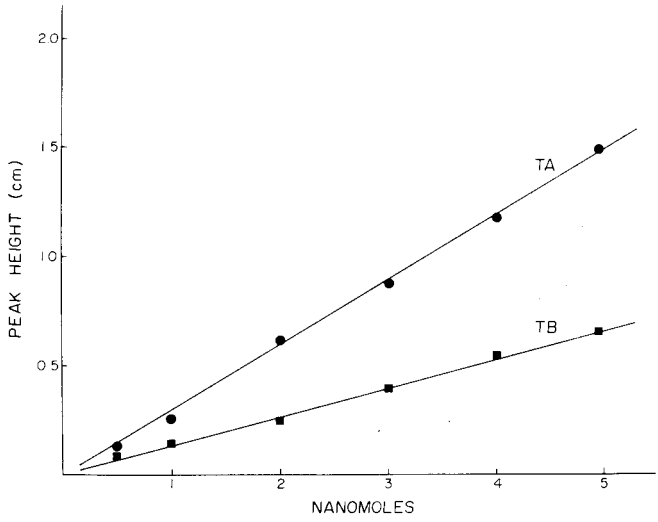

Fig. 2. Standard curves for amount (nmoles) of TA or TB maleylated and injected *vs.* peak height (measured peak height × attenuation factor). HPLC conditions were those described in Fig. 1B. The correlation coefficients for the curves are 0.999 (TA) and 0.998 (TB).

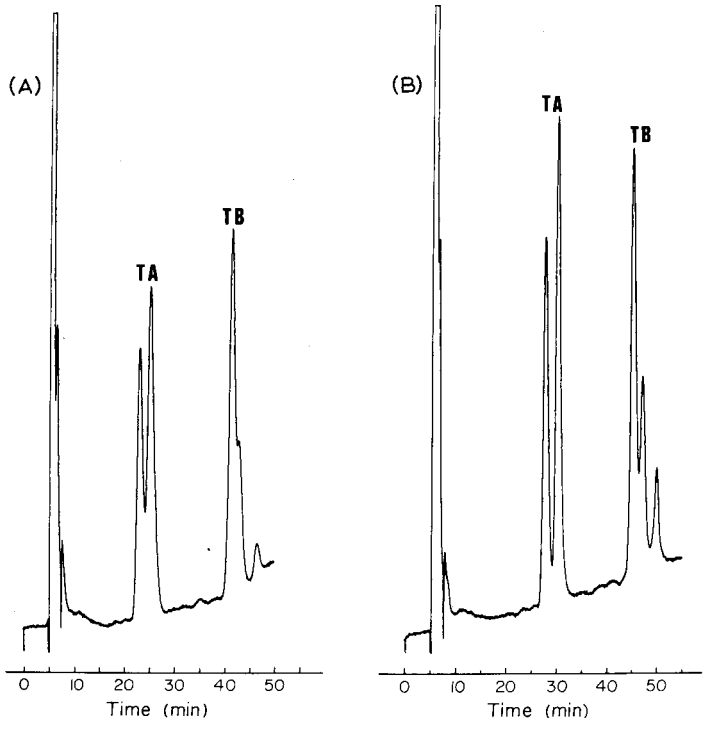

Fig. 3. HPLC of phytotoxins isolated from *A. alternata* f. sp. *lycopersici*, showing separation of TA and TB into their components. (A) Conditions: mobile phase, 60-min gradient from 50:50 to 70:30 methanol–potassium phosphate buffer (pH 3.5); flow-rate, 0.5 ml/min; UV detection at 250 nm, 0.05 a.u.f.s.; sample size 10 μl. Conditions for (B) were identical to those for (A), except that the potassium phosphate was buffered at pH 2.7. The sample was identical in both cases and contained 12 nmole of toxin. The small peak eluting after the TB peaks is a contaminant often found in the fungal extracts.

with biological assays; the ability to remove non-destructively the derivatizing group from the toxin molecules before biological assay. Maleic anhydride as a derivatizing reagent met all of these criteria since elevated temperatures were not required, the reaction took place in aqueous solution, and high pH was maintained for only a very short time. Excess maleic acid and dioxane in the reaction mixture eluted close to the solvent peak and did not interfere with chromatography of the phytotoxins. Toxin samples which were maleylated at pH 9.2 and then demaleylated at pH 3.0 as described above showed no detectable loss in biological activity.

Due to the presence of three carboxylic acid groups on the maleylated toxin molecules, ion suppression HPLC was achieved by including 0.05 *M* phosphate buffer with a pH of 2.7–3.5 in the mobile phase. The net charge on the maleylated toxin molecules under these conditions would be close to zero, for maximal selectivity in the reversed-phase mode during chromatography.

Baseline separation of maleylated TA and TB was achieved using an isocratic solvent system with 60% methanol–phosphate buffer (pH 3.5) as the mobile phase and a flow-rate of 2 ml/min (Fig. 1A). In contrast, Fig. 1B shows the effect on peak

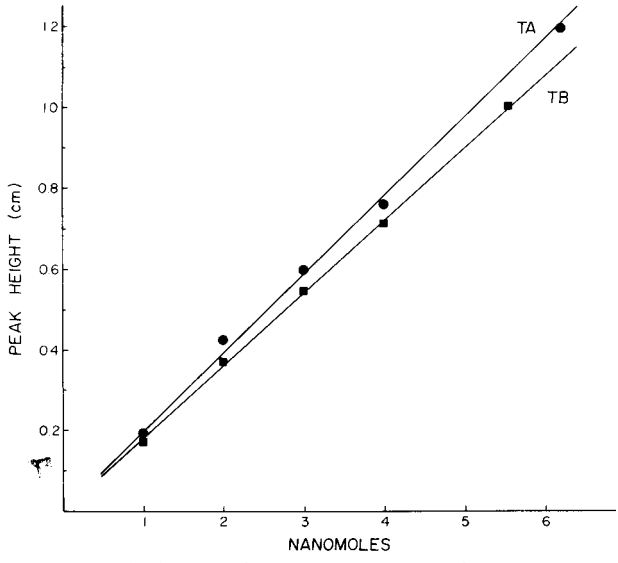

Fig. 4. Standard curves for amount (nmoles) of TA or TB maleylated and injected *vs.* peak height (measured peak height × attenuation factor). HPLC conditions were those described in Fig. 3A. The correlation coefficients for the curves are 0.999 (TA) and 0.999 (TB).

sharpening of a 60:40 to 70:30 (10 min) gradient of methanol–phosphate buffer (pH 3.5) with flow-rate of 2 ml/min.

Standard curves (Fig. 2) for quantitative analysis of the toxins were prepared by maleylation of known amounts of TA and TB, which were then analyzed by HPLC separately and together under the conditions described for Fig. 1B. Indistinguishable retention times and peak heights for TA and for TB were obtained when the toxins were maleylated and analyzed together or separately. These results show that both the recorder response and the maleylation reaction are linear within the limits of amounts of toxin used. The toxins were quantified on the basis of nanomoles of amino groups by reactions with TNBS as described in methods.

Maleylated TA and TB were further resolved into two components each with a 60-min gradient from 50:50 to 70:30 methanol–potassium phosphate buffer, (pH 3.5) and a flow-rate of 0.5 ml/min (Fig. 3A). Standard curves for this system at pH 3.5 were prepared as described above except that the sum of the peak heights of the two components of TA and TB, respectively, were plotted against the amount of TA or TB maleylated and injected (Fig. 4). The effect of the pH of the mobile-phase buffer on maleylated toxin separation was investigated by lowering the pH of the phosphate buffer to 2.7. A better resolution of the four toxin components with this solvent system was achieved at pH 2.7 (Fig. 3B). The ratio of components of TA and TB was constant at both pH 2.7 and 3.5 for a given sample, but varied in different fungal extracts. The peak areas for each of the toxin components were identical when the same sample was chromatographed at pH 2.7 or 3.5 (calculated as peak height times width at half height) although peak heights varied. Standard curves prepared with the pH 2.7 system were also linear.

The identities of the peaks corresponding to TA and TB for both gradient

systems were confirmed by spiking extracts with purified TA and TB as well as by collection of the HPLC eluate fractions corresponding to the TA and TB peaks from several HPLC runs, de-maleylation of the toxin as described above, concentration, and TLC analysis. In all cases the HPLC analysis indicated that the toxin peaks initially ascribed to TA and TB were duplicated with spiking and rechromatography by HPLC. The TLC R_F values of the demaleylated toxins agreed with those for authentic TA and TB (0.32 and 0.44, respectively), and no other ninhydrin positive compounds were detected. Following demaleylation, biological activity was detected in fractions corresponding to TA and TB. The relative standard deviations were typically less than 0.7% for retention times and 2–4% for peak heights.

The HPLC procedure described in this report has been useful both as an analytical method for detection and quantification of toxins in fungal extracts and infected plant tissue and as a semi-preparative method for TA and TB and their two components, since the use of a reversible derivatizing reagent allows us to obtain small amounts of the phytotoxins in a purified state for further chemical and biological studies.

ACKNOWLEDGEMENTS

The authors thank Ann Martensen for both technical assistance and preparation of the line drawings.

The research was supported in part by National Science Foundation Grant (PCM 80-1173) and USDA: Competitive Research Grant (59-2063-01406).

REFERENCES

1 D. G. Gilchrist and R. G. Grogan, *Phytopathology*, 66 (1976) 165.
2 A. T. Bottini, J. R. Bowen and D. G. Gilchrist, *Tetrahedron Lett.*, (1981) 2723.
3 P. J. G. Butler, J. I. Harris, B. S. Hartley and R. Leberman, *Biochem. J.*, 112 (1969) 679.
4 M. H. Freedman, A. L. Grossberg and D. Pressman, *Biochemistry*, 7 (1968) 1941.
5 K. Uyeda, *Biochemistry*, 8 (1969) 2366.
6 E. D. Moffat and R. I. Lytle, *Anal. Chem.*, 31 (1959) 929.
7 A. F. S. A. Habeeb, *Anal. Biochem.*, 14 (1966) 328.

Journal of Chromatography, 238 (1982) 175–182
Elsevier Scientific Publishing Company, Amsterdam — Printed in The Netherlands

CHROM. 14,547

NEW LIQUID CHROMATOGRAPHIC APPROACHES FOR FREE AMINO ACID ANALYSIS IN PLANTS AND INSECTS

MARIA DE LOS ANGELES BARCELÓN
University of Florida Agricultural Research and Education Center, 3205 S.W. College Avenue, Fort Lauderdale, FL 33314 (U.S.A.)
(Received November 13th, 1981)

SUMMARY

A simple and rapid method of analysis for free amino acids in plants and insects is presented. The amino acids were determined as their 5-dimethylaminonaphthalene-1-sulfonyl (Dns) derivatives. Two-dimensional thin-layer chromatography on polyamide sheets and high-performance liquid chromatography on μBondapak C_{18} columns were used to resolve the Dns derivatives. R_F values of 45 Dns derivatives are reported.

INTRODUCTION

Researchers in the field of agriculture believe that information on the free amino acid contents of plant tissues and exudates could be relevant to the expression of plant disease and the feeding preference of certain insects. Differences in the pattern of free amino acid contents of disease-resistant plants from those of non-resistant plants, if correlated to the specific needs of the insect vector or the microorganism involved, could be a way of determining what plants or plant varieties can be grown in infested areas. Amino acid patterns could also be a clue to the nutrients needed for the artificial rearing of insects and/or culture of microorganisms in question.

Since the pioneering works of Hartley and Gray[1–3] in the early sixties, a number of reports[4–8] have appeared in the literature using 5-dimethylaminonaphthalene-1-sulfonyl chloride (Dns-Cl) as a labelling reagent in protein chemistry. However to our knowledge, there are no published reports on the use of free amino acid Dns derivatization as a possible routine method of analysis for free amino acids in plants and plant disease carrier insects.

We report here a simple method of extraction, separation, derivatization and resolution of free amino acids applicable to plants as well as insect specimens.

EXPERIMENTAL

Extraction and separation of the free amino acids

Leaves. After weighing, 10 g of leaves were cut into small pieces and placed in a

0021-9673/82/0000–0000/$02.75

blender (spiking with standard amino acids to determine recovery was done at this point). The leaves were blended for 2 min with 50 ml of a solution of methanol–water–12 *M* hydrochloric acid (90:5:5). The supernatant liquid was vacuum filtered. This procedure was repeated using the remaining leaf pulp. The combined total filtrate was *ca.* 90 ml.

The resulting leaf extract was divided into two aliquots, for two separate analyses. In each, *ca.* 40 ml of the leaf extract were diluted with 15 ml of deionized water and extracted with 15 ml of chloroform. The chloroform extract removes most of the non-polar organic components of the leaf extract, leaving the free amino acids in the acidic aqueous layer. The aqueous layer was passed through an ion-exchange column (7 × 1 cm; Amberlite IR-120 H, medium porosity). The column was washed with deionized water until neutral to pH paper. The amino acids were eluted using 10 ml of 4 *M* NH_4OH followed by 5 ml of deionized water. The eluate was evaporated to dryness in a rotary evaporator. The resulting residue was then dansylated.

Phloem sap. Phloem exudate (15–20 ml) was mixed with an equal volume of the above methanol–water–hydrochloric acid mixture and treated in the same way as the leaf extract.

Insects. Approximately 0.1 g of the insect in question was carefully ground to a thick paste using a mini agate mortar and pestle. The resulting paste was dissolved in *ca.* 1.5 ml of methanol–water–hydrocholoric acid (90:5:5). The mixture was filtered through a Pasteur pipet plugged with glass wool. The filtered solution was diluted with an equal volume of deionized water and then extracted with chloroform. The rest of the procedure is the same as that followed for the leaf extract.

Preparation of the Dns derivatives

Standard amino acids and/or amines. Some 10–20 mg of a standard amino acid and/or amine (Sigma, St. Louis, MO, U.S.A.) were dissolved in 1.5 ml of $NaHCO_3$ buffer (pH 10.5, 0.1 *M*). Next, 0.5 ml of Dns-Cl (Sigma) solution (15 mg/ml acetone) was added, mixed thoroughly, incubated at 40°C for 2 h, and evaporated to dryness under reduced pressure. The residue was taken up in methanol (HPLC grade; J. T. Baker, Phillipsburgh, NJ, U.S.A.), and filtered through a Pasteur pipet plugged with glass wool. The resulting clear solution was used directly for spotting with no further purification.

Amino acids from plant and insect extracts. The procedure followed for the Dns derivatization of the free amino acids in the plant and insect extracts was basically the same as above, except for an occasional need for a clean-up step after Dns derivatization. For the clean-up step, the acetone in the reaction mixture was removed by passing nitrogen gas. Excess unhydrolyzed Dns-Cl was then removed by extracting the reaction mixture two to three times with toluene. Alternatively, the Dns-amino acids were extracted into ethyl acetate leaving the bulk of Dns-OH and Dns-NH_2 in the aqueous layer.

Chromatographic separation of Dns derivatives

High-performance liquid chromatography (HPLC). HPLC was done using Waters Associates solvent delivery system Models 6000-A and M-45; solvent programmer Model 660; injector Model U6K; and μBondapak C_{18} column. The detector was a Tracor 970A variable wavelength, and the recorder was a Houston Instrument Omni Scribe recorder.

TABLE I

THE 45 AMINO ACIDS AND RELATED COMPOUNDS STUDIED

		Abbreviation			*Abbreviation*
1	Alanine	Ala	24	Lysine	Lys
2	Asparagine	AsN	25	ε-lysine	ε-Lys
3	Aspartic acid	Asp	26	Methionine	Met
4	Arginine	Arg	27	Methionine sulfone*	Mes
5	Aziridine	Azi	28	Methionine sulfoxide*	Meo
6	α-butyric acid	AABA	29	Norleucine	Nle
7	γ-butyric acid	GABA	30	Norvaline	Nval
8	Cadaverine	Cad	31	Ornithine*	Orth
9	Carboxymethyl cysteine*	Cmc	32	Phenylalanine	Phe
10	Cysteic acid	Cya	33	Pimelic acid*	Pim
11	Cystine	Cys	34	Proline	Pro
12	Dansylic acid	Dns-OH	35	Sarcosine	Sar
13	Dansylsulfonamide	Dns-NH_2	36	Serine	Ser
14	Diaminobutyric acid*	di-ABA	37	Speridine*	Spd
15	Diaminopropionic acid	di-APA	38	Spermine*	Spm
16	Glutamic acid	Glu	39	Taurine*	Tau
17	Glutamine	GlN	40	Threonine	Thr
18	Glycine	Gly	41	Tryptamine	TrN
19	Histidine*	His	42	Tryptophan	Trp
20	Hydrazine	Hydz	43	Tyrosine	Tyr
21	Hydroxyproline	HO-Pro	44	bis-Tyrosine	bis-Tyr
22	Isoleucine	Ile	45	Valine	Val
23	Leucine	Leu			

* Dns derivative prepared as outlined in the Experimental section.

Thin-layer chromatography (TLC). Spotting was done on 5 × 5 cm sheets (Schleicher & Schüll, Keene, NH, U.S.A.) using a 10-μl Hamilton syringe. Development of the plates was carried out in a filter-paper-lined 250-ml beaker with two pieces of glass rod cut to fit diagonally at the bottom of the beaker to hold the plates upright and covered by an inverted 600-ml beaker. Solvent I (1.5% formic acid) and solvent II (benzene–acetic acid, 4.5:1) were run perpendicular to each other. The chromatograms were viewed under a UV chromatogram viewer equipped with both long-wave (366 nm) and short-wave (254 nm) UV light source.

DISCUSSION

To investigate the feasibility of using Dns derivatization coupled with HPLC[9–13] and/or two-dimensional TLC on polyamide sheets[14,15] as a routine method of analysis for free amino acids in plants and insects, we experimented first on the standard Dns derivatives of the twenty common amino acids. After successfully resolving the Dns derivatives of the twenty common amino acids, we experimented on the Dns derivatives of 25 other very closely related compounds to determine if they would interfere in the resolution of the twenty common amino acids of interest. Of the 45 Dns derivatives (Table I), 34 were obtained commercially and II were prepared in our laboratory as outlined in the Experimental section.

Our first attempt to resolve the twenty amino acids was made using HPLC with

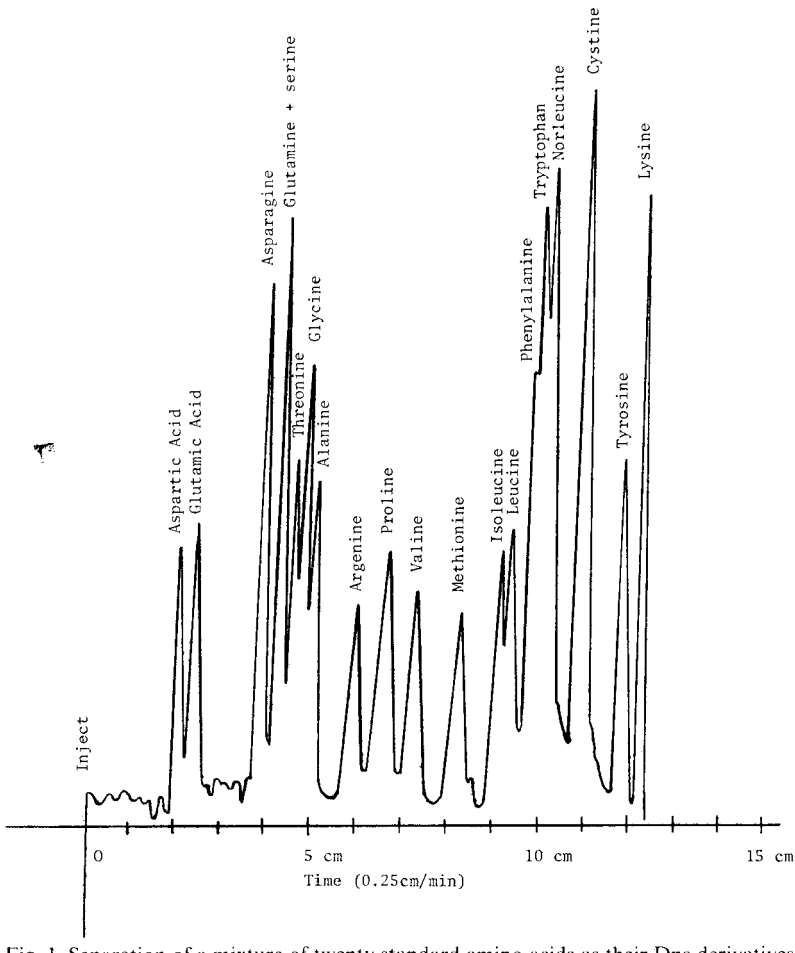

Fig. 1. Separation of a mixture of twenty standard amino acids as their Dns derivatives. Packing, μBondapak C_{18}; column, 30 cm × 4 mm; solvent, (A) 0.01 *M* K_2HPO_4 pH 6.7, (B) acetonitrile, isocratic for 10 min at 10% B, then curve No. 8: 15% B → 45% B in 35 min; flow-rate, 1.4 ml/min; detector, UV at 254 nm; chart speed, 0.25 cm/min.

a gradient solvent system (acetonitrile–phosphate buffer) on a μBondapak C_{18} column. The parameters varied in the attempt to resolve the common amino acids were: the ion concentration and pH of the phosphate buffer; the solvent strength or amount of acetonitrile; the time; and the flow-rate. Our best results gave eighteen peaks (Fig. 1) for a mixture of twenty Dns amino acids. Each run required *ca.* 1 h, not including re-equilibration time.

We then tried the two-dimensional TLC on a 5 × 5 cm polyamide sheet. As a first step we tried resolving a mixture containing the twenty common amino acids using different solvent systems. We tested solvent systems suggested by other workers[16] as well as solvent systems that we thought could be of some use. The solvent system suggested by Lee and Safille[15] gave us the best results. This method completely resolved the twenty common amino acids (Fig. 2a). Each run from the initial spotting to the final air-drying takes only 15–20 min.

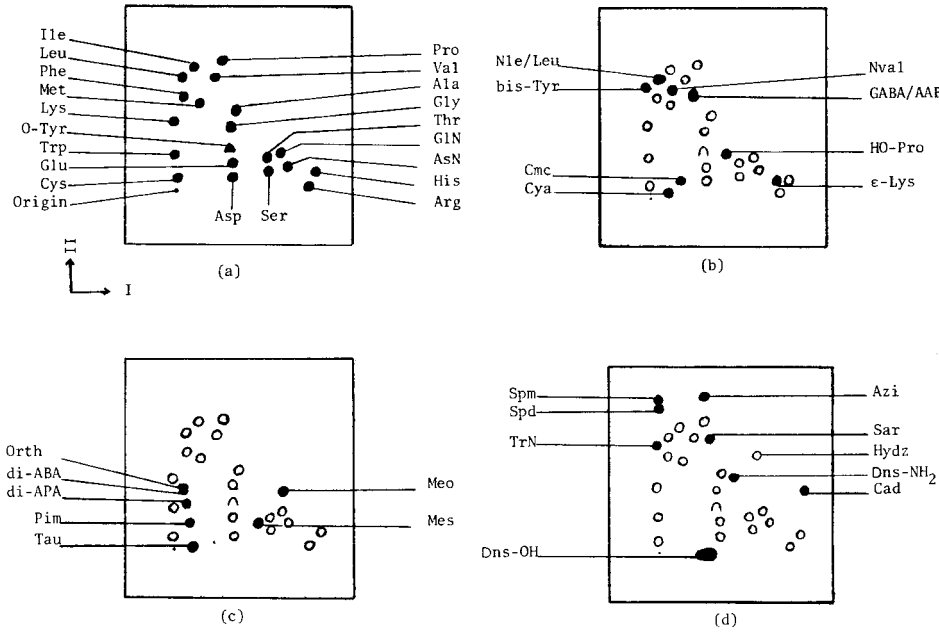

Fig. 2. (a) Chromatogram of a mixture of the twenty common amino acids. (b)–(d) Chromatograms showing the position of 25 other compounds [●] relative to those of the twenty common amino acids [○].

RESULTS AND EVALUATION

HPLC

Our attempts to use HPLC to separate the Dns-amino acids did not result in the complete resolution of the twenty amino acids in a single run, but there was a reasonably good resolution (Fig. 1). The fact that the pairs glutamine/serine and phenylalanine/tryptophan completely overlapped did not pose serious problems in the identification of the amino acids. It was possible to zero in on these pairs and resolve them by altering the conditions of the chromatogram after the other amino acids had been identified. However, after evaluating our results, we thought that for a routine analysis, merely for identification and not necessarily for a detailed or quantifying analysis, the use of HPLC may not be warranted. Another unfavorable factor was the time element, since each HPLC run required approximately three times longer than the two-dimensional TLC, which completely resolves the twenty most common amino acids.

TLC

The use of polyamide TLC in protein chemistry has been popular for some time now. The literature reports the sensitivity of detection of Dns derivatives to be in the nanomole range[5,17] and in some cases in the picomole range[18]. Therefore we started experimenting on the Dns derivatives of standard amino acids. From our results we found that the modified solvent system suggested by Lee and Safille[15] completely resolved the Dns derivatives of the twenty common amino acids. Fig. 2a is a tracing of the chromatogram of a mixture containing all twenty common amino

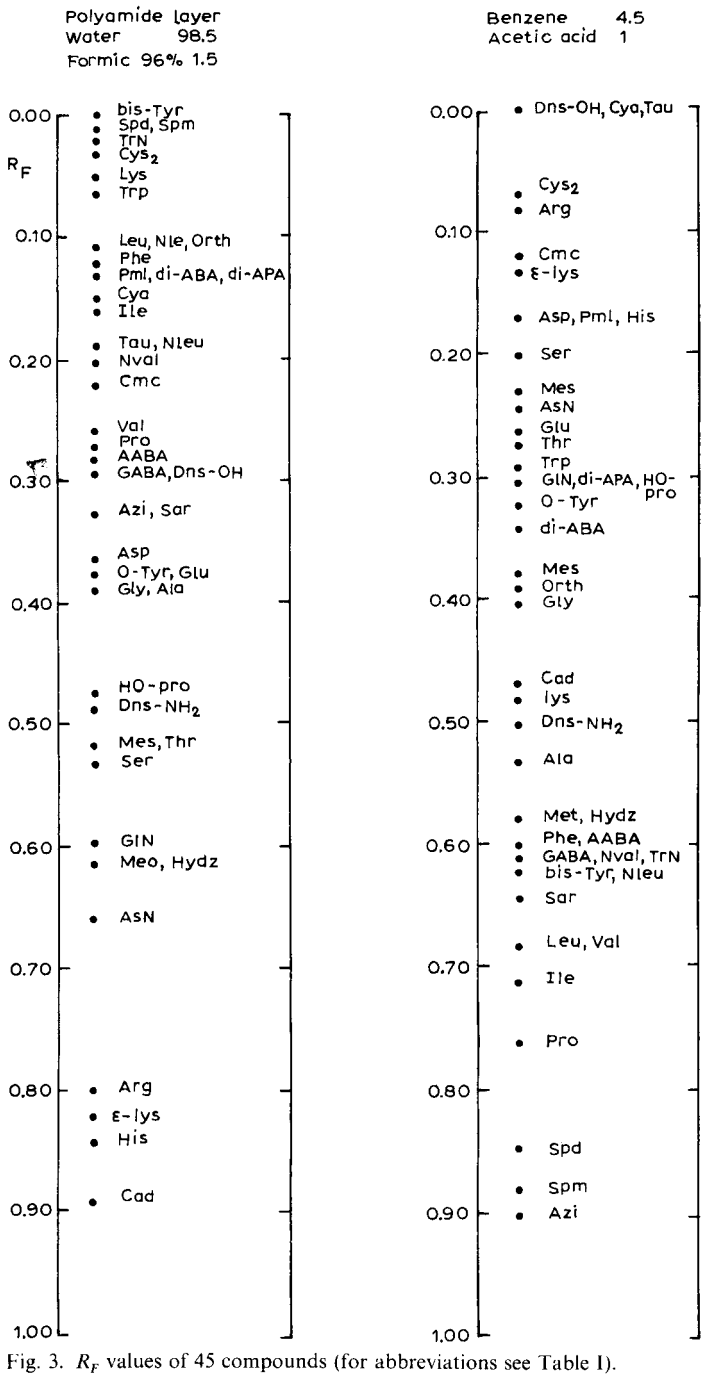

Fig. 3. R_F values of 45 compounds (for abbreviations see Table I).

acids, after it had been developed using solvent systems I and II (see Experimental section) at right angles to each other.

While our primary interest was to separate and identify the twenty common amino acids, it was necessary to determine the relative positions or R_F values of

compounds that are often associated with the amino acids found in living organisms, such as taurine, ornithine, tryptamine, etc. Figs. 2b–2d are plates showing the positions of 25 such compounds relative to those of the twenty common amino acids. As can be observed, with the exception of the pair norleucine/leucine, none of the 25 other compounds studied overlaps with any of the common amino acids. Mono-Dns-lysine, if present in large amounts, may fuse with arginine and histidine. The presence of large amounts of mono-Dns-lysine, however, is not likely under the conditions we use in the preparation of the Dns derivatives. Under saturating concentrations of Dns-Cl, most of the lysine will be present in the di-Dns form, which has an R_F value quite distinct from any of the other compounds.

In Fig. 3, we give the R_F values of all 45 compounds in solvent systems I and II separately.

Application

Once we had determined the R_F values of the Dns derivatives of appropriate compounds, we turned our attention to application of the method in the identification of free amino acids in plants and insect specimens. We devised a general scheme (see Experimental section) for the extraction, separation, and derivatization of the free amino acids found in the above specimens.

TABLE II

AMINO ACID ANALYSIS

− = not observed; + = observed; ++ = bright; ± = faint.

Amino acids	*Sample specimens*		
	Phloem sap Veitchia merrilli (palm)	*Leaves Syzigium jambos (rose-apple)*	*Insect Myzus persicae (green pea aphids)*
Alanine	++	++	++
Asparagine	++	+	+
Aspartic acid	+	+	+
Arginine	+	±	−
α-butyric acid/γ-butyric acid	++	+	+
Carboxymethyl cysteine	+	−	−
Cysteic acid	−	+	+
Cystine	−	−	−
Glutamic acid	++	+	+
Glutamine	+	+	+
Glycine	++	+	+
Histidine	−	−	+
Hydroxyproline	+	−	−
Isoleucine	+	+	+
Leucine/Norleucine	+	+	++
Lysine	+	+	++
Methione	+	−	−
Phenylalanine	+	+	+
Proline	++	++	++
Serine	++	+	+
Threonine	+	+	+
Tryptophan	+	++	+
O-Tyrosine	−	−	+
bis-Tyrosine	±	+	++
Valine	−	++	+

To determine if the amino acids would survive the proposed procedure of extraction, separation and derivatization, we chose eight different amino acid standards at random (alanine, isoleucine, lysine, methionine, proline, threonine, tyrosine and valine) and used them to spike eight different leaf samples. Approximately 0.1 g of standard amino acid was added to a 10-g sample of leaves. The chromatograms of these test runs gave us bright spots for the free amino acids found in leaves and very intense spots for the added standard amino acids. The intensities of the added standard amino acids were such that the readings of adjacent spots were rendered difficult. This indicates that 0.1 g amino acid in 10 g of leaves was a concentration that was out of proportion relative to the concentration of free amino acids found in 10 g of leaves. The spiking was done to test the effectiveness of the work-up procedure. The amount used for spiking was arbitrary and was chosen for convenience. Evidently the sensitivity of the method is good. At this stage, no effort had been made to quantify the sensitivity limits of the method. Our present interest is geared more to identification and only to a relative or rough quantification.

In Table II we report the results of sample analysis obtained following the scheme outlined in the Experimental section; an analysis of phloem sap, leaves, and insects. Besides the twenty common amino acids, we have also included in Table II a number of other amino acids that were observed in the specimens cited. It is interesting to note that while cystine was not observed in any of the three sample analyses, cysteic acid was observed in both the rose-apple leaves and the green pea aphids, and carboxymethylcysteic acid in the palm phloem sap. Tyrosine, like lysine, seemed to be present mostly in the di-Dns form, except in the green pea aphids where tyrosine was observed in both forms, with the di-Dns-tyrosine in relatively large concentration.

Identification of the amino acids was done by spiking with marker mixtures of standard Dns-amino acids, as well as by comparison with identification maps.

We feel that this method of analysis for free amino acids, using the scheme for extraction, separation, derivatization and resolution in two-dimensional TLC as described in this report, can be of value because the method is simple, does not require sophisticated instrumentation, is reliable and is easily adaptable to a variety of specimens.

REFERENCES

1 W. R. Gray and B. S. Hartley, *Biochem. J.*, 89 (1963) 379.
2 W. R. Gray and B. S. Hartley, *Biochem. J.*, 89 (1963) 59.
3 W. R. Gray, *Ph. D. Thesis*, University of Cambridge, 1964.
4 W. R. Gray, *Methods Enzymol.*, 25 (1972) 121.
5 B. S. Hartley, Biochem. J., 119 (1970) 805.
6 J. Rosmus and Z. Deyl, *Chromatogr. Rev.*, 13 (1971) 163.
7 C. Gros and B. Labouesse, *Eur. J. Biochem.*, 7 (1969) 463.
8 F. Orrego and M. C. Doria de Lorenzo, *Neurochem. Res.*, 5 (1980) 523.
9 D. C. Olson, G. J. Schmidt and W. Slavin, *Chromatogr. Newslett.*, 7 (1979) 22.
10 J. M. Wilkinson, *J. Chromatogr. Sci.*, 16 (1978) 547.
11 G. Powis and M. M. Ames, *J. Chromatogr.*, 170 (1979) 195.
12 L. S. O'Keefe and J. J. Warthesen, *J. Food Sci.*, 43 (1978) 1297.
13 E. Bayer, E. Grom, B. Kaltenegger and R. Uhmann, *Anal. Chem.*, 48 (1976) 1106.
14 K. R. Woods and K.-T. Wang, *Biochim. Biophys. Acta*, 133 (1967) 369.
15 M.-L. Lee and A. Safille, *J. Chromatogr.*, 116 (1976) 462.
16 A. Niederwieser, *Methods Enzymol.*, 25 (1972) 60.
17 A. M. Weiner, T. Platt and K. Weber, *J. Biol. Chem.*, 247 (1972) 3242.
18 K.-S. Hui, M. Salschutz, B. Davis and A. Lajtha, *J. Chromatogr.*, 192 (1980) 341.

Journal of Chromatography, 238 (1982) 183–192
Elsevier Scientific Publishing Company, Amsterdam — Printed in The Netherlands

CHROM. 14,591

MEDIUM-PRESSURE LIQUID CHROMATOGRAPHY OF LEOZYM, A PECTIC ENZYME PREPARATION, ON ION-EXCHANGE DERIVATIVES OF SPHERON

L'. REXOVÁ-BENKOVÁ and J. OMELKOVÁ
Institute of Chemistry, Slovak Academy of Sciences, 809 33 Bratislava (Czechoslovakia)
and
O. MIKEŠ* and J. SEDLÁČKOVÁ
Institute of Organic Chemistry and Biochemistry, Czechoslovak Academy of Sciences, 166 10 Prague 6 (Czechoslovakia)
(Received November 30th, 1981)

SUMMARY

Leozym, a commercial pectic enzyme preparation, was subjected to medium-pressure liquid chromatography on weakly, medium, and strongly acidic cation exchangers and on weakly and strongly basic anion exchangers, and to hydrophobic chromatography on the ionogenically unsubstituted glycomethacrylate macroreticular gel of the Spheron type. The course of the gradient chromatography was examined by continuous measurement of the absorbance of the effluent at 285 and 254 nm, by pH and conductivity measurements on the fractions collected and by specific measurements of selected enzyme activities. Fractions containing endo-D-galacturonanase, pectin-lyase and pectin-esterase activity were successfully resolved. The presence of multiple forms of endo-D-galacturonanase and pectin-lyase in the preparation examined was shown. The technological importance of these findings is briefly discussed.

INTRODUCTION

Commercial pectic enzymes used in the canning industry contain components showing the activity of endo-D-galacturonanase*, exo-D-galacturonanase, pectin-lyase and pectin-esterase. During the past few years, in order to increase the efficiency of production and quality, there has been a trend towards the use in certain industrial processes of exclusively enzyme preparations that contain certain components of the pectic complex only; such preparations are composed of, *e.g.*, pectin depolymerases

* Nomenclature of enzymes and abbreviations used: endo-D-galacturonanase and exo-D-galacturonanase, poly(1–4)-α-D-galactosiduronate glycanohydrolase, E.C. 3.2.1.15 and E.C. 3.2.1.67; pectin-lyase, poly(methyl-D-galactoside uronate)lyase, E.C. 4.2.2.10; pectin-esterase, pectin pectyl-hydrolase, E.C. 3.1.1.11; the earlier trivial names of the first two enzymes were endopolygalacturonase and exopolygalacturonase; HPLC, high-pressure liquid chromatography; MPLC, medium-pressure liquid chromatography.

0021-9673/82/0000–0000/$02.75

only, or show an increased content of a certain pectic enzyme, such as endo-D-galacturonanase or pectin-lyase. The preparation and analysis of these commercial products require rapid and efficient procedures that permit one or several enzymes to be separated from the original mixture. Of the laboratory procedures used so far for the separation or purification of microbial pectic enzymes, only bioaffinity chromatography, which permits the selective resolution of endo-D-galacturonanase[1] and pectin esterase[2], appears to be possibly useful.

During the past few years high- and medium-pressure liquid chromatography have been used for the separation of biopolymers[3–5]. For such separations of enzymes[6] and certain other proteins[7] macroreticular ion exchangers with a matrix of a hydrophilic glycolmethacrylate gel (Spheron) have been employed. The possibilities for their application in the analytical separation of pectic enzymes from two commercial preparations. Pectinex Ultra (AG Ferment, Basle, Switzerland) and Rohament P (Röhm and Haas, Darmstadt, G.F.R.), by medium-pressure liquid chromatography have been discussed earlier[8].

This study was designed to examine the applicability of the procedures developed for the separation of pectic enzymes present in Leozym (Slovlik, Leopoldov, Czechoslovakia); this preparation is obtained in a pilot plant from fermented media of *Aspergillus niger*, which is a waste product from citric acid manufacture. Leozym contains endo-D-galacturonanase as the main component, together with pectin-lyase, pectin-esterase and trace amounts of exo-D-galacturonanase. The preparation is used predominantly for the processing of fruits and vegetables. The analytical procedures developed should provide information on the prospective large-scale separation on Spheron derivatives.

EXPERIMENTAL

Materials

Enzyme. Leozym contained 19.7% of protein, pectic enzymes endo-D-galacturonanase (0.188 katal/kg), exo-D-galacturonanase ($5 \cdot 10^{-7}$ katal/kg), pectin-esterase ($1.5 \cdot 10^{-7}$ katal/kg)[9] and pectin-lyase, the activity of which cannot be determined in the crude preparation because of the large amounts of coloured contaminants (the activity of the enzymes is expresed in moles of reducing groups or carboxyl groups liberated in 1 sec).

Ion exchangers. Spheron C-1000 (1.85 mequiv./g), Spheron Phosphate-1000 (3.1 mequiv./g), Spheron S-1000 (1.72 mequiv./g), Spheron DEAE-1000 (1.5 mequiv./g), Spheron TEAE-1000 (1.4 mequiv./g) and unsubstituted Spheron 1000 (0.044 mequiv./g) were products of Lachema (Brno, Czechoslovakia). The particle size of all products was 25–40 μm, except for the phospho derivative (40–60 μm).

Substrates. Citrus pectin, employed for the determination of the activity of pectin esterase, degree of esterification (DE) 65.1%, was a preparation obtained from commercial Genu Pectin. Type B (Københavns Pektinfabrik, Copenhagen, Denmark) by washing with 60% ethanol containing 5% hydrochloric acid and then with 60 and 96% ethanol. Pectic acid used for the determination of the activity of endo-D-galacturonanase was prepared from purified citrus pectin by repeated alkaline deesterification in 0.1 *M* sodium hydroxide solution, followed by precipitation at pH 2.5. Highly esterified pectin (DE 93.8%) was prepared by esterification of pectic acid in a 1 *M* solution of sulphuric acid in methanol[10].

Methods

Chromatographic methods. The general principles of the work with Spheron ion exchangers and the medium-pressure liquid chromatography apparatus have been described previously[3,6,11]. The technique of rapid chromatographic analysis of pectic enzymes has been described elsewhere[8].

Assays. The activity of endo-D-galacturonanase was examined in terms of increase in reducing groups by the method of Somogyi[12] after a 10-min incubation of a reaction mixture composed of 0.8 ml of a 0.5 % solution of pectic acid in 0.1 *M* acetate buffer (pH 4.2) and 0.2 ml of the effluent fraction. The activity of pectin-esterase was determined by titration with 0.1 *M* sodium hydroxide solution of carboxyl groups liberated during a 60-min incubation of a mixture of 5 ml of a 0.5 % solution of pectin in 0.1 *M* acetate buffer (pH 4.4) and 1 ml of the effluent from the column. The activity of pectin-lyase was determined in terms of increase in absorbance at 235 nm[13] of a reaction mixture containing 2.5 ml of a 0.5 % solution of highly esterified pectin in 0.1 *M* acetate buffer (pH 5.6) and 0.5 ml of the effluent fraction.

RESULTS

The possibilities of using MPLC on Spheron and its ion-exchange derivatives for the separation of pectic enzymes in Leozym were examined under experimental conditions similar to those described in the preceding study[8] dealing with the separation of enzymes from Pectinex Ultra and Rohament P. Because of the enzyme composition of the preparation examined and the character of the microbial producer (*Aspergillus niger*), we expected that the behaviour of the enzymes would be similar to that of enzymes in Pectinex Ultra. The preparation was chromatographed on Spheron 1000 and on its ion-exchange derivatives: weakly, medium and strongly acidic cation exchangers and on weakly and strongly basic anion exchangers.

Pectin-esterase S was well separated on the weakly acidic carboxyl cation exchanger Spheron C as the middle peak (Fig. 1) from a large amount of endo-D-galacturonanase N. The tailing, small peak of pectin-lyase L indicates considerable sorption of this enzyme by the resin. Enzymes S and N were eluted from the column in the same order and by the same buffer concentrations as with Pectinex Ultra (Fig. 2 in ref. 8). Endo-D-galacturonanase N, however, formed in Leozyme only one fraction, which was identical with the major fraction of Pectinex Ultra. The position of the peak of pectin-lyase, however, was entirely different. It emerged as the first peak when Leozym was chromatographed whereas with Pectinex Ultra it was contained in the last peak.

Chromatography on the medium acidic cation exchanger Spheron-phosphate (Fig. 2) resulted in the separation of pectin-esterase S, present in the most retarded peak, from the mixed peak of pectin-lyase L and the main fraction of endo-D-galacturonanase N. These two enzymes were not separated, however, even when Pectinex Ultra was chromatographed (Fig. 3 in ref. 8; see also the remark on p. 102 of ref. 8).

A partial separation of all three pectic activities was achieved on the strongly acidic sulpho acid cation exchanger Spheron-S (Fig. 3). The course of the separation and the order of the enzymes eluted, *i.e.*, pectin-esterase S, pectin-lyase L, endo-D-galacturonanase N, shows that this ion exchanger in combination with a milder elution gradient could be used for the isolation of specific preparations from Leozym.

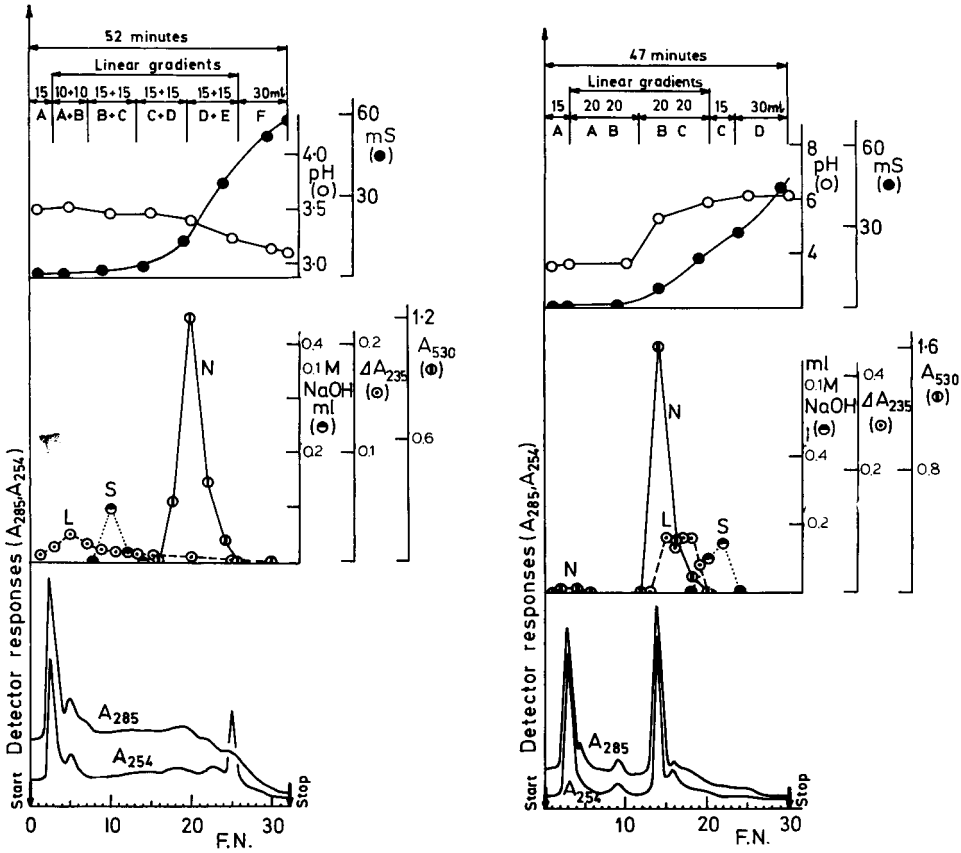

Fig. 1. Chromatography of Leozym (25 mg) on Spheron C-1000 (20 × 0.8 cm; particle size 25–40 μm). Enzyme activities: L, pectin-lyase; N, endo-D-galacturonanase; S, pectin-esterase. The electrical conductivity is given in millisiemens. The buffers were prepared from sodium hydroxide of the given final concentration whose pH was adjusted to 3.5 with formic acid: A, 0.05 *M*; B, 0.1 *M*; C, 0.2 *M*; D, buffer C, 1 *M* in sodium chloride; E, unbuffered 2 *M* sodium chloride solution was used for preliminary regeneration of the column and for washing out any protein remaining in the column. Flow-rate, 3 ml/min; temperature, 25°C, counterpressure, 4 atm. Fractions (4.5 ml) collected at 90-sec intervals. F.N. = Fraction number.

Fig. 2. Chromatography of Leozym (25 mg) on Spheron-phosphate 1000 (40–60 μm). Counterpressure, 6 atm; other details as in Fig. 1. Buffers: A, 0.005 *M* ammonia solution + formic acid (pH 3.5); B, 0.3 *M* ammonia solution + acetic acid (pH 6); C, 1 *M* ammonia solution + acetic acid (pH 8), 0.5 *M* in sodium chloride; D, 2 *M* sodium chloride solution.

A better separation was obtained with Pectinex Ultra (Fig. 4 in ref. 8). The pectin-lyase L and endo-galacturonanase N present in both Leozym and Pectinex Ultra were resolved into multiple forms, but only one member of the pair was identical in both preparations (peak L in fraction 12 and the highest peak N in both figures). In contrast, the second peak L emerged last (Fig. 3) rather than first as in the earlier study (Fig. 4 in ref. 8). The positions of the peaks of pectin-esterase S in the elution patterns obtained with the two preparations were different.

The above similarities in the behaviour of certain enzymes in Pectinex Ultra and Leozym, especially during their chromatography on the weakly acidic cation

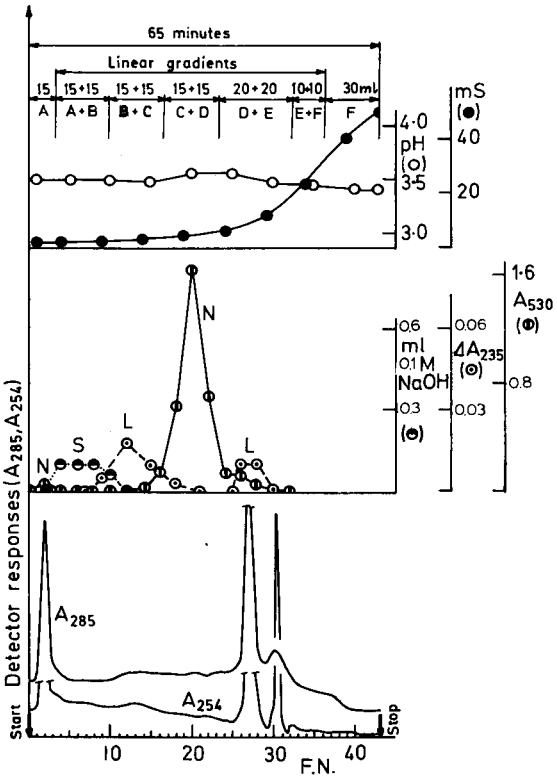

Fig. 3. Chromatography of Leozym (25 mg) on Spheron S-1000. Counterpressure, 8 atm; other details and buffers A, B and C as in Fig. 1. The remaining buffers were prepared from sodium hydroxide of the given final concentration, whose pH was adjusted to 3.5 with formic acid; D, 0.3 *M*; E, 0.5 *M*, 1 *M* in sodium chloride; F, unbuffered 2 *M* sodium chloride solution.

exchanger (Fig. 1), were not observed when these preparations were chromatographed on anion exchangers. The chromatography of Leozym on the weakly basic Spheron-DEAE (Fig. 4) resulted in a poorer separation of enzymes than that obtained with Pectinex Ultra (Fig. 7 in ref. 8) where all the enzymes present, including the two forms of endo-D-galacturonanase, were well separated in Tris–hydrochloric acid buffer at pH 7. The position of the peak of Leozym endo-D-galacturonanase N in Fig. 4 does not correspond to the position of any of the multiple forms N observed in Pectinex Ultra (Fig. 7 in ref. 8). A decrease in the pH of the elution buffer to pH 5, which is convenient with respect to the stability of microbial pectic enzymes, led to unfavourable retardation of pectin-esterase and thus to a shift to a peak containing the remaining two enzymes. In this experiment, not illustrated here, the minor form of endo-D-galacturonanase N emerged only at the beginning of the chromatogram; this form was obviously overlapped by the major form and emerged in one peak (N) under the conditions used to obtain Fig. 4.

A similar course of chromatography can be seen in Fig. 5, which illustrates experiments with the strongly basic (quaternized) anion exchanger Spheron-TEAE. The pattern of three separated enzymes, S, L and N, resembles that obtained with the

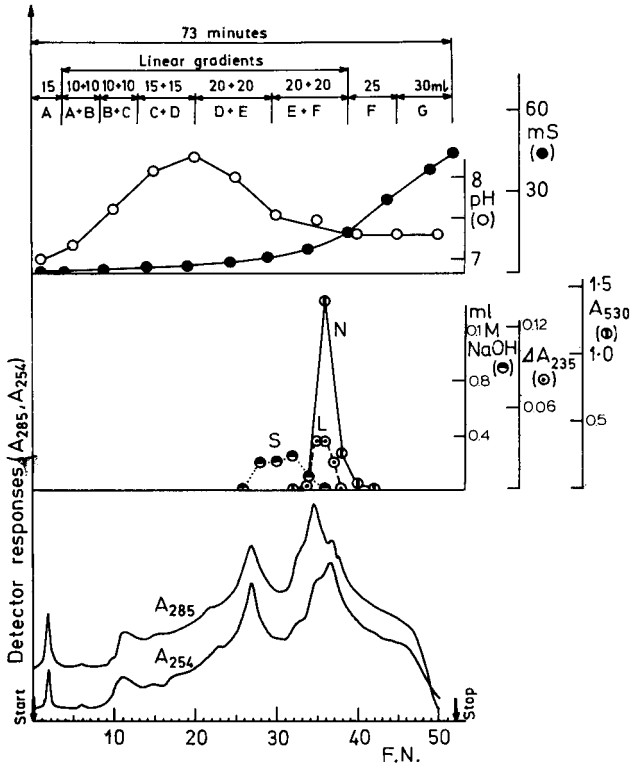

Fig. 4. Chromatography of Leozym (25 mg) on Spheron DEAE-1000. Counterpressure, 6–8 atm; other details as in Fig. 1. The buffers were prepared from hydrochloric acid of the given final concentration whose pH was adjusted to 7 with Tris: A, 0.005 *M*; B, 0.05 *M*; C, 0.1 *M*; D, 0.2 *M*; E, 0.4 *M*; F, buffer E, 1 *M* in sodium chloride; G, unbuffered 2 *M* sodium chloride solution.

weakly basic anion exchanger (Fig. 4). Another multiple form of endo-D-galacturonanase N was well separated. We cannot explain why this form was not separated also on the weakly basic anion exchanger (a separation was observed when Pectinex Ultra was chromatographed on Spheron-DEAE; *cf.*, Fig. 7 in ref. 8).

We considered it of interest to examine the behaviour of pectic enzymes on unmodified Spheron 1000, *i.e.*, on the matrix itself, as a comparison of this behaviour with the experiments with ion exchangers should provide information on the effects of the individual ionogenic groups. In earlier experiments with Pectinex Ultra and Rohament P (Figs. 1 and 9 in ref. 8) conditions similar to those employed for ion-exchange chromatography were used, the elution being started with solutions of low ionic strength. Under these conditions, however, it is difficult to distinguish the participation of ion exchange due to trace amounts of carboxyls (originating in the monomer used as the starting material in the production of Spheron and responsible for a cation-exchange capacity of 0.04 mequiv./g of Spheron 1000) from the participation of hydrophobic interactions (with aliphatic hydrocarbon chains of the matrix; *cf.*, Fig. 1 in ref. 7). Therefore, Leozym was chromatographed under conditions of hydrophobic chromatography: a support equilibrated in a buffer of high ionic strength was used and the latter was decreased in a gradient manner. Under these

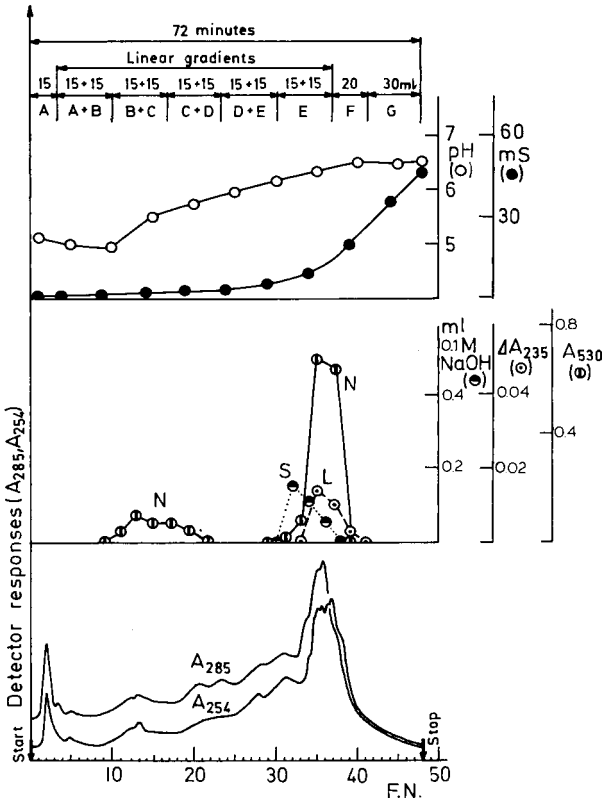

Fig. 5. Chromatography of Leozym (25 mg) on Spheron TEAE-1000. Counterpressure, 11 atm; other details as in Fig. 4, except that the pH was adjusted to 5.

conditions the proteins cannot be retained by the ionogenic groups, but are first "salted" on to the matrix and then the hydrophobic bonds are successively released during the chromatography.

The result is shown in Fig. 6. All of the enzymes present, *i.e.*, N, L and S, emerged almost in one peak in the void volume. Pectin-lyase L only was slightly retarded; this can be ascribed to its hydrophobicity, which is slightly higher than that of the remaining enzymes. The small peak of endo-D-galacturonanase N at the end of the chromatogram, emerging at a very low ionic strength, can be explained either by the existence of a multiple form, characterized by a strong hydrophobic bond to the matrix, or by the low capacity of hydrophobic bonds of the matrix capable of binding part of the hydrophobic form N only and leaving most of the enzyme to emerge in the void volume.

DISCUSSION

The results obtained in this study confirmed the advantages MPLC on ion-exchange derivatives of Spheron for the analysis of commercial pectic enzyme preparations mentioned previously[8]. These advantages are as follows:

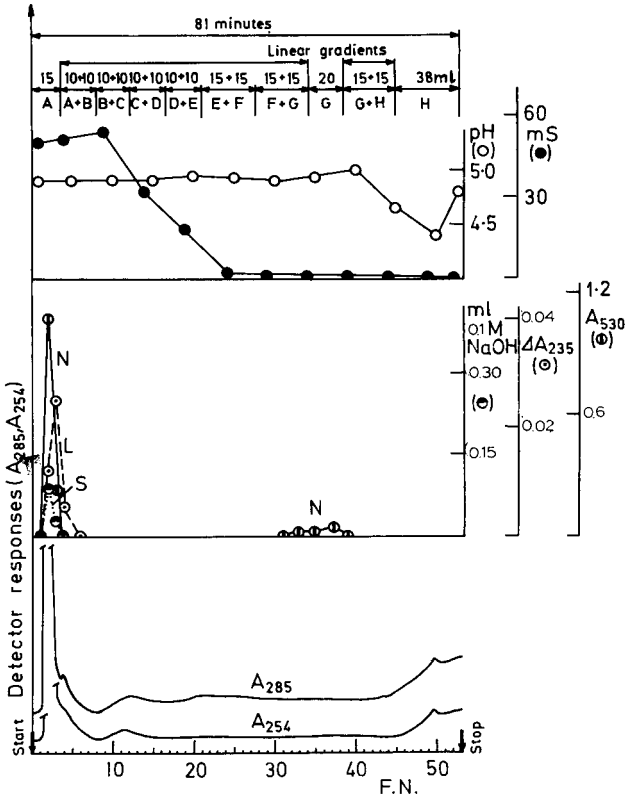

Fig. 6. Hydrophobic chromatography of Leozym on ionogenically unsubstituted Spheron 1000. Counter-pressure, 5 atm; other details as Fig. 1. The buffers were prepared from sodium hydroxide of the given final concentration whose pH was adjusted to 5 with acetic acid; A, 0.2 *M*, 2 *M* in sodium chloride; B, 0.1 *M*, 1 *M* in sodium chloride; C, 0.05 *M*, 0.5 *M* in sodium chloride; D, 0.05 *M*, 0.1 *M* in sodium chloride; E, 0.05 *M*; F, 0.01 *M*; G, distilled water; H, water–ethanol (3:1).

(a) Improved reliability of the determination of the individual enzyme activities as a result of the elimination of the simultaneous action of several enzymes on the same substrate, provided by the possibility of rapid separation of the enzymes. The simultaneous separation of the reducing compounds present in the preparation, which usually also emerge in the void volume, is possible. These compounds interfere in the analyses of the unfractioned preparation.

(b) The possibility of the determination of the presence and activity of pectinlyase by a spectrophotometric method and the higher sensitivity of the spectrophotometric determination of the activity of D-galacturonanases as a result of the separation of the coloured contaminants. This can be explicitly observed by a comparison of UV absorbance curves with the enzyme activity curves; this comparison shows that sometimes a completely negligible part of the absorbance of the commercial preparation can be accounted for by the enzyme present.

(c) The possibility of identifying multiple forms of pectic enzymes. According to these analyses commercial preparations of different origin can be distinguished chromatographically, thus establishing the technological regime of production, the

conditions of enzyme maturation and material handling and storage. Multiple forms need not necessarily be caused genetically or by differences in quaternary structure as is the case with numerous isoenzymes. They can result from complementary modification of originally homogeneous extracellular enzymes after secretion from the cell; such a modification can be due to limited proteolysis, changes in the sugar moiety of glycoproteins and conformational changes caused by temperature, ions or other compounds (the appearance of so-called conformers; see, *e.g.*, ref. 14). These modifications need not necessarily result in a decrease in the activity of the enzyme. Numerous enzymes are known with peptide chains interrupted at several sites; these enzymes retain full enzymatic activity. Such changes, however, are responsible for changes in electrophoretic or chromatographic behaviour and are readily detected by HPLC or MPLC. In general these methods are therefore of possible importance for the rapid checking of technological processes, enzyme maturation and storage and transportation of crude commercial enzyme preparations. Deviation from the permitted temperature and time limits usually manifests itself by the appearance of or increase in multiple enzyme forms with a simultaneous decrease in the enzyme activity[5]. The purification and characterization of two forms of vegetable pectin esterases has been described elsewhere[15].

The results obtained in this study show the potential use of MPLC in the preparation of products with modified contents of pectic enzymes and the possibilities of the preparation of specific products by MPLC. Likewise, preparations containing pectin-depolymerizing enzymes only, *i.e.*, free from pectin-esterase (which liberates methanol from pectin and can be the cause of toxicity of depectinized fruit juices, especially for children), could be obtained by removal of pectin-esterase via its sorption by a medium acid cation exchanger (Fig. 2), where it is retained. The use of the thus purified enzyme preparation in immobilized form would be economical for industrial application. Specific pectin esterase for research applications can be prepared by chromatography on a weakly basic anion exchanger (Fig. 4), from which it is eluted as the first peak, and in enriched form by chromatography on a weakly acidic cation exchanger (Fig. 1). The separation of all three enzyme activities could also be effected on a strongly acidic cation exchanger (*cf.*, Fig. 3) by rechromatography of the fractions.

The flow-rates used in this study (3 ml/min in columns of 0.8 cm diameter, *i.e.*, 5 ml/cm^2 · min) correspond to a total flow-rate of 30 l/min through a technical filter of 80 cm diameter at medium pressures of 5–10 atm. The time necessary for one run is around 1 h (and could be reduced for industrial applications). In general, this is very convenient in the production of enzyme preparations where the obtaining of high activities depends on the rate of processing. These are possibilities for future technical developments in the chromatography of enzymes. A necessary prerequisite of such developments, however, is the adequate production of chemically and biochemically stable, rigid, macroporous and hydrophobic ion exchangers at a reasonable cost.

ADDENDUM

While this manuscript was being prepared we obtained a reprint of the paper by Castino and Ubigli[16] describing the separation of two commercial pectic enzyme preparations and the characterization of the fractions obtained.

REFERENCES

1 L'. Rexová-Benková and V. Tibenský, *Biochim. Biophys. Acta*, 268 (1972) 187.
2 M. A. Vijayalakshmi, C. Bonaventura, D. Picque and E. Segard, in O. Hoffmann-Ostenhof (Editor), *Affinity Chromatography, Proc. Int. Symp.*, Pergamon Press, Oxford, 1978, p. 115.
3 O. Mikeš, *Int. J. Peptide Protein Res.*, 14 (1979) 393.
4 E. F. Regnier and K. M. Gooding, *Anal. Biochem.*, 103 (1980) 1.
5 O. Mikeš, *Ernährung*, 5 (1981) 88.
6 O. Mikeš, P. Štrop and J. Sedláčková, *J. Chromatogr.*, 148 (1978) 237.
7 O. Mikeš, P. Štrop, J. Zbrožek and J. Čoupek, *J. Chromatogr.*, 119 (1976) 339.
8 O. Mikeš, J. Sedláčková, L'. Rexová-Benková and J. Omelková, *J. Chromatogr.*, 207 (1981) 99.
9 O. Markovič, L'. Rexová-Benková and K. Heinrichová, unpublished work.
10 W. Heri, H. Neukom and H. Deuel, *Helv. Chim. Acta*, 44 (1961) 1939.
11 O. Mikeš, P. Štrop, M. Smrž and J. Čoupek, *J. Chromatogr.*, 192 (1980) 159.
12 M. Somogyi, *J. Biol. Chem.*, 195 (1952) 19.
13 P. Albershein, H. Neukom and H. Deuel, *Helv. Chim. Acta*, 42 (1960) 1422.
14 O. Mikeš, K. Worowski and J. Turková, *Collect. Czech. Chem. Commun.*, 38 (1973) 3339.
15 C. Versteeg, F. M. Rombouts and W. Pilnik, *Lebensm. Wiss. Technol.*, 11 (1978) 267.
16 M. Castino and M. Ubigli, *Frazionamento per Gel Filtrazione delle Attività Enzimatiche di Preparati Pectolitici Commerciali*, Istituto Sperimentale per l'Enologia di Asti, Tipolitografia Editrice Scarpis, Conegliano, Italy, No. 2, 1977, pp. 28.

Journal of Chromatography, 238 (1982) 193–202
Elsevier Scientific Publishing Company, Amsterdam — Printed in The Netherlands

CHROM. 14,534

HIGH-PERFORMANCE LIQUID CHROMATOGRAPHY OF PROTEINS: ANALYTICAL APPLICATIONS*

K. BUCHHOLZ and B. GÖDELMANN
Dechema-Institute, D-6000 Frankfurt 97 (G.F.R.)
and
I. MOLNAR*
Knauer, Hegauer Weg 38, D-1000 Berlin 37 (G.F.R.)
(First received February 23rd, 1981; revised manuscript received November 10th, 1981)

SUMMARY

Analysis of proteins in solution by high-performance liquid chromatography is presented with respect to structural changes in solution, adsorption processes and differentiation concerning specific activities. Trypsin and cellulases were taken as examples.

INTRODUCTION

Radioimmunoassay, ultracentrifugation, electrophoresis, gel filtration, size-exclusion, ion-exchange and affinity chromatography, and membrane osmometry are commonly used methods for the characterization of proteins. These techniques are, however, time consuming and difficult to automate, and they have, therefore, often been replaced by high-performance liquid chromatographic (HPLC) methods, which offer advantages in these respects.

Aqueous size-exclusion HPLC is increasingly being used for the separation and characterization of biologically important macromolecules[1–4]. In particular, improvements in column technology and the introduction of stationary phases based on chemically modified silica gel[5–10], which are mechanically stable under high pressures, have advanced the use of this technique although its specificity and resolution are still relatively low. In this paper we describe some applications of size-exclusion HPLC to the analysis of proteins in solution. It will be shown that this method is a useful tool for the rapid characterization of proteins and for monitoring the degradation of enzymes in solution.

In addition, size-exclusion HPLC was used for studying the hydrolysis of cellulose by cellulases, complex mixtures of enzymes of different activity which catalyse the successive reaction steps in this process[11,12]. The development of rapid methods

* Dedicated to Professor G. Manecke on the occasion of his 65th birthday.

0021-9673/82/0000–0000/$02.75

for analysing the adsorption of these enzymes on their substrate, their separation and the identification of the active fractions is an important topic in enzyme technology and reaction engineering[13]. Although the separation of cellulases by conventional methods has recently been improved[11,14,15], a correlation of the activity and the molecular size of the cellulase components, measured by HPLC, has to our knowledge so far not been reported. In this paper, we report a study of this correlation and compare the separation of cellulases on DEAE-Sephadex with that obtained on LiChrosorb DIOL columns.

EXPERIMENTAL

Apparatus

The high-pressure size-exclusion chromatograph was obtained from Knauer (Berlin, G.F.R.).

Fast screening of proteins was performed with a double-head reciprocating high-pressure pump (Type 52.00, Knauer), and a high-pressure sample introduction valve (RH 71-25, Knauer). The column (250 × 4.6 mm) was packed with LiChrosorb DIOL (5 μm) with an average pore size of 100 Å (103.07.16.005, Knauer). As mobile phase we used 0.1 *M* phosphate buffer, pH 2.1, at a flow-rate of 2.0 ml/min. Proteins (20 μg per injection) were detected with a spectrophotometer operating at 200 nm (Type 87.00, Knauer). The flow cell of the detector had a volume of 8 μl. The elution volume was accurately measured with an electronic volumeter (Type 68.00, Knauer) with a cell volume of 8.51 μl. This instrument generates a small heat impulse which is carried by the eluent flow and is detected by a small thermocouple. When the voltage of the thermocouple exceeds a threshold level, a new heat impulse is generated electronically and the cycle repeats itself as long as the eluent flows through the cell. A

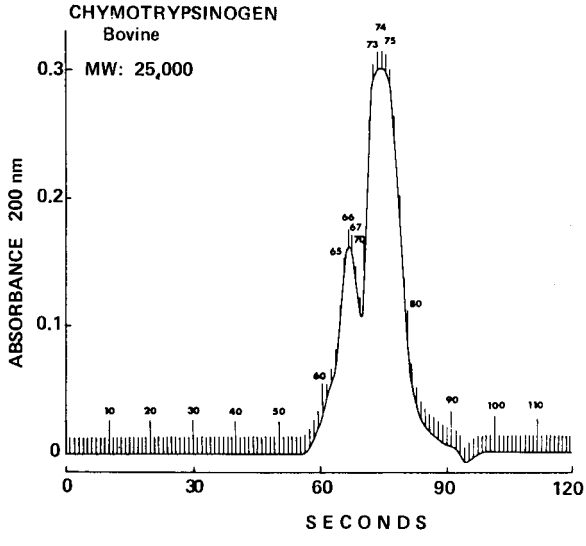

Fig. 1. High-speed, high precision separation of bovine chymotrypsimogen by size-exclusion HPLC. For fast screening conditions see Experimental section.

chromatogram using electronic volume measurement is shown in Fig. 1. Each mark on the chromatogram corresponds to cell volumes.

For trypsin analysis a 5-μm LiChrosorb DIOL column (250 × 4.6 mm) (103.07.16.005, Knauer) was used, eluted with 0.1 *M* phosphate buffer, pH 5, at a flow-rate of 1 ml/min and a pressure drop of 100 bar. Proteins were detected spectrophotometrically at 200 nm.

For adsorption studies of cellulases five columns of LiChrosorb DIOL, 5 μm, as specified above, were operated in series. The flow-rate was 0.5 ml/min, the pressure drop 300 bar, and the sample volume 20 μl. Buffer and detector were the same as above.

For activity studies and correlation of enzyme activity with HPLC data two LiChrosorb DIOL columns (250 × 16 mm) (105.09.16.005, Knauer) were coupled in series. The flow rate was 1 ml/min, the pressure *ca.* 2 bar, while other conditions were as above, except for the sample volume, which was 100 μl.

Materials

Protein samples of different molecular weight were purchased from Serva (Heidelberg, G.F.R.).

Trypsin (crystalline) and buffers were obtained from E. Merck (Darmstadt, G.F.R.). Cellulase from *Penicillium funiculosum* were a gift from J.a.E. Sturge (Selby, Great Britain): two preparations with different activities were used. Avicel (microcrystalline cellulose) was from Serva.

Methods

Trypsin inactivation. This was investigated in solution at a concentration of 0.05 g/l, 25°C, pH 8.2, 0.3 m*M* Tris buffer, 1 m*M* NaCl. The activity was determined from the kinetics of the hydrolysis of 1 m*M* N-α-benzoyl–arginine–*p*-nitroanilide, under the same conditions as before. The release of product was measured by monitoring its absorbance at 410 nm.

Adsorption of cellulases. Adsorption was investigated by incubation of the protein (1 g/l) with Avicel (0, 10, 50 g/l) for 10 min or for various times at 40°C, in 0.05 *M* citrate buffer, pH 5.

Chromatography of cellulases. Chromatography of cellulases (100 mg) on DEAE-Sephadex A-50 (15 g) was performed in a column with a volume of 0.96 l, and a length of 48 cm, which was eluted with 0.01 *M* citrate buffer, pH 4.3, at 1 ml/min. Samples of 10 ml were collected.

Determination of cellulase activities. Glucanases were analysed by incubation with Avicel (25 g/l) at 40°C, in 0.05 *M* citrate buffer, pH 4.5. Samples were taken at various times, centrifuged and analysed for glucose and cellobiose by HPLC, using LiChrosorb NH_2 (103.07.17.010, Knauer), acetonitrile–water (70:30), 2 ml/min, and a differential refractometer as detector (Type 98.00, Knauer). β-Glucosidases were analysed by incubation with cellobiose, 5 m*M*, under similar conditions as before.

RESULTS AND DISCUSSION

In size-exclusion chromatography, proteins are eluted according to their molecular weights. However, as discussed by Schmidt *et al.*[1], deviations may occur,

mainly as a result of interactions of the charged proteins with dissociated residual silanol groups on the silica surface. Negatively charged proteins will tend to elute faster than expected owing to repulsion by the negatively charged surface of the stationary phase. As a result, the calculated molecular weights will be higher than the real molecular weights. Positively charged proteins, on the other hand, will be retained more strongly by the stationary phase, resulting in too low values for the calculated molecular weights. For a meaningful correlation between elution volumes and molecular weight, therefore, pH control and complete coverage of the silica surface are essential. In LiChrosorb DIOL the latter requirement is achieved by covering the surface with covalently bound $-O-CH_2-CHOH-CH_2OH$ groups.

To investigate the retention characteristics of this stationary phase for proteins, a mixture of standard proteins of known molecular weight was chromatographed on a LiChrosorb DIOL column (Fig. 2).

The relationship between the molecular weights and the elution volumes on a 250 × 4.6 mm column packed with 5-μm LiChrosorb DIOL is shown in Fig. 3, which demonstrates the validity of the function

$$\log MW = A - BV_e$$

(where MW = molecular weight, V_e = elution volume of the protein, A and B = constants) even under conditions of high speed and low pore volume.

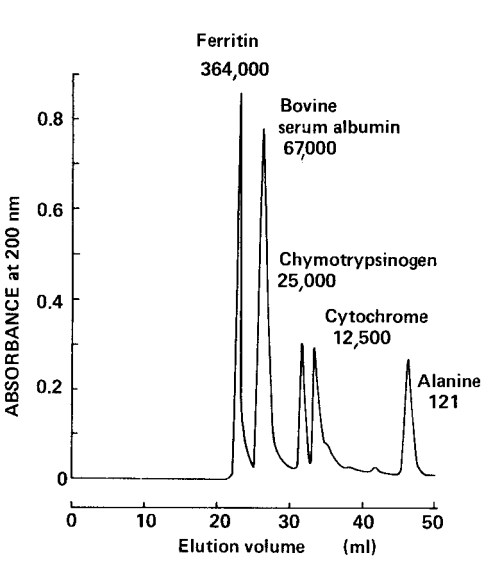

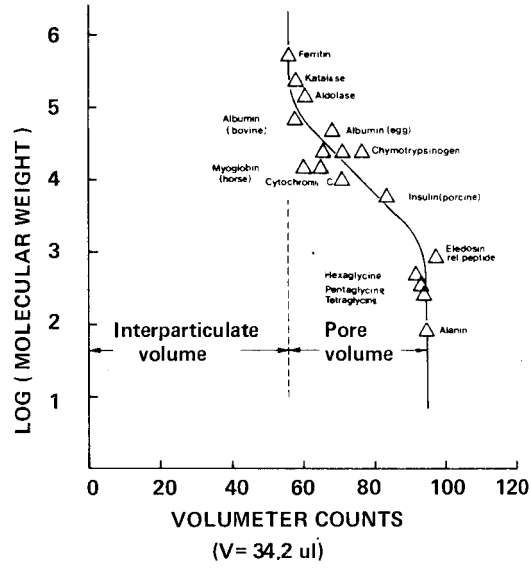

Fig. 2. Separation of protein molecular weight standards by size-exlusion HPLC. Column: prepacked with LiChrosorb DIOL, 5 μm (Knauer, 105.09.16.005) (250 × 16 mm); mobile phase: 0.1 M phosphate buffer, pH 5; flow-rate: 2.5 ml/min; low pressure drop; detection: 200 nm, spectrophotometer; sample amount: 20 μg each.

Fig. 3. Correlation between elution volume and molecular weight. For fast screening conditions see Experimental section.

As a demonstration of the high speed of this type of analysis, Fig. 1 shows a chromatogram of bovine chymotrypsinogen, which was obtained in less than 100 sec on a column with a liquid volume of *ca.* 3.3 ml. The shoulder preceding the main peak in the chromatogram is probably due to the formation of dimers or polymers as it disappeared upon dilution of the sample solution. In experiments with bovine trypsin it was shown that the reproducibility of this type of "molecular-size screening" is excellent.

Degradation of trypsin

Trypsin is in solution subject to autolysis, the kinetics of which depend on the experimental conditions[16].

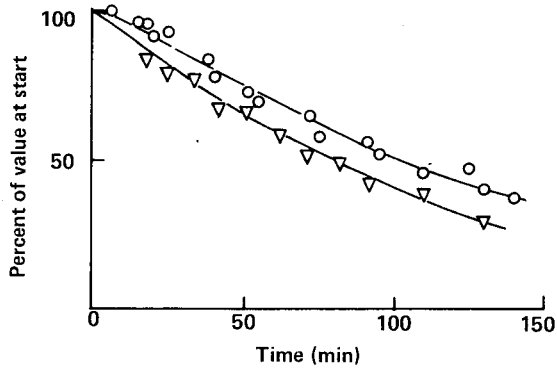

Fig. 4. Degradation (autolysis) of trypsin in solution. For conditions see Experimental section. O, Activity test (BAPNA); △, first peak in HPLC.

Fig. 4 shows the decrease in trypsin activity with time as well as the decrease in the height of the first peak in the HPLC chromatogram. As can be seen, both lines run parallel, suggesting that the first peak in HPLC corresponds to the integral active enzyme.

Adsorption of cellulases on cellulose

Adsorption of the enzymes on the substrate is the first step in enzymic cellulose hydrolysis. This process is also important in technical processes, where the active enzyme and the substrate are kept together within the reactor. We investigated by HPLC the adsorption of cellulases on Avicel, which served as a model substrate.

Fig. 5a shows a chromatogram of the cellulases. Fig. 5b presents the superimposed HPLC chromatograms of two fractions which had been separated previously on DEAE-Sephadex. Fig. 5c shows a chromatogram of cellulase preparation can be identified. Fig. 6a and b shows the decrease in peak heights (concentration in the supernatant) after adsorption of the enzyme on increasing amounts of Avicel. The components with α values of 0.68 and 0.92 are not, or only weakly, adsorbed ($\alpha = V_e/V_0$; V_e and V_0 = elution volumes of protein and buffer, respectively). The main peaks with α values of 0.72 and 0.75 are strongly adsorbed, but not completely. Even

at high concentrations of Avicel the peak heights were still about 20% of the values found in the absence of Avicel, suggesting that these peaks correspond to more than one protein each. One component ($\alpha = 0.87$) was adsorbed only moderately.

Fig. 7a, b and c shows that the adsorption equilibrium is established within *ca.* 10 min, and that part of the enzymes is released into solution after a considerable reaction time. For a detailed characterization of the cellulase system preparation No. 2 was separated by ion-exchange chromatography on DEAE-Sephadex (Fig. 8a). Fractions (10 ml each) were taken and were further investigated as described below.

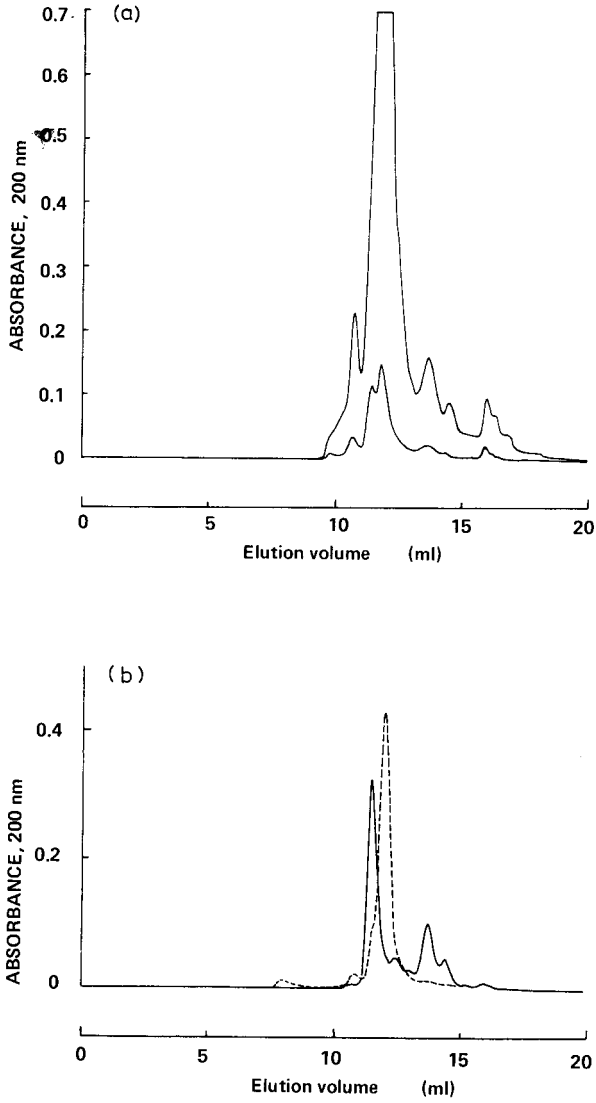

Fig. 5.

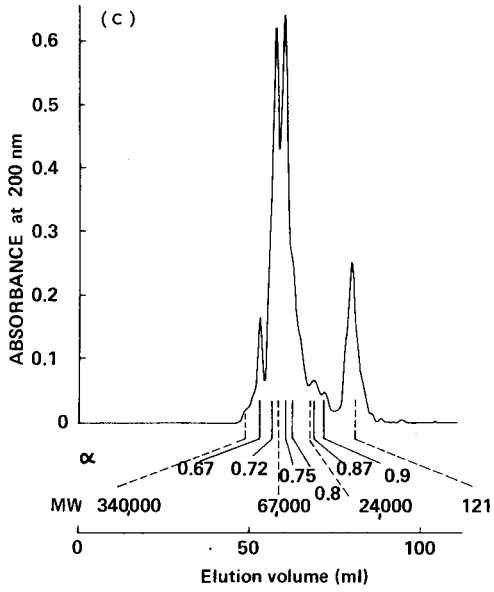

Fig. 5. (a) HPLC of cellulase, preparation No. 1 (5 g/l and 0.5 g/l, respectively); five columns with 4.6 mm diameter; for conditions see Experimental section. (b) Same as in (a); superimposition of chromatograms of two main fractions which had been separated by chromatography on DEAE-Sephadex; two columns with 16 mm diameter; for conditions see Experimental section. (c) HPLC of cellulases, preparation No. 2. For conditions see Experimental section. Retention indices ($\alpha = V_e/V_0$) are given, those of molecular weight standards are indicated.

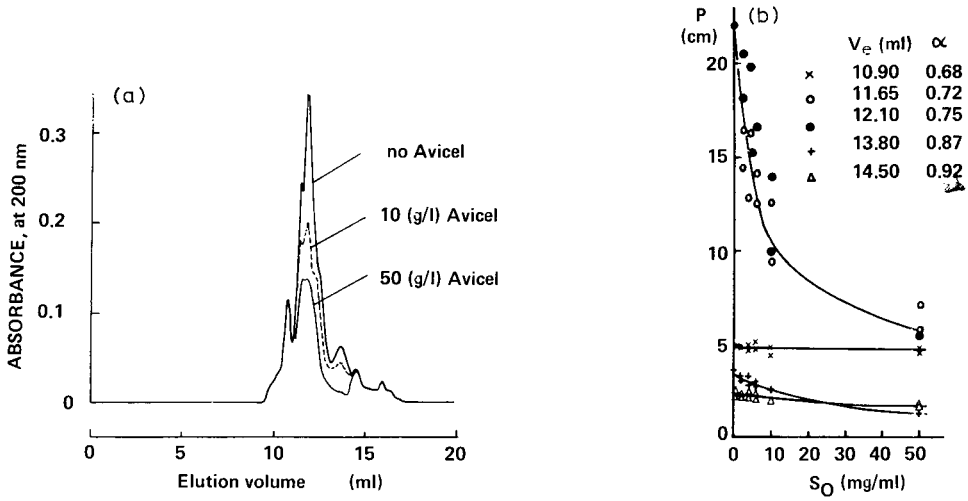

Fig. 6. Adsorption of cellulases (1 g/l) (a) On cellulose (Avicel, 0, 10 and 50 g/l) after 10 min, 40°C, pH 5, citrate buffer 0.05 *M*; HPLC from the supernatant. (b) Peak height (*P*) as a function of cellulose concentration (S_0), conditions as in (a).

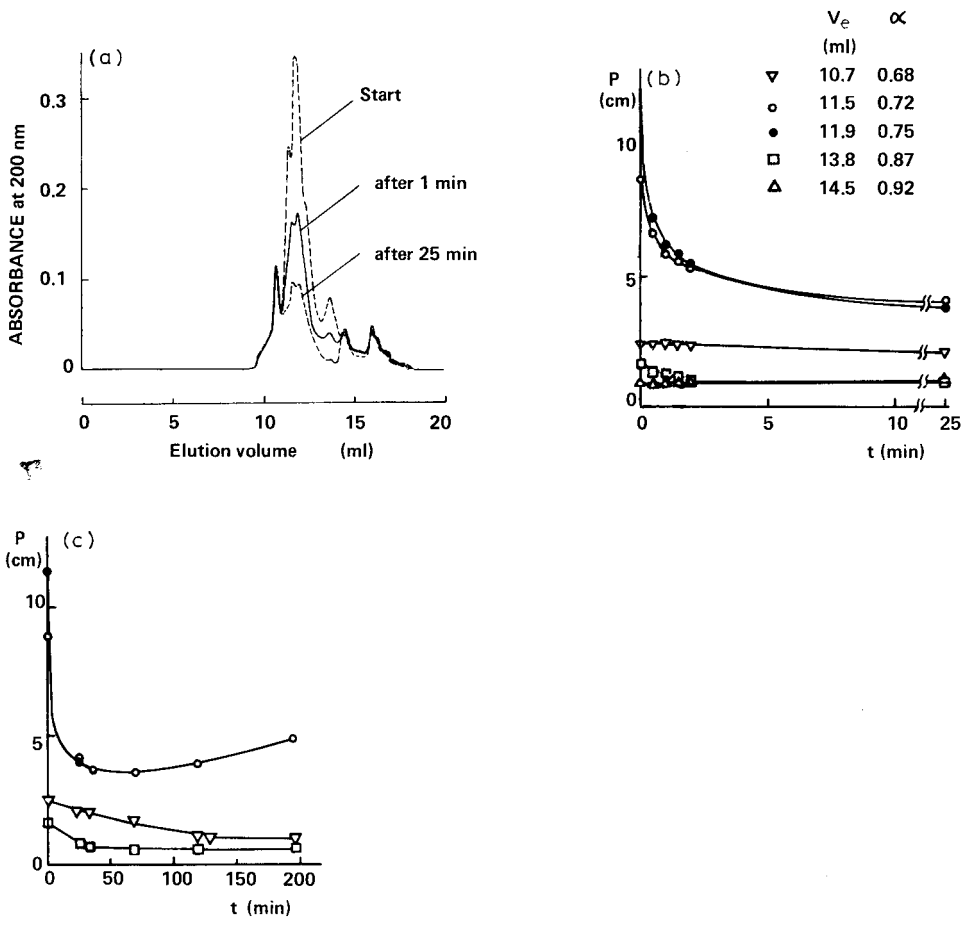

Fig. 7. (a) Time course of cellulase adsorption (0, 1, 25 min), conditions as in Fig. 6a (b, c) Peak height in HPLC as a function of time (0.5 g/l protein, 25 g/l Avicel). Conditions as in Fig. 6a.

Measurements of (β-glucosidases)$_{E2}$ and (glucanases)$_{E1}$ activities

endo-Glucanases randomly split bonds between glucose units in a cellulose chain. *exo*-Glucanases split cellobiose units from the end of a cellulose chain. Their activity was measured with Avicel (consisting mainly of crystalline cellulose) as substrate which can only be attacked by combined action of *endo*- and *exo*-glucanases. β-Glucosidases hydrolyse the cellobiose into two glucose units. The activity was measured with cellobiose as substrate.

Cellobiose and glucose were separated on LiChrosorb-NH_2 (see Experimental section). The activities of the cellulase fractions separated on DEAE-Sephadex are shown in Fig. 8b and c.

Relationship between fractions separated on DEAE-Sephadex and their molecular size, estimated by HPLC on LiChrosorb DIOL

Each fraction collected from the DEAE-Sephadex column was injected on two

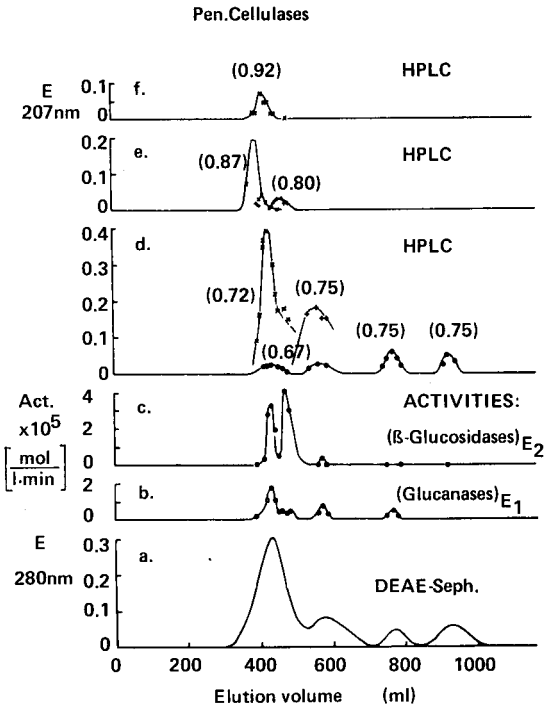

Fig. 8. (a) Chromatogram of cellulases (0.1 g) on DEAE-Sephadex (15 g, 0.96 l, h = 48 cm, citrate buffer 0.01 *M*, pH 4.3, Q = 1 ml/min). (b, c) Activity determination in fractions from (a). E_1 = activity with Avicel as substrate. E_2 = activity with cellobiose as substrate. Note: several different proteins with similar activity are present. (d–f) HPLC of the fractions from (a). The peak height of different peaks in HPLC (ordinate) is given for the fractions from (a) (abscissa). For conditions see Experimental section.

LiChrosorb DIOL columns (16 mm diameter). The fractions consisted of more than one component, as was expected. The first peak of the DEAE-Sephadex chromatogram was shown by HPLC to contain five different species with approximate molecular weights of 80,000 (α = 0.67), 50,000 (α = 0.72), 24,000 (α = 0.80), 12,500 (α = 0.87) and some low-molecular-weight species (α = 0.92). Three further peaks contained proteins with a molecular weight of *ca.* 37,000 (α = 0.75). For clarity these results are shown in three different figures (Fig. 8d, e and f).

The first two peaks in HPLC (α = 0.67 and 0.72) (Fig. 8d), which eluted at V_e = 430 ml from DEAE-Sephadex, appear to be associated with glucanases and a β-glucosidase activity.

Two species, both with α = 0.75 in HPLC, and with V_E = 570 and 770 ml, respectively, in the chromatogram obtained on DEAE-Sephadex, exhibited glucanase activities. Since they produced cellobiose they are most probably *exo*-glucanases. There was furthermore an inactive protein with α = 0.75 and with V_E = 950 ml. The peak (α = 0.80) normally hidden as a shoulder under the second main component of the HPLC separation seems to be a β-glucosidase since it corresponds to one of the two maxima in this activity (Fig. 8e and c).

In Fig. 8e and f two HPLC peaks (α = 0.87 and 0.92) seem to be due to inactive

material: the first peak ($\alpha = 0.87$) does not correlate with any activity, and the second peak is of low molecular weight ($\alpha = 0.92$). Similarly one main peak ($\alpha = 0.75$) apparently contains inactive protein as stated before.

This assignment of activities, though tentative, is expected to be a valuable tool for the localization of activities in enzyme reactors, as it can be performed much more readily than other tests.

CONCLUSIONS

The main advantage of size-exclusion HPLC is its speed without the need for regeneration of the system, enabling the rapid monitoring of alterations in protein mixtures due to degradation or adsorption processes.

Even from a complex mixture of enzymes, information on the activities of the different components can be obtained using relatively simple methods. The main activities in the cellulase system were found to be associated with the main HPLC peaks ($\alpha = 0.72$ and 0.75) and with a minor one ($\alpha = 0.80$). These components are rather strongly adsorbed on to the substrate, a finding that is important for reaction engineering in cellulose hydrolysis[14].

Chromatograms from DEAE-Sephadex columns show peaks which often contain several species of different molecular weight (Fig. 8). On the other hand peaks of different retention volume on DEAE-Sephadex can be proteins of the same molecular weight (see also Fig. 8).

ACKNOWLEDGEMENT

Support by the Federal German Ministry for Research and Technology is gratefully acknowledged.

REFERENCES

1 D. E. Schmidt, Jr., R. W. Giese, D. Conron and B. L. Karger, *Anal. Chem.*, 52 (1980) 177.
2 H. Engelhardt and D. Mathes, *J, Chromatogr.*, 142 (1977) 311.
3 P. Roumeliotis and K. K. Unger, *J. Chromatogr.*, 185 (1979) 445.
4 C. T. Wehr and S. R. Abbott, *J. Chromatogr.*, 185 (1979) 453.
5 F. E. Regnier and R. Noel, *J. Chromatogr. Sci.*, 14 (1976) 316.
6 K. K. Unger and N. P. Becker, *28th Pittsburgh Conference on Analytical Chemistry and Applied Spectroscopy, 1977, Cleveland, OH*, Abstr. No. 171.
7 D. Mathes and H. Engelhardt, *Naturwissenschaften*, 66 (1979) 551.
8 I. Molnar, *Chromatographia*, 12 (1979) 371.
9 H. Engelhardt and D. Mathes, *J. Chromatogr.*, 185 (1979) 305.
10 J. F. K. Huber and F. Eisenbeiss, *J. Chromatogr.*, 149 (1978) 127.
11 T. K. Ghose, in T. K. Ghose, A. Fiechter and N. Blakebrough (Editors) *Advances in Biochemical Engineering*, Vol. 6, Springer, Berlin, 1977, pp. 39–76.
12 P. Linko, *Chem.-Ing.-Techn.*, 50 (1978), 655.
13 K. Buchholz, J. Puls, B. Gödelmann and H. H. Dietrichs, *Process Biochemistry*, 16 (1980/81) 37.
14 F. J. Bissett, *J. Chromatogr.*, 178 (1979) 515.
15 S. P. Shoemaker, R. D. Brown, *Biochim. Biophys. Acta*, 523 (1978) 133, 147.
16 D. Gabel, V. Kasche, *Acta Chem. Scand.*, 27 (1973) 1971.

Journal of Chromatography, 238 (1982) 203–215
Elsevier Scientific Publishing Company, Amsterdam — Printed in The Netherlands

CHROM. 14,687

APPLICATION OF LIQUID CHROMATOGRAPHIC AND SPECTROSCOPIC METHODS FOR THE CHARACTERISATION OF FATTY ACID ANILIDES IN CONTAMINATED COOKING OILS

B. B. WHEALS*, M. J. WHITEHOUSE and C. J. CURRY
Metropolitan Police Forensic Science Laboratory, 109 Lambeth Road, London SE1 (Great Britain)
(Received December 24th, 1981)

SUMMARY

High-performance liquid chromatographic and spectroscopic (mass spectrometric and infrared spectroscopic) methods were used to characterise the presence of oleic, linoleic, linolenic and stearic anilides in contaminated cooking oils from Spain. The procedures provide the basis for a screening technique to ensure the absence of such components in oils.

INTRODUCTION

The toxic effects of cooking oil sold in Spain during 1981 produced widespread illness and death[1]. The Department of Forensic Medicine at the University of Seville asked this Laboratory to assist their investigation by carrying out some trace metal analyses. However, it seemed worthwhile extending the examination to other possible toxic components. For this purpose it is necessary to use a primary screening technique that would allow a comprehensive examination to be made. The procedure that most nearly approaches the ideal for this is size exclusion chromatography which has been used as a forensic screening technique for some years[2], albeit with UV detection (*i.e.*, a selective rather than a universal detector). Comparison of the size exclusion chromatograms of control oils with those from Spanish cooking oils indicated that the latter contained components that were unusual. These components could be extracted from the oil with acetonitrile, and spectroscopic (mass spectrometric, MS, and infrared, IR, spectroscopic) examination of the extract indicated that they were fatty acid anilides. A series of standard anilides were prepared and it was found that they could be separated well under reversed-phase high-performance liquid chromatographic (HPLC) conditions and could be readily monitored by their UV absorbance. Comparison of the retention time data of standard anilides and the extracted compounds before and after bromination enabled a tentative identification to be made. Confirmation was achieved by using the HPLC system in a preparative mode and subjecting individual fractions to spectroscopic examination. The reversed-phase HPLC procedure was also used to confirm that the compounds characterised could be produced by heating aniline with rapeseed oil.

0021-9673/82/0000–0000/$02.75

This paper describes the procedures used in comparing suspect and control oils, isolation of the unknown components and their characterisation. In addition chromatographic and IR spectroscopic screening methods are proposed.

EXPERIMENTAL

Six samples of Spanish cooking-oil were examined and the following authenticated vegetable oils were tested for control purposes: olive oil (five samples), rapeseed oil (two samples), safflower oil, palm oil, palm kernel oil, cotton seed oil, soyabean oil, groundnut oil, castor oil, coconut oil, sunflower-seed oil, grape-seed oil, maize oil and sesame oil. In appearance and odour the Spanish oils did not differ markedly from many of the authenticated vegetable oils.

Size exclusion chromatography

Conditions very similar to those previously reported[2] were used in this study: column, 25 cm × 8 mm I.D. stainless steel; packing, a microparticulate silica of *ca.* 5 μm particle size, with the pore size 130 Å, pore volume 1.25 ml/g, and surface area 320 m^2/g; eluent, tetrahydrofuran (HPLC grade, Fisons)–water (99:1); flow-rate, 2 ml/min; detection, UV absorbance at 254 nm (SpectroMonitor III, LDC); injection, Rheodyne valve (Model 7125) with 20-μl loop.

A 0.2-g amount of each oil was dissolved in 5 ml of eluent and 20 μl of the solution were injected. A molecular weight (size) *versus* retention volume calibration curve was produced by injecting polystyrene standards.

Solvent extraction and spectroscopic examination

A 50-ml volume of oil was extracted with 2 × 50 ml of acetonitrile (Laboratory grade, May & Baker). The combined extracts were washed with 2 × 100 ml of pentane (Distol grade, Fisons) and the acetonitrile solution was evaporated to dryness at 70°C using a rotary evaporator. The residue was dissolved in 5 ml of diethyl ether. A 100-μl volume of this extract was streaked on to a silica thin-layer chromatography plate and developed with chloroform. The compounds of interest ran with an R_F of about 0.7 and this portion of the plate was removed and extracted with diethyl ether. The cleaned sample was then examined by IR spectroscopy and MS using the conditions described below.

IR spectroscopy. The IR spectra were recorded on a Nicolet MX-1 Fourier transform infrared spectrometer employing a Nicolet 7000 MX (× 4) mirror beam condenser when appropriate. The oil extract was evaporated on to KBr powder, pressed into 1.5-mm discs using an ultra-micro die (Perkin-Elmer) and spectra were acquired for 16 min (*i.e.*, 512 scans).

Mass spectrometry. Mass spectra were obtained using a direct insertion probe on a VG 12-12F quadrupole mass spectrometer (VG Analytical) linked to a 2050 Data system (VG Analytical). Electron impact (EI) and chemical ionisation spectra were recorded under the following experimental conditions: *electron impact:* source temperature, 200°C; electron energy, 70 eV; emission current, 500 μA; mass range, 35–535 a.m.u.; scan rate, 6 sec; and *chemical ionisation:* source temperature, 160°C; electron energy, 50 eV; emission current, 1000 μA; reagent gas, isobutane at $5 \cdot 10^{-5}$ Torr at the source housing; mass range, 200–500 a.m.u.; scan rate, 6 sec.

Preparation of fatty acid anilides

A 1-g amount of each of the following fatty acids was weighed into test tubes (Soveril tubes): oleic, linoleic, linolenic, lauric, myristic, palmitic, stearic and erucic acid. A 2-ml volume of aniline was added to each sample and the stoppered test tube was heated in an oven at 150°C for 18 h. The contents of each tube were dissolved in 50 ml of diethyl ether and extracted with 2 × 50 ml of 10% hydrochloric acid to remove excess aniline. The ether solution was neutralised by adding it to a beaker containing solid sodium bicarbonate (*ca.* 5 g) and the solution was then filtered and evaporated to dryness. The products were recrystalised from methanol or methanol–water. With the exception of the anilides of oleic, linoleic and linolenic acids which formed as oils, all other products were crystalline.

Reversed-phase HPLC of fatty acid anilides and oil extracts

A packing material made in the Laboratory was used in these studies. The preparation was as follows: 50 g of the silica described above under *Size exclusion chromatography* was oven dried at 150°C for 24 h, and was refluxed for 1 h with 250 ml of xylene containing 25 ml of octadecyltrichlorosilane. After this period 25 ml of trimethylchlorosilane was added and refluxing was continued for a further hour. The product was filtered and washed in succession with xylene, acetone and methanol, and was then vacuum dried at 75°C. This packing material is a typical end-capped C_{18} modified silica and gave a weight loss of 19.5% on ashing at 600°C. The retention characteristics of this material can be correlated with that of commercially available supports. Thus: Spherisorb 5 μm ODS displays less retention, factor 0.8; Zorbax ODS displays greater retention, factor 1.2–1.7.

The following chromatographic conditions were used: column, 12.5 cm × 5 mm I.D. stainless steel; packing, as described above; eluent, methanol–water (95:5); flow-rate, 1 ml/min; detection, UV absorbance at 254 nm (SpectroMonitor III, LDC); injection, Rheodyne valve (Model 7125) with 20-μl loop.

Standard anilides were dissolved in methanol for injection. Oils were shaken with methanol or acetonitrile (0.2–0.5 g of oil + 5 ml of solvent) and an aliquot of the extract was injected. In addition to running the anilides under the conditions just described samples were also mixed with an equal volume of a brominating solution (20 drops of bromine in 25 ml of acetonitrile). The reaction was allowed to progress for 10 min and the reaction mixture was injected.

Preparative HPLC was carried out on the same column system using a sample which consisted of 1 ml of the ether extract prepared as described above under *Solvent extraction and spectroscopic examination* dried down and redissolved in 400 μl of the eluent. Monitoring at 280 nm three fractions were collected; these fractions corresponding to the three major UV absorbing components. The bulked fractions were added to 50 ml of water and extracted with 4 × 10 ml of ether. The extracts were filtered, dried and examined by chromatography and spectroscopy.

Formation of fatty acid anilides by heating oils with aniline

Rapeseed oil and aniline were mixed in different proportions and heated in sealed test tubes at 150°C for 18 h. Aliquots of the mixtures were dissolved in tetrahydrofuran and examined under the reversed-phase conditions described above.

Screening procedures

Either of the two chromatographic systems can be used to screen oils for the presence of anilides. The optimum monitoring wavelength is about 240 nm and in the case of the reversed-phase system the detection limit for individual anilides is about 1 ng (*i.e.*, injected). Quantitation merely requires the use of stock solutions prepared from the standard anilides.

The following procedure was used when screening by IR: 1 g of oil was dissolved in 2 ml of isooctane and shaken for 5 min with 3 ml of methanol. After centrifugation, the methanol layer was removed and washed with 5 ml of isooctane. The methanol fraction was separated, evaporated to dryness and the oil residue taken up in 500 μl of dry ether. About half of the ether solution was spotted as evenly as possible on to a pre-prepared 13-mm KBr disc. Spectra were acquired for 5 min (*i.e.*, 160 scans).

RESULTS AND DISCUSSION

Size exclusion chromatography

The chromatograms obtained with the Spanish cooking-oils and some of the control oils are shown in Fig. 1. The retention volume *versus* molecular weight data for polystyrene standards are shown in Table I.

The Spanish oils and most of the control oils displayed UV absorption at 254 nm and hence the size exclusion chromatograms provided information on how the UV absorbance varied as a function of molecular weight (or size). All oils had a major peak of elution volume 8.2 ml (mol.wt. *ca.* 1780) and the intensity of this peak varied

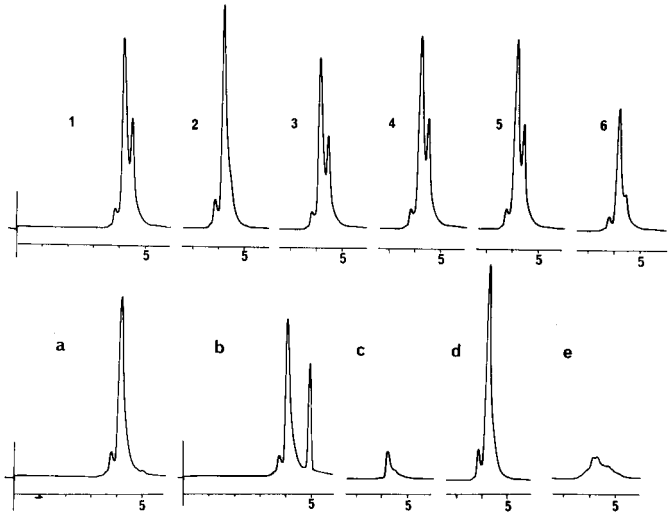

Fig. 1. Size exclusion chromatograms of vegetable oils. Column, 25 cm × 8 mm I.D.; packing, 5 μm silica (see text); eluent, tetrahydrofuran–water (99:1); flow-rate, 2 ml/min; detection, UV at 254 nm; sample concentration, 0.2 g/5 ml of eluent; injection volume, 20 μl. Samples: 1–6 = Spanish cooking oils numbers 1–6, respectively; a = rapeseed oil; b = rapeseed oil + aniline (at 500 ppm); c = olive oil; d = maize oil; e = soya oil. The time scale on these chromatograms is marked in 1-min intervals.

TABLE I

RETENTION VOLUME DATA FOR POLYSTYRENE STANDARDS ON A COLUMN PACKED WITH SILICA OPERATING IN A SIZE EXCLUSION MODE

Column, 25 cm × 8 mm I.D.; packing, 5 μm silica (see text); eluent, tetrahydrofuran–water (99:1).

Molecular weight (polystyrene)	*Retention volume (ml)*
125,000	5.3
25,000	5.9
10,000	6.8
4000	7.7
1400	8.3
650	8.8
92 (toluene)	9.6

considerably in different samples. A feature unique to the Spanish oils, with the exception of sample 2, was a peak of elution volume 9.0 ml (mol.wt. *ca.* 370); this was sufficiently unusual to justify the study that was initiated.

Solvent extraction and spectroscopic examination

By using size exclusion chromatography it was possible to ascertain that the components of molecular weight of about 370 could be extracted from the Spanish oil by acetonitrile. This method of enrichment was used to provide the crude extract suitable for spectroscopic examination. The IR spectrum and the EI mass spectrum of the extract are shown in Fig. 2.

The IR spectrum has strong CH stretching bands in the region of 2850–2950 cm^{-1} together with characteristic features associated with fatty acid anilides[3]. In Fig. 2a the bands at A (1661 cm^{-1}) and B (1546 cm^{-1}) correspond to the amide I (CO stretch) and amide II (NH in plane deformation) modes of a secondary amide. The weaker band C (1310 cm^{-1}) may be attributed to the amide III mode but the amide IV band is obscured by the absorption (D) due to the $(-CH_2-)_n$ rocking mode at 724 cm^{-1}. The band (E) at 3330 cm^{-1} is probably due to the NH stretching mode of a hydrogen bonded secondary amide in the *trans* configuration. The bands (Ar) at 3009, 1601, 1500, 754, and 691 cm^{-1} are all indicative of a monosubstituted benzene ring. The weak band (F) at 1745 cm^{-1} is probably due to the CO stretch of the unreacted glyceride. The EI mass spectrum (Fig. 2b) resembles that of acetanilide in exhibiting a base peak at m/z 93 due to the $(C_6H_5NH_2)^+$ ion and a prominent ion at m/z 135 is attributable to $(C_6H_5NHCOCH_3)^+$. However, the spectrum shows features at masses higher than the molecular weight of acetanilide (*i.e.*, 135), notably an ion at m/z 148. In the case of spectra in which the base peak was well overloaded peaks of low abundance are seen at m/z 355 and 357. The IR and MS data strongly suggested that the extract contained a mixture of fatty acid anilides.

Reversed-phase HPLC of fatty acid anilides and oil extracts

The chromatograms obtained with methanol extracts of Spanish oils and solutions of standard anilides are shown in Fig. 3. It will be seen that with the exception of sample 2, each oil extract contained the same components in the same relative ratios and that the intensity of these peaks in the chromatograms correlated well with the

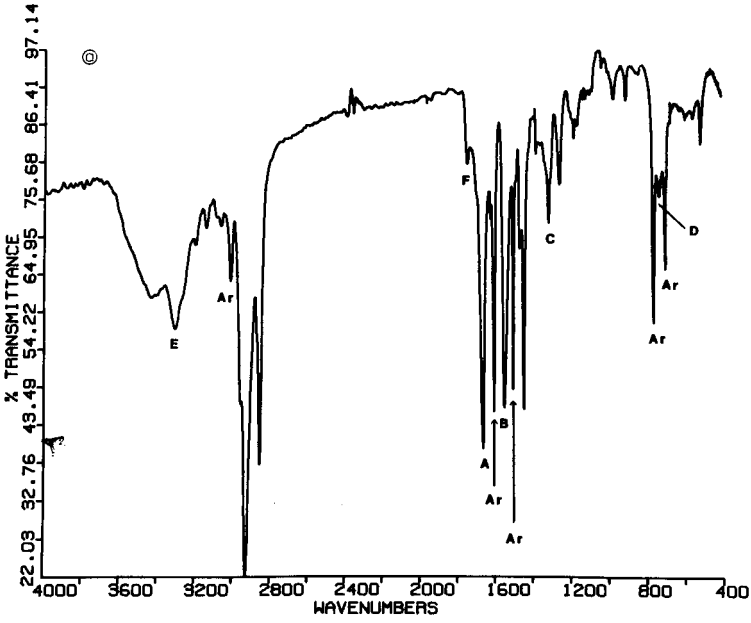

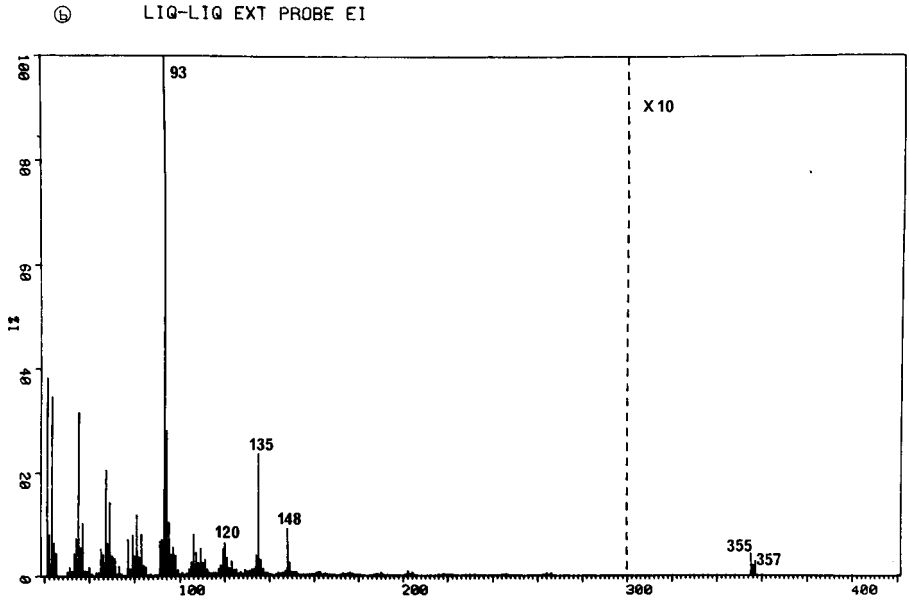

Fig. 2. (a) IR spectrum and (b) EI mass spectrum of an acetonitrile extract of contaminated Spanish cooking oil.

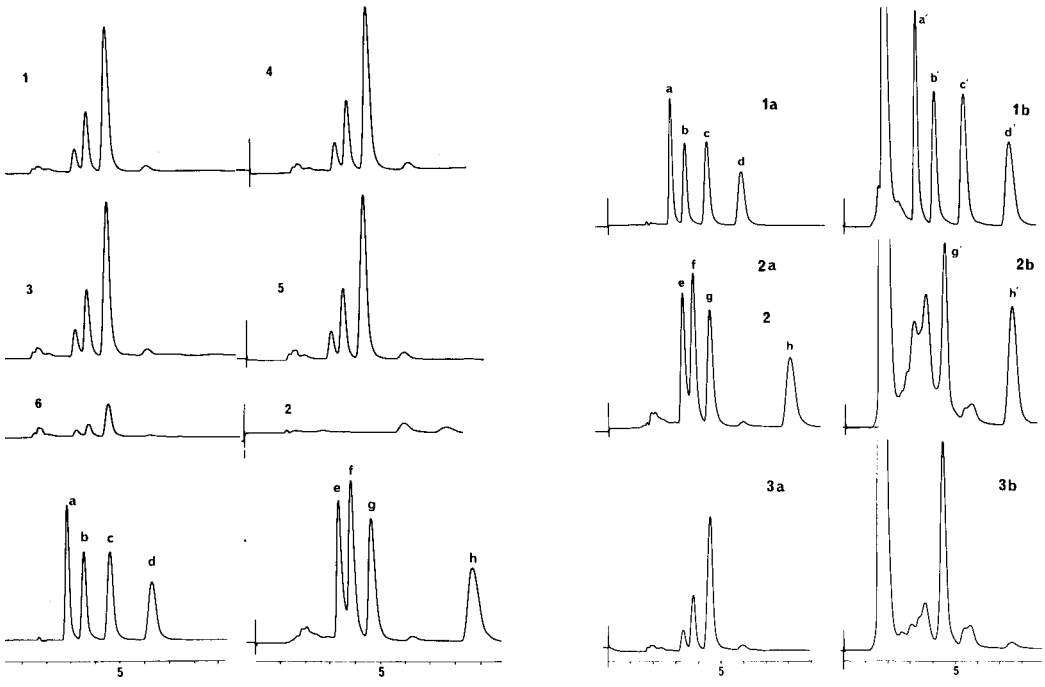

Fig. 3. Reversed-phase liquid chromatograms of oil extracts and standard anilides. Column, 12.5 cm × 5 mm I.D.; packing, C_{18} modified silica (see text); eluent, methanol–water (95:5); detection, UV at 254 nm, sensitivity 1.0; injection volume, 20 μl. Samples: 1–6 = Spanish cooking oils extracts in 5 ml of methanol (sample weights were 348, 484, 399, 464, 373, and 446 mg, respectively); a = lauric anilide; b = myristic anilide; c = palmitic anilide; d = stearic anilide; e = linolenic anilide; f = linoleic anilide; g = oleic anilide; h = erucic anilide. The time scale on these chromatograms is marked in 1-min intervals.

Fig. 4. Reversed-phase liquid chromatograms of an oil extract and standard anilides before and after bromination. Conditions as in Fig. 3. Samples: 1a = anilides of saturated fatty acids; 1b = the same mixture after bromination; 2a = anilides of unsaturated fatty acids; 2b = the same mixture after bromination; 3a = a methanol extract of Spanish oil 1; 3b = same sample after bromination. The compounds are designated in the same coding as in Fig. 3. The peaks shown with a suffixed letter correspond to the bromination products formed from the parent anilide.

intensity of the suspect peak in the size exclusion chromatograms. In Fig. 4 are shown chromatograms run under the same conditions before and after bromination. With the exception of oil 2 all the Spanish oil extracts behaved in the same way on bromination and hence the chromatograms illustrated (*i.e.*, 3a and 3b in Fig. 4 derived from oil 1) are typical of all the results. The retention volume data are summarised in Table II.

The retention of fatty acid anilides under reversed-phase conditions is largely determined by differences in the chain length and degree of unsaturation of the fatty acid moiety. Bromination provides a convenient method of producing additional qualitative information, with anilides of saturated fatty acids yielding a single product (probably the monobromo derivative) of slightly longer retention and greater UV absorbance than the parent compound. The unsaturated fatty acid anilides display a somewhat different pattern after bromination —oleic and erucic anilides, with

TABLE II

RETENTION VOLUMES OF STANDARD ANILIDES, EXTRACTS OF SPANISH COOKING OIL AND THEIR BROMINATION PRODUCTS ON A COLUMN PACKED WITH A C_{18} MODIFIED SILICA

Column, 12.5 cm × 5 mm I.D.; packing, C_{18} modified silica (see text); eluent, methanol–water (95:5) at 1 ml/min.

Compound	*Retention volume (ml)*	*Retention volume after bromination (ml)*
Lauric anilide	2.8	3.2
Myristic anilide	3.5	4.0
Palmitic anilide	4.5	5.3
Stearic anilide	6.3	7.4
Linolenic anilide	3.3	*
Linoleic anilide	3.7	*
Oleic anilide	4.6	4.6
Erucic anilide	8.8	8.3
Peak 1	3.3	*
Peak 2	3.7	*
Peak 3	4.6	4.6
Peak 4	6.3	7.4

* A mixture of several products formed

one double bond in the aliphatic side chain yield major products of slightly lower retention volume and slightly greater UV absorbance than the parent anilide. In contrast linoleic and linolenic anilides which have a greater level of unsaturation, yield several products none of which produce chromatographic peaks of an intensity greater than that of the starting product. Thus a comparison of chromatograms run before and after bromination can give additional evidence to aid in the characterisation of individual anilides.

The retention characteristics and bromination patterns of the components extracted from contaminated Spanish cooking oils supported the conclusions derived from the spectroscopic interpretation. Thus it seems that these oils contain oleic, linoleic and linolenic anilides together with a smaller proportion of stearic anilide. Oil sample 2 was not found to contain anilides.

Fig. 3 indicates that the relative proportion of the four anilides in the Spanish oil extracts is constant and on a peak area basis corresponds to: linolenic anilide, 8%; linoleic anilide, 24%; oleic anilide, 64%; and stearic anilide, 4%. It should be appreciated that these values apply only to the extracts and will only relate to the levels in the oil if extraction does not lead to preferential enrichment of any of these compounds.

To obtain some idea of the levels of anilides actually present in the oil samples, a control oil was fortified with known amounts of oleic anilide, and was then examined by both chromatographic methods. The failure to obtain a crystalline oleic anilide prevented accurate quantitation from being performed, but the results suggested that four of the samples (*i.e.*, 1, 3, 4 and 5) contain about 5 mg of anilide per g of oil; that sample 6 contained about 1 mg/g and that sample 2 was anilide-free.

Spectroscopic confirmation

Confirmation of the identity of the three major UV absorbing components in the Spanish oils was achieved by the spectroscopic examination of the fractions corresponding to the three major peaks on the chromatograms shown in Fig. 3. The IR spectra of the three fractions showed only minor differences between them and were very similar to that given by the crude extract as shown in Fig. 2. The EI

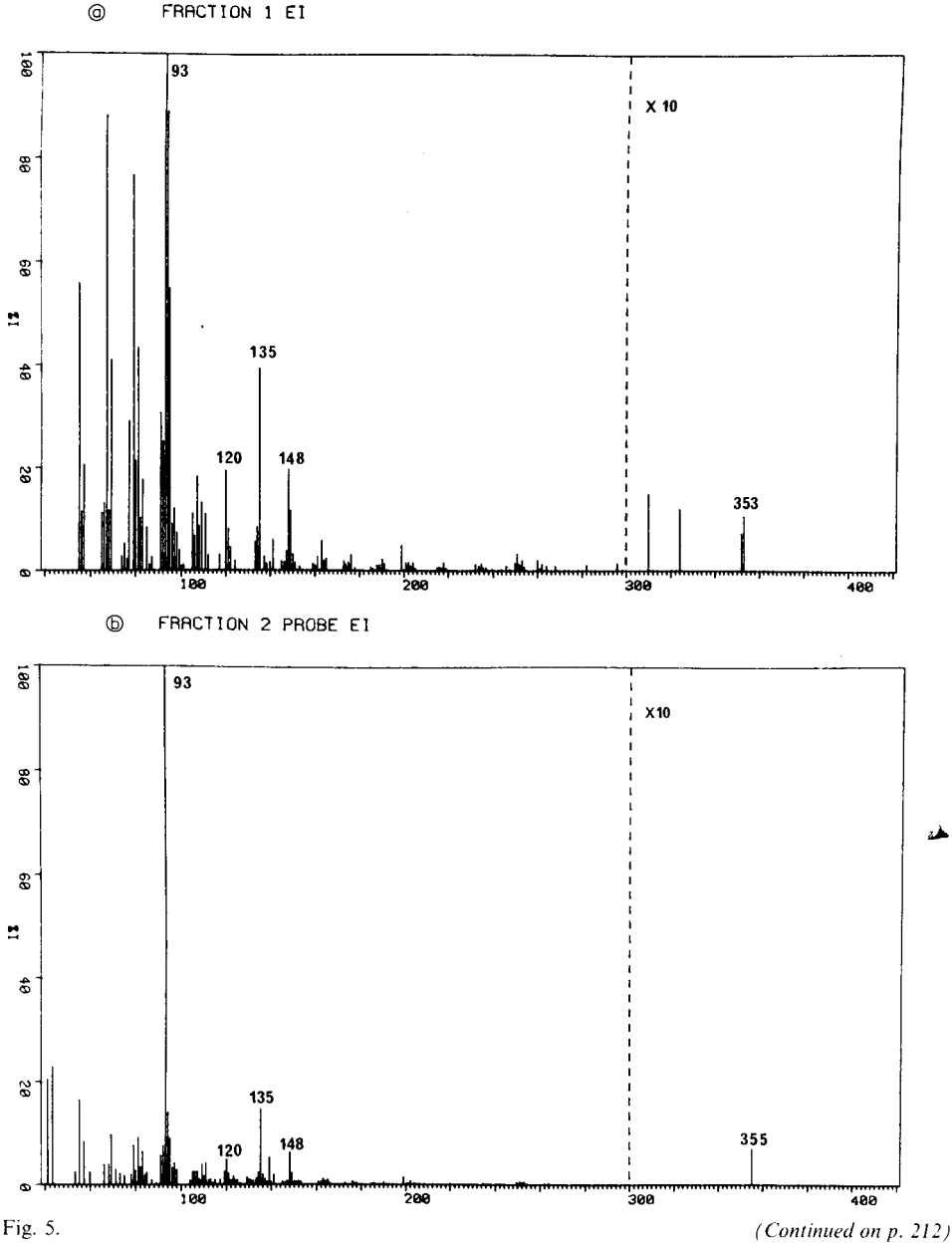

Fig. 5.

(Continued on p. 212)

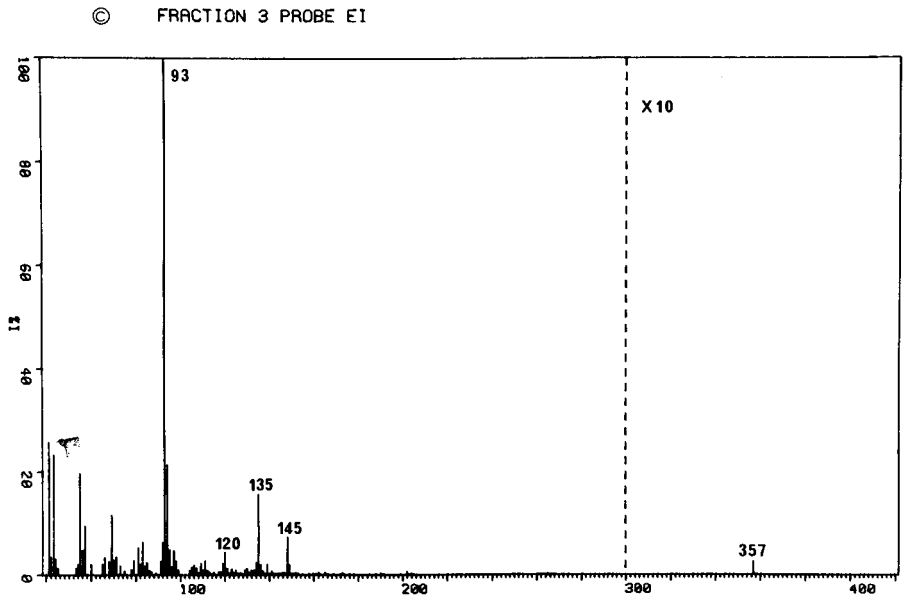

Fig. 5. EI mass spectra of preparative HPLC fractions. (a) Fraction 1 (*i.e.*, the first major retained peak on the chromatogram); (b) fraction 2 (*i.e.*, the second major retained peak); (c) fraction 3 (*i.e.*, the third major retained peak).

mass spectra of the fractions (see Fig. 5) were also similar to each other and that of the crude extract in that the base peak of *m/z* 93 and ions of *m/z* 135 and 148 were common to all. Weak molecular ions were observed in overloaded spectra at *m/z* 353, 355, and 357 for fractions 1 to 3 inclusive. These ions could be assigned to linolenic, linoleic and oleic anilides. Further confirmation was obtained from the isobutane chemical ionisation spectra which exhibited as base peaks the pseudo molecular $(M + 1)^+$ ions at *m/z* 354, 356, and 358 respectively. In the third fraction there was also evidence of the presence of stearic anilide from the $(M + 1)^+$ ion at *m/z* 360.

Heating experiments

The earlier studies showed that all but one of the Spanish oil samples submitted to our Laboratory were contaminated with fatty acid anilides. Although we cannot be certain that these compounds gave rise to the observed poisoning outbreak in Spain it cannot be ruled out, and hence we felt that it was necessary to establish that they could be formed in processes through which the oil had been taken prior to human consumption. The only information available were a few press reports, and it was not possible to simulate exactly the way in which they became contaminated. Apparently vegetable oils not destined for human consumption are sometimes denatured by heating with aniline. This process causes the oils to become darkly coloured and obviously unpalatable. In the case of the Spanish oil poisoning it seems likely that the colour and odour was removed from the denatured oil by some process that failed to remove the anilides that were also present.

The results obtained by heating a control rapeseed oil with aniline in different

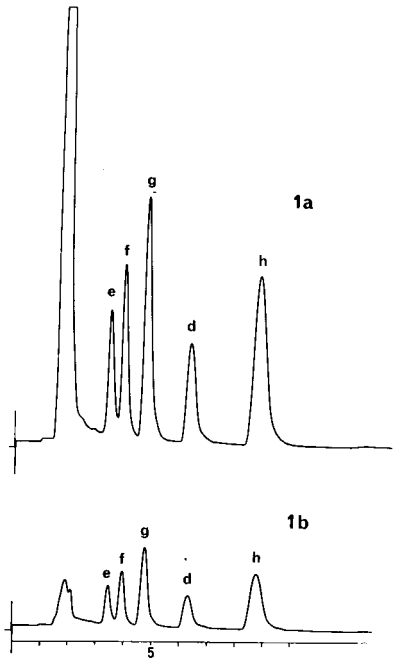

Fig. 6. Reversed-phase liquid chromatograms of a rapeseed oil heated with aniline at 150°C. Conditions as in Fig. 3. Samples: 1a = 0.4 g of rapeseed oil and 0.4 g of aniline heated for 18 h at 150°C. The sample was then dissolved in 5 ml of tetrahydrofuran and 100 μl of this solution was diluted with 5 ml of eluent to provide the solution for injection; 1b = 0.4 g of rapeseed oil and 0.03 g of aniline heated for 18 h at 150°C. Sample dilution as for 1a. The anilide peaks are coded as in Fig. 3.

proportions are typified by the chromatograms shown in Fig. 6. Regardless of whether the oil or the aniline were in excess, heating resulted in a blackening of the oils and the chromatograms show that a mixture of anilides of constant relative proportion were formed. Present in the mixture were four of the anilides identified in the Spanish cooking oils, but a comparison of Figs. 3 and 6 shows that in the latter the levels of stearic and erucic anilides formed by heating give the chromatograms a quite different appearance. This may reflect a difference in the composition of the oils prior to the formation of the anilides or could possibly result from the treatment used in removing the dark colour from the Spanish oils.

Screening methods

For screening purposes either of the HPLC methods described above could be used to provide rapid and sensitive analysis of oils contaminated with anilides. For those laboratories without HPLC equipment the IR screening method offers an alternative approach. Typical spectra derived from contaminated and uncontaminated oils are shown in Fig. 7. Comparison of these spectra and that given in Fig. 2 shows that the simple extraction procedure described is adequate to indicate the presence of anilides in a contaminated sample. The procedure takes about 30 min but could be reduced if smaller volumes of solvent were used, because evaporation of the methanol

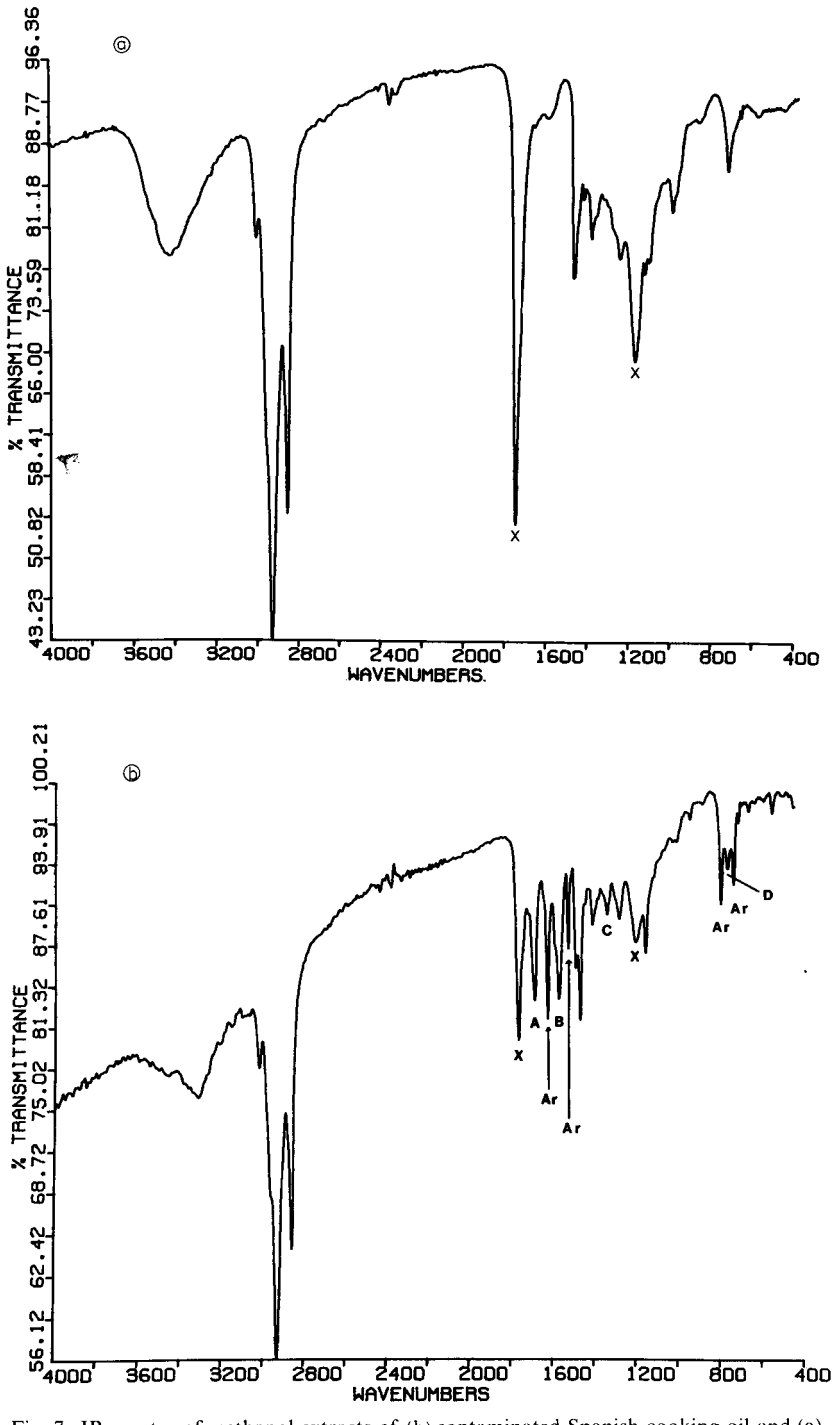

Fig. 7. IR spectra of methanol extracts of (b) contaminated Spanish cooking oil and (a) an uncontaminated rapeseed oil.

extract is the time consuming step. The isooctane wash could also be omitted although the ester bands (X) of the co-extracted glyceride would be very much stronger.

CONCLUSIONS

The analytical study presented in this paper shows that Spanish cooking oils associated with the epidemic in Madrid contain mixtures of oleic, linoleic, linolenic and stearic anilides. Such compounds can be formed by heating aniline with a rapeseed oil and the chromatographic and spectroscopic methods that have been used in this study would provide procedures suitable for screening for the presence of such compounds in contaminated oils.

REFERENCES

1 J. M. Tabuenca, *Lancet*, (1981) 567.
2 B. B. Wheals, *J. Liquid Chromatogr.*, 2 (1979) 91.
3 G. Dijkstra and A. P. de Junge, *Rec. Trav. Chim.*, 75 (1956) 1173.

Journal of Chromatography, 238 (1982) 217–225
Elsevier Scientific Publishing Company, Amsterdam — Printed in The Netherlands

CHROM. 14,566

HIGH-PERFORMANCE LIQUID CHROMATOGRAPHIC DETERMINATION OF CAROTENE AND VITAMIN A AND ITS GEOMETRIC ISOMERS IN FOODS

APPLICATIONS TO CHEESE ANALYSIS

BRUNO STANCHER* and FABIO ZONTA
Istituto di Merceologia, Università di Trieste, Via A. Valerio 6, 34127 Trieste (Italy)
(Received November 23rd, 1981)

SUMMARY

A fractionation of retinol geometric isomers and of carotene was achieved, by straight-phase high-performance liquid chromatography, using a LiChrosorb Si 60 5-μm prepacked column and an isocratic mobile phase of methyl ethyl ketone–hexane (10:90). The wavelengths selected for detection of carotene and retinols were 450 nm and 340 nm respectively, and were changed during the chromatographic run. Two internal standards were used for quantitative analysis: 2-nitrofluorene for retinols and azobenzene for carotene. The proposed method, which has the advantage that all vitamin A active compounds can be evaluated simultaneously, was applied to the analysis of Italian cheese samples. The percentage recoveries of retinol and carotene were 75.7 and 79.6, respectively, and were not affected by cheese fat content, at least in the explored range.

INTRODUCTION

The biological activity of vitamin A should be referred to two large classes of compounds: retinoids and carotenoids[1].

Retinoids, such as retinyl aldehyde, retinol (usually referred to as vitamin A), retinyl esters, retinoic acid and its esters and related derivatives and metabolites (*e.g.*, 4-keto- or 4-hydroxyretinoic acid), as well as retinoid geometric isomers were previously determined by means of high-performance liquid chromatography (HPLC)[2–5]. HPLC was successfully been applied also in the separation of carotenoids, such as α- and β-carotene, cryptoxanthin and lycopene[6–9]. Some papers dealt with the separation of both carotenoids and retinoids, in an attempt to determine all vitamin A active compounds together[9–11].

In a previous note[12], we reported the HPLC separation of retinol isomers; this paper deals with a simultaneous, rapid separation of retinol isomers and carotene, suggesting a new HPLC method for assaying total vitamin A activity in food samples with a single analysis.

2-Nitrofluorene is used as an internal standard for determining retinol isomers,

0021-9673/82/0000–0000/$02.75

and azobenzene is proposed for carotene. The procedure has been developed as a tentative general method for food samples; an application to three different samples of Italian cheeses (selected with high, average and low fat contents) is presented. A study of the percentage recoveries of retinol and carotene was performed and total vitamin A activity in cheese samples was estimated.

EXPERIMENTAL

Apparatus

The liquid chromatographic apparatus was as previously described[12].

A prepacked HPLC column of LiChrosorb Si 60, 5 μm (250 × 4 mm) (E. Merck, Darmstadt, G.F.R.), equipped with a precolumn dry-packed with 40-μm silica pellicular packing (Supelco, Bellefonte, PA, U.S.A.) was employed.

Reagents and materials

All-*trans*-retinol (puriss.), 2-nitrofluorene (purum) and azobenzene (puriss.) were purchased from Fluka (Buchs, Switzerland). The β-carotene (Type III, crystalline, natural from carrots; 10–20% α-isomer, 80–90% β-isomer) was obtained from Sigma (St. Louis, MO, U.S.A.).

The hexane used for extractions was extrapure (96% GC, E. Merck). All other solvents (hexane, methyl ethyl ketone, ethanol) were HPLC grade (E. Merck).

L-(+)-Ascorbic acid (cryst. extra pure) (E. Merck), potassium hydroxide pellets (GR, E. Merck), anhydrous sodium sulphate (RPE; Carlo Erba, Milan, Italy) and sodium chloride (AnalaR; BDH, Poole, Great Britain) were also employed.

The working solutions of standards were prepared in hexane containing 10% (v/v) of methyl ethyl ketone (the same as the eluting phase). The concentration of the standard solution of retinol and carotene used for the calibration graphs was 3.00 mg all-*trans*-retinol plus 0.60 mg β-carotene per 100 ml. The internal standard solution was 2.00 mg 2-nitrofluorene plus 28.00 mg azobenzene per 100 ml.

Sample preparation

A 10-g amount of fresh cheese, ground in a food chopper or cut very finely, were digested in a 250-ml centrifuge tube with 25 ml of distilled water, 50 ml of ethanol and 25 ml of potassium hydroxide aqueous solution (100 g KOH in 100 g water). A 0.5-g amount of ascorbic acid was added as antioxidant as previously proposed[13,14]. The centrifuge tube was flushed with nitrogen, sealed with Parafilm® and occasionally shaken. After alkaline digestion overnight[15], the suspension was centrifuged at 2000 *g* for 15 min. The supernatant was poured into a 500-ml separatory funnel and extracted four times (shaking for 2 min) with 50-ml portions of hexane. The pooled extracts were washed twice with 50 ml of a saturated NaCl solution and once with 50 ml of distilled water. The washed organic layer was filtered through a Whatman No. 1 filter-paper (containing 30 g of anhydrous sodium sulphate) into a 250-ml flask, and the filter was rinsed twice with 10-ml portions of hexane.

A 2.50-ml volume of the internal standard solution (2-nitrofluorene plus azobenzene) was added to the flask. The solution was concentrated by means of a rotary vacuum evaporator (water-bath temperature $\leqslant 40^{\circ}C$) to a volume of about 2 ml. The concentrated solution was transferred quantitatively into a 5-ml volumetric flask,

which was then filled to the mark with a 10% (v/v) solution of methyl ethyl ketone in hexane. A 25-μl volume of the sample thus obtained was used for chromatographic injection.

Cheese samples were chosen from among those listed in the Italian Gazzetta Ufficiale (Italian legal gazette) and were selected according to their fat content. Thus Parmigiano Reggiano (fat content 32%), Montasio (40%) and Taleggio (48%) were analyzed, with a view to exploring samples containing the lowest, average and the highest fat contents, in order to establish its influence on the recovery of retinol and carotene.

Chromatographic procedure

The isocratic eluent mixture consisted of 10% (v/v) methyl ethyl ketone in hexane. With an operating flow of 1 ml/min, the pressure drop was 4.3–4.5 MPa at room temperature (25°C). The detection wavelength, λ, was 450 nm for carotene and azobenzene. After the elution of azobenzene, λ was quickly shifted to 340 nm in order to detect 2-nitrofluorene and retinol isomers. With an injection of 25 μl of cheese extract solution, the sensitivity setting was 0.1 a.u.f.s. The chart speed was adjusted to 10 mm/min or to 60 mm/min as required to compute peak areas.

Data processing

Statistical analysis of data was performed with an Olivetti P6040 desk calculator. The linearity of the calibration graphs was tested by the analysis of the variance (ANOVA) for the regression, using R^2 and F ratios as criteria of adequacy[16]. R^2 is the ratio between the sum of squares attributable to regression and the total sum of squares, and F is the ratio between the variance attributable to regression and the variance attributable to deviation from regression.

RESULTS AND DISCUSSION

Peak identification

Fig. 1 shows the chromatogram obtained with an injection of a test solution.

Peak identification of retinol, its isomers and 2-nitrofluorene has been accomplished according to the procedure described previously[12]. Owing to the fact that UV-cut-off of methyl ethyl ketone occurs at 330 nm, with this eluent it is obviously not possible to record UV spectra of eluting peaks at lower wavelengths. The identification of retinol isomer peaks was therefore based on the cited reference as well as on their relative retention times.

Carotene and azobenzene were identified by means of the stop flow method, recording their absorption spectra (see Fig. 2).

Internal standards

The use of 2-nitrofluorene as the internal standard for quantitation of retinol was discussed previously[12].

Azobenzene is proposed as internal standard for quantitation of carotene, since both these compounds show an absorbance maximum in the region of 450 nm and their chromatographic peaks are well resolved. The internal standard solution must be freshly prepared. On standing, azobenzene isomerizes into the *cis*-form which is detectable in chromatograms of aged internal standard solutions.

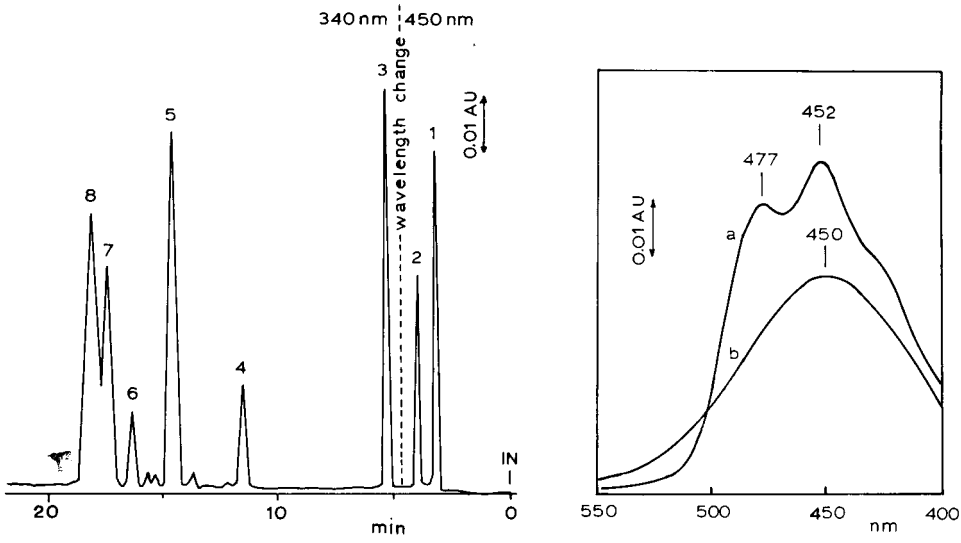

Fig. 1. Chromatogram of a test mixture of retinol geometric isomers, carotene and internal standards. Column. 5-μm Si 60 (250 × 4 mm) with precolumn, 40-μm pellicular silica (50 × 4 mm). Mobile phase: isocratic mixture of methyl ethyl ketone–hexane (10:90). Temperature: 25° C. Flow-rate: 1 ml/min. Pressure drop: 4.5 MPa. Detection wavelengths: 450 and 340 nm. Recorder sensitivity: 0.1 a.u.f.s. Chart speed: 10 mm/min. Peaks: 1 = carotene; 2 = azobenzene; 3 = 2-nitrofluorene; 4 = 11,13-di-*cis*-retinol; 5 = 13-*cis*-retinol; 6 = 9,13-di-*cis*-retinol; 7 = 9-*cis*-retinol; 8 = all-*trans*-retinol.

Fig. 2. Absorption spectra of β-carotene (a) and azobenzene (b). Spectra were recorded in a 8-μl spectrophotometer cell with the stop-flow method. Solvent system: methyl ethyl ketone–hexane (10:90).

Calibration graphs

Solutions used for construction of the calibration graphs were obtained as follows: aliquots of retinol plus carotene standard solution were added to 10-ml volumetric flasks containing 5.00 ml of internal standard solution; the flasks were then filled to the mark with 10% (v/v) methyl ethyl ketone in hexane. After chromatography of these solutions, calibration graphs were obtained by plotting the ratios A_R/A_{S1} and A_C/A_{S2} *versus* the concentrations of retinol and carotene respectively (A_R = retinol peak area; A_C = carotene peak area; A_{S1} = 2-nitrofluorene peak area; A_{S2} = azobenzene peak area).

The calibration graphs are shown in Fig. 3. They are linear over the explored range of concentration. Table I shows the values of the parameters a and b of the equation $y = a + bx$, where y is the ratio (analyte peak area/internal standard peak area) and x is the concentration, expressed in mg per 100 ml. The values of the standard deviation of the slope, s_b, and of the intercept, s_a, as well as F- and R^2-test values are also reported.

Cheese analysis

Analysis of cheese was performed by the standard-addition technique. Identical cheese samples were added of known quantities of retinol and carotene before starting the alkaline digestion. Analyses were carried out in quintuplicate, with four samples added with four different aliquots of analytes and one with no addition. Internal stan-

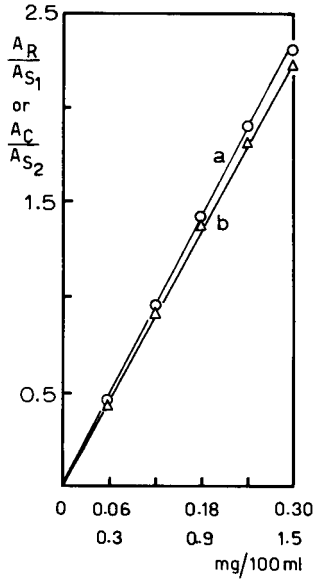

Fig. 3. Calibration graphs of carotene (a) and all-*trans*-retinol (b). Graph a shows A_C/A_{S2} *versus* concentration of carotene (upper scale on x axis); A_C = carotene peak area, A_{S2} = azobenzene peak area. Graph b shows A_R/A_{S1} *versus* concentration of retinol (lower scale on x axis); A_R = all-*trans*-retinol peak area, A_{S1} = 2-nitrofluorene peak area.

TABLE I

VALUES OF a, b, s_a, s_b, OF F AND R^2 TESTS AND OF PERCENTAGE RECOVERIES ($Q \pm s_Q$)

The values refer to the calibration graphs of retinol and carotene and to the standard-addition technique graphs of the analytes to three different cheese samples. As $y = a + bx$ is the general equation of the graphs, s_a and s_b represent the standard deviation of the intercept and of the slope respectively. s_Q is the standard deviation of the percentage recovery of analyte in the sample considered. Recovery values are obtained dividing b values of samples by the corresponding b value of the calibration graph. Cheese samples: 1 = Parmigiano Reggiano; 2 = Montasio; 3 = Taleggio.

	a	s_a	b	s_b	F	R^2	$Q \pm s_Q$
Retinol							
Calibration	0.001	0.022	1.503	0.022	4658	0.9993	
Cheese sample 1	0.666	0.024	1.135	0.025	2079	0.9985	75.5 ± 2.0
2	0.532	0.021	1.142	0.022	2756	0.9989	76.0 ± 1.8
3	0.566	0.024	1.138	0.024	2180	0.9986	75.7 ± 1.8
Carotene							
Calibration	0.012	0.016	7.766	0.080	2142	0.9986	
Cheese sample 1	2.230	0.028	6.153	0.143	1850	0.9984	79.2 ± 1.1
2	2.769	0.028	6.137	0.143	1838	0.9984	79.0 ± 1.0
3	1.864	0.038	6.270	0.156	1608	0.9981	80.7 ± 1.9

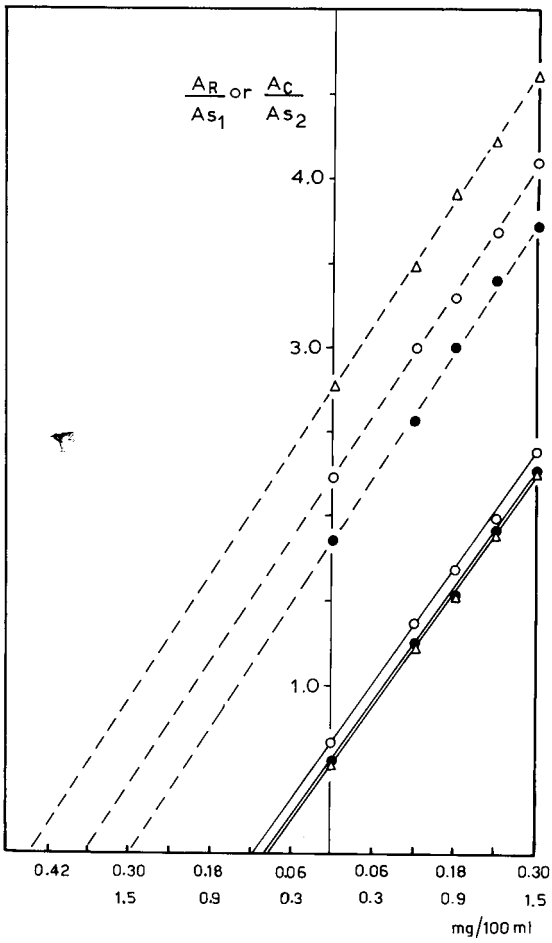

Fig. 4. Graphs obtained by means of the standard-addition technique of analytes to cheeses. x and y axes as in Fig. 3. Dotted lines refer to carotene, continuous lines to retinol. Cheeses: ○, Parmigiano Reggiano; ●, Taleggio; △, Montasio.

dards were also added (see *Sample preparation*) and at the end of the procedure the ratios A_R/A_{S1} and A_C/A_{S2} were plotted *versus* the known concentrations of added analytes. These graphs are shown in Fig. 4 and their parameters are listed in Table I. The quantities of retinol and carotene in a sample with no analytes added are then given by the intercepts of the graphs with the x axis.

Since the graphs obtained using the standard-addition technique were linear in the explored range of concentrations, the recovery of the analytes is unaffected by their concentrations. Furthermore, percentage recoveries of the analytes can be obtained by dividing the slope of these graphs by the slopes of the calibration graphs. Percentage recoveries were found to be unaffected by the fat content of cheese in the explored range (from 32 to 48%) since the slopes of the standard-addition graphs of different cheese samples were equal within the experimental error (see Table I). It follows that, in routine analysis of samples, it is possible to perform tests simply as

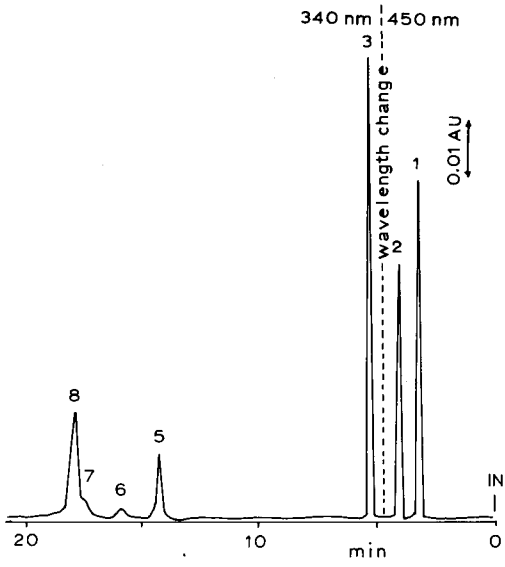

Fig. 5. Chromatogram of a Taleggio cheese extract. Chromatographic conditions and peak identification as in Fig. 1. 25 μl injected.

stated in *Sample preparation*. The quantities of analytes are obtained by comparing the values of A_R/A_{S1} and A_C/A_{S2} with those of the calibration graphs, and multiplying the obtained values by the known percentages recoveries.

Fig. 5 shows, as an example, the chromatogram obtained with the extract from a sample of Taleggio cheese. Peak 5 demonstrates the presence of 13-*cis*-retinol. Other retinol isomers (peak 6, 7) present in small amounts were not taken into account considering their low biological activity.

Retinols

Owing to the alkaline digestion of the sample, only retinols are detected because esters are completely hydrolyzed into alcohols. The completeness of this hydrolysis is indicated (as previously suggested[14]) by the lack of any ester peak in the chromatograms.

Since retinol geometric isomers have been found to have different biological activities[1], and the 13-*cis*-isomer has already been reported as naturally occurring in foods[14], it is advisable to quantify retinol separately from its isomers. The absorptivity ratio (1.08) of all-*trans*- to 13-*cis*-retinol at 328 nm has been used to calculate the 13-*cis*-retinol content[14]. Referring to available literature data[17,18], it can be seen that at 340 nm the absorptivity ratio of all-*trans*- to 13-*cis*-retinol is very close to 1.0. Therefore there is no need for any correction factor in order to quantitate these two isomers at this wavelength.

Carotenes

Owing to the great polarity difference between carotenes and retinols, the difficulty in resolving carotene isomers together with retinol isomers is not unexpected. Under the adopted chromatographic conditions, carotene is eluted very early,

TABLE II

CHEESE CONTENTS OF ALL-*trans*-RETINOL, 13-*cis*-RETINOL AND CAROTENE

Values for 13-*cis*-retinol and carotene equivalent to the biological activity of all-*trans*-retinol, as well as the resultant total vitamin A activity, are reported (in Italics). All values are expressed in μg per 100 g of fresh cheese.

Cheese	*Sample 1 (Parmigiano Reggiano)*	*Sample 2 (Montasio)*	*Sample 3 (Taleggio)*
All-*trans*-retinol	*293*	*233*	*249*
13-*cis*-Retinol	53	130	117
13-*cis*-Retinol × 0.75 (all-*trans*-retinol equivalents)	*39.7*	*97.5*	*87.7*
Carotene	181	225	149
Carotene × 1/6 (all-*trans*-retinol equivalents)	*30.1*	*37.5*	*24.8*
Total vitamin A activity	*363*	*368*	*361*

and no separation of α- and β-carotene can be achieved. Therefore only total carotene is determined with the proposed method.

Evaluation of total vitamin A active compounds

13-*cis*-Retinol is only 75% as active as all-*trans*-retinol[1], and it is necessary to multiply the weight of the former by 0.75 to obtain the equivalent weight of the latter. Vitamin A activity is then given by:

$$\mu g \text{ of retinol equivalents} = \mu g \text{ of all-}trans\text{-retinol} + 0.75 \cdot \mu g \text{ of 13-}cis\text{-retinol}$$

Considering only the more common and wide spread carotenoids, those which exhibit a vitamin A activity in mammals can be narrowed down to three species: α-carotene, β-carotene and cryptoxanthin[6]. To evaluate their vitamin A activity, the following formula was proposed[7]:

$$\mu g \text{ of retinol equivalents} = (\mu g\ \beta\text{-carotene})/6 + (\mu g\ \alpha\text{-carotene})/12 + (\mu g\ \beta\text{-cryptoxanthin})/12.$$

Parrish[19], referring specifically to margarine and butter, took into account only total carotene, and the above formula thus simplifies to: μg of retinol equivalents = (μg carotene)/6.

Total vitamin A activity, of retinols and carotene is then given by:

$$\mu g \text{ of retinol equivalents} = \mu g \text{ of all-}trans\text{-retinol} + 0.75 \cdot \mu g \text{ of 13-}cis\text{-retinol} + (\mu g \text{ of carotene})/6.$$

Table II reports the values for all-*trans*-retinol, 13-*cis*-retinol and carotene, and the resulting total vitamin A activity found in the considered cheese samples.

REFERENCES

1 W. H. Sebrell, Jr. and R. S. Harris, *The Vitamins*, Vol. II, Academic Press New York, 2nd ed., 1967.
2 C. D. B. Bridges, S. L. Fong and R. A. Alvarez, *Vision Res.*, 20 (1980) 355.
3 B. A. Halley and E. C. Nelson, *J. Chromatogr.*, 175 (1979) 113.
4 J. E. Paanakker and G. W. T. Groenendijk, *J. Chromatogr.*, 168 (1979) 125.
5 A. M. McCormick, J. L. Napoli and H. F. DeLuca, *Methods Enzymol.*, 67 (1980) 220.
6 S. K. Reeder and G. L. Park, *J. Ass. Offic. Anal. Chem.*, 58 (1975) 595.
7 I. Stewart, *J. Ass. Offic. Anal. Chem.*, 60 (1977) 132.
8 A. Fiksdahl, J. T. Mortensen and S. Liaaen-Jensen, *J. Chromatogr.*, 157 (1978) 111.
9 T. Van de Weerdhof, M. L. Wiersum and H. Reissenweber, *J. Chromatogr.*, 83 (1973) 455.
10 W. O. Landen, Jr. and R. R. Eitenmiller, *J. Ass. Offic. Anal. Chem.*, 62 (1979) 283.
11 W. O. Landen, Jr., *J. Chromatogr.*, 211 (1981) 155.
12 B. Stancher and F. Zonta, *J. Chromatogr.*, 234 (1982) 244.
13 D. B. Parrish, *CRC Crit. Rev. Food Sci. Nutr.*, 9 (1977) 375.
14 D. C. Egberg, J. C. Heroff and R. H. Potter, *J. Agr. Food Chem.* 25 (1977) 1127.
15 J. N. Thompson, W. B. Maxwell and M. L'Abbe', *J. Ass. Offic. Anal. Chem.*, 60 (1977) 998.
16 N. R. Draper and H. Smith, *Applied Regression Analysis*, Wiley, New York, 1966, 7.
17 R. Hubbard, *J. Amer. Chem. Soc.*, 78 (1956) 4662.
18 C. D. Robeson, J. D. Cawley, L. Weisler, M. H. Stern, G. C. Eddinger and A. J. Chechak, *J. Amer. Chem. Soc.*, 77 (1955) 4111.
19 D. B. Parrish, *J. Ass. Offic. Anal. Chem.*, 63 (1980) 468.

Journal of Chromatography, 238 (1982) 226–231
Elsevier Scientific Publishing Company, Amsterdam — Printed in The Netherlands

CHROM. 14,653

Note

Apparatus for the recovery of proteins from polyacrylamide gels during electrophoresis

M. FAUPEL*, M. DE GASPARO and E. VON ARX
Chemical and Biological Research Laboratories, Pharmaceuticals Division, Ciba-Geigy Limited, CH-4002 Basle (Switzerland)

(Received December 15th, 1981)

Disc electrophoresis is used extensively[1] as a sensitive technique for the analysis of biological materials. To overcome the major problem associated with this technique, *viz.*, the elution of separated compounds from the gel, we have devised a disc electrophoresis elution apparatus that permits the recovery, during electrophoresis, of materials which are then readily available for further characterization. We have demonstrated its efficiency in the separation of the two insulins of rat pancreas extracts.

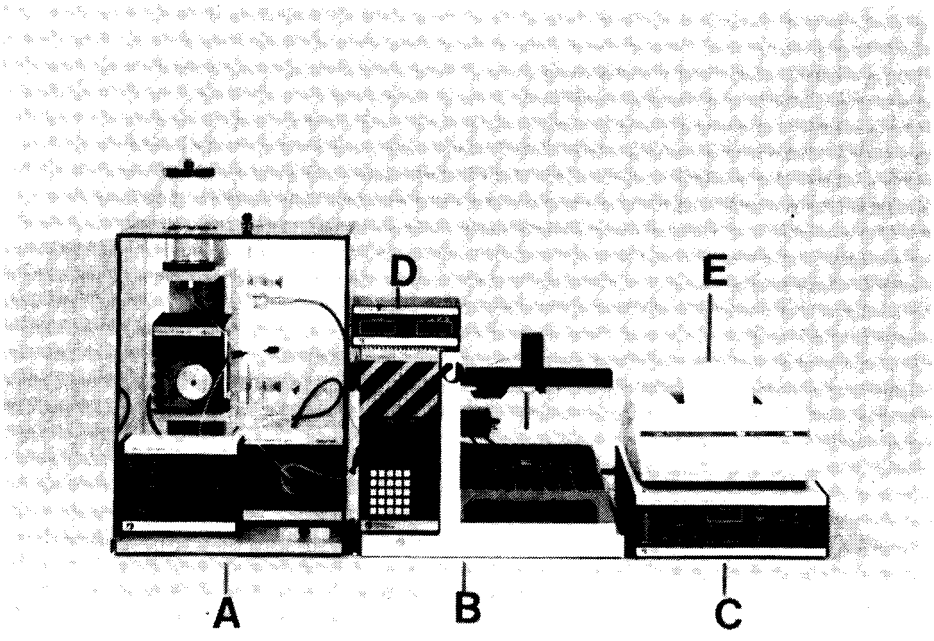

Fig. 1. (A) Separation unit detailed in Figs. 3 and 4; (B) fraction collector; (C) electrophoresis constant power supply; (D) volt–hour integrator; (E) Hewlett-Packard recorder.

0021-9673/82/0000–0000/$02.75

EXPERIMENTAL

Chemicals

All chemicals were of analytical-reagent grade from Fluka (Buchs, Switzerland). Rat insulins were obtained from the Novo Research Institute (Bagswerd, Denmark).

Apparatus

The disc electrophoresis apparatus (Fig. 1) consists of a glass tube (Fig. 2) inserted in two buffer chambers containing the electrodes (Fig. 3) and connected to a peristaltic pump (Pharmacia P.1), a buffer reservoir and a detection system consisting of an optical unit (Pharmacia UV-1 single path monitor, a control unit (Fig. 4) (Pharmacia single path monitor), a recorder (Hewlett-Packard 3390A integrator) and a fraction collector (Pharmacia FRAC-300). The electrophoresis constant-power

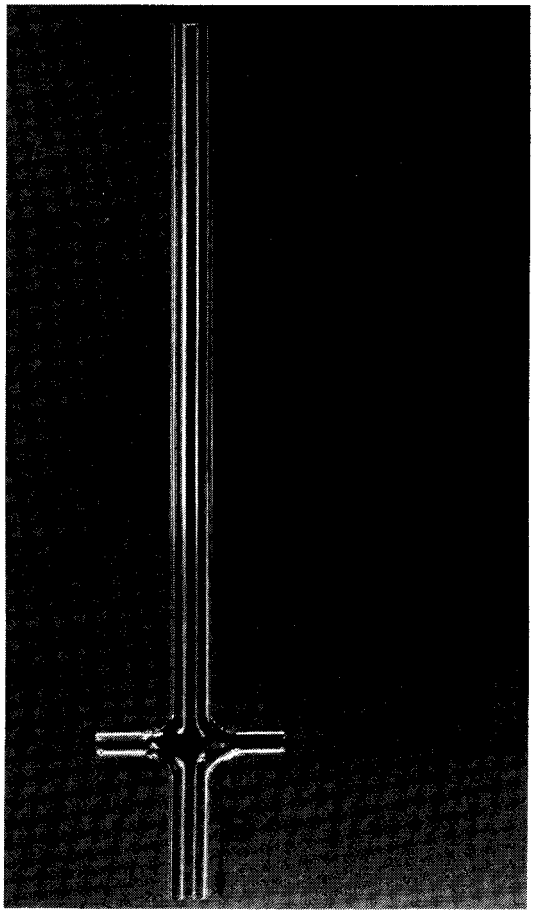

Fig. 2. Glass tube. (A) Upper part (containing the "separating gel"); (B) lower part (containing the "plug gel"); (C) elution channel.

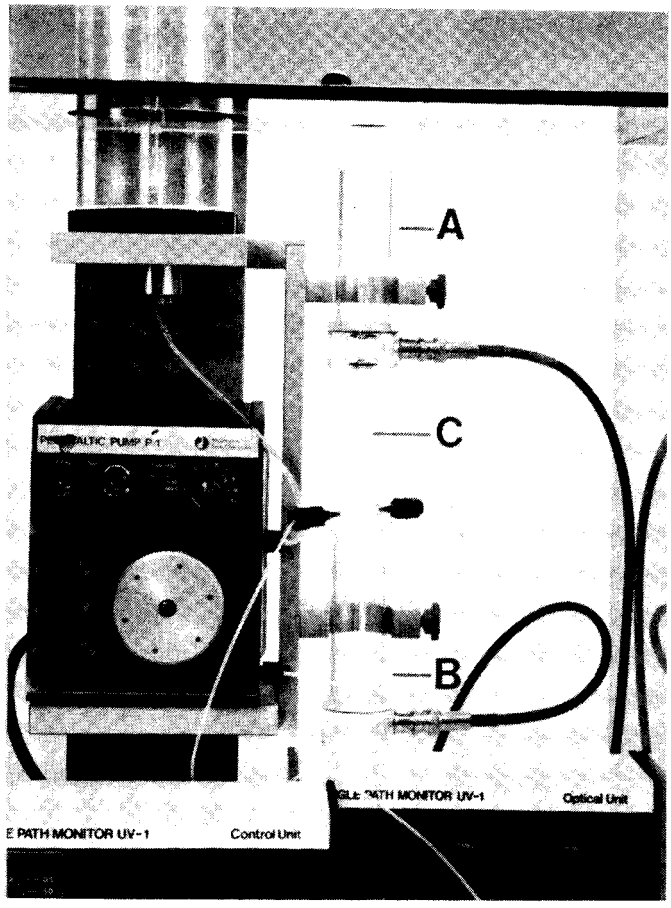

Fig. 3. (A) Upper electrode chamber; (B) lower electrode chamber; (C) glass tube.

supply (Pharmacia ECPS 3000/150) was connected to a volt–hour integrator (Pharmacia VH-1).

Polyacrylamide gels

The lower part of the tube was sealed with Parafilm foil and filled to a height of 2.5 cm with plug gel consisting of 40% acrylamide, 0.02% bisacrylamide and 0.375 *M* Tris–HCl (pH 8.3), which was polymerized with 9 μl of N,N,N′,N′-tetramethylethylenediamine (TEMED) and 30 μl of 10% ammonium persulphate solution. The gel was overlayed with circulating buffer, which was removed after polymerization. The elution channel (Fig. 2A) was filled with a mixture of 50% glycerol in circulating buffer. The separating gel, consisting of three gels as described by Rall *et al.*[2], was introduced and overlayed with pH 8.3 buffer during polymerization. The channel solution was finally washed out with elution buffer.

Electrophoresis conditions

A 100-μg amount of Novo rat insulin was dissolved in 50 μl of pH 8.3 buffer

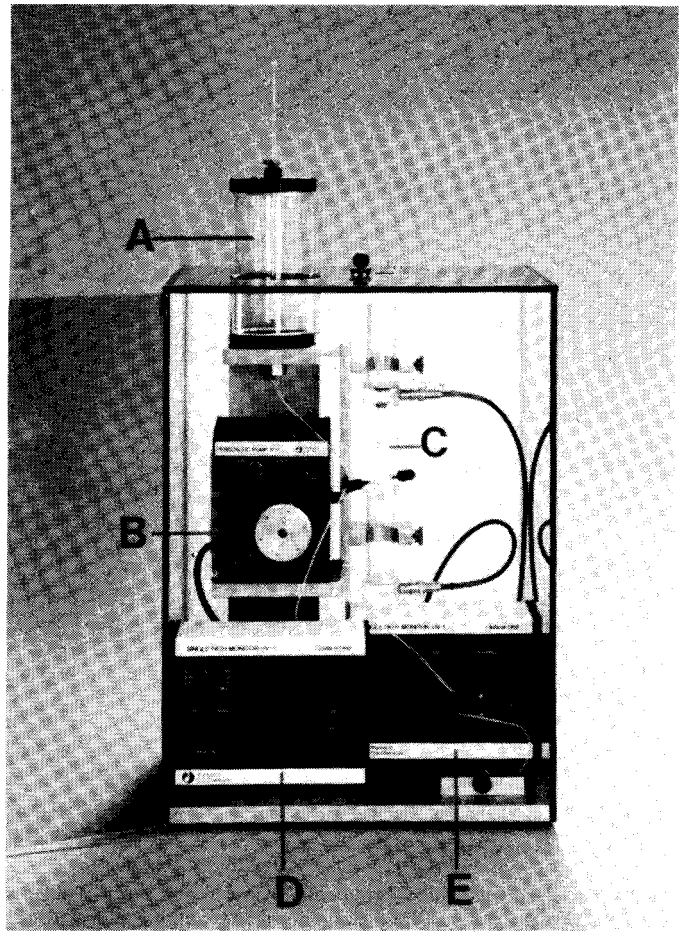

Fig. 4. (A) Buffer reservoir; (B) peristaltic pump; (C) glass tube; (D) control unit; (E) optical unit.

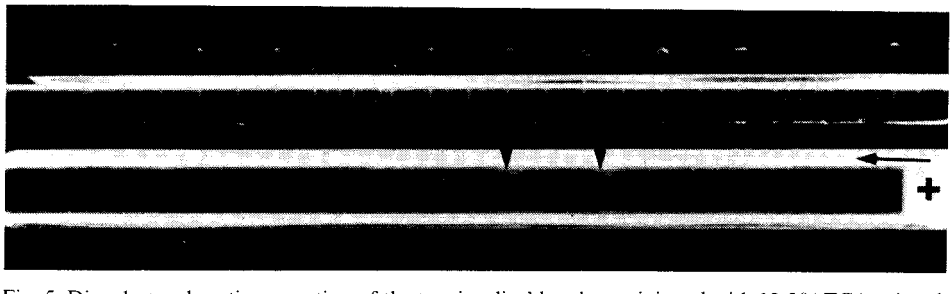

Fig. 5. Disc electrophoretic separation of the two insulins' bands precipitated with 12.5% TCA using the method of Rall *et al.*[2].

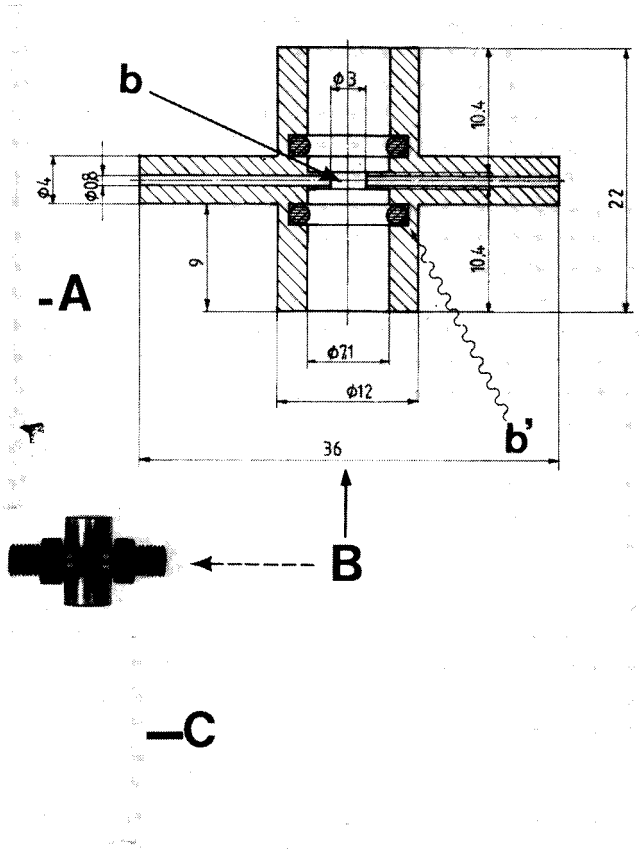

Fig. 6. Fine calibre cell. (A) Standard borosilicate glass tube (containing the separating gel); (B) detailed calibre cell, (b) elution channel and (b') O-ring; (C) borosilicate glass tube (containing the plug gel).

and applied with a Hamilton syringe on top of the gel (cathode side). This solution was overlayed with 0.01 % bromophenol blue solution containing 6 *M* urea (50 μl). The degassed electrode buffer and the degassed circulating buffer respectively contained a 10 % and 5 % solution of 6.0 g of Tris and 28.8 g of glycine in 1 l of water. Electrophoresis was carried out at 2 mA for 10 h.

RESULTS AND DISCUSSION

Fig. 5 shows the disc electrophoretic separation of the two insulins' bands precipitated with 12.5 % trichloroacetic acid (TCA) in a separated gel (4 h running time) and demonstrates the excellent reproducibility of the work of Rall *et al.*[2].

The blue band of bromophenol blue was eluted after 4 h. From experience, we know that the first band of insulin reaches the elution channel after 8 h. The UV photometer was then started and 1-ml fractions were collected at 254 nm. The second band was collected in the same way. The eluted fractions were analysed, after separation of buffer on Pharmacia PD-10 columns and concentration, by high-performance

thin-layer chromatography on cellulose (Merck) with 1-butanol–pyridine–water–acetic acid (34:25:12:30) as eluent. For detection, Pauly's reagent[3] and N,N,N′,N′-tetramethyl-4,4′-diaminodiphenylmethane[4] were used. This apparatus is of great potential value for the purification and recovery of proteins after isoelectric focusing[5]. A new narrow bore cell (Fig. 6) has been developed to optimize its use for establishing the biosynthesis and secretion of mutant (functionally defective) insulins responsible for insulinopathies[6–9].

ACKNOWLEDGEMENTS

We thank M. Vernier, K. Wagner for constructing the apparatus, J. Kieffer and G. Hostetter for technical assitance and K. Kuhn for making the glass tube.

REFERENCES

1 R. C. Allen and H. R. Maurer, *Electrophoresis and Isoelectric Focusing in Polyacrylamide Gel*, Walter de Gruyter, Berlin, New York, 1974.
2 L. B. Rall, R. L. Pictet and W. J. Rutter, *Endocrinology*, 105 (1978) 835.
3 M. Faupel and E. von Arx, *J. Chromatogr.*, 157 (1978) 253.
4 E. von Arx, M. Faupel and M. Brugger, *J. Chromatogr.*, 120 (1976) 224.
5 M. Faupel and M. de Gasparo, *Diabetologia*, 21 (1981) 269 (abstract).
6 H. Tager, B. Given, D. Baldwin, M. Mako, J. Markese and A. Rubinstein, *Nature (London)*, 281 (1979) 122.
7 G. R. Milner, M. de Gasparo, R. Kay and R. D. G. Milner, *J. Endocrinol.*, 82 (1979) 179.
8 S. J. Chan and D. F. Steiner, *Trends Biochem. Sci.*, 2 (1977) 254.
9 K. H. Gabbay, *N. Eng. J. Med.*, 302 (1980) 165.

Journal of Chromatography, 238 (1982) 232–236
Elsevier Scientific Publishing Company, Amsterdam – Printed in The Netherlands

CHROM. 14,579

Note

Devices for packing preparative chromatographic columns by "dry-packing" techniques

KRYSTYNA PRUSIEWICZ*, MARIAN KAMIŃSKI and JAN KLAWITER
Institute of Inorganic Chemistry and Technology, Technical University of Gdańsk, 80-952 Gdańsk (Poland)
(Received October 12th, 1981)

Column packings with particle diameters over 25 μm are still widely used in liquid chromatography, especially for preparative purposes, since they are considerably cheaper than the high-performance packings having smaller particles. Packing of columns with packing of such large size is generally carried out by so-called "dry-packing" methods. It follows from previous papers[1–6] that the material used as column packing should be introduced uniformly onto the entire cross-sectional area of the column. Such operations as column vibrating or tapping are frequently automated[3,4,6]. Similarly, feeding the packing to columns during filling can be automated and should considerably improve the reproducibility of filling.

This paper describes devices for filling columns which should be useful in many chromatographic laboratories.

The following column packing techniques were taken into consideration:

(1) tap-fill method, found[6] to be optimal when using a tapping frequency of 120 min^{-1} and column drop from a height of 2 cm

(2) vibration method, optimal at a frequency of *ca.* 1 kHz and acceleration of 5 *g* (ref. 6). Two methods of feeding the packing were investigated.

(1) from the packer shown in Fig. 1a, attached to the column packed by the tap-fill method

(2) from the packer shown in Fig. 1b, undergoing transverse vibrations of frequency 50 Hz, coupled to the column packed vibrationally. Perforated plates (0.1 mm thick) with holes distributed as shown in Fig. 1b or gauzes with various mesh sizes were placed in both cases at the bottom of the packer containers. In order to ensure uniform distribution of silica gel, the perforated plates had seven, three and one hole for the columns of diameter 52, 16.8 and 2–8 mm, respectively.

The following particle fractions of silica gel were used; $\bar{d} = 33$ μm, 65 μm, 124 μm and 240 μm, where $\bar{d}_p$ is the average particle diameter according to Krumbein[7]. More detailed granulometric characteristics of these packings will be presented elsewhere[6].

The results of investigations of the effect of the hole diameter in perforated plates or the mesh size in gauzes on the packing feeding rate for each method of column filling are shown in Figs. 2–4.

On the basis these results it was found that:

(1) the use of the packing devices shown in Fig. 1 for filling columns by tap-fill

0021-9673/82/0000-0000/$02.75

and vibration methods ensures good reproducibility of the mass feeding rate, particularly for particle fractions with $\bar{d}_p$ = 124 μm and 240 μm.

(2) slightly worse reproducibility was obtained when using packing fractions with $\bar{d}_p$ = 33 μm and 65 μm. This is probably due to the presence in these fractions of particles with diameters less than 15 μm, which are usually introduced by "slurry packing" techniques

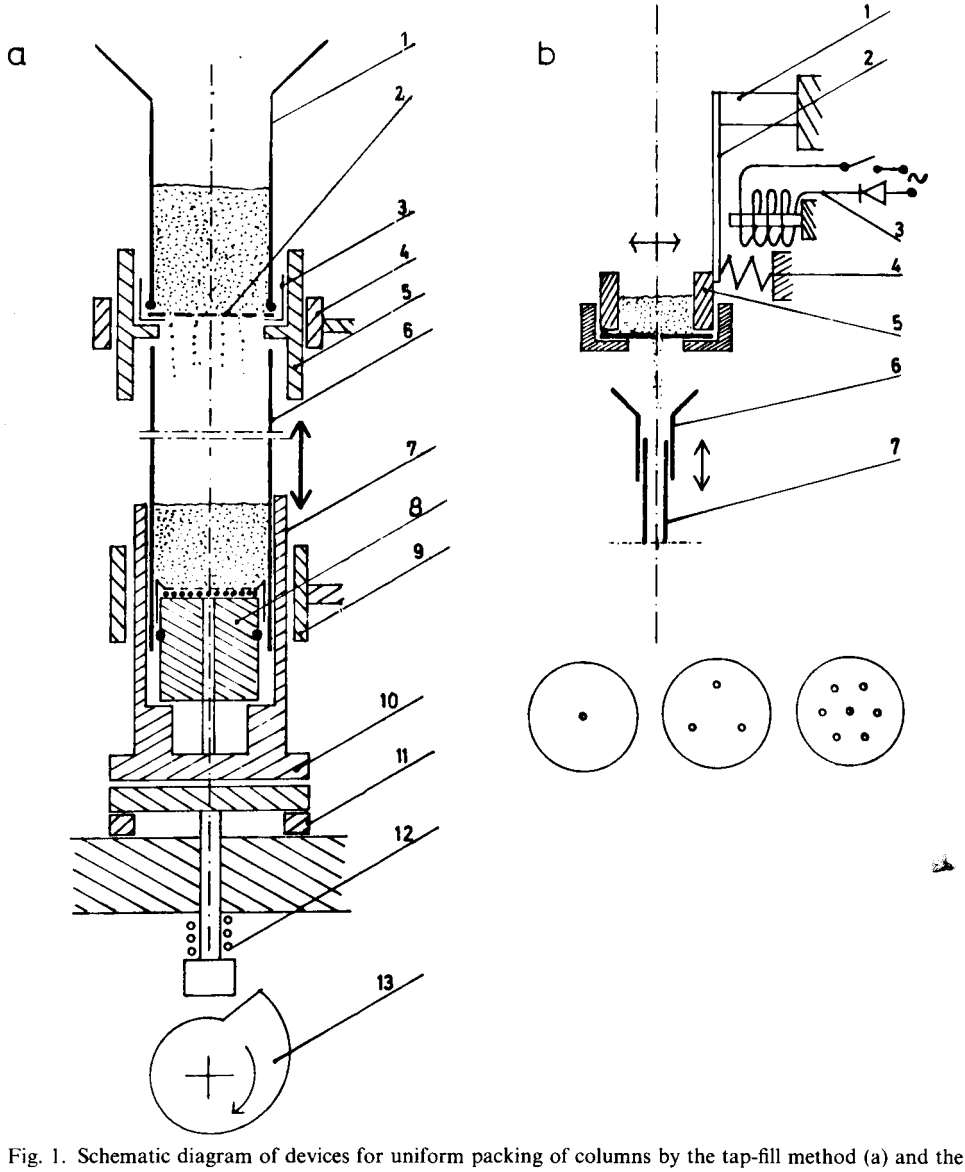

Fig. 1. Schematic diagram of devices for uniform packing of columns by the tap-fill method (a) and the vibration method (b). a, 1 = Container; 2 = perforated plate, 0.1 mm thick; 3 = nut; 4,9 = guiding rings; 5 = coupling; 6 = columns; 7 = nut; 8 = outlet head; 10 = sliding table; 11 = hard rubber washer; 12 = spring; 13 = motor-driven cam. b, 1 = Holder; 2 = elastic plate; 3 = electric circuit 6.3 V a.c. with electromagnet; 4 = spring; 5 = container; 6 = funnel; 7 = column.

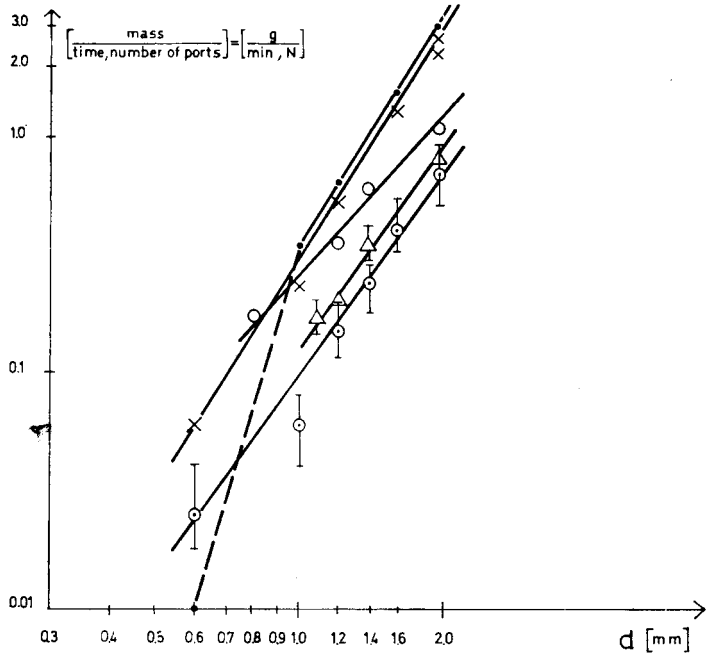

Fig. 2. The effect of hole diameter, d, of the perforated plate on the mass feeding rate of silica gel to chromatographic columns filled by the tap-fill method (Fig. 1a). $\bar{d}_p$ = 240 μm (●), 124 μm (×) or 33 μm (⊙) for columns of diameter 2.8 and 17 mm; 33 μm (○) for columns of diameter 52 mm; 65 μm (△).

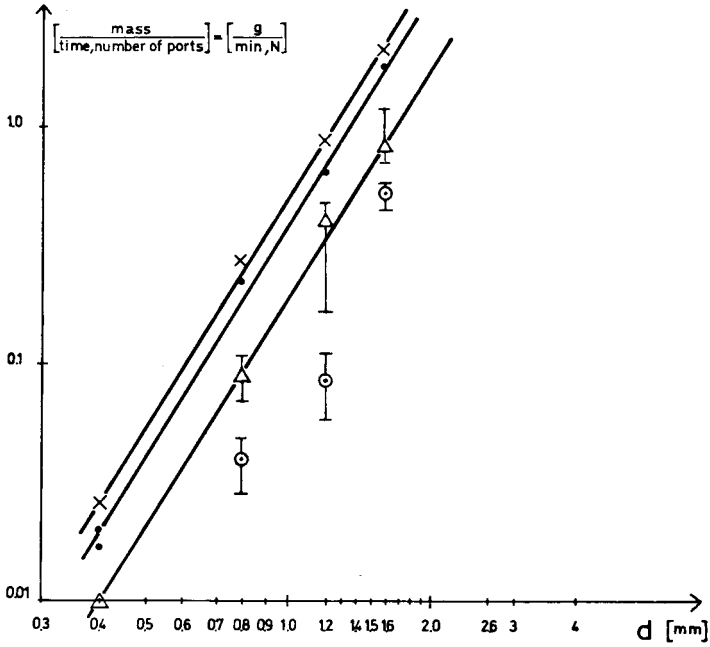

Fig. 3. The effect of hole diameter, d, of the perforated plate on the mass feeding rate of silica gel to chromatographic columns filled by the vibration method (Fig. 1b) $\bar{d}_p$ = 240 μm (●), 124 μm (×), 65 μm (△) and 33 μm (⊙).

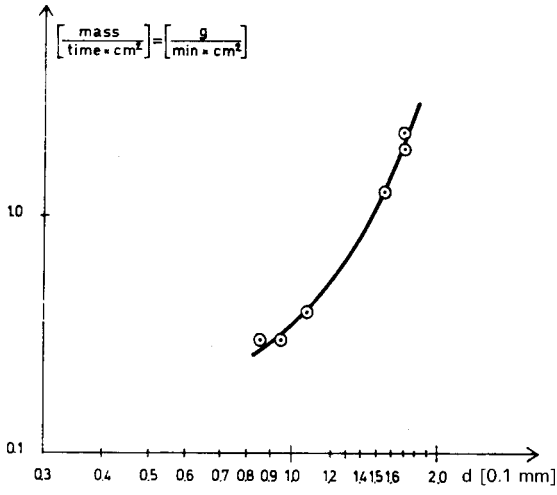

Fig. 4. The effect of gauze mesh size, d, on the mass feeding rate of silica gel with $\bar{d}_p = 33$ μm to chromatographic columns filled by the tap-fill method (Fig. 1a).

(3) the average density of the packing for columns filled by the tap-fill method was 0.56 g/cm^3

(4) in order to achieve favourable filling conditions the height of the bed of packing in the container should be constant, the actual value being immaterial for fractions with $\bar{d}_p = 124$ and 240 μm, whereas for fractions with $\bar{d}_p = 65$ and 33 μm the optimal height was 20 μm

(5) the use of perforated plates with hole diameters lower than 1.2 mm had a deleterious effect on the reproducibility of the results, even for the smallest particles with $\bar{d}_p = 33$ mm

(6) no effect of column diameter on the feeding rate of packings of the silica gel type was observed with the exception of the particle fraction with $\bar{d}_p = 33$ μm fed to a column of diameter 52 mm packed by tap-fill method. An increase in tapping intensity through increase of column mass resulted in an increase in feeding rate.

(7) no difference in the efficiency of columns of diameter 52 mm packed by the tap-fill method was observed when packings of a given particle size were introduced at the same feeding rate, using at the bottom of the packer a gauze or a perforated plate with seven holes

(8) employing in the packer the plate with not less than one hole per 3 cm^2 of cross-sectional area of the column ensures homogeneity of the packing, as evidenced by the symmetrical peaks of test substances. Analogous results were obtained with a gauze.

In conclusion, the experimental results permit one to predict and adjust the feeding rate of packings of the silica gel type through the choice of diameter and number of holes in a perforated plate. Presumably the packing methods described will also be useful for other types of packings, *e.g.*, alumina and magnesium oxide. In addition, it seems probable that these packers can also be employed for filling columns by other "dry-packing" methods.

REFERENCES

1 J. C. Giddings and E. N. Fuller, *J. Chromatogr.*, 7 (1962) 255.
2 J. Halász and M. Naefe, *Anal. Chem.*, 44 (1972) 76.
3 S. T. Sie and N. van den Hoed, *J. Chromatogr. Sci.*, 7 (1969) 257.
4 J. N. Done and J. H. Knox, *J. Chromatogr. Sci.*, 10 (1972) 606.
5 J. Halász, *Z. Anal. Chem.*, 277 (1975) 257.
6 J. Klawiter, M. Kamiński and J. S. Kowalczyk, *J. Chromatogr.*, 241 (1982) in press.
7 M. Beyer (Editor), *Handbuch der Mikroskopie*, Verlag Technik VEB, Berlin, 1973.

Journal of Chromatography, 238 (1982) 237–240
Elsevier Scientific Publishing Company, Amsterdam — Printed in The Netherlands

CHROM. 14,613

Note

Configurational analysis and test of racemization of N-methylamino acids by capillary gas chromatography

WILFRIED A. KÖNIG*, INGRID BENECKE and JÜRGEN SCHULZE
Institut für Organische Chemie und Biochemie der Universität, D-2000 Hamburg 13 (G.F.R.)
(Received December 4th, 1981)

Although N-methylamino acids are frequently encountered in natural compounds, especially as constituents of peptide antibiotics[1,2], the identification of their configuration has so far been possible only by comparison of their optical rotation with that of reference compounds[2] or by NMR spectroscopy[3]. An even more difficult problem is the determination of the degree of racemization of N-methylamino acids during various steps of peptide synthesis. It has been reported that N-methylamino acids give significant racemization during peptide bond formation[4,5].

For configurational analysis of amino acids sensitive gas chromatographic methods have been developed. Direct separation of enantiomers on optically active stationary phases has proved to be a particularly valuable tool[6–9]. Esterification and N-acylation are necessary for converting amino acids into volatile derivatives suitable for separation of enantiomers. When these reactions are applied to N-methylamino acids the expected derivatives are not obtained, but an intramolecular redox reaction occurs and cyclic alkylidene-oxazolidin-5-ones are formed[10]. In these compounds the hydrogen atom of the asymmetric centre is rearranged to yield a racemate of the heterocyclic compound. The enantiomers of N-methylamino acid esters without an N-acyl group are not separated on chiral phases.

In this paper we describe a procedure for the separation of diastereomeric (+)-3-methyl-2-butyl esters of N-methylamino acids by capillary gas chromatography.

EXPERIMENTAL

Materials

N-Methylamino acids were prepared from L- and DL-amino acids according to the procedure of McDermott and Benoiton[11]. (+)-3-Methylbutan-2-ol was prepared as described by Halpern and Westley[12]. Reagents for trimethylsilylation and for deactivation of capillary columns were purchased from Regis Chemical Co. (U.S.A.) and Machery, Nagel & Co. (Düren, G.F.R.).

Formation of derivatives

The (+)-3-methyl-2-butyl esters of N-methylamino acids were obtained according to the procedure described previously[13].

0021-9673/82/0000–0000/$02.75

Gas chromatography

For the separation of diastereomeric esters of N-methylamino acids 25-m fused silica and Pyrex glass columns coated with CpSil-5 (Chrompack, Berlin, G.F.R.) and SE-30AMAC (Franzen Analysentechnik, Bremen, G.F.R.) and a Model 2101 gas chromatograph (Carlo Erba, Milan, Italy), were used.

RESULTS AND DISCUSSION

The separation of diastereomeric derivatives has been suggested as an alternative to direct separation of enantiomers. We have shown that N-acylated amino acid (+)-3-methyl-2-butyl esters are well separated on capillary columns[13]. The precision of this method depends mainly on the optical purity of the chiral reagent. (+)-3-Methylbutan-2-ol can be prepared in about 99% optical purity.

Gas chromatography of N-methyl-DL-amino acid (+)-3-methyl-2-butyl esters gave unsymmetrical, tailing peaks and incomplete separations, even on highly deactivated fused silica capillaries. We therefore tried to reduce the polarity of the derivatives by N-trimethylsilylation. Gas chromatographic–mass spectrometric investigation of the reaction products, however, revealed that not one but a mixture of products was obtained, consisting mainly of unreacted N-methylamino acid ester, some N-silylated derivative and some N-methyl-N-trimethylsilylamino acid trimethylsilyl ester. The N-methyl-N-trimethylsilyl-DL-amino acid (+)-3-methyl-2-butyl esters were not completely separated in the case of N-methylalanine and N-methylleucine. Complete separations were observed for N-methylphenylalanine, N-meth-

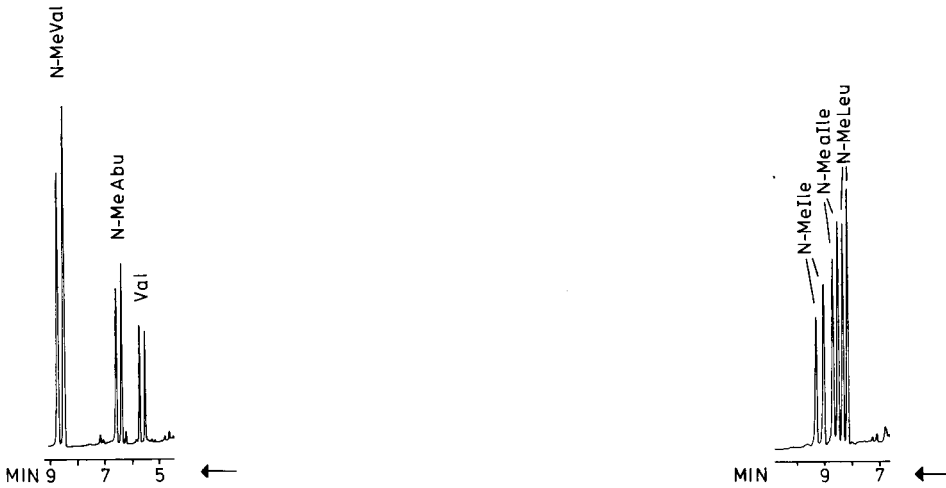

Fig. 1. Separation of (+)-3-methyl-2-butyl esters of DL-valine, N-methyl-DL-α-aminobutyric acid and N-methyl-DL-valine on a 25 m × 0.23 mm I.D. fused silica capillary column coated with CpSil-5. Column temperature, 90°C. Carrier gas, hydrogen (0.6 bar). Co-injection of 0.5 μl of MSTFA.

Fig. 2. Separation of (+)-3-methyl-2-butyl esters of N-methyl-DL-leucine, N-methyl-DL-*allo*-isoleucine and N-methyl-DL-isoleucine. Column as in Fig. 1. Column temperature, 100°C. Co-injection of 0.5 μl of MSTFA.

TABLE I

SEPARATION FACTORS (α) AND OPERATING TEMPERATURES FOR SEPARATION OF N-METHYL-DL-AMINO ACID (+)-3-METHYL-2-BUTYL ESTERS (A) AND N-METHYL-N-TRIMETHYLSILYL-DL-AMINO ACID-(+)-3-METHYL-2-BUTYL ESTERS (B) ON A 25 m PYREX GLASS CAPILLARY COLUMN COATED WITH CpSIL-5

Co-injection of 0.5 μl of MSTFA.

Racemate	*A*		*B*	
	α	*Column temperature (°C)*	α	*Column temperature (°C)*
N-Methylalanine	1.038	80	1.018	100
N-Methylaminobutyric acid	1.041	80	Not tested	–
N-Methylvaline	1.030	100	1.050	110
N-Methylleucine	1.024	100	1.015	120
N-Methylisoleucine	1.032	100	1.038	120
N-Methyl-*allo*-isoleucine	1.026	100	Not tested	–
N-Methylphenylalanine	Not tested	–	1.046	160

ylvaline and N-methylisoleucine. In all these instances the D-enantiomer has a longer retention time than the L-enantiomer.

The most surprising result was that the unchanged N-methyl-DL-amino acid (+)-3-methyl-2-butyl esters were now eluted as symmetrical and completely resolved peaks, the L-enantiomer having the longer retention time (Figs. 1 and 2 and Table I). The same result could be obtained when 0.5 μl of the silylating reagent was co-injected with 1 μl of a solution of N-methyl-DL-amino acid (+)-3-methyl-2-butyl esters in methylene chloride. This effect was independent of the type of silylating agent when using N-methyl-N-trimethylsilyltrifluoroacetamide (MSTFA), N,O-bistrimethylsilyltrifluoroacetamide (BSTFA), hexamethyldisilazane (HMDS), N-methyl-N-trimethylsilylheptafluorobutyramide (MSHFBA); N,N-dimethyl-N-trimethylsilylamine (TMSDMA) and N,O-bistrimethylsilylacetamide (BSA). Only

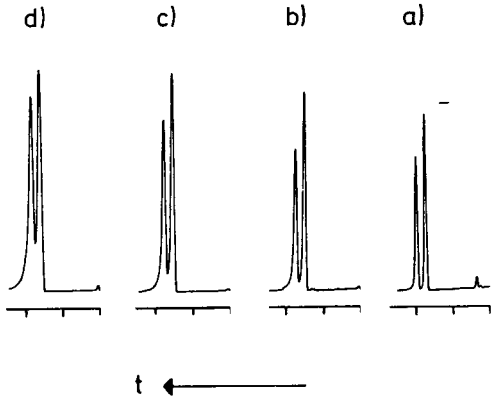

Fig. 3. Separation of (+)-3-methyl-2-butyl esters of N-methyl-DL-valine. (a) Co-injection of 0.5 μl of MSTFA; (b) re-injection without MSTFA after 10 min; (c) after 20 min; (d) after 40 min.

trimethylchlorosilane (TMCS) was ineffective. The deactivation phenomenon is only observed on co-injection and cannot be achieved with equal quality by injection of a silylating agent more than 10 sec before or after injection of the sample. The deactivating effect also is only temporary, as demonstrated in Fig. 3. This indicates that the molecules of the silylating agent cover the active centres of the inner surface of the column by adsorption rather than reacting chemically with free Si–OH groups still present. This hypothesis is also supported by the observation that the deactivation effect decreases markedly at temperatures above 120°C.

REFERENCES

1 H. Brockmann, *Fortschr. Chem. Org. Naturst.*, 13 (1960) 1.
2 A. Rüegger, M. Kuhn, H. Lichti, H.-R. Loosli, R. Huguemin, Ch. Quiquerez and A. von Wartburg, *Helv. Chim. Acta*, 59 (1976) 1075.
3 J. S. Davies and R. J. Thomas, in I. Z. Siemion and G. Kupryszewski (Editors), *Peptides 1978*, Wroclaw University Press, Wroclaw, 1979, p. 173.
4 M. Goodman and R. C. Stueben, *J. Org. Chem.*, 27 (1962) 3409.
5 J. R. McDermott and N. L. Benoiton, *Can. J. Chem.*, 51 (1973) 2562.
6 E. Gil-Av, B. Feibush and R. Charles-Sigler, in A. B. Littlewood (Editor), *Gas Chromatography 1966*, Institute of Petroleum, London, 1966, p. 227.
7 W. A. König and G. J. Nicholson, *Anal. Chem.*, 47 (1975) 951.
8 H. Frank, G. J. Nicholson and E. Bayer, *J. Chromatogr.*, 146 (1978) 197.
9 W. A. König, S. Sievers and I. Benecke, in R. E. Kaiser (Editor), *Proceedings of 4th International Symposium on Capillary Chromatography, Hindelang, 1981*, Institut für Chromatographie, Bad Dürkheim, and Dr. Hüthig Publishers, Heidelberg, 1981, p. 703.
10 W. A. König and U. Hess, *Justus Liebigs Ann. Chem.*, (1977) 1087.
11 J. R. McDermott and N. C. Benoiton, *Can. J. Chem.*, 51 (1973) 1915.
12 B. Halpern and J. W. Westley, *Aust. J. Chem.*, 19 (1966) 1533.
13 W. A. König, W. Rahn and J. Eyem, *J. Chromatogr.*, 133 (1977) 141.

Journal of Chromatography, 238 (1982) 241–246
Elsevier Scientific Publishing Company, Amsterdam — Printed in The Netherlands

CHROM. 14,652

Note

Gas–liquid chromatographic assay of mixtures of camphor, menthol, and methyl salicylate in ointments*

HENRY S. I. TAN*, PATRICIA A. KEMPER and PETRA E. PADRON
College of Pharmacy, University of Cincinnati-Medical Center, Cincinnati, OH 45267 (U.S.A.)
(Received December 15th, 1981)

Many over-the-counter (OTC) preparations to relieve pain due to strains, sprains, sore muscles and joints, rheumatism, neuralgia and similar disorders by topical application contain mixtures of camphor, menthol, and methyl salicylate as active ingredients. These compounds serve as counterirritants and by rubbing them into the skin stimulate circulation and relax muscle tension. Since preparations containing these three active ingredients are marketed by numerous manufacturers there is need for a simple, rapid, and reliable assay method to aid in the quality control of these OTC products. This is particularly important for methyl salicylate because U.S. federal law requires that preparations containing more than 5% of methyl salicylate must be dispensed in child-resistant containers with warning to use only as directed for external use.

Assay methods for the quantitative determination of combinations of any two of these drugs have been reported[1–3]. These methods were based on gas–liquid chromatography (GLC) since these drugs are volatile substances. However, only a few methods were published which allowed the assay of mixtures containing all three drugs[4–6]. Bruno[4] isolated the three compounds from the sample by steam distillation, followed by extraction of the distillate into chloroform. After washing with sodium bicarbonate and drying, the chloroform solution was injected onto the gas chromatograph. The isolation step was time-consuming and great care must be taken to prevent the loss of the compound(s) during distillation. Although Stevens and Warren[5] analyzed methyl salicylate in the presence of menthol and camphor by GLC after extraction or steam distillation, the latter two compounds were not quantitated. Douglas[6] assayed mixtures of all three compounds by GLC using phenol as internal standard. However, this method dealt with oily solutions and hydrophobic ointments only and was not applicable to many hydrophilic ointments containing the three compounds.

This paper describes a simple, rapid, and reliable GLC internal standard method for the quantitation of camphor, menthol, and methyl salicylate in both hydrophobic and hydrophilic OTC preparations.

---

* To be presented at the meeting of the Pharmaceutical Analysis and Control Section, APhA Academy of Pharmaceutical Sciences, Las Vegas, NV, U.S.A., April 1982.

0021-9673/82/0000–0000/$02.75

EXPERIMENTAL

Apparatus

We used a Varian Aerograph Model 2740 flame ionization gas chromatograph equipped with Disc chart integrator (Model 200, Disc Instruments, Santa Ana, CA, U.S.A.), a Sargent-Welch Model SRG strip-chart recorder, and 10-μl Hamilton Series 700 syringes.

Reagents and materials

The following reagents and materials were used: *d*-camphor, *l*-menthol, methyl salicylate, and benzyl alcohol (Eastman Kodak, Rochester, NY, U.S.A.); cyclohexane and methanol (99 mole % pure, Fisher, Fair Lawn, NJ, U.S.A.); Carbowax 20M and Chromosorb W-HP 80–100 mesh (Supelco, Bellefonte, PA, U.S.A.).

GLC conditions

A 6 ft. × 1/8 in. I.D. glass column packed with 5% Carbowax 20M on 80–100 mesh Chromosorb W-HP was used. Nitrogen was the carrier gas delivered at a flow-rate of about 30 ml/min. The flow-rates for hydrogen gas and air were approximately 30 and 300 ml/min, respectively. The injector port was heated at 200 C and the detector was maintained at 200° C. The temperature of the oven was programmed between 130° and 170°C at 6°/min. A flame ionization detector current of 1×10^{-9} A was used. Attenuation was adjusted to keep all peaks on the chart paper.

Internal standard solution

One ml of benzyl alcohol was diluted to 25.0 ml with methanol.

Standard solution preparation

About 0.5 g each of camphor, menthol, and methyl salicylate were weighed accurately and transferred into a 50-ml volumetric flask. After 1.0 ml of the internal standard solution was added, the solution was diluted to volume with methanol. For most applications, this solution was diluted again ten-fold using a volumetric flask with methanol. A different dilution might be necessary to accomodate a particular sample.

Sample solution preparation

Hydrophilic products (creams and ointments with water-soluble bases). A sample of about 3 g was weighed accurately in a 100-ml volumetric flask and dissolved or suspended in methanol. After 1.0 ml of internal standard solution was added, the mixture was diluted to volume with methanol and then filtered through dry filter paper, if necessary, discarding the first 5 ml of filtrate. Five milliliters of the filtrate were pipetted into a 50-ml volumetric flask and diluted to volume with methanol.

Hydrophobic products (ointments with water-insoluble bases). A sample of about 3 g was weighed accurately in a 25-ml beaker and dissolved in 7 ml of cyclohexane. The solution was transferred quantitatively into a 50-ml volumetric flask. The beaker was rinsed twice with 3-ml portions of cyclohexane, and the washings were combined with the cyclohexane solution in the volumetric flask. After 1.0 ml of

internal standard solution was added, methanol was slowly added to the mark while the mixture was shaken vigorously. The precipitated ointment base was allowed to settle and the supernatant was filtered through dry filter paper, if necessary, discarding the first 5 ml of filtrate. Five milliliters of the filtrate were pipetted into a 50-ml volumetric flask and diluted to volume with methanol.

Chromatographic procedure

Using a 10-μl syringe, 1.5 μl of the sample solution and 1.5 μl of the standard solution were injected into the gas chromatograph under the operating conditions described above. Quantitation was based on relating the compound–internal standard peak area ratio of the sample to that of the standard.

RESULTS AND DISCUSSION

The almost quantitative removal of water-insoluble bases from hydrophobic products prolonged column life. With the method of Douglas[6], for example, a solution of the ointment was directly injected onto the column. Since a relatively high carrier gas flow-rate was used, in time the deposited ointment base diffused through the column, thereby changing the column characteristics.

Under the proposed experimental conditions camphor, menthol, methyl salicylate, and benzyl alcohol eluted as symmetrical sharp peaks and were well-separated from one another (Fig. 1). The approximate retention times were for camphor 1.4, menthol 1.8, methyl salicylate 2.8, and benzyl alcohol 3.6 min. The entire elution can be completed within 4 min which is much faster than previously reported methods[1,5,6].

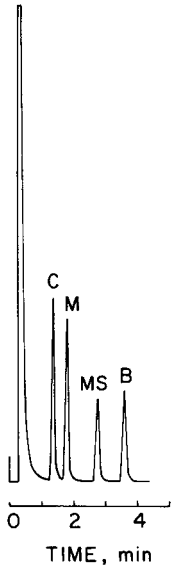

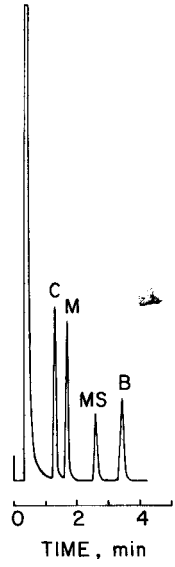

Fig. 1. Gas chromatogram of a standard solution run under conditions described in text. C = camphor; M = menthol; MS = methyl salicylate; and B = benzyl alcohol.

Fig. 2. Gas chromatogram of the extract from a hydrophilic synthetic mixture run under conditions described in text. C = camphor; M = menthol; MS = methyl salicylate; and B = benzyl alcohol.

TABLE I

RECOVERY DATA FROM SYNTHETIC OINTMENTS

Sample	*Camphor*			*Menthol*			*Methyl salicylate*		
	Amount (mg/g)		*Recovery (%)*	*Amount (mg/g)*		*Recovery (%)*	*Amount (mg/g)*		*Recovery (%)*
	Weighed	*Found*		*Weighed*	*Found*		*Weighed*	*Found*	
Hydrophilic									
1	165.0	167.8	101.7	161.4	166.0	102.9	179.4	183.8	102.5
2	222.3	215.6	97.0	160.3	152.4	95.1	223.6	220.2	98.5
3	214.7	215.3	100.3	156.7	154.7	98.7	223.4	218.5	97.8
4	175.3	173.9	99.2	159.0	159.0	100.0	164.5	159.1	96.7
5	162.8	156.7	96.2	166.4	166.1	99.8	183.0	177.9	97.2
Overall recovery (%)			98.9			99.3			98.5
S.D.			2.3			2.8			2.3
Hydrophobic									
1	165.9	167.0	100.7	166.2	163.2	98.2	172.9	168.2	97.3
2	174.9	176.1	100.7	152.6	151.2	99.1	222.5	215.8	97.0
3	165.1	158.5	96.0	168.6	169.1	100.3	165.6	166.1	100.3
4	158.2	148.8	97.8	152.6	156.4	102.5	154.8	157.6	101.8
5	166.3	164.3	98.8	167.2	166.1	99.3	187.8	180.3	96.0
Overall recovery (%)			98.8			99.9			98.5
S.D.			2.0			1.6			2.5

The relationship between compound-internal standard peak area ratio and amount of compound injected was established. Linearity was obtained between 10.4–83.0 μg of camphor, 10.2–81.5 μg of menthol, and 9.4–93.6 μg of methyl salicylate injected. Typical regression equations were for camphor: $A = 0.026\ C + 0.160$; for

TABLE II

RECOVERY DATA FROM COMMERCIAL OTC PRODUCTS

Product	*Component*	*Label claim (mg/g)*	*Amount found* (mg/g)*	*Label claim (%)*
Hydrophilic A**	Camphor	50	49.5 ; 53.8	103.6
	Menthol	70	72.7 ; 75.8	106.1
	Methyl salicylate	70	73.6 ; 73.4	105.1
Hydrophilic B**	Camphor	50	47.9 ; 50.4	98.2
	Menthol	50	54.7 ; 56.3	110.9
	Methyl salicylate	50	17.6 ; 20.7	42.8
Hydrophobic A	Camphor	–	–	–
	Menthol	70	73.4 ; 74.3	105.5
	Methyl salicylate	150	150.1 ; 146.3	99.0
Hydrophobic B	Camphor	90	70.8 ; 69.4	77.9
	Menthol	13.5	20.1 ; 20.7	153.2
	Methyl Salicylate	–	–	–

* Values of duplicate assays.

** Contains eucalyptol 10 mg/g.

menthol: $A = 0.029\ C + 0.099$; and for methyl salicylate: $A = 0.020\ C + 0.047$, where A = compound-internal standard area ratio, and C = amount of compound injected in micrograms. The correlation coefficients r were for camphor 0.9986; for menthol 0.9997; and for methyl salicylate 0.9997.

Recovery studies were performed on synthetically prepared mixtures containing all three compounds. The hydrophilic base consisted of a prepared mixture of cetyl alcohol, white wax, sodium lauryl sulfate, polyethylene glycol 400, and water. The hydrophobic base consisted of white petrolatum. Fig. 2 shows a typical gas chromatogram from a synthetic hydrophilic mixture. Overall percent recoveries ($\pm$ S.D.) ($n = 5$) from hydrophilic synthetic mixtures for camphor, menthol, and methyl salicylate were 98.9 $\pm$ 2.3, 99.3 $\pm$ 2.8, and 98.5 $\pm$ 2.3%, respectively (Table I). The overall percent recoveries ($\pm$ S.D.) from hydrophobic synthetic mixtures were ($n = 5$) 98.8 $\pm$ 2.0, 99.7 $\pm$ 1.6, and 98.5 $\pm$ 2.5% for camphor, menthol, and methyl salicylate, respectively. Addition of eucalyptol in concentrations usually found in commercial products did not interfere with the assay. The eucalyptol peak was hardly noticeable

The method was applied to commercial hydrophilic and hydrophobic products. Table II shows the recovery data. The overall percent label claim from these commercial preparations varied considerably from one brand to another. This would confirm the need for better quality control of these OTC products. In one brand the methyl salicylate content was only 42.8% of label claim (Hydrophilic B) whereas in another brand (Hydrophobic B) the menthol was 153.2% of label claim. Fig. 3 shows the gas chromatogram of Hydrophilic B. The gas chromatogram of Hydrophobic A is shown in Fig. 4.

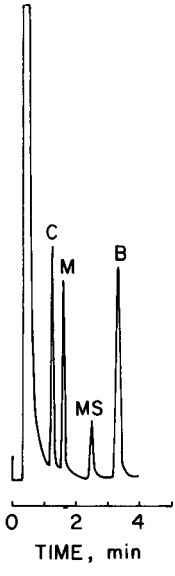

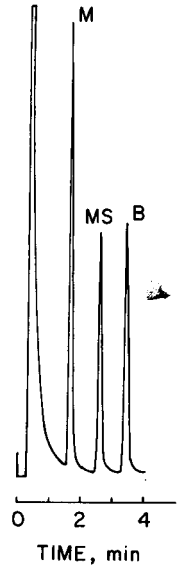

Fig. 3. Gas chromatogram of the extract from a commercial hydrophilic preparation run under conditions described in text. C = camphor; M = menthol; MS = methyl salicylate; and B = benzyl alcohol.

Fig. 4. Gas chromatogram of the extract from a commercial hydrophobic preparation run under conditions described in text. M = menthol; MS = methyl salicylate; and B = benzyl alcohol.

REFERENCES

1 K. S. Bahjat, *J. Pharm. Sci.*, 52 (1963) 1006.
2 K. R. Wernich, *Proc. Soc. Anal. Chem.*, 11 (1974) 297.
3 W. Groebel, *Arch. Pharm.*, 300 (1967) 226.
4 E. Bruno, *Atti Congr. Qual., 6th*, (1967, Publ. 1968) 121; *C.A.*, 73 (1970) 91279u.
5 S. G. E. Stevens and B. Warren, *J. Pharm. Pharmacol., Suppl.*, 16 (1964) 32T.
6 C. C. Douglas, *J. Ass. Offic. Anal. Chem.*, 55 (1972) 610.

Journal of Chromatography, 238 (1982) 247–249
Elsevier Scientific Publishing Company, Amsterdam — Printed in The Netherlands

CHROM. 14,615

Note

High-performance liquid chromatographic determination of phosphate esters of dexamethasone and prednisolone and their sulphite adducts

J. DIJKSTRA*
Hospital Venlo-Tegelen, Hogeweg 19, 5914 BA Venlo (The Netherlands)
and
D. DEKKER
Servier Nederland B.V., Storkstraat 5, 2722 NN Zoetermeer (The Netherlands)
(Received December 4th, 1981)

Corticosteroids are widely used in therapeutics in different formulations. During the preparation of a formulation containing corticosteroids and during its storage decomposition may occur. To prevent oxidative decomposition of corticosteroid esters in aqueous solution sodium metabisulphite is used as an antioxidant.

Decomposition of corticosteroids due to this added bisulphite has been reported for prednisolone[1,2] and dexamethasone[2]. Smith *et al.*[2] reported that addition of bisulphite took place at the A-ring system at C-1. When prednisolone was used both the 1α- and 1β-sulphonates were detected[2], but with dexamethasone only the 1β-sulphonate was detected[2]. This addition is illustrated for prednisolone in Fig. 1.

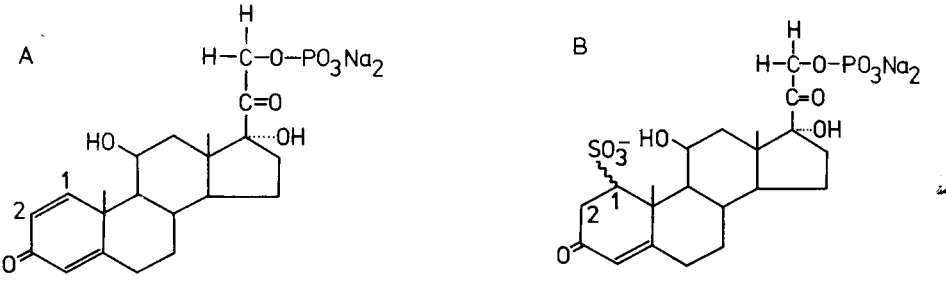

Fig. 1. Prednisolone sodium phosphate (A) and its bisulphite adduct (B).

Specific and sensitive methods are required to study the addition of bisulphite to corticosteroids in aqueous solutions and to determine the adducts formed and the remaining undecomposed corticosteroid phosphates in aqueous formulations. Therefore we developed an ion-pair reversed-phase high-performance liquid chromatographic procedure for the determination of the phosphate esters of dexamethasone and prednisolone and their respective sulphite adducts.

0021-9673/82/0000–0000/$02.75

MATERIALS AND METHODS

The chemicals used were of European Pharmacopoeia quality unless mentioned otherwise. Prednisolone sodium phosphate and dexamethasone sodium phosphate were of B.P. quality. PIC-A reagent (tetrabutylammonium phosphate in phosphate buffer) was purchased from Waters Assoc. (Milford, MA, U.S.A.).

A liquid chromatograph (Waters Assoc.), a stainless-steel column (30 cm × 3.9 mm I.D.) and a UV detector Model 440 (Waters Assoc.) were used. Detection was performed at 254 nm. The column packing comprised porous silica particles, permanently bonded to a monomolecular layer of organosilane (μBondapak C_{18}; Waters Assoc.). The mobile phase was methanol (analytical reagent grade)–water (1:1 v/v), containing 0.01 or 0.02 *M* PIC-A.

Peak areas were measured and computed with an Hewlett-Packard Type 3390 A integrator. The flow-rate was 1.5 ml/min and the sensitivity was 1 a.u.f.s. The temperature was 24°C. After dilution of aqueous solutions containing the corticosteroids and adducts formed, volumes of 5 μl and 20 μl respectively were injected.

Dilution appeared to have no influence on the equilibrium between the corticosteroid and the adducts.

RESULTS AND DISCUSSION

A chromatogram of an aqueous solution of dexamethasone sodium phosphate (peak 1) and the adduct formed (peak 2) is illustrated in Fig. 2A. A chromatogram of

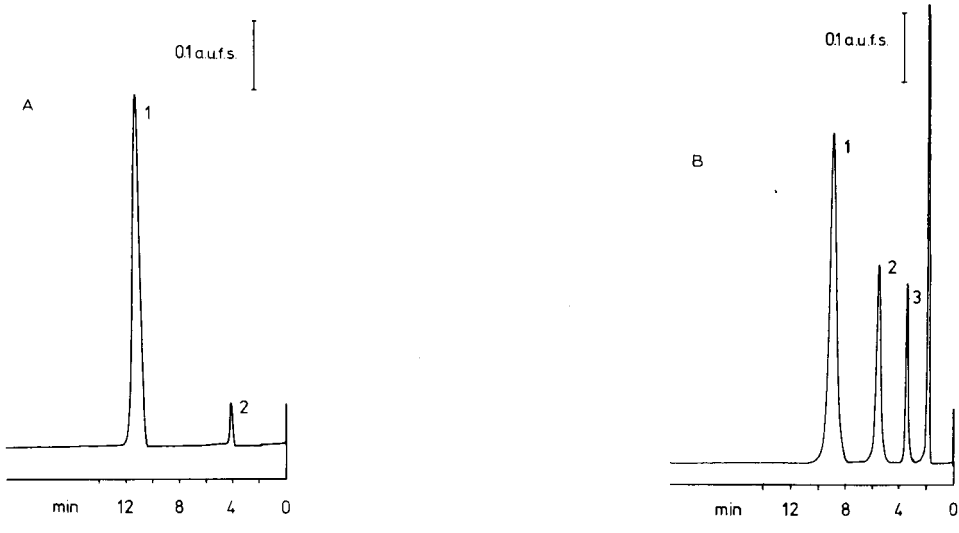

Fig. 2. A, HPLC of an aqueous solution of dexamethasone sodium phosphate (peak 1) (11 μg) and the adduct formed (peak 2) (0.6 μg). Solvent: 0.01 *M* PIC-A in methanol–water (1:1, v/v). Injection volume, 20 μl. Column: μBondapak C_{18} (30 cm × 3.9 mm I.D.). Temperature: 24°C. Flow-rate; 1.5 ml/min. Wavelength 254 nm. Sensitivity: 1 a.u.f.s. B, HPLC of an aqueous solution of prednisolone sodium phosphate (peak 1) (4.1 μg) and the adducts formed (peaks 2 and 3) (1.4 μg each). Solvent: 0.02 *M* PIC-A in methanol–water (1:1, v/v). Injection volume: 5 μl. Other parameters as in A.

prednisolone sodium phosphate (peak 1) and the two adducts formed (peaks 2 and 3) is shown in Fig. 2B.

Detailed studies on the addition of bisulphite to corticosteroids revealed that the molar absorption of the adducts at 254 nm was about 10% less than the molar absorption of the intact A-ring system. Consequently, peak area measurements should be corrected for these absorption differences.

REFERENCES

1 P. F. G. Boon and J. M. Busse, *J. Pharm. Pharmacol.*, 13 (1961) 62.
2 G. B. Smith, L. M. Weinstock, L. M. Roberts, F. E. Brenner, G. S. Hoinowsky, B. H. Arison and A. W. Douglas, *J. Pharm. Sci.*, 61 (1972) 708.

Journal of Chromatography, 238 (1982) 250–252
Elsevier Scientific Publishing Company, Amsterdam — Printed in The Netherlands

CHROM. 14,614

Note

Ready separation of ergocornine, α-and β-ergocryptine by high-performance liquid chromatography

BULCSU HERÉNYI and SÁNDOR GÖRÖG*
Scientific Department, Chemical Works of Gedeon Richter Ltd., H-1475 Budapest (Hungary)
(Received December 9th, 1981)

In recent years there has been increasing interest in the therapeutic use of ergot alkaloids. This has posed serious analytical problems and high-performance liquid chromatography (HPLC) has played an important rôle in solving them. One of the most delicate analytical problems in this field is the separation of the components of the ergotoxine and dihydroergotoxine groups, respectively: ergocornine (I), α and β-ergocryptine (II, III) and ergocristine (IV) or their dihydro derivatives (Ia–IVa).

Most workers dealing in this area have used reversed-phase HPLC systems: chemically bonded C_{18} or C_8 phases with buffered mixtures of water and acetonitrile or methanol. With slightly alkaline or neutral eluents, only partial separation of the components has been achieved. Vivilecchia *et al.*[1] separated Ia, IIa + IIIa and IVa using a mixture of acetonitrile and 0.01 *M* aqueous ammonium carbonate, while Dolinar[2], Szepesy *et al.*[3] and Fankel and Slad[4], using similar mixtures, and Hartman *et al.*[5], using a mixture of methanol and aqueous ammonium acetate, have achieved partial separation of the isomeric ergocryptines. The complete separation of the four components has been achieved by Hartmann *et al.*[5] and Ali and Strittmatter[6] with the aid of strongly alkaline eluents (mixtures of water, acetonitrile and tri- or diethylamine with pH values above 12). Szepesi *et al.*[7] successfully used chromatography on silica for the separation of several ergot alkaloids, among them the above mentioned derivatives.

The aim of this paper is to describe a reversed-phase HPLC system enabling the separation of ergocornine, α- and β-ergocryptine by using a neutral eluent.

EXPERIMENTAL

A Hewlett-Packard 1010B high-pressure liquid chromatograph was used equipped with a 1030B variable-wavelength UV detector and Valco loop injector.

The separation was carried out at ambient temperature, using a column (25 cm × 4.6 mm) of LiChrosorb RP-18, 10 μm (Chrompak, Middelburg, The Netherlands), and tetrahydrofuran–0.01 *M* aqueous ammonium acetate (4:6) as the eluent at a flow-rate of 1.5 ml/min. The chromatograms were monitored at 280 nm in the case of the dihydroergotoxine series and at 322 nm in the case of the ergotoxine series.

The samples (methanesulphonates, free bases or dried extracts of fermentation liquors) were dissolved in the eluent and 5-μl portions of the solutions thus obtained were injected into the chromatograph.

0021-9673/82/0000–0000/$02.75

TABLE I

SEPARATION OF ERGOTOXINES AND DIHYDROERGOTOXINES

Compound		*Capacity factor, k'*
I	Ergocornine	4.22
Ia	Dihydroergocornine	4.38
II	α-Ergocryptine	5.00
IIa	Dihydro-α-ergocryptine	5.44
III	β-Ergocryptine	5.78
IIIa	Dihydro-β-ergocryptine	5.91

RESULTS AND DISCUSSION

Although the strongly alkaline eluent described for the separation of the four components of ergotoxines[5] has been claimed not to be as corrosive as might have been expected[8] and the method based on it seems to be generally accepted, it is still reasonable to search for neutral eluents assuring longer column lifetimes. After having tried a number of eluents we have found that the alkaline eluent of Hartmann

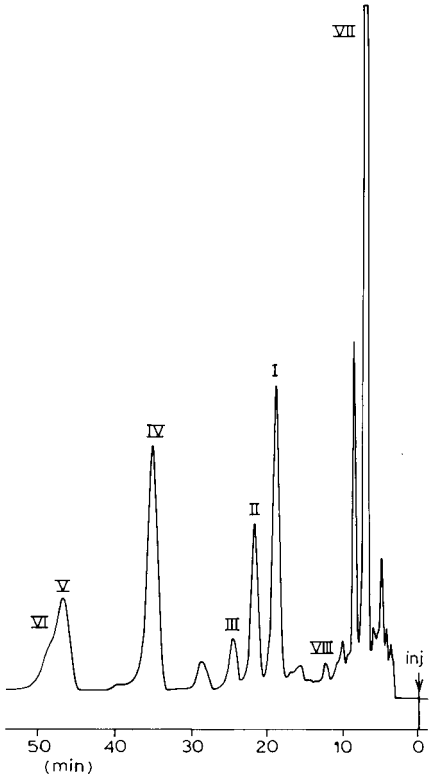

Fig. 1. Chromatogram of the fermentation liquor in the production of ergocornine-ergocryptine. For details see Experimental. Peaks: I = ergocornine; II = α-ergocryptine; III = β-ergocryptine; IV = ergocorninine; V = α-ergocryptinine; VI = β-ergocryptinine; VII = ergometrine; VIII = ergometrinine.

et al.[5] really affords the only possibility to separate the four components. However, tetrahydrofuran–0.01 *M* aqueous ammonium acetate (4:6) is suitable for the complete separation of ergocornine, α and β-ergocryptine (ergocristine is eluted together with β-ergocryptine). As is seen from the data of Table I, this system is suitable for the solution of any analytical problems where the task is the separation of I, II and III or Ia, IIa and IIIa.

We have routinely used this system for the estimation of I, II and III in fermentation liquors where IV (ergocristine) is not present. Fig. 1 shows the chromatogram of an extract of a typical fermentation liquor.

ACKNOWLEDGEMENTS

The authors wish to thank Dr. K. Zalai for valuable discussions and Mrs. M. Melegh for technical assistance.

REFERENCES

1 R. V. Vivilecchia, R. L. Cotter, R. J. Limpert, N. Z. Thimot and J. N. Little, *J. Chromatogr.*, 99 (1974) 407.
2 J. Dolinar, *Chromatographia*, 10 (1977) 364.
3 L. Szepesy, I. Fehér, G. Szepesi and M. Gazdag, *J. Chromatogr.*, 149 (1978) 271.
4 R. Fankel and I. Slad, *Z. Anal. Chem.*, 303 (1980) 208.
5 V. Hartmann, M. Rödiger, W. Ableidinger and H. Bethke, *J. Pharm. Sci.*, 67 (1978) 98.
6 S. L. Ali and T. Strittmatter, *Int. J. Pharm.*, 4 (1979) 111.
7 G. Szepesi, M. Gazdag and L. Terdy, *J. Chromatogr.*, 191 (1980) 101.
8 A. Wehrli, J. C. Hildenbrand, H. P. Keller, R. Stampfli and R. W. Frei, *J. Chromatogr.*, 149 (1978) 199.

Journal of Chromatography, 238 (1982) 253–257
Elsevier Scientific Publishing Company, Amsterdam — Printed in The Netherlands

CHROM. 14,540

Note

Reversed-phase high-performance liquid chromatography of procyanidins and other phenolics in fresh and oxidising apple juices using a pH shift technique

ANDREW G. H. LEA
University of Bristol, Long Ashton Research Station, Long Ashton, Bristol BS18 9AF (Great Britain)
(Received November 12th, 1981)

The principal phenolic constituents of apple juice and ciders are phenolic acids, catechins, phloridzin and procyanidins[1,2]. Typical examples are shown in Fig. 1. These compounds, particularly procyanidins, are important for their contribution to flavour and to oxidative browning, but until recently they have been very difficult to quantify in apple juices or ciders without pre-treatment. The method described here enables the direct determination of these components, which greatly assists the study of rapid enzymic browning.

Separation of apple phenolics

Although it is possible to separate the procyanidins, epicatechin and phloridzin in apple juice and cider extracts by reversed-phase high-performance liquid chromatography (HPLC) in acidified water–methanol gradients with detection at 280 nm[3,4], analysis of complete juices or ciders is not possible without modifying the method. This is because large amounts of phenolic acids are eluted in a non-ionic form at similar retention times to procyanidins of interest. Fig. 2 demonstrates the interference caused by phenolic acids at pH 2.5.

The pK_a of chlorogenic acid[5] is 3.5 and its retention time is thus pH-dependent in the range pH 1.5–5.5. It is therefore possible to take advantage of a pH shift during the run to improve the resolution of procyanidins and so to permit the analysis of complete cider or juices. By operating the column initially at pH 7.0 the phenolic acids are quickly eluted in an ionised form, but by reverting to pH 2.5 for the remainder of the run the procyanidins are eluted free from interference. Fig. 3 shows the improvement which is possible by this technique. For example, *ca.* 50 ppm of procyanidin B2 may now be detected in a Cox apple juice even in the presence of 300 ppm of chlorogenic acid. Since the phenolic acids are eluted close to the void volume with other non-phenolic materials, it is advisable to re-run the sample at pH 2.5 throughout if it is necessary to quantify these acids, and in this case to monitor at 320 nm where interference from catechins and procyanidins is effectively nil.

It has been found that buffer salts must be kept to a minimum if good procyanidin peak shape is to be maintained. The pH of the neutral eluent is not critical so long as it is above pH 5.5, which can be maintained by adding a trace of ammonia to

0021-9673/82/0000–0000/$02.75

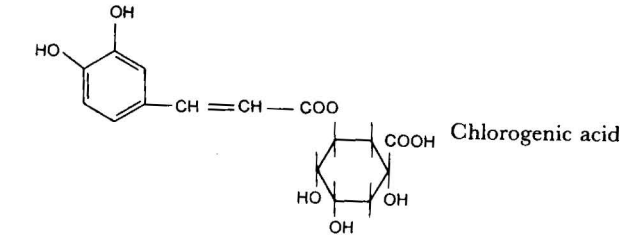

Chlorogenic acid

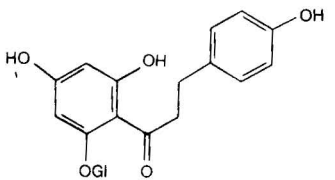

Phloridzin

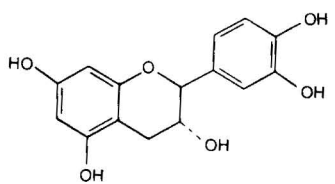

(−) Epicatechin

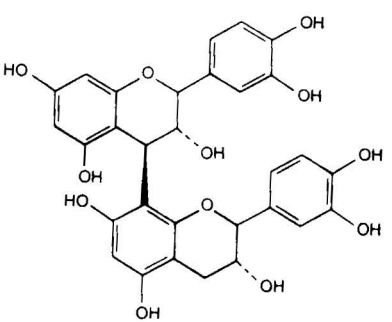

Procyanidin B2

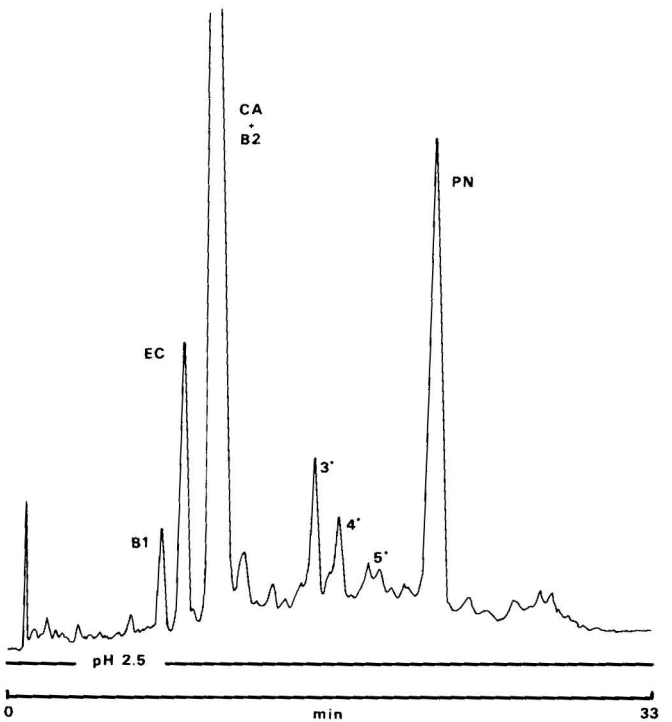

Fig. 1. The principal phenolic constituents of apple juice.

Fig. 2. Separation of Dabinett cider phenolics at pH 2.5. Peaks: CA = chlorogenic acid; EC = epicatechin; B1 and B2 = procyanidin dimers; 3°, 4° and 5° = procyanidin oligomers; PN = phloridzin.

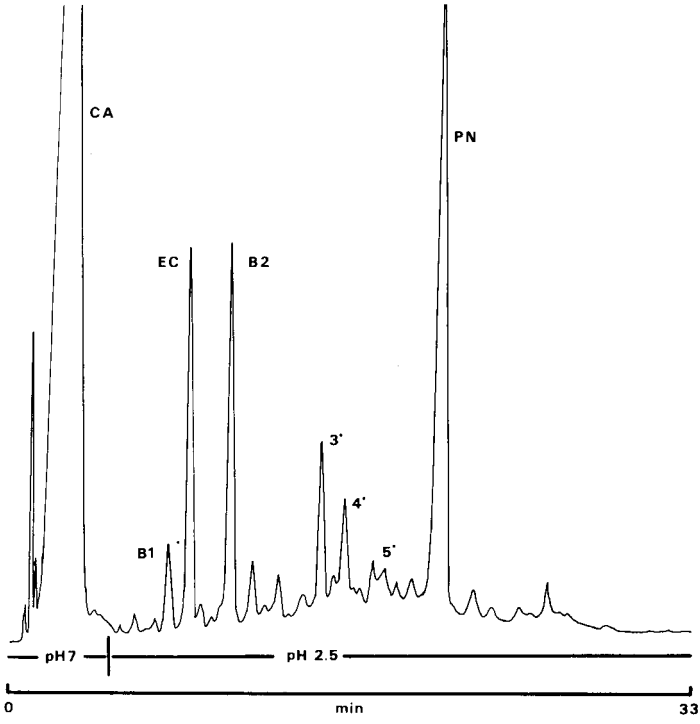

Fig. 3. Separation of Dabinett cider phenolics by the pH shift technique. Peaks as in Fig. 2. For conditions see text.

distilled water in equilibrium with aerial CO_2. Operating much above pH 7.0 may lead to solution of the silica-based packing and decrease the resolution of procyanidins. The shift from neutrality to pH 2.5 is essential for good peak shape during the remainder of the run, so it is important to allow sufficient equilibration time for neutral conditions to be restored at the beginning of the next run. Although this method was developed for the study of ciders, it is equally applicable to similar problems in red or white wines.

Study of oxidising juices

The system described above now permits detailed study of phenolic changes in oxidising apple juices, particularly when dual wavelength monitoring is used. Fig. 4 shows the separation of a totally unoxidised apple juice monitored both at 280 nm and 420 nm. Fig. 5 shows an analysis of the same juice after natural enzymic oxidation for 1 h. All the native phenolic compounds have diminished to differing extents and several new coloured peaks have appeared. Amongst these is the broad peak (Y), which is believed to consist largely of procyanidin polymers whose chromatographic behaviour following a sharp change in gradient steepness has been discussed previously[3]. Thus the new method provides a powerful tool for investigating the detailed mechanism of colour formation in apple juice.

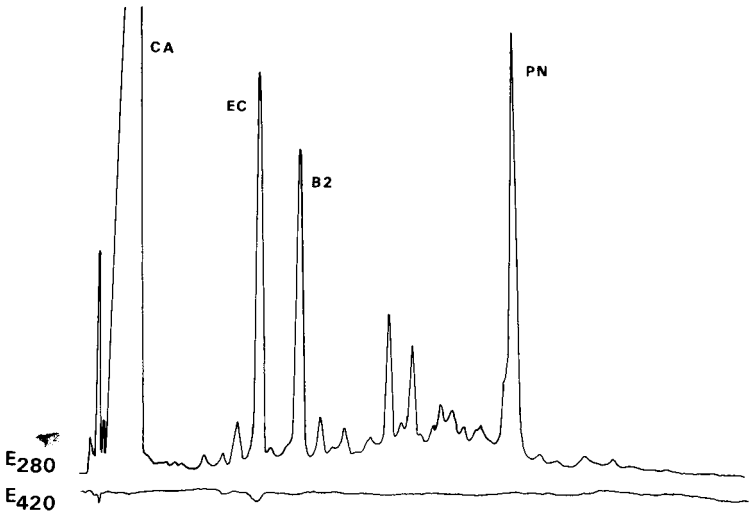

Fig. 4. Separation of phenolics in unoxidised Dabinett apple juice by the pH shift technique. Conditions as in Fig. 3.

EXPERIMENTAL

Chromatography

A Spectra-Physics SP 8000A machine was used, with detection at 280 nm supplemented by a variable-wavelength LC3 detector (Pye Unicam). The column was 100 × 5 mm I.D. (Shandon) packed in this laboratory with Spherisorb 5 Hexyl

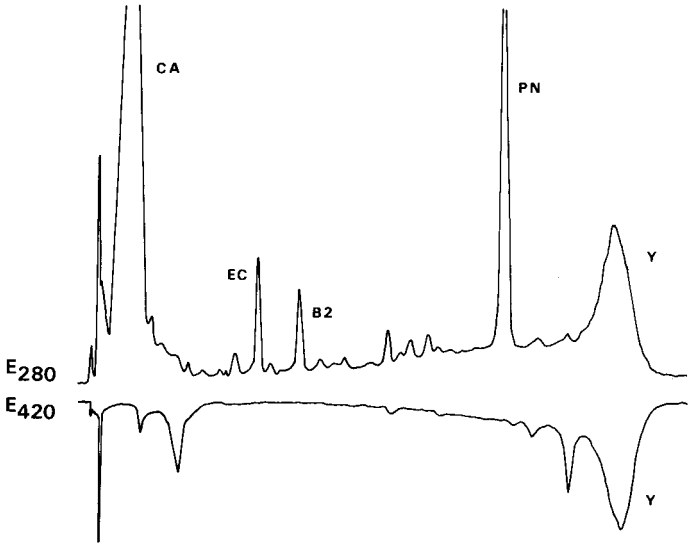

Fig. 5. Separation of phenolics in oxidised Dabinett apple juice by the pH shift technique. Conditions as in Fig. 3.

TABLE I

PERCENTAGE COMPOSITION OF THE SOLVENT

Time (min)	*A (water, pH 2.5)*	*B (methanol)*	*C (water, pH 7.0)*
0	0	2	98
3	0	5	95
3.1	95	5	0
23	75	25	0
33	2	98	0
35.9	2	98	0
36	0	98	2
40	0	98	2
45	0	2	98

(Phase Separations) and operated at 45°C. Sensitivity was 0.02–0.16 a.u.f.s. depending on the sample, and 20 or 50 μl of juice or cider was injected. Solvent A was charcoal-filtered and de-ionised (Elga) water brought to pH 2.5 with *ca.* 0.1% perchloric acid; solvent B was methanol redistilled from KOH; solvent C was water neutralised to pH 6.5–7.0 with ammonia. The flow-rate was 1.5 ml/min and the solvent gradient was as shown in Table I.

After the run, a further 30 ml of starting solvent was pumped to ensure complete neutrality. All solvents and samples were filtered through 0.45-μm HATF membranes (Millipore) before use (FHUP for methanol).

Preparation of apple juice

Typically, one apple of the cider variety "Dabinett" was chilled to 4°C for several hours and then extracted in a domestic juice extractor consisting of a grater plate and basket centrifuge (Moulinex). Part of the juice was collected into a helium-filled tube, centrifuged briefly, and filtered through a 0.45-μm membrane before direct injection into the machine. Since the cider apple polyphenoloxidase is tightly membrane bound[6], this prevented any oxidation and resulted in a water-white juice. The remainder of the juice was allowed to brown naturally in the presence of its solids and was centrifuged and filtered for analysis after 1 h.

ACKNOWLEDGEMENT

The financial assistance of the Cider Sponsors Committee of the National Association of Cidermakers is acknowledged.

REFERENCES

1 A. G. H. Lea and C. F. Timberlake, *J. Sci. Food Agric.*, 25 (1974) 1537.
2 A. G. H. Lea, *J. Sci. Food Agric.*, 29 (1978) 471.
3 A. G. H. Lea, *J. Chromatogr.*, 194 (1980) 62.
4 E. L. Wilson, *J. Sci. Food Agric.*, 32 (1981) 257.
5 C. F. Timberlake, *J. Chem. Soc.*, 561 (1959) 2795.
6 P. W. Goodenough and A. G. H. Lea, *Rep. Long Ashton Research Station for 1979*, University of Bristol, Bristol, 1980, p. 207.

Journal of Chromatography, 238 (1982) 258–260
Elsevier Scientific Publishing Company, Amsterdam — Printed in The Netherlands

CHROM. 14,573

Note

Separation of triarylsulfonium salts by thin-layer chromatography

ALAN A. BORNSTEIN*
American Can Company, Princeton Research Center, P.O. Box 50, Princeton, NJ 08540 (U.S.A.)
(Received November 24th, 1981)

Triarylsulfonium salts are important as photoinitiators for cationic polymerization[1–3]. The synthesis of these salts can often be accompanied by the formation of similar side products, occasionally in significant quantities[3]. Because of these considerations, a definite need exists to define the types and amounts of triarylsulfonium salts in these products.

Thin-layer chromatography (TLC) is usually a powerful tool for separating similar compounds, in this case for molecules which have similar aromatic moeities, but different polarities. While there has been some work on the chromatographic separation of alkylsulfonium iodides[4] and phosphonium salts[5], there has been no report on the separation of triarylsulfonium salts. A TLC separation was therefore developed to accomplish this task.

EXPERIMENTAL

Materials

Purified triarylsulfonium hexafluorophosphate salts were obtained from S. Schlesinger and W. Watt of American Can Company (Princeton, NJ, U.S.A.). Methanol and hydrochloric acid, 1.0 *N*, were obtained from Fisher Scientific (Springfield, NJ, U.S.A.). Hexafluorophosphoric acid, 65% solution in water, was obtained from Aldrich (Milwaukee, WI, U.S.A.). All reagents were of the highest purity available and used without further purification.

TLC plates were purchased from Whatman (Clifton, NJ, U.S.A.).

Methods

1.0% Methanolic solutions each of bis[4-(diphenylsulfonio)phenyl] sulfide dihexafluorophosphate (BDS), S-phenylthianthrylium hexafluorophosphate (SPT), triphenylsulfonium hexafluorophosphate (TPS) and diphenyl-4-thiophenoxyphenylsulfonium hexafluorophosphate (DPTS) were made up. These solutions were stored in the dark at 4°C prior to use.

Analytical TLC was performed using 250-μm precoated silica gel K6 plates without any preconditioning. Samples (up to 500 μg) were spotted on the plate with a

* Present address: Philip A. Hunt Chemical Corporation, P.O. Box 800, Palisades Park, NJ 07650, U.S.A.

0021-9673/82/0000–0000/$02.75

disposable capillary tube. Similarly, preparative TLC was performed using 1000-μm precoated silica gel plates. In this case, samples were applied as streaks at the 2000 μg/cm loading level.

Ascending development (to a distance about 10 cm above the starting line) was performed using methanol–water–1 *N* hydrochloric acid (90:10:5), in a well-equilibrated chromatographic tank. After solvent evaporation, visualization was accomplished by UV fluorescence quenching of the TLC plate phosphor (*caution*: HCl, HF and PF_5 vapors may be released on visualization). Although not used here, an alternative method of visualizing sulfonium compounds on the TLC plate is spraying with cobaltous ammonium thiocyanate solution[6,7]. Zones containing onium compounds subsequently appear red.

Zones containing the separated triarylsulfonium compounds were scraped off and eluted with additional mobile phase solvent. Samples were not collected from zones exposed to UV radiation used in visualization. After evaporating the solvent, the solid products were redissolved in methanol. Purified hexafluorophosphate salts of the TLC separated components were isolated by precipitation following the addition of a stoichiometric excess of hexafluorophosphoric acid to the water diluted methanol solution (4 parts water to 1 part methanol). Infrared and proton nuclear magnetic resonance spectroscopic analysis and further TLC were performed to check for sample decomposition.

RESULTS AND DISCUSSION

The four standard triarylsulfonium compounds (Fig. 1) were separated with good resolution and minimal tailing (Table I). Preparative TLC was used to separate mg quantities of the triarylsulfonium compounds. The hexafluorophosphate salts of the separated components were recovered in each case and their IR spectra compared. Excellent IR spectral correlations before and after TLC were seen for each compound, indicating the absence of decomposition during the separation procedure.

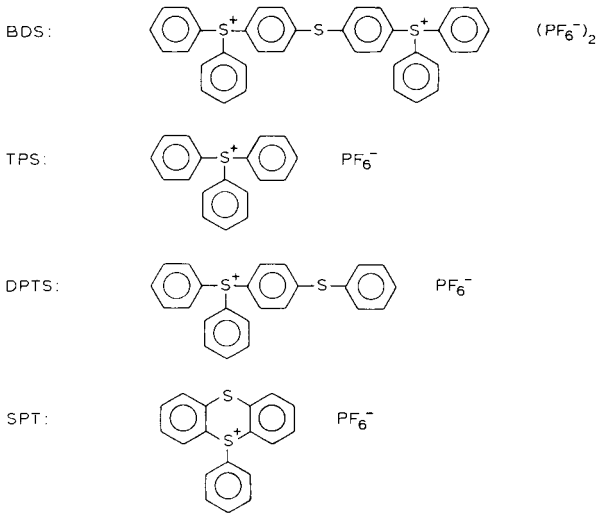

Fig. 1. Triarylsulfonium compounds separable by TLC.

The TLC artifact indicated in Table I is probably due to the formation of the so-called second solvent front. This effect occurs if the mobile phase contains a mineral acid, such as hydrochloric acid.

TABLE I

TLC RESULTS (R_F VALUES)

Synthetic mixture	*Identification*
0.14–0.26	TLC artifact
0.35	BDS
0.52	SPT
0.58	TPS
0.71	DPTS

The order of retention appeared to be related to the relative importance of the triphenylsulfonium (TPS) segment in the molecule. It was concluded that the more predominant the TPS segment, the greater is the compound's affinity for the silica gel stationary phase. Furthermore, the R_F values were found to be highly dependent on the pH of the mobile phase, tending rapidly towards zero as the pH exceeded 2.0 [BDS in methanol–water (90:10), pH adjusted with HCl to pH 1.0, $R_F = 0.35$; at pH 2.0, R_F 0.05; for TPS at pH 1, $R_F = 0.58$; at pH 2, $R_F = 0.28$].

Spectroscopic analysis of the recovered compounds showed silica contamination and anionic exchange, *i.e.*, chloride substituting for hexafluorophosphate. Silica contamination of the isolated products is due to the appreciable solubility of silica in acidic methanol–water solvent. A significant portion of this solubilized silica probably exists as methyl esters of silicic acid. Thus, the isolation of pure TLC separated compounds must allow for the removal of these esters. Pure hexafluorophosphate salts were found to be obtainable by adding an excess of the hexafluorophosphate anion (see *Methods*).

ACKNOWLEDGEMENTS

The author thanks Mr. H. Pobiner for suggesting TLC as a potential method for separating these compounds, Drs. S. Schlesinger and W. Watt for samples of the triarylsulfonium salts and their helpful suggestions, Drs. F. Loprest, H. Hoffman and L. Schkolnick for their comments and support and the American Can Company for permission to publish this paper.

REFERENCES

1 W. R. Watt, *U.S. Pat.*, 4,201,640 (May 6, 1980).
2 K. T. Chang, *U.S. Pat.*, 4,197,174 (April 8, 1980).
3 J. V. Crivello and J. H. W. Lam, *J. Polym. Sci., (Polym. Chem. Ed.)*, 18 (1980) 2697.
4 L. Kronrad and K. Panek, *Z. Anal. Chem.*, 191 (1962) 199.
5 H. Schindlbauer and F. Mitterhofer, *Z. Anal. Chem.*, 221 (1966) 394.
6 H. A. Potratz and J. M. Rosen, *Anal. Chem.*, 21 (1949) 1276.
7 G. H. Wiegand and W. E. McEwen, *J. Org. Chem.*, 33 (1968) 2671.

Journal of Chromatography, 238 (1982) 261–263
Elsevier Scientific Publishing Company, Amsterdam — Printed in The Netherlands

CHROM. 14,563

Note

Thin-layer chromatographic analysis of 1-(1-phenylcyclohexyl)pyrrolidine in urine

ROBERT D. BUDD*
Rancho Los Amigos Hospital, Downey, CA 90242 (U.S.A.)
(Received November 20th, 1981)

1-(1-Phenylcyclohexyl) pyrrolidine (PHP) is growing in popularity on the U.S. drug scene as a replacement for phencyclidine (PCP), as the operators of illicit drug laboratories try to beat the legal restrictions being placed on the chemicals required for the synthesis of PCP[1]. Because of its growing abuse[1] and because of its overdose potential[2], toxicology laboratories are being more and more frequently required to analyze for its presence. A procedure for the analysis of PHP is needed. To meet this need, a thin-layer chromatography (TLC) procedure for the determination of PHP in urine samples has been developed.

PROCEDURE

PHP is analyzed by TLC as follows. To a 50-ml conical centrifuge tube, add 15 ml of the urine sample to be tested, 2 ml of 2 *M* Tris buffer, and 20 ml of isopropanol–chloroform (5:95). Cap and shake the tube at slow speed on a horizontal platform shaker for 15 min. After the extraction, aspirate and discard the top, urine layer, then filter the organic layer into a 40-ml conical centrifuge tube. Add two drops of 1% HCl–methanol and then evaporate the organic layer to dryness in a 70°C water-bath under nitrogen. Reconstitute the residue in 0.1 ml of methanol and spot the resulting solution on a Merck silica gel G TLC plate. Develop the plate in an unsaturated tank containing 100 ml of a solvent system of *n*-hexane–acetone–diethylamine (70:30:1). After development, air-dry the plate and spray it with acidified iodoplatinate to visualize the purple-gray PHP spots.

RESULTS AND DISCUSSION

The TLC method described allows rapid, accurate determination of PHP in urine samples down to a level of 1.0 μg/ml. PHP is readily separated from other drugs of abuse (particularly PCP), metabolites, and urinary substances by the *n*-hexane–acetone–diethylamine (70:30:1) solvent system (Table I).

Other solvent systems (Table I) have been tried, but found to be not quite as good as the *n*-hexane–acetone–diethylamine solvent system. The ethyl acetate–methanol–diethylamine solvent system is slightly more sensitive, but PHP is subject to

* Present address: Los Angeles County Medical Examiner-Coroner, Los Angeles, CA, 90033, U.S.A.

0021-9673/82/0000–0000/$02.75

TABLE I

TLC SEPARATION OF PHP FROM OTHER DRUGS AND METABOLITES

I, *n*-Hexane–acetone–diethylamine (70:30:1); II, ethyl acetate–methanol–diethylamine (90:10:1.6); III, ethyl acetate–*o*-dichlorobenzene–methylene chloride–methanol–concentrated ammonium hydroxide (40:20:25:15:0.7).

Drug	R_F *values on solvent systems*		
	I	*II*	*III*
PHP	0.61	0.32	0.65
Benzoylecgonine	0.01	0.03	0.04
Caffeine	0.48	0.49	0.63
Cocaine	0.52	0.55	0.79
Codeine	0.20	0.20	0.35
Methadone	0.71	0.35	0.61
Methadone metabolite*	0.56	0.30	0.46
Methaqualone	0.63	0.88	0.85
Morphine	0.15	0.16	0.19
Nicotine	0.37	0.26	0.58
Norpropoxyphene	0.28	0.23	streak**
PCP	0.86	0.58	0.79
Propoxyphene	0.64	0.59	0.77

* 2-Ethylidene-1,5-dimethyl-3,3-diphenylpyrrolidine.
** 0.15–0.30.

interference from methadone and its major metabolite. The ethyl acetate–*o*-dichlorobenzene–methylene chloride–methanol–concentrated ammonium hydroxide solvent system is nearly as sensitive, but PHP is subject to interference from caffeine which is found in a large proportion of the general population due to the use of coffee, tea, and colas. If the simultaneous analysis of another drug(s) is important, either of the other two solvent systems may be advantageous for this purpose.

Several parts of the procedure are quite critical. (1) It is important that the initial extraction be done at slow speed to minimize emulsion formation and avoid a centrifugation step. (2) It is critical that the acidic methanol be added before the

TABLE II

DETECTION LIMITS

PHP concentration (μg/ml)	*Samples run*	*Samples in which PHP was detected*	*%*
5	10	10	100
2.5	10	10	100
1.0	10	10	100
0.75	10	8	80
0.50	10	4	40
0.25	10	1	10
0.1	10	0	0

concentration step. This converts PHP to a hydrochloride which is much higher boiling and, therefore, less likely to be lost.

PHP, when present in levels on the order of 5 μg/ml or more can be detected by the Roche radioimmunoassay PCP procedure[3-4]; however, some method to differentiate PHP from PCP is still needed. Due to its insensitivity to PHP, radioimmunoassay is only of use in PHP overdose cases.

If further confirmation of a positive result is required, the sample can be analyzed using another TLC solvent system (such as the ethyl acetate–methanol–diethylamine solvent system) or the sample can be analyzed by a gas–liquid chromatography procedure[2].

The TLC procedure described obtained good sensitivity and reliable results (Table II). It is well suited for the analysis of urine samples on a large-scale basis. Two technicians can analyze 250–300 samples in an 8-h day.

REFERENCES

1 R. D. Budd, *New Engl. J. Med.*, 303 (1980) 588.
2 G. R. Nakamura, E. C. Griesemer, L. E. Joiner and T. T. Noguchi, *Clin. Toxicol.*, 14 (1979) 383–388.
3 *Abuscreen, Radioimmunoassay for Phencyclidine (PCP)*, Roche Diagnostics, Nutley, NJ, 1979.
4 R. D. Budd, *Clin. Toxicol.*, 18 (1981) 1033–1041.

Journal of Chromatography, 238 (1982) 264–265
Elsevier Scientific Publishing Company, Amsterdam — Printed in The Netherlands

CHROM. 14,581

Letter to the Editor

Determination of hydroxyl groups and water content in silica by nuclear magnetic resonance spectroscopy

Sir,

Holík and Matějková[1] recently reported results on the determination of residual hydroxyl groups on silanized silica gel which differed markedly from our results[2] based on a chemical reaction of hydroxyl groups and/or adsorbed water with a dimethylzinc complex. According to the former authors, the hydroxyl concentration determined by means of hydrogen–deuterium exchange lies between 4 and 8 OH groups per nm^2 and the water content corresponds to about 1.5–3 H_2O groups per nm^2. This water content, determined by the displacement of adsorbed water by deuterated trifluoroacetic acid, was in good agreement with thermogravimetrical measurements. Our chemical determination[2] of hydroxyl groups and adsorbed water showed 0.1–1.5 OH groups per nm^2 and 0.5–2 H_2O groups per nm^2. Thus the question arises, what is the reason for this discrepancy.

First, the recent paper does not mention any drying of samples prior to the measurements. It is well known that silica gel rehydrates on standing in air and rehydrated samples show a high content of adsorbed or even capillary condensed water. In such cases, concentrations above 8 OH groups per nm^2 have been found even using chemical methods[3]. However, a part of this water is lost rapidly by heating of samples at 150–200°C. Also unclear is what is the "water content" measured by means of thermogravimetry[1]. Owing to the dehydration of vicinal and/or geminal hydroxyl groups it is almost impossible to distinguish between adsorbed water and hydroxyl groups using thermogravimetry (TG)[4]. Moreover, Holík and Matějková reported neither any TG curves nor the conditions of their TG experiments.

Another possible source of the differences between chemical determinations and the hydrogen–deuterium exchange is well known[4]. On silanized silica surfaces, there may be hydroxyl groups that are inaccessible to the relatively bulky molecules of chemical reagents[5], although these hydroxyl groups can be determined using deuterium-labelled water, the molecules of which are relatively small and readily permeative. On the other hand, the molecular size of deuterated trifluoroacetic acid, which is recommended by Holík and Matějková for the quantitative exchange of adsorbed water, is comparable with the molecular sizes of other chemical reagents.

The chemical determination of surface hydroxyls is believed to be closely dependent on the sorption properties of the silanized silicas, because the chemical reaction as well as the sorption of relatively bulky solute molecules are sensitive to the accessible hydroxyl groups only. However, there is an additional amount of inaccessible hydroxyl groups shielded by bonded alkyl chains. This is also shown by the results of Holík and Matějková. The relative changes of hydroxyl concentration due to drying, silanization and capping, which they have reported, are surprisingly low —

0021-9673/82/0000–0000/$02.75

see, for example, Samples 1–4, because they are superimposed on the "background" of the unknown concentration of these inaccessible hydroxyls.

The feasibility of the two methods should be judged only on the basis of relationships between the hydroxyl concentration and the chromatographic properties of silanized silica gels.

Institute of Chemical Process Fundamentals,
Czechoslovak Academy of Science,
Praha 6-Suchdol 2 (Czechoslovakia)

L. NONDEK

1 M. Holík and B. Matějková, *J. Chromatogr.*, 213 (1981) 33.
2 L. Nondek and V. Vyskočil, *J. Chromatogr.*, 206 (1981) 581.
3 W. Hanke, *Z. Anorg. Allg. Chem.*, 395 (1973) 191.
4 K. K. Unger, *Porous Silica (Journal of Chromatography Library*, Vol. 16), Elsevier, Amsterdam, Oxford, New York, 1979, Ch. 3.1.1.
5 R. K. Iler, *J. Chromatogr.*, 209 (1981) 341.

(Received October 28th, 1981)

Journal of Chromatography, 238 (1982) 266–267
Elsevier Scientific Publishing Company, Amsterdam — Printed in The Netherlands

CHROM. 14,599

Book Review

High-performance liquid chromatography —Advances and perspectives, Vol. 2, edited by Cs. Horváth, Academic Press, New York, 1980, XVI + 341 pp., price US$ 39.50, ISBN 0-12-312202-3.

This volume is the second in a series which had a very good start with its first volume which contained excellent articles on various important and interesting topics in liquid chromatography (LC). The contributors to the second volume are equally well qualified and the reviewer expected a very good book indeed.

However, these expectations were not completely fulfilled. The best, in fact an excellent part of the book, is the chapter by Engelhardt and Elgass, who discuss LC on silica and alumina from a practical point of view. Exactly the right amount of theoretical knowledge about adsorption onto these solids is given in order to enable practicing chromatographers to understand and organize their experimental results. There are also many important hints for the choice of techniques and conditions. Although no revolutionary developments have taken place in this field during recent years, a review of this type is timely.

Melander and Horváth treat reversed-phase (RP) chromatography in the third chapter, which occupies about two thirds of the whole book. This is justified in view of the importance of this technique, with which the majority of LC applications are carried out. The authors do a very good job in explaining the basic concepts of the method. However, most practising chromatographers will have difficulties in following the detailed theoretical expositions on solvophobic theory and the "mechanism" of ion-pair chromatography. These matters are still under discussion and such mathematical exercises are not necessary in a book of this type. Moreover, the development of a model for ion-pairing equilibria is approached in an inappropriate manner, starting with and adding up reactions rather than species. This leads to final equations in which the same species occurs several times, and to ambiguities such as "... if a Maxwell demon exploring the stationary phase could determine by inspection of the complex how each eluite it encountered had been bound..." Since retention is an equilibrium phenomenon, the (microscopic) history of molecules and ions should be of no concern. Another defect is the absence of the electroneutrality concept, which I believe should play a central role. The chapter closes with well written sections on physico-chemical measurements using RP-LC and on analytical applications, leading to a respectable, very useful and up to date reference list (635 items!).

The first chapter by Guiochon, on optimization in LC, is of much narrower scope than the title suggests, as it treats only the time-resolution trade off. An adequate theoretical approach to this problem was given in 1969 by Knox and Saleem. The present treatment, which ultimately results in the same equations, is much more complicated and gives an unnecessary large number of equations and figures. It is doubtful whether this will be of much use for those chromatographers working on

applications, while those concerned with higher efficiency and speed will probably invent their own equations if they do not want to use the treatment by Knox. The chapter closes with sections on practical considerations and equipment specifications. The demands on the equipment, *e.g.*, on the time constant of the detector, are very much exaggerated here. Several erroneous and unclear statements were found in this chapter and these may lead to additional confusion.

In summary, this book is of variable quality. Some parts are very valuable, others are superfluous or will generate confusion. The printing is good, the number of errors not too high, except sometimes in Chapter III, and the price is reasonable.

Amsterdam (The Netherlands) H. POPPE

Vol. 238, No. 1

journal of chromatography news section

SYMPOSIUM PROGRAM

VI INTERNATIONAL SYMPOSIUM ON COLUMN LIQUID CHROMATOGRAPHY

The VI International Symposium on Column Liquid Chromatography will be held in Philadelphia, PA, U.S.A., from June 7th to 11th, 1982, at the Cherry Hill Inn in Cherry Hill, NJ, U.S.A. The Symposium is organized by The Chromatography Forum of Delaware Valley and co-sponsored by The Chromatography Discussion Group, Arbeitskreis Chromatographie der Gesellschaft Deutscher Chemiker, and GAMS.

The proceedings will be published in a special issue of the *Journal of Chromatography*. The language of the Symposium will be English.

For further information contact:

Dr. R.A. Barford
Program General Chairman)
ERRC-SEA
U.S. Dept. of Agriculture
600 E. Mermaid Lane
Philadelphia, PA 19118
U.S.A.

or

Dr. J.L. Glajch
(Program Co-Chairman)
Central Research & Development Dept.
Experimental Station 262/315
E.I. du Pont de Nemours & Co.
Wilmington, DE 19898
U.S.A.

The detailed program of the Symposium is given below.

MONDAY, JUNE 7, 1982

SELECTIVITY, I

Session Chairman: J.J. Kirkland

8:30 Welcome and Introduction (R.A. Barford)

8:45 L.R. Snyder (Technicon Corp., Tarrytown, NY, U.S.A.) – Mobile phase effects in liquid–solid chromatography

9:10 J.F.K. Huber and R. Hirz (University of Vienna, Vienna, Austria) – Multichannel switching including peak compression, ultimate performance and selectivity in multicolumn liquid chromatography

9:35 J.L. Glajch, J.J. Kirkland and J.M. Minor (E.I. du Pont de Nemours & Co., Wilmington, DE, U.S.A.)

10:00 R.K. Gilpin (IBM Instruments, Danbury, CT, U.S.A.) and M.E. Gangoda (Kent State University, Kent, OH, U.S.A.) – Investigations of solvation and mobility of alkyl chains attached to liquid chromatographic surfaces

10:25–11:00 Coffee break

SELECTIVITY, II

Session Chairman: G. Schill

11:00 E. Grushka, R. Leshem and C. Gilon (The Hebrew University, Jerusalem, Israel) – On the mechanism of enantiomeric resolution by reversed-phase liquid chromatography

11:25 P. Roumeliotis and K.K. Unger (Johannes Gutenberg-Universität, Mainz, G.F.R.) and A.A. Kurganov and V.A. Davankov (Academy of Sciences, Moscow, U.S.S.R.) – High-performance ligand exchange chromatography of enantiomers: studies on monomerically bonded chiral silica phases

11:50 A.A. Kurganov, A.B. Tevlin and V.A. Davankov (Academy of Sciences, Moscow, U.S.S.R.) and P. Roumeliotis and K.K. Unger (Johannes Gutenberg-Universität, Mainz, G.F.R.) – High-performance ligand exchange chromatography of enantiomers: studies on polystyrene-type chiral phases bonded to microparticulate silicas

12:15–14:00 Lunch

14:00–15:15 POSTER SESSION

1. G. Szepesi, M. Gazdag and R. Ivancsics (Chemical Works of Gedeon Richter, Ltd., Budapest, Hungary) – Separation of optical isomers by using normal-phase solvent-generated molecular complexation chromatography
2. W. Lindner and H. Ruckendorf (Institute of Pharmaceutical Chemistry, University of Graz, Austria) – Applications of HPLC (MD-HPLC); potencies and limitations of this technique in trace analysis
3. C.J. Little, D. Tompkins and O. Stahel (Kontron Electrolab, Middlesex, Great Britain) and R.W. Frei and C.E. Werkhoven-Goewie (Amsterdam, The Netherlands) – Applications of a microprocessor-controlled valve-switching unit in high-performance liquid chromatography. Part 1: Sample cleanup and trace enrichment
4. S.A. Wise, P.A. White and W.E. May (National Bureau of Standards, Washington, DC, U.S.A.) – The effect of C_{18} surface coverage on selectivity on reversed-phase liquid chromatography of polycyclic aromatic hydrocarbons
5. L.A. D'Avila, H. Colin and G. Guiochon (Ecole Polytechnique, Palaiseau, France) – Use of secondary equilibria in HPLC of azaarenes
6. H. Englehardt and H. Elgass (Universitat des Saarlandes, Saarbrucken, G.F.R.) – Gradient-elution as a pilot technique for isocratic analysis
7. M.T.W. Hearn and B. Grego (St. Vincent's School of Medical Research, Fitzroy, Victoria, Australia) – Reversed-phase liquid chromatographic analysis of dansyl-amino acids: evaluation of selectivity effects due to different buffer and pairing-ion systems
8. C.E. Werkhoven-Goewie, U.A.Th. Brinkman and R.W. Frei (Free University, Amsterdam, The Netherlands) and G.J. deJong, C.J. Little and O. Stahel (Kontron Electrolab, Middlesex, Great Britain) – Automated determination of drugs in blood samples after enzymatic hydrolysis, using pre-colomn switching and post-column detection
9. W.E. May, W.J. Sonnefeld, J.M. Brown-Thomas and S.A. Wise (National Bureau of Standards, Washington, DC, U.S.A.) – Multidimensional HPLC techniques applied to the determination of polycyclic aromatic compounds in complex mixtures
10. R. Lewis, T. May and R.K. Gilpin (IBM Instruments, Danbury, CT, U.S.A.) – Further investigations of retention predictability using the solubility parameter concept
11. T. Hanai and J. Hubert (University of Montreal, Montreal, Quebec, Canada) – Liquid chromatographic behaviour of amines
12. A.D. Nunn (Squibb Institute for Medical Research, New Brunswick, NJ, U.S.A.) – Structure distribution relationships of radiopharmaceuticals. A correlation between lipophilicity of 99mTc-HIDA derivatives as determined by HPLC and their protein binding and renal elimination
13. C. Li and L.J. Crane (J.T. Baker Chemical Company, Phillipsburg, NJ, U.S.A.) – Comparative evaluations of two new silica-based strong and weak cation exchange packings with several commercially available products

14. D.L. Reynolds, L.A. Sternson and A.J. Repta (The University of Kansas, Lawrence, KS, U.S.A.) – The retention behavior of quaternary and bis-quaternary ammonium compounds in reversed-phase HPLC systems
15. M. Gimpel and K.K. Unger (Johannes Gutenberg-Universitat, Mainz, G.F.R.) – Monomeric vs. polymeric bonded iminodiacetate silica supports in high-performance ligand exchange chromatography (HPLEC)
16. R. Eksteen, D.A. Bartley and L.A. Witting (Supelco, Inc., Bellefonte, PA, U.S.A.) – Chromatographic reproducibility and stability for *n*-alkyl bonded phases used in high-performance liquid chromatography
17. J.M. DiBussolo and W.R. Nes (Drexel University, Philadelphia, PA, U.S.A.) – The effect of configuration at C-20 on the retention of sterols on octyl and octadecyl bonded phases
18. D.J. Pietrzyk (University of Iowa, Iowa City, IA, U.S.A.) – Ion interaction chromatography: the separation of organic and inorganic anions
19. S. Alenmark and B. Bomgren (Linkoping University, Linkoping, Sweden) – Direct resolution of enantiomers by liquid affinity chromatography: a new tool for studies of stereoselectivity in biochemical reactions?
20. S.L. Abidi and I. Schmeltz (U.S. Fish and Wildlife Service, Dept. of Interior, La Crosse, WI, U.S.A.) – High-performance liquid chromatography of quinoidal imminium compounds derived from triphenylmethanes

15:30–17:00 DISCUSSION SESSION (L.R. Snyder, Chairman)

TUESDAY, JUNE 8, 1982

PROTEINS AND BIOMOLECULES, I

Session Chairman: J.F.K. Huber

8:30 Introduction

8:45 B. Grego, P.G. Stanton and M.T.W. Hearn (St. Vincent's School of Medical Research, Fitzroy, Victoria, Australia) – Further studies on the role of the organic modifier on resolution and solute recovery in the reversed-phase high-performance liquid chromatography of polypeptides and proteins

9:10 F.E. Regnier and J. Pearson (Purdue University, West Lafayette, IN, U.S.A.) – High-performance anion exchange chromatography of oligonucleotides

9:35 S.A. Cohen, Y. Tapuhi, J.C. Ford and B.L. Karger (Northeastern University, Boston, MA, U.S.A.) – Studies in the reversed-phase liquid chromatographic separation of proteins

10:00 M. Zakaria and P.R. Brown (University of Rhode Island, Providence, RI, U.S.A.) – Reversed-phase retention mechanism of purine and pyrimidine compounds: stationary phase effects

10:25–11:00 Coffee break

PROTEINS AND BIOMOLECULES, II

Session Chairman: R.S. Deelder

11:00 R.A. Barford and B.J. Sliwinski (Eastern Regional Research Center, U.S. Dept. of Agriculture, Philadelphia, PA, U.S.A.) – Physicochemical properties of mobile phase modifiers and protein retention by alkyl silicas

11:25 J.P. Larmann, J.J. DeStefano, A.P. Goldberg, J.A. Schmit and R.W. Stout (E.I. du Pont de Nemours & Co., Wilmington, DE, U.S.A.) – Effect of pore size and surface chemistry on reversed-phase high-performance liquid chromatography of macromolecules

11:50 N.H.C. Cooke, B.G. Archer, M.J. O'Hare, E.C. Nice and M. Capp (Altex Scientific Inc., Berkeley, CA, U.S.A., and Ludwig Institute for Cancer Research, London, Great Britain) – Effect of chain length and carbon load on the performance of alkyl bonded silicas for protein separations

12:15–14:00 Lunch

14:00–15:15 POSTER SESSION

1. G. Hoogewijs and D.L. Massart (Vrije Universiteit Brussel, Brussels, Belgium) – Plasma determinations of basic drugs using a general strategy involving ion-pair extractions and HPLC
2. Dietrich and Henke (Enka AG, Research Institute, Obernburg, G.F.R.) – Selective preparative gel-chromatographic separation of compounds with a low molecular weight on Sephadex LH-20
3. L.L. Ng (Merck, Sharp, and Dohme Research Laboratories, West Point, PA, U.S.A.) – A sample treatment for quantitation of drugs in biological fluids in HPLC
4. I.R. West, J. Dekker and R.L. Owen (American Maize-Products Company, Hammond, IN, U.S.A.) – Improved high-pressure liquid chromatographic determination of 5-(hydroxymethyl)-2-furaldehyde in corn syrups
5. T.D. Splittler and R.A. Marafioti (Cornell University, Geneva, NY, U.S.A.) – An efficient method for the HPLC analysis of carbofuran and its metabolites
6. J.D. Manes (Mead-Johnson Nutritional Division, Evansville, IN, U.S.A.) – Food grade protein hydrolysates and their peptides profiles
7. W. Roy Day and P.D. McDonald (Waters Associates Pty. Ltd., Chippendale, NSW, Australia) – A comparison of HPLC techniques for sugar analysis
8. M.L. Fishman, P.E. Pfeffer, L.W. Doner, R.A. Barford and P.D. Hoagland (Eastern Regional Research Center, U.S. Dept. of Agriculture, Philadelphia, PA, U.S.A.) – Characterization of pectin by high-performance size exclusion chromatography (HPSEC) on E Linear Micro Bondagel
9. G.W.K. Fong, R.N. Johnson and B.T. Kho (Ayerst Labs., Rouses Point, NY, U.S.A.) – A study on the rate of epimerization of Amoxicillin beta-Penicilloic Acid to its alpha-form in aqueous solutions using high-performance liquid chromatography
10. M. Johansson, S. Eksborg and A. Arbin (ACO Lakemedel AB, Solna, Sweden) – Liquid chromatographic determination of noscapine in plasma
11. B. Bjorkquist (Kemira Oy, Espoo Research Centre, Espoo, Finland) – Rapid simultaneous measurement of urea and biuret
12. L.W. Doner and An-F. Hsu (Eastern Regional Research Center, U.S. Department of Agriculture, Philadelphia, PA, U.S.A.) – High performance liquid chromatographic separation of alkaloids from *Papaver somniferum* – papaverine, thebaine, narceine, codeine and morphine
13. J.D. Stuart, E.R. Nemergut and D.W. Hill (University of Connecticut, Storrs, CT, U.S.A.) – A sensitive high-performance liquid chromatographic determination of primary amino acids in various biological fluids
14. T. Hosain and F. Hosain (University of Connecticut Health Center, Farmington, CT, U.S.A.) – Protein recovery in high-performance size exclusion chromatography: studies with radioactive human serum albumin and different columns
15. M.J. Kessler (University of Texas Health Science Center, Medical School, Houston, TX, U.S.A.) – Quantitation of radiolabeled biological molecules separated by high-performance liquid chromatography
16. G.D. Wachob (J.T. Baker Chemical Co., Phillisburg, NJ, U.S.A.) – A new sample processing technique for water soluble vitamin analyses
17. C.M. Riley, L.A. Sternson and A.J. Repta (The University of Kansas, Lawrence, KS, U.S.A.) – The assessment of cisplatin reactivity with peptides and proteins by reversed-phase high-performance liquid chromatography
18. M.P. Henry (J.T. Baker Chemical Co., Phillisburg, NJ, U.S.A.) – Separation of oligonucleotides by HPLC
19. J.L. DiCesare and F.L. Vandemark (Perkin-Elmer Corp., Norwalk, CT, U.S.A.) – High resolution preparative separation of peptides and proteins by reversed-phase liquid chromatography
20. D.T. Organisciak and H.M Wang (Wright State University, Dayton, OH, U.S.A.) – HPLC analysis of two antioxidants in the rat retina
21. K.G. Symms (Ecology and Environment, Inc., Pennsauken, NJ, U.S.A.) – Rapid separation and correlation in relative retentions of a diversity of glucuronide and corresponding sulfate conjugates by reverse-phase high-performance liquid chromatography
22. J.M. Bartlett and A.B. Segelman (Rutgers University, Piscataway, NJ, U.S.A.) – Bioanalysis of Cimetidine by high-performance liquid chromatography
23. C.K. Lim (Clinical Research Centre, Harrow, Middlesex, Great Britain) – High-performance liquid chromatography of tetrahydronaphthalene lignans

15:30–17:00 DISCUSSION SESSION (B.L. Karger, Chairman)

WEDNESDAY, JUNE 9, 1982

FIELD-FLOW FRACTIONATION

Session Chairman: G. Guiochon

8:30 Introduction

8:45 J.C. Giddings, K.D. Caldwell, M.N. Myers, F.-S. Yang and G. Karaiskakis (University of Utah, Salt Lake City, UT, U.S.A.) – Separation and characterization of particulate materials by field-flow fractionation

9:10 J.J. Kirkland, C.H. Dilks, Jr. and W.W. Yau (E.I. du Pont de Nemours & Co., Wilmington, DE, U.S.A.) – Sedimentation field-flow fractionation (SFFF) at high force fields

9:35 M. Martin, J. Gril, O. Besancon and R. Reynaud (Ecole Polytechnique, Palaiseau, France) – Influence of inertia effects on particle retention in field-flow fractionation

10:00 K.D. Caldwell, M.N. Myers and J.C. Giddings (University of Utah, Salt Lake City, UT, U.S.A.) – Field-flow fractionation of biological macromolecules and particles

10:25–11:00 Coffee break

UNIQUE STATIONARY PHASE EFFECTS

Session Chairman: K.P. Hupe

11:00 Cs. Horváth, J. Frenz and Z. El Rassi (Yale University, New Haven, CT, U.S.A.) – Theory and applications of high-performance displacement chromatography

11:25 H. Colin, Y. Zihou and G. Guiochon (Ecole Polytechnique, Palaiseau, France) – Stationary phase effects in reversed-phase liquid chromatography

11:50 J. Kohler and G. Schomburg (Max-Planck-Institut für Kohlenforschung, Mülheim Ruhr, G.F.R.) – Platinum complexes in reversed- and normal-phase chromatography: analytical and preparative scale separations of enantiomeric olefins

12:15 F.F. Cantwell, S. Afrashtehfar and R.A. Hux (University of Alberta, Edmonton, Alberta, Canada) – Double layer ionic adsorption and exchange on low capacity ion exchangers

12:15–14:00 Lunch

THURSDAY, JUNE 10, 1982

COLUMN TECHNOLOGY, I

Session Chairman: H. Englehardt

8:30 Introduction

8:45 J.W. Jorgenson and E.J. Guthrie (University of North Carolina, Chapel Hill, NC, U.S.A.) – Liquid chromatography in open-tubular columns

9:10 D. Ishii and T. Takeuchi (Nagoya University, Chikusa-ku, Nagoya-shi, Japan) – High-resolution micro-HPLC using flexible fused-silica packed columns

9:35 J.C. Giddings, J.P. Chang and M.N. Myers (University of Utah, Salt Lake City, UT, U.S.A.) – Capillary LC in FFF-type channels

10:00 F.J. Yang (Varian Instrument Group, Walnut Creek, CA, U.S.A.) – Narrow-bore microparticulate packed column HPLC

10:25–11:00 Coffee break

COLUMN TECHNOLOGY, II

Session Chairman: R.W. Frei

11:00 H. Poppe and J.C. Kraak (University of Amsterdam, Amsterdam, The Netherlands) – Mass loadability of chromatographic columns

11:25 G. Guiochon, L.A. D'Avila, H. Colin, M.S. Gonnard, A. Siouffi and M. Zacria (Ecole Polytechnique, Palaiseau, France) – Liquid chromatography using a bidimensional column

11:50 H.H. Lauer, G.P. Rozing and K.P. Hupe (Hewlett-Packard, G.F.R.) Determination of band spreading effects in HPLC instruments, II

12:15–14:00 Lunch

14:00–15:15 POSTER SESSION

1. J. Crommen (Universite de Liege, Belgium) – Detection of amino acids and peptides in reversed-phase ion-pair chromatographic systems with a UV-absorbing ion in the mobile phase
2. E.J Parks, R.B. Johannesen and F.E. Brinckman (National Bureau of Standards, Washington, DC, U.S.A.) – Characterization by SEC of organometallic polymers and polymerization
3. H.H. Wisneski, R.L. Yates and H.M. Davis (Food and Drug Administration, Washington, DC, U.S.A.) – High-pressure liquid chromatographic–fluorometric determination of 1,2-methylenedioxy-4-allyl-benzene (Safrole) in fragrances
4. M. Novotny, A. Hirose and V. McGuffin (Indiana University, Bloomington, IN, U.S.A.) – Separation and characterization of heavy components in fossil fuels by micro-HPLC and its ancillary techniques
5. G.W.C. Hung (Woodson-Tenant Labs., Inc., Memphis, TN, U.S.A.) – High-performance liquid chromatographic determination of carbohydrates in food products
6. P.D. McDonald and H.S. Schultz (Waters Associates, Inc., Milford, MA, U.S.A.) – Ultra-high-efficiency size separation of small organic molecules
7. M.A. Elchisak and J.D. Evanseck (Purdue University, West Lafayette, IN, U.S.A.) – Determination of conjugated compounds by HPLC using post-column hydrolysis: specific application to dopamine sulfate isomers
8. R. Gill, S.C. Qua and A.C. Moffat (Home Office Central Research Establishment, Berkshire, Great Britain) – High-performance liquid chromatography of paraquat and diquat in urine with rapid sample preparation involving ion-pair extraction on disposable cartridges of octadecyl-silica
9. J.M. Colin (Total, Compagnie Francaise de Raffinage Research Centre, Harfleur, France) – Hydrocarbon group type analyses in petroleum residue by HPLC
10. H. Noda, K. Saito, A. Nakamoto and Y. Ishida (Shimadzu Corp., Kyoto, Japan) – A microbore column system in liquid chromatography – performance and applications
11. V.L. Osborne and W.C. Randolph (Smith Kline and French Labs., Philadelphia, PA, U.S.A.) – Analysis of SK&F 82526 in plasma by high-performance liquid chromatography with electrochemical detection (LCEC)
12. B.F.H. Drenth and T. Jagersma (State University Groningen, Groningen, The Netherlands) – Data acquisition and processing system for HPLC with an on-line radioactivity detector
13. M.W. Dong and J.L. DiCesare (Perkin-Elmer Corp., Norwalk, CT, U.S.A.) – Environmental analysis using very-high-speed liquid chromatography
14. J.N. Little, G.L. Hawk and F.H. Zenie (Zymark Corp., Hopkinton, MA, U.S.A.) – Automated sample preparation for chromatography using robotics
15. R.T. Krause (U.S. Food and Drug Administration, Washington, DC, U.S.A.) – Determination of fluorescent pesticides, metabolites and industrial chemicals using reversed-phase high-performance liquid chromatography
16. N. Petroff and J.P. Durand (Institut Francais du Petrole, Reuil-Malmaison, France) – Fast determination of hydrocarbon groups in heavy petroleum products by liquid–liquid chromatography
17. S. George and H. Elgass (Hewlett-Packard GmbH, Waldbronn, G.F.R.) – Application of a photodiode-array HPLC detection system
18. S.-T. Lai and D.C. Locke (City University of New York, Queens College, Flushing, NY, U.S.A.) – Step-wise pyrolysis–liquid chromatography and pyrolysis–gas chromatography of polystyrene
19. T. Suortti and A.V. Wright (Technical Research Centre of Finland, Food Laboratory, Espoo, Finland) – HPLC separation of mutagenic compounds from wild edible mushroom *Lactarius necator*
20. R.E. Shoup (Bioanalytical Systems Inc., West Lafayette, IN, U.S.A.) – Recent advances in electrochemical detectors for LC

15:30–17:00 DISCUSSION SESSION (H. Poppe, Chairman)

FRIDAY, JUNE 11, 1982

DETECTION, I

Session Chairman: Cs. Horváth

8.30 Introduction

8:45 R.S. Deelder, J.H.M. van den Berg and A.T.J.M. Kuijpers (DSM Research, Geleen, The Netherlands) – Evaluation and comparison of reaction detectors

9:10 P. Kucera and H. Umagat (Hoffman-La Roche, Inc., Nutley, NJ, U.S.A.) – Design of post-column fluorescence derivatization system for use with microbore columns

9:35 J.J. Donkerbroek, C. Gooijer, N.H. Velthorst and R.W. Frei (Free University, Amsterdam, The Netherlands) – New detection method for liquid chromatography on room temperature phosphorescence

10:00 H. Englehardt and B. Lillig (Universität des Saarlandes, Saarbrücken, G.F.R.) – High-performance ion-exchange chromatography and reaction detection

10:25–11:00 Coffee break

DETECTION, II

Session Chairman: W. Simon

11:00 G. Schill and L. Hackzell (University of Uppsala, Uppsala, Sweden) – Detection of non-UV absorbing compounds in reversed-phase systems by use of ion-pairing techniques

11:25 I.S. Krull and D. Bushee (Northeastern University, Boston, MA, U.S.A.) and S.B. Smith, Jr., R. Schleicher and P. Demko (Instrumentation Laboratory, Wilmington, MA, U.S.A.) – Applications of HPLC-inductively coupled plasma emission spectroscopy for metal cation and anion analysis and speciation

11:50 V.V. Berry and R.E. Shansky (Polaroid Corp., Cambridge, MA, U.S.A.) – Halide analysis in silver photo-products with HPLC and UV detection using classical ion pairing and novel injection loading of ion pairing agent

12:15 Concluding remarks

PUBLICATION SCHEDULE FOR 1982

Journal of Chromatography (incorporating *Chromatographic Reviews*) and *Journal of Chromatography, Biomedical Applications*

MONTH	J	F	M	A	M	J	J	A	S	O	N	D
Journal of Chromatography	234/1 234/2 235/1 235/2	236/1 236/2	237/1 237/2 237/3	238/1 238/2 239	240/1 240/2 241/1	The publication schedule for further issues will be published later.						
Chromatographic Reviews		251/1		251/2								
Biomedical Applications	227/1	227/2	228	229/1	229/2							

INFORMATION FOR AUTHORS

(Detailed *Instructions to Authors* were published in Vol. 209, No. 3, pp. 501-504. A free reprint can be obtained by application to the publisher.)

Types of Contributions. The following types of papers are published in the *Journal of Chromatography* and the section on *Biomedical Applications:* Regular research papers (Full-length papers), Short communications and Notes. Short communications are preliminary announcements of important new developments and will, whenever possible, be published with maximum speed. Notes are usually descriptions of short investigations and reflect the same quality of research as Full-length papers, but should preferably not exceed four printed pages. For review articles, see page 2 of cover under Submission of Papers.

Submission. Every paper must be accompanied by a letter from the senior author, stating that he is submitting the paper for publication in the *Journal of Chromatography*. Please do not send a letter signed by the director of the institute or the professor unless he is one of the authors.

Manuscripts. Manuscripts should be typed in double spacing on consecutively numbered pages of uniform size. The manuscript should be preceded by a sheet of manuscript paper carrying the title of the paper and the name and full postal address of the person to whom the proofs are to be sent. Authors of papers in French or German are requested to supply an English translation of the title of the paper. As a rule, papers should be divided into sections, headed by a caption (*e.g.,* Summary, Introduction, Experimental, Results, Discussion, etc.). All illustrations, photographs, tables, etc., should be on separate sheets.

Introduction. Every paper must have a concise introduction mentioning what has been done before on the topic described, and stating clearly what is new in the paper now submitted.

Summary. Full-length papers and Review articles should have a summary of 50–100 words which clearly and briefly indicates what is new, different and significant. In the case of French or German articles an additional summary in English, headed by an English translation of the title, should also be provided. (Short communications and Notes are published without a summary.)

Illustrations. The figures should be submitted in a form suitable for reproduction, drawn in Indian ink on drawing or tracing paper. Each illustration should have a legend, all the *legends* being typed (with double spacing) together on a *separate sheet*. If structures are given in the text, the original drawings should be supplied. Coloured illustrations are reproduced at the author's expense, the cost being determined by the number of pages and by the number of colours needed. The written permission of the author and publisher must be obtained for the use of any figure already published. Its source must be indicated in the legend.

References. References should be numbered in the order in which they are cited in the text, and listed in numerical sequence on a separate sheet at the end of the article. Please check a recent issue for the lay-out of the reference list. Abbreviations for the titles of journals should follow the system used by *Chemical Abstracts*. Articles not yet published should be given as "in press", "submitted for publication", "in preparation" or "personal communication".

Proofs. One set of proofs will be sent to the author to be carefully checked for printer's errors. Corrections must be restricted to instances in which the proof is at variance with the manuscript. "Extra corrections" will be inserted at the author's expense.

Reprints. Fifty reprints of Full-length papers, Short communications and Notes will be supplied free of charge. Additional reprints can be ordered by the authors. An order form containing price quotations will be sent to the authors together with the proofs of their article.

News. News releases of new products and developments, and information leaflets of meetings should be addressed to: The Editor of the News Section, Journal of Chromatography/Journal of Chromatography, Biomedical Applications, Elsevier Scientific Publishing Company, P.O. Box 330, 1000 AH Amsterdam, The Netherlands.

Advertisements. Advertisement rates are available from the publisher on request. The Editors of the journal accept no responsibility for the contents of the advertisements.

THREE VOLUMES IN THE ANALYTICAL CHEMISTRY SYMPOSIA SERIES

Volume 4: (NEW)

Recent Developments in Mass Spectrometry in Biochemistry and Medicine, 6

Proceedings of the 6th International Symposium on Mass Spectrometry in Biochemistry and Medicine, Venice, 21 and 22 June, 1979

A FRIGERIO, *Mario Negri Institute for Pharmacological Research, Milan, Italy, and* M. McCAMISH, *University of Queensland, Brisbane, Australia (Editors)*

This book, comprising 52 papers, presents the latest research and developments in biochemistry, medicine, forensic science, drug research, clinical chemistry and pollution, as reported at the meeting.

Sections: Endogenous compounds : qualitative studies *(6 papers).* Endogenous compounds: quantitative studies *(14 papers).* Exogenous compounds: qualitative studies *(10 papers).* Exogenous compounds: quantitative studies *(5 papers).* Instrumentation and methodology *(12 papers).* Environmental studies *(5 papers).*

1980 about 550 pages
US $ 83.00/Dfl. 170.00
ISBN 0-444-41870-9

Volume 3: (NEW)

Recent Developments in Chromatography and Electrophoresis, 10

Proceedings of the 10th International Symposium on Chromatography and Electrophoresis, Venice, 19 and 20 June, 1979

A. FRIGERIO and M. McCAMISH *(Editors)*

Comprising a total of 34 papers, this volume is devoted to potential applications of chromatography and electrophoresis with special emphasis on newer developments.

Sections: Drug analysis *(9 papers).* Electrophoresis *(5 papers).* Analysis of endogenous compounds *(7 papers).* Environmental studies *(3 papers).* Fluorometry *(5 papers).* Instrumental *(5 papers).*

1980 350 pages
US $ 68.25/Dfl. 140.00
ISBN 0-444-41871-7

Volume 1:

Recent Developments in Chromatography and Electrophoresis

Proceedings of the 9th International Symposium on Chromatography and Electrophoresis, Riva del Garda, 15-17 May, 1978

A. FRIGERIO, *Mario Negri Institute for Pharmacological Research, Milan, Italy, and* L. RÉNOZ, *Belgian Society for Pharmaceutical Sciences, Belgium (Editors)*

These proceedings, providing 34 general reviews on chromatography and electrophoresis, cover a wide range of potential applications of these techniques.
Of interest to: research workers in chemistry, biochemistry, medicine, toxicology, drug metabolism, forensic science, clinical chemistry and pollution studies

1979 368 pages
US $ 58.50/Dfl. 120.00
ISBN 0-444-41785-0

ELSEVIER

P.O. Box 211,
1000 AE Amsterdam,
The Netherlands
52 Vanderbilt Avenue
New York, N.Y. 10017

The Dutch guilder price is definitive. US $ prices are subject to exchange rate fluctuations.